La conservation inattendue du métabolisme du glycogène chez les Chlamydiae souligne une fonction essentielle des polysaccharides de réserve dans leur cycle de développement

Matthieu Colpaert

Université de Lille

Ecole Doctorale Biologie-Santé

THESE DE DOCTORAT

En vue de l'obtention du diplôme de docteur en biochimie

Rédigée et présentée par

Matthieu COLPAERT

Unexpected conservation of the glycogen metabolism pathway underlines a pivotal function of storage polysaccharides in the developmental cycle of *Chlamydiae*

La conservation inattendue du métabolisme du glycogène chez les Chlamydiae souligne une fonction essentielle des polysaccharides de réserve dans leur cycle de développement.

Directeur de Thèse : Christophe COLLEONI

Equipe de Génétique Microbienne UGSF UMR 8576

Thèse soutenue le 22 janvier 2021

Les membres du jury :

Rapporteurs :

- Agathe SUBTIL, Directrice de Recherche à l'Institut Pasteur Paris
- Marcelo GUERIN, Ikerbasque Research Professor at CIC bioGUNE

Examinateurs :

- Matthew GENTRY, Professor at the University of Kentucky
- Gilbert GREUB, Professeur au CHUV de Lausanne
- Steven BALL, Professeur de l'Université de Lille

Président :

- Christophe D'HULST, Professeur de l'Université de Lille

Abstract

For almost a century, the *Chlamydiae* phylum contained only the *Chlamydiaceae* family, which encompasses etiological agents of severe infectious diseases in humans. Today, fifteen families have enriched this phylum in which the so-called Chlamydia-like bacteria or environmental *Chlamydiae* are distributed. The hallmark of all *Chlamydiae* is a huge genome reduction leading to an obligate intracellular lifestyle and a biphasic developmental cycle including a highly metabolically active intracellular form (i.e., reticulate bodies) and an extracellular (i.e., elementary body) form. While glycogen metabolism loss is viewed as an adaptation to the intracellular lifestyle, all *Chlamydiae* are singularly distinguished from other intracellular pathogens by the maintenance of the GlgC-pathway, which is the one described in *Escherichia coli*. Some environmental *Chlamydiae*, however, seemed to deviate from this rule. Indeed, the *glgC* gene, encoding the ADP-glucose pyrophosphorylase activity is missing in the genomes of *Estrella lausannensis* (family *Criblamydiaceae*) and *Waddlia chondrophila* (family *Waddliaceae*). The lack of this key enzyme suggested that chlamydial strains are therefore defective in glycogen biosynthesis.

However, electron microscopic observation of thin sections of *E. lausannensis* and *W. chondrophila* elemental bodies stained with PATAg (specific glycogen staining) clearly refuted this presumption. In order to explain this unexpected result, 220 genomes reflecting chlamydial diversity were examined for their gene content of the glycogen biosynthesis pathway reported in bacteria: the GlgC pathway and the GlgE pathway, recently evidenced in *Mycobacterium tuberculosis*. We thus identified *in E. lausannensis* and *W. chondrophila* but also in phylogenetically related *Chlamydiae* the GlgE pathway, which is based on four enzymatic reactions enabling the synthesis of glycogen from trehalose. The enzymatic characterizations of TreS-Mak; a bifunctional enzyme that converts trehalose to maltose-1-phosphate and GlgE; a maltosyltransferase activity responsible for the synthesis of α-1,4 glucan chains, confirmed that this pathway is functional in these two environmental *Chlamydiae*. In addition, we show that, like the glycogen synthase (GlgA) of the GlgC pathway, GlgE activity is capable of initiating *de novo* glycogen synthesis without the aid of a glucan primer. Finally, preliminary studies suggest that acetylation of lysine residues, a post-translational modification involved in the regulation of many enzymes of the carbon metabolism in bacteria, may activate GlgE activity.

Altogether this study demonstrates that glycogen metabolism is conserved in all *Chlamydiae*, without exception, despite the genome reduction process, thus underlining an essential function, underestimated to date, of this storage polysaccharide. We propose that the degradation of glycogen may provide the energy required to sustain basal metabolic functions, which are essential for the survival and virulence of extracellular forms, i.e., elementary bodies.

Keywords : Chlamydia, glycogen, GlgE

Résumé

Pendant près d'un siècle, le phylum *Chlamydiae* n'a contenu que la famille des *Chlamydiaceae*, qui regroupe les agents étiologiques de sévères maladies infectieuses chez l'Homme. Aujourd'hui, quinze familles enrichissent ce phylum où se répartissent les bactéries dites *Chlamydia*-like ou *Chlamydiae* environnementales. Les *Chlamydiae*, bactéries intracellulaires obligatoires, se caractérisent par une réduction importante de leur génome et un cycle de développement biphasique comprenant une forme intracellulaire métaboliquement très active (le corps réticulé) et une forme extracellulaire dormante et infectieuse (le corps élémentaire). Alors que la perte du métabolisme du glycogène est décrite comme une adaptation à la vie intracellulaire, les *Chlamydiae* se distinguent singulièrement des autres pathogènes intracellulaires par un maintien de la voie GlgC qui est identique à celle décrite chez *Escherichia coli*. Cependant, certaines *Chlamydiae* environnementales semblaient déroger à cette règle. En effet, le gène *glgC*, codant l'activité ADP-glucose pyrophosphorylase, est absent dans les génomes d'*Estrella lausannensis* (famille *Criblamydiaceae*) et de *Waddlia chondrophila* (famille *Waddliaceae*). L'absence de cette enzyme clef laissait supposer que ces espèces sont, par conséquent, défectueuses dans la biosynthèse du glycogène.

L'observation au microscope électronique de fines sections colorées au PATAg (coloration spécifique du glycogène) de corps élémentaires d'*E. lausannensis* et de *W. chondrophila* ont toutefois clairement réfuté cette idée reçue. Afin d'expliquer ce résultat inattendu, 220 génomes représentant la diversité des *Chlamydiae* ont été scrutés pour leur contenu en gènes des voies de biosynthèse du glycogène documentés chez les bactéries : la voie GlgC et la voie GlgE, récemment décrite chez *Mycobacterium tuberculosis.* Nous avons ainsi identifié chez *E. lausannensis* et *W. chondrophila* mais aussi chez des *Chlamydiae* phylogénétiquement apparentées, la voie GlgE qui repose sur quatre réactions enzymatiques permettant la synthèse du glycogène à partir du tréhalose. Une caractérisation biochimique de l'activité TreS-Mak ; une enzyme bifonctionnelle qui convertit le tréhalose en maltose-1-phosphate et de l'activité GlgE ; une activité maltosyltransférase responsable de la synthèse de chaînes d'α-1,4 glucanes, ont confirmé que la voie GlgE était bien fonctionnelle chez ces deux *Chlamydiae* environnementales. En outre, nous avons montré que, à l'instar de la glycogène synthase (GlgA) de la voie GlgC, l'activité GlgE est capable d'initier la synthèse du glycogène *de novo* sans l'aide d'une amorce glucanique. Enfin, des études préliminaires suggèrent que l'acétylation des résidus lysines, une modification post-traductionnelle qui intervient dans la régulation de nombreuses enzymes impliquées dans le métabolisme carboné chez les bactéries, activerait l'activité GlgE.

L'ensemble de cette étude démontre que le métabolisme du glycogène est conservé chez toutes les *Chlamydiae,* sans exception, et ce malgré le processus de réduction du génome, soulignant ainsi une fonction essentielle, sous-estimée à ce jour, de ce polysaccharide de réserve. Nous proposons que le catabolisme du glycogène fournisse l'énergie nécessaire au maintien des fonctions métaboliques basales, qui sont indispensables à la survie et à la virulence des formes extracellulaires c'est-à-dire des corps élémentaires.

Mots-clés : Chlamydia, glycogène, GlgE

Acknowledgements

Tout d'abord, je souhaite remercier le Pr. Christophe Colleoni, alias Coco, mon directeur de thèse, mon chef, mon mentor. Merci de m'avoir guidé et aidé durant toute cette thèse, de m'avoir fait découvrir et aimer le monde de la recherche. Merci de m'avoir transmis tant de savoirs, de savoir-faire. Merci de m'avoir fait confiance, de m'avoir poussé et mis la pression quand il le fallait. Bref, un énorme MERCI !

Je souhaite également remercier chaleureusement le Pr. Steven Ball, pour m'avoir accepté au sein de son équipe dès mon Master 2. Merci de m'avoir aidé à obtenir ma bourse de thèse, ce qui m'a permis de passer 3 ans de plus au sein d'une équipe géniale !

I would also like to thank all the members of my Ph.D. committee:

Merci au Dr. Agathe Subtil d'avoir accepté d'être examinatrice de ma thèse. Je te remercie sincèrement pour tes conseils et pour nos discussions, hélas toujours trop courtes, lors de mes Comités de Suivi Individuels.

Thanks to Pr. Marcelo Guerin for accepting to be an examiner for my Ph.D. Even if we did not have the opportunity to talk a lot to each other in the Slovakian countryside, I remember you as a great man and a great scientist.

Thanks to Pr. Matthew S. Gentry to be part of my Ph.D. committee. It was a real pleasure to meet you at the Alamy conference, but also to visit your lab at the University of Kentucky. I had a great moment and met amazing people during this month (that went too fast). Thank you again for your warm welcome!

Merci également au Pr. Gilbert Greub de faire partie de mon jury de thèse. Un grand merci pour tes remarques durant notre rencontre à l'ICES, et pour ton aide précieuse dans l'avancée de ce projet.

Et merci au Pr. Christophe d'Hulst d'avoir accepté de présider mon jury de thèse. Merci pour ton humour et pour toutes ces années à prendre soin de nous au sein de l'UGSF.

J'aimerai ensuite remercier l'ensemble des membres de mon équipe. Ugo, malgré la faute d'orthographe dans ton prénom, c'est toujours un immense plaisir de discuter avec toi, que ce soit de sujets sérieux ou non. Malika, merci pour ta bonne humeur, mais également pour toute ton aide, autant pour le travail que dans la vie privée. J'ai pu ouvrir les yeux sur certaines

choses. Marie, merci pour ta bonne humeur débordante (pour ne pas dire folie). Grâce à toi, je n'ai jamais eu faim au laboratoire.

Merci également aux anciens de l'équipe ! Derifa, pour m'avoir aidé à prendre mes marques au sein du laboratoire et qui m'a appris le sens du #ifficacité. Et bien sûr Sylvain, qui trainait un peu trop par chez nous, mais tellement plein de bonne humeur communicative (et d'histoires drôles (et de bières)) qu'on ne pouvait pas lui en vouloir.

Un grand merci également aux camarades et amis de bureaux, avec qui j'ai pu passer de très bons moments. Merci à François et Maud (et encore félicitations), à Stan et Marine. Merci également à Corentin pour avoir fait de moi une star internationale (dans le monde des films d'art contemporains).

Merci plus généralement, merci à l'ensemble des membres de l'UGSF !

Une grande pensée à mes proches. Gros bisous à mon fwewo et à Charles, qui m'ont permis de garder le moral et le sourire pendant toutes ces années. Je vous aime.

Comment ne pas remercier Léa ? Quel bonheur d'avoir croisé ta route au moment où je m'y attendais le moins. Grâce à toi, cette période difficile s'est transformée en joie de tous les instants. Quand je doute, il suffit que je te regarde (trop mimi) pour retrouver toute mon énergie. Merci ❤

Et évidemment, une pensée émue pour toute ma famille. Ça y est, j'y suis. C'est grâce à vous. Merci pour votre support, à tous ! Merci de m'avoir supporté durant toutes ces années (même si vous n'aviez pas le choix). Plein de bisous !

Et à tous ceux qui ont lu ces remerciements, qui pensaient voir leur nom, et ne l'ont pas vu, pardon. Et merci !

Abbreviations

ABC : ATP-binding cassette
AcCoA : acetyl-coenzyme A
AckA : acetate kinase
AcP : acetyl-phosphate
Acs : AMP-forming acetyl-CoA synthetase
ADP-glucose : adenosine diphosphoglucose
ATP : adenosine triphosphate
cAMP : cyclic adenosine monophosphate
CAZy : carbohydrate-active enzymes
CTP : cytidine triphosphate
DP : degree of polymerization
DTT : 1,4-dithiothreitol
EB : elementary body
EMP : Embden-Meyerhof-Parnas
FACE : fluorophore assisted carbohydrate electrophoresis
FBC : Fibrobacteres Chlorobi Bacteroidetes
G1P : glucose-1-phosphate
G6P : glucose-6-phosphate
GH : glycoside hydrolase
GlgA : glycogen synthase
GlgB : branching enzyme
GlgC : ADP-glucose-pyrophosphorylase
GlgE : α-1,4-glucan:maltose-1-phosphate maltosyltransferase
GlgM : maltose-1-phosphate synthase
GlgP : glycogen phosphorylase
GlgX : debranching enzyme
GT : glycosyltransferase
GTP : guanosine triphosphate
HAT : histone acetyltransferase
HDAC : histone deacetylase
IPTG : isopropyl β-D-1-thiogalactopyranoside
KAT : lysine acetyltransferase
KDAC : lysine deacetylase
LB : Lysogeny broth
M1P : maltose-1-phosphate
Mak : maltokinase
MalP : maltodextrin phosphorylase
MalQ : 4-α-glucanotransferase
MATH : *Ménage à trois* hypothesis
MOS : malto-oligosaccharide
NAD : nicotinamide adenine dinucleotide
NTT : nucleotide triphosphate transporter
OPP : oxidative pentose phosphate
OtsA : trehalose-6-phosphate synthase
OtsB : trehalose-6-phosphate phosphorylase
PAL : alkaline phosphatase
PGM : phosphoglucomutase
Pi : orthophosphate
PPi: pyrophosphate
PTA: phosphotransacetylase
PTM : post-translational modification
PTS : phosphoenol-pyruvate: sugar phosphotransferase system
PVC : Planctomycetes Verrucomicrobia Chlamydiae
RB : reticulate body
T3SS : type III secretion system
T6P : trehalose-6-phosphate
TB : Terrific Broth
TCA cycle : tricarboxylic acid cycle
TreP : trehalose phosphorylase
TreS : trehalose synthase
TreT : trehalose glycosyltransferring synthase
TreY : maltooligosyl-trehalose synthase
TreZ : maltooligosyl-trehalose trehalohydrolase
UDP-glucose : uridine diphosphoglucose
UTP : uridine triphosphate

Résumé de la thèse en français

I. Introduction générale

I-A. Le métabolisme du glycogène chez les bactéries

Le glycogène, homopolymère soluble de glucoses liés en α-1,4 et branchés en α-1,6, constitue la principale forme de stockage du carbone et d'énergie chez les procaryotes et les cellules eucaryotes (Wilson *et al.*, 2010). Chez les bactéries, deux voies principales de biosynthèse du glycogène peuvent être définies selon les enzymes impliquées.

La voie classique du métabolisme du glycogène rencontrée chez les eucaryotes et les bactéries, reposant sur l'activité GlgC, sera nommée voie GlgC dans la suite de cette étude. Dans cette voie de biosynthèse, trois réactions enzymatiques sont requises pour la synthèse du glycogène : (i) la synthèse du nucléotide-sucre (ADP-glucose chez les bactéries) à partir d'ATP et de glucose-1-phosphate par une ADP-glucose pyrophosphorylase (GlgC) (ii) la formation des liaisons α-1,4 catalysée par les glycogène synthases (GlgA) en transférant le résidu glucose de l'ADP-glucose sur l'extrémité non-réductrice d'une chaîne de glucose en croissance et (iii) l'introduction de points de branchement par les enzymes de branchement (GlgB). Ces dernières clivent une liaison α-1,4 et transfèrent la chaîne ainsi clivée en position α-1,6 (Figure R1). Une voie similaire existe chez les eucaryotes qui ont toutefois substitué l'utilisation de l'ADP-glucose par celle de l'UDP-glucose, un substrat commun à beaucoup d'autres voies métaboliques (Wilson *et al.*, 2010).

Contrairement à la voie classique GlgC, qui est de loin la plus étudiée et qui est retrouvée chez environs 20 % des bactéries (Syson *et al.*, 2020), la voie GlgE n'a été étudiée que chez un nombre restreint d'*Actinobacteria* alors qu'elle est présente dans au moins 14 % des génomes bactériens (Rashid *et al.*, 2016). Il est important de noter que les voies GlgC et GlgE cohabitent parfois dans le même organisme (Chandra *et al.*, 2011). A l'inverse de la voie GlgC, la voie GlgE repose sur l'utilisation du tréhalose (deux glucoses liés par une liaison α,α-1,1). A l'exception des vertébrés, ce disaccharide est produit chez de nombreux organismes, tels que les bactéries, les champignons, les plantes et les invertébrés, comme réserve de carbone (Opperdoes *et al.*, 2011), mais également comme molécule protectrice face à divers stress environnementaux (stress osmotique, dessiccation, changement de température, oxydation). Il entre aussi, sous forme conjuguée à des lipides, dans la composition des enveloppes bactériennes des mycobactéries et corynebactéries (Argüelles, 2000).

La voie GlgE repose sur trois réactions enzymatiques pour synthétiser une chaîne de glucose à partir du tréhalose : (i) la tréhalose synthase (TreS) convertit de manière réversible le tréhalose en maltose, (ii) lequel est ensuite phosphorylé par la maltokinase (Mak) en maltose-1-phosphate (M1P) (iii) avant que la maltosyltransférase GlgE transfert le groupement maltosyl du M1P sur une chaîne de glucose en élongation (Figure R1) (Kalscheuer *et al.*,

2010). En plus de ces activités, une deuxième enzyme produisant du M1P, nommée maltose-1-phosphate synthase (GlgM), a été identifiée chez les *Actinobacteria* (Koliwer-Brandl *et al.*, 2016).

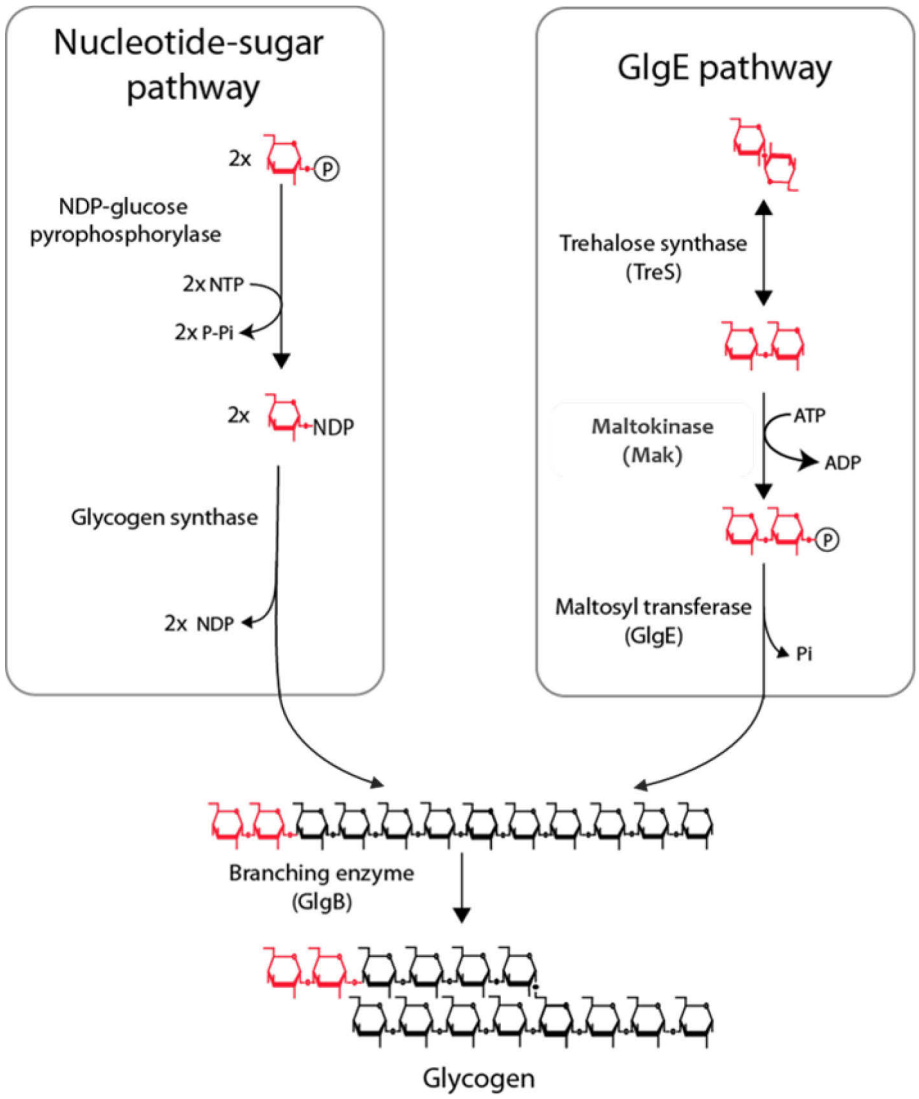

Figure R 1 : Deux voies métaboliques conduisent à la synthèse de particules de glycogène chez les bactéries. La voie la plus répandue pour la synthèse du glycogène est basée sur l'utilisation de nucléotides-sucre (panneau de gauche). Cette voie repose sur deux activités enzymatiques. Premièrement, une NDP-glucose pyrophosphorylase synthétise des nucléotides-sucres à partir de NTP et de glucose-1-phosphate. Alors que les eucaryotes hétérotrophes ne dépendent que de l'UDP-glucose pour la synthèse du glycogène, les bactéries utilisent l'ADP-glucose. La deuxième activité est une glycogène synthase qui catalyse l'élongation des chaînes de α-1,4 glucanes, transférant le résidu glucose de la molécule de NDP-glucose sur l'extrémité non réductrice d'une chaîne linéaire. La voie alternative est, quant à elle, spécifique aux bactéries (panneau de droite). Moins étudiée mais néanmoins répandue parmi la plupart des phylums bactériens, la voie GlgE repose sur 3 activités enzymatiques. Le point d'entrée de cette voie est le tréhalose, qui est converti de manière réversible en maltose par la tréhalose synthase TreS. Ensuite, le maltose est phosphorylé par la maltokinase Mak en maltose-1-phosphate, substrat de l'activité d'élongation. La maltosyltransférase GlgE transfère finalement le résidu maltosyl du maltose-1-phosphate sur l'extrémité non réductrice d'une chaîne linéaire de glucose. Les deux voies finissent par partager une étape commune : l'insertion de points de branchements (liaisons α-1,6) par une enzyme de branchement (GlgB).

I-B. Les *Chlamydiae*

Les *Planctomycetes*, les *Verrucomicrobia* et les *Chlamydiae* forment un groupe monophylétique très ancien et phylogénétiquement éloigné des autres eubactéries (Fuerst, 2013). Un regain d'intérêt s'est récemment porté sur l'embranchement des *Chlamydiae*. En effet, un nombre croissant d'indices phylogénétiques et fonctionnels suggère que les *Chlamydiae* auraient contribué à l'établissement de l'endosymbiose primaire du plaste ; un évènement unique et fondateur des cellules eucaryotes photosynthétiques (algues vertes/plantes, algues rouges et Glaucophytes, regroupés sous le terme d'*Archaeplastida*). Résumé dans la théorie du « ménage à trois », ce modèle propose que les *Chlamydiae* auraient facilité l'établissement du lien symbiotique entre la cyanobactérie ancestrale et la cellule hôte notamment par l'intermédiaire du métabolisme des polysaccharides de réserve (Facchinelli *et al.*, 2013 ; Ball *et al.*, 2015).

Les progrès techniques réalisés dans la détection des *Chlamydiae* révèlent une étonnante diversité au sein de cet embranchement. Ainsi, à la famille des *Chlamydiaceae,* la première décrite, s'est ajoutée quinze autres familles : les *Parachlamydiaceae*, *Waddliaceae*, *Criblamydiaceae*, *Simkaniaceae*, *Rhabdochlamydiaceae, Candidatus* Parilichlamydiaceae, *Ca.* Novochlamydiaceae, *Ca.* Pelagichlamydiaceae, *Ca.* Enkichlamydiaceae, *Ca.* Limichlamydiaceae, *Ca.* Arenachlamydiaceae, *Ca*. Kinetochlamydiaceae, *Ca.* Clavichlamydiaceae, *Ca*. Piscichlamydiaceae and *Ca*. Motilichlamydiaceae. Ces bactéries sont responsables de maladies chez les mammifères, les poissons, les invertébrés et elles représentent également des agents pathogènes pour la plupart des amibes. Leur pathogénicité s'explique par une étape de vie obligatoire au sein d'une cellule eucaryote, suivie d'une sortie entrainant généralement la mort de l'hôte par lyse cellulaire.

La réduction du génome des *Chlamydiae* due au mode de vie intracellulaire (Henrissat *et al.*, 2002) entraine *de facto* des incapacités métaboliques qui sont plus particulièrement prononcées chez les *Chlamydiaceae*, ultraspécialisées pour infecter une ou quelques espèces de vertébrés, que chez les autres familles de *Chlamydiae*. Ces autres familles, regroupées sous le terme de *Chlamydiae* environnementales, car essentiellement isolées à partir de prélèvements environnementaux, ont quant à elles un spectre d'hôtes plus large. (Omsland *et al.*, 2014). Toutefois, s'il existe des différences entre les *Chlamydiaceae* et les *Chlamydiae* environnementales, toutes les *Chlamydiae* sont des parasites énergétiques qui importent, *via* des transporteurs spécifiques, des nucléotides (comme l'ATP), des acides aminés, et du carbone sous la forme de glucose-6-phosphate, en provenance de la cellule infectée. De plus, la vie intracellulaire obligatoire des *Chlamydiae* s'accompagne par la sécrétion dans le cytosol de la cellule hôte de nombreux effecteurs de virulence, dont font partie les enzymes du métabolisme du glycogène, par le biais du système de sécrétion de type III. Il est intéressant de noter que contrairement aux autres bactéries pathogènes ou

symbiotiques intracellulaires qui ont également subi une réduction de leur génome, le métabolisme du glycogène fut maintenu chez les *Chlamydiae* (Henrissat *et al.*, 2002).

I-C. Le métabolisme du glycogène chez les *Chlamydiae*

La compréhension de la synthèse du glycogène chez les *Chlamydiae* porte essentiellement sur des études menées sur les *Chlamydiaceae* et plus particulièrement sur *C. trachomatis*. Cet agent pathogène de l'Homme infecte les cellules épithéliales, ce qui entraine une suraccumulation de glycogène dans la cellule infectée qui peut être visualisée en colorant un frottis avec une solution d'iode. Cette méthode est d'ailleurs utilisée pour diagnostiquer les chlamydioses chez l'Homme. La dérégulation du métabolisme du glycogène de la cellule hôte passe par la sécrétion des enzymes chlamydiennes de biosynthèse et de dégradation du glycogène dans le cytosol de la cellule hôte *via* le système de sécrétion de type III.

En cas d'infection à *C. trachomatis*, la synthèse de glycogène se produit à la fois dans le cytosol de la bactérie, dans la lumière de la vésicule parasitophore (également appelée inclusion) qui contient les *Chlamydiae* et dans le cytosol de la cellule infectée. L'objectif serait pour les *Chlamydiae* de déréguler la synthèse de glycogène de l'hôte et d'importer du carbone sous la forme de glucose-6-phosphate, mais également sous forme de malto-oligosaccharides que la cellule eucaryote ne peut pas métaboliser. Alors que les *Chlamydiae* environnementales sécrètent l'ADP-glucose pyrophosphorylase (GlgC) afin de produire de l'ADP-glucose requis à l'activité glycogène synthase (GlgA), également sécrétée, *Chlamydia trachomatis* sécrète toutes ses enzymes du métabolisme du glycogène à l'exception de GlgC (Gehre *et al.*, 2016). Ce résultat, à première vue surprenant, s'explique d'une part par le recrutement d'un transporteur de nucléotides-sucres (SLC35D2) de l'hôte au niveau de la membrane d'inclusion qui permet d'importer l'UDP-glucose de l'hôte, et d'autre part par la capacité de GlgA de *C. trachomatis* à utiliser à la fois l'ADP-glucose et l'UDP-glucose pour allonger les chaînes de glucose (Gehre *et al.*, 2016). Ainsi, même en absence de sécrétion de GlgC au sein de l'inclusion, la synthèse de glycogène peut se dérouler grâce à l'import de l'UDP-glucose et à son intégration au sein de la particule de glycogène par GlgA.

I-D. L'acétylation des protéines chez les bactéries

Durant leur vie, les bactéries doivent s'adapter à de rapides changements de leur environnement pour ne pas périr. Une stratégie permet de répondre rapidement aux variations d'environnement, tout en consommant peu d'énergie : la modification de protéines préexistantes, également appelée modification post-traductionnelle (Christensen *et al.*, 2019a). Alors que plus de 600 types de modifications post-traductionnelles ont été identifiées à ce jour, on retrouve parmi les plus courantes la phosphorylation, l'ubiquitination, ou encore l'acétylation. Deux types d'acétylation existent : l'acétylation N-terminale des protéines (ou N^{α} acétylation), et l'acétylation des lysines sur leur groupement ε (ou N^{ε} acétylation) (Drazic *et al.*, 2016; Soppa, 2010), cette dernière étant plus commune chez les bactéries. La N^{ε} acétylation, tout comme les autres modifications post-traductionnelles, peut influer sur de

nombreuses propriétés d'une protéine, comme sur son activité enzymatique, son repliement, sa stabilité, sa localisation, voire même sur son interaction avec d'autres protéines.

Le mécanisme d'acétylation des lysines fut originellement découvert sur les histones, où il permet de réguler de manière réversible la transcription de nombreux gènes en influant sur la compaction de la chromatine (Fischer *et al.*, 1959). Depuis, de nombreuses autres cibles de N^{ε} acétylation ont été mises en évidence, notamment chez les bactéries, et les protéines impliquées dans leur acétylation sont appelées lysine acétyltransférases. Cette modification post-traductionnelle est réversible, grâce à des enzymes permettant de cliver les résidus acétyles, nommées lysine déacétylases. Chez les bactéries, en plus de l'acétylation catalysée par les lysine acétyltransférases, qui utilisent l'acétyl-coenzyme A comme cofacteur, il existe deux mécanismes d'acétylation non enzymatiques, basés sur le transfert d'un groupement acétyle, soit d'une molécule d'acétyl-coenzyme A, soit de phosphate d'acétyle, sur un résidu lysine (Ramponi *et al.*, 1975). Il est intéressant de noter que ces trois mécanismes de N^{ε} acétylation, enzymatique ou non-enzymatiques, ciblent chacun des protéines différentes, mais également des résidus lysine différents au sein de la même protéine (Baeza *et al.*, 2015).

II. Résultats

II-A. État de l'art du métabolisme du glycogène dans le phylum des *Chlamydiae*

Depuis de nombreuses années, mon laboratoire d'accueil s'intéresse au rôle des *Chlamydiae* dans l'établissement de l'endosymbiose primaire du plaste. Lors de cet événement unique, survenu il y a environ 1,5 milliards d'années, un eucaryote phagotrophe a internalisé une cyanobactérie et a établi avec elle une relation symbiotique, aboutissant à l'émergence de la photosynthèse eucaryote. Suite à cet évènement symbiotique, trois lignées ont divergé, regroupées sous le nom d'Archaeplastida : les glaucophytes (composés d'algues unicellulaires) ; les algues rouges ou *Rhodophyceae* ; et les *Chloroplastida* dans lesquels on retrouve les algues vertes et l'ensemble des plantes terrestres. Cet intérêt a conduit mon laboratoire à formuler l'hypothèse du ménage à trois, hypothèse selon laquelle la présence d'une *Chlamydiae* ancestrale aurait facilité la mise en place rapide d'un lien symbiotique, notamment grâce au métabolisme des polysaccharides de réserve, entre le cyanobionte et l'eucaryote hétérotrophe ancestraux (Ball *et al.*, 2011). Dans ce contexte, un intérêt tout particulier a été porté sur les enzymes du métabolisme du glycogène des *Chlamydiae*, ce qui permit de démontrer un transfert des gènes chlamydiens *glgA* et *glgX*, codant respectivement pour une glycogène synthase et une enzyme de débranchement directe, à l'ancêtre des *Archaeplastida* (Ball *et al.*, 2011, 2015; Facchinelli *et al.*, 2013). Cependant, durant cette étude du métabolisme du glycogène chez les *Chlamydiae*, nous nous sommes aperçus d'une particularité au sein des familles des *Waddliaceae* (*Waddlia chondrophila*) et des *Criblamydiaceae* (*Estrella lausannensis* et *Criblamydia sequanensis*) : aucun gène codant pour une ADP-glucose pyrophosphorylase (*glgC*) n'est détecté au sein de leur génome. De plus, leurs gènes *glgA* et *glgB*, codant respectivement pour une glycogène synthase et une

enzyme de branchement, sont fusionnés, avec la présence d'un codon stop prématuré dans la partie *glgA* de ce gène de fusion chez *E. lausannensis*. Alors que, malgré la réduction de leur génome lié au mode de vie intracellulaire obligatoire, toutes les espèces de *Chlamydiae* ont conservé un métabolisme du glycogène fonctionnel, les *Waddliaceae* et *Criblamydiaceae* semblent faire exception à la règle. Cependant, des observations au microscope électronique à transmission de coupes ultrafines colorées au PATAg (coloration spécifique des polysaccharides) révèlent clairement l'accumulation de particules de glycogène dans le cytosol d'*E. lausannensis* et de *W. chondrophila*, suggérant la présence d'une voie alternative de synthèse de glycogène parmi ces deux familles.

Nous avons donc entrepris l'analyse de 220 génomes (disponibles sur https://chlamdb.ch/), issus de 47 espèces et représentant la diversité du phylum des *Chlamydiae* connues à ce jour. Cette analyse a permis de confirmer la présence de la voie GlgC chez toutes les espèces chlamydiennes, à l'exception des *Waddliaceae* et *Criblamydiaceae*. De plus, un opéron codant pour la voie GlgE (*glgE-treSmak-glgB2*) a été découvert chez *W. chondrophila*, *E. lausannensis*, *C. sequanensis*, mais également chez *Parachlamydia* sp. C2, *Protochlamydia naegleriophila* et *Protochlamydia massiliensis*. Ces trois dernières espèces ne possèdent cependant pas le gène *glgB2* (opéron *glgE-treSmak*), mais ont conservé le gène *glgB*, codant pour l'enzyme de branchement associée à la voie GlgC. La voie GlgE ainsi découverte est décrite comme permettant la synthèse de glycogène à partir de tréhalose, en utilisant le maltose-1-phosphate (M1P) comme métabolite intermédiaire.

Afin d'avoir un aperçu de l'origine de l'opéron GlgE chez les *Chlamydiae*, une analyse phylogénétique a été réalisée sur les séquences protéiques de GlgE et de TreS-Mak. Celle-ci a permis de déterminer que la voie GlgE est monophylétique chez les *Chlamydiae*, suggérant que l'ancêtre commun des familles des *Criblamydiaceae*, *Waddliaceae* et des *Parachlamydiaceae* possédait cet opéron. De plus, la phylogénie de GlgE indique que deux classes de GlgE existent parmi les bactéries. Comme les maltosyltransférases actinobactériennes, les seules caractérisées jusqu'à présent, et les GlgE chlamydiennes appartiennent respectivement aux classes II et I, nous avons décidé d'entreprendre la caractérisation des GlgE chlamydiennes afin de (i) vérifier qu'elles possèdent bien l'activité maltosyltransférase mais également (ii) déterminer si elles possèdent des particularités fonctionnelles différant des GlgE de classe II.

II-B. Caractérisation des homologues de GlgE d'*E. lausannensis* et de *W. chondrophila*

Les gènes annotés comme GlgE d'*E. lausannensis* et de *W. chondrophila* ont été clonés puis exprimés chez *E. coli*. Après purification des protéines recombinantes, nous avons tout d'abord entrepris de démontrer que ces enzymes portent une activité maltosyltransférase. L'activité maltosyltransférase de GlgE étant réversible, elle peut, en plus d'allonger des α-glucanes, les dégrader en présence d'orthophosphate pour produire du M1P (Kalscheuer *et*

al., 2010). Nous avons pu montrer que les GlgE recombinantes sont capables de dégrader des α-glucanes en présence d'orthophosphate, libérant ainsi un composé que nous avons analysé par (i) déphosphorylation à la phosphatase alcaline, (ii) spectrométrie de masse et (iii) résonance magnétique nucléaire du proton, afin de démontrer qu'il s'agisse d'α-maltose-1-phosphate. Le M1P ainsi produit a permis de poursuivre la caractérisation des GlgE chlamydiennes dans l'autre sens réactionnel, c'est-à-dire l'élongation des α-glucanes, démontrant ainsi qu'elles possèdent bel et bien une activité maltosyltransférase.

La détermination des paramètres cinétiques de la GlgE d'*Estrella lausannensis* nous a permis de confirmer que cette enzyme est efficace pour allonger les α-glucanes. En plus de leur activité maltosyltransférase réversible, les GlgE d'*E. lausannensis* et de *W. chondrophila* possèdent une activité annexe qui permet de disproportionner les malto-oligosaccharides composés d'au moins six résidus de glucose par le transfert de groupements maltosyl d'une chaîne de glucoses à une autre. L'activité d'élongation est quant à elle possible sur des malto-oligosaccharides composés d'au moins quatre résidus de glucose, avec néanmoins une plus grande efficacité sur le maltohexaose et les malto-oligosaccharides plus longs. De manière intéressante, en présence de malto-oligosaccharides plus courts (glucose, maltose, maltotriose), voire uniquement avec du M1P, les GlgE chlamydiennes sont capables d'initier la synthèse de longues chaînes qui possèdent jusqu'à 32 résidus de glucose. Les maltosyltransférases d'*E. lausannensis* et de *W. chondrophila* semblent donc, à l'instar de la glycogène synthase GlgA dans la voie GlgC, capables d'initier la synthèse de glycogène en absence d'amorce de malto-oligosaccharides. Cette caractéristique a été confirmée par la synthèse *in vitro* d'un α-polysaccharide branché de haute masse, uniquement à partir de M1P incubé en présence de la GlgE d'*E. lausannensis* et de l'enzyme de branchement de *W. chondrophila*.

Ainsi, nous avons pu démontrer que les protéines recombinantes d'*E. lausannensis* et de *W. chondrophila*, annotées comme GlgE, sont fonctionnelles et possèdent une activité maltosyltransférase. Ces enzymes sont capables d'allonger des malto-oligosaccharides existants avec une activité distributive, mais également d'initier leur synthèse *de novo* avec une activité qui semble processive, afin de produire du glycogène en coopération avec l'enzyme de branchement.

Nous nous sommes ensuite demandé si la voie GlgE est pleinement fonctionnelle chez *E. lausannensis*, c'est-à-dire si TreS-Mak synthétise le M1P requis à l'activité maltosyltransferase de GlgE.

II-C. Caractérisation de la protéine TreS-Mak d'*E. lausannensis*

Le clonage du gène *treS-mak* d'*E. lausannensis* pour son expression dans *E. coli* a permis de montrer indirectement que cette enzyme est capable de synthétiser du M1P à partir de tréhalose. En effet, l'accumulation de M1P est toxique chez les bactéries (Kalscheuer *et al.*,

2010), et l'expression basale de la TreS-Mak d'*E. lausannensis* dans une souche Rosetta d'*E. coli* a empêché la formation de colonies dans des conditions permettant la synthèse endogène de tréhalose. Deux méthodes ont permis de contourner cette toxicité. Premièrement, l'utilisation d'une souche d'*E. coli* BL21 AI, qui permet de diminuer la transcription basale des gènes recombinants, nous a permis d'obtenir de nombreuses colonies, démontrant ainsi que la toxicité est liée à l'expression de TreS-Mak. Deuxièmement, sachant que la synthèse de tréhalose chez *E. coli* est induite en cas de stress osmotique, nous avons décidé d'utiliser un milieu de culture dépourvu de sel (Terrific Broth) à la place du LB utilisé précédemment, qui contient quant à lui 170 mM de NaCl, pour exprimer TreS-Mak. Là encore, de nombreuses colonies furent obtenues, montrant que la toxicité induite par l'expression de TreS-Mak est liée à la présence de tréhalose endogène.

Nous avons par la suite exprimé et purifié TreS-Mak afin de caractériser chacune des deux activités qu'elle porte. Premièrement, le domaine maltokinase est fonctionnel, puisque la TreS-Mak d'*E. lausannensis* catalyse la phosphorylation du maltose en M1P en utilisant un nucléotide triphosphate (NTP) comme donneur de groupement phosphate. Nous avons déterminé que son NTP préférentiel est l'ATP, même si l'UTP et le GTP permettent de garder un bon niveau d'activité. En revanche, le CTP s'avère être un donneur de phosphate très peu efficace. Comme la plupart des phosphotransférases, l'activité maltokinase nécessite la présence d'un cation divalent pour stabiliser le donneur de phosphate et être active. Dans le cas des maltokinases, le Mg^{2+} est généralement le meilleur activateur (Mendes *et al.*, 2010). Cependant, pour la TreS-Mak d'*E. lausannensis*, le meilleur activateur s'est avéré être, de loin, le Mn^{2+}.

Nous avons ensuite montré que l'activité tréhalose synthase de la TreS-Mak d'*E. lausannensis* est également fonctionnelle et catalyse la conversion du tréhalose en maltose, tout en relâchant une faible quantité de glucose libre. Cette activité est néanmoins partiellement inhibée par de fortes concentrations d'ATP et de Mn^{2+}, ce qui est étonnant étant donné que ce sont les substrats préférentiels de l'activité maltokinase. Néanmoins, ce résultat permet de confirmer que la voie GlgE est fonctionnelle chez *E. lausannensis* et permet de synthétiser du glycogène à partir du tréhalose et de NTP.

II-D. Reconstruction de la voie métabolique complète associée à GlgE et permettant la synthèse de glycogène chez les *Chlamydiae*

Alors que la voie GlgE nécessite la présence de tréhalose, aucune trace de gène codant un transporteur de tréhalose n'a été trouvé dans les génomes chlamydiens. En revanche, au moins une voie métabolique permettant de synthétiser du tréhalose est retrouvée chez chacune des espèces possédant la voie GlgE. De plus, la majorité des *Chlamydiae* environnementales semblent capables de synthétiser du tréhalose, à l'inverse des *Chlamydiaceae* qui en semblent incapables. La voie de synthèse du tréhalose chez les *Criblamydiaceae* et les *Waddliaceae* repose sur deux activités enzymatiques : la tréhalose-6-

phosphate synthase OtsA qui catalyse la synthèse de tréhalose-6-phosphate à partir de glucose-6-phosphate et d'un nucléotide-sucre, et la tréhalose-6-phosphate phosphatase OtsB qui déphosphoryle le tréhalose-6-phosphate en tréhalose (Strøm and Kaasen, 1993). Nous avons également trouvé dans ces 2 familles la présence d'une UDP-glucose pyrophosphorylase homologue de UGP3 chez les plantes (Okazaki *et al.*, 2009). Nous supposons qu'UGP3 permet d'alimenter OtsA en UDP-glucose afin de synthétiser du tréhalose par cette voie. La présence d'UGP3, limitée à quelques espèces de *Chlamydiae* environnementales et aux *Archaeplastida*, suggère qu'un transfert horizontal de gène ancien a eu lieu entre ces deux phylums.

Chez les trois espèces de *Parachlamydiaceae* qui possèdent les deux voies de synthèse du glycogène (GlgC et GlgE), des activités enzymatiques autres que OtsA et OtsB permettent de synthétiser le tréhalose : la maltooligosyl tréhalose synthase TreY convertit la liaison α-1,4 à l'extrémité non-réductrice d'un malto-oligosaccharides en liaison α,α-1,1, formant ainsi un maltooligosyl tréhalose. La maltooligosyl tréhalose tréhalohydrolase TreZ clive ensuite le résidu tréhalose afin de le libérer. Cette voie de synthèse du tréhalose a donc au préalable besoin, *ad minima*, de malto-oligosaccharides, ou de particules de glycogène. Ces derniers pouvant être synthétisés par la voie GlgC, on peut supposer que TreY et TreZ permettent de créer un lien entre les deux voies métaboliques de synthèse du glycogène chez les *Parachlamydiaceae*.

De par leur caractère intracellulaire obligatoire, les *Chlamydiae* possèdent également de nombreux transporteurs afin de détourner de nombreuses voies métaboliques de leur hôte. Parmi les transporteurs chlamydiens utiles pour la synthèse du glycogène reposant sur GlgE, on retrouve UhpC, qui permet d'importer du glucose-6-phosphate, divers transporteurs de nucléotides triphosphates NTT qui permettent d'importer l'ATP, le GTP et/ou l'UTP nécessaires aux activités UGP3 et maltokinase, et également des protéines importatrices de manganèse, nécessaire à l'activité maltokinase.

De plus, il est important de rappeler que les *Chlamydiae* sécrètent la majorité de leurs enzymes impliquées dans la synthèse et la dégradation du glycogène au sein de la cellule hôte par le système de sécrétion de type III afin de détourner des voies métaboliques à son avantage (Kadouche, 2016). En utilisant le système de sécrétion hétérologue *Shigella flexneri*, nous avons pu montrer que les enzymes GlgE et TreS-Mak d'*E. lausannensis* et de *W. chondrophila* portent un signal de sécrétion par le système de sécrétion de type III. Nous préférons cependant décrire cette sécrétion comme potentielle, en attente d'une preuve de leur sécrétion *in situ*.

Grâce à tous ces résultats, nous avons résumé le métabolisme du glycogène retrouvé chez les *Criblamydiaceae* et les *Waddliaceae* sur la Figure R2.

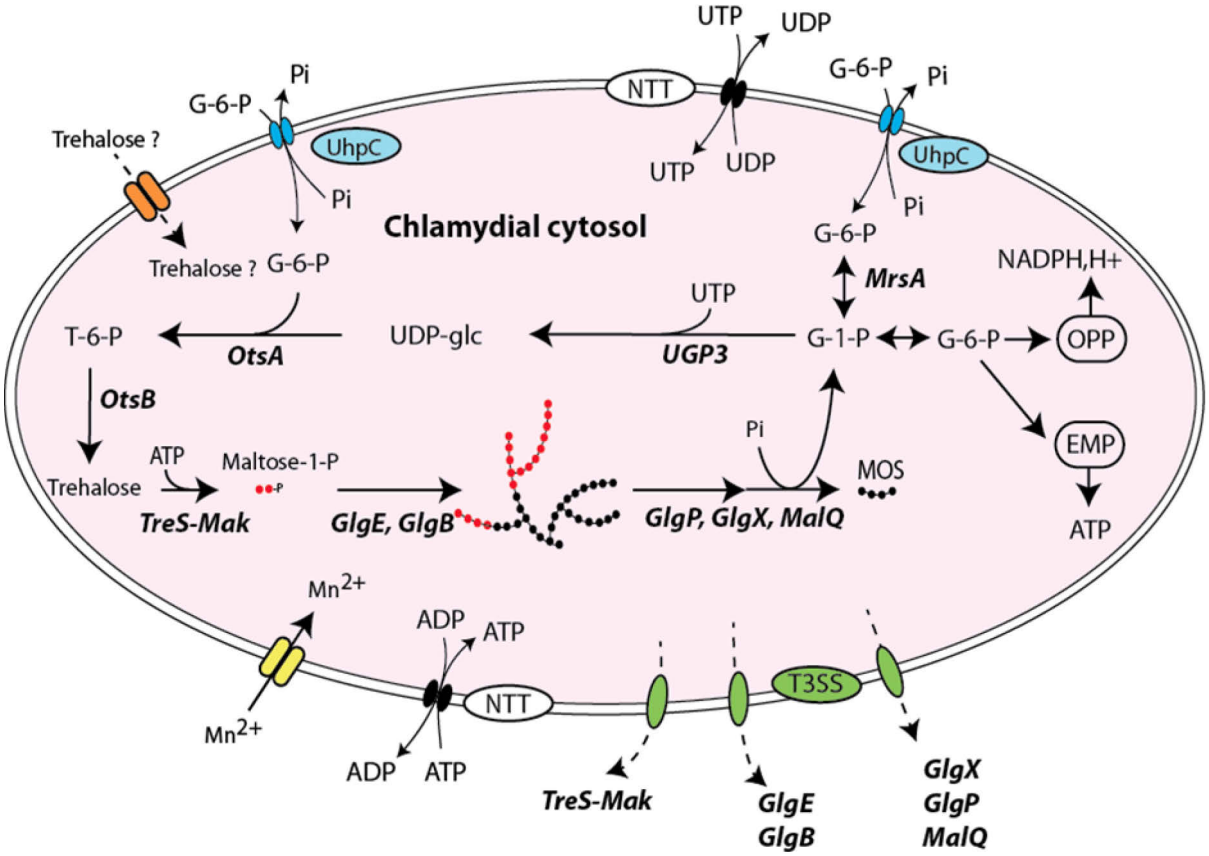

Figure R 2 : Réseau métabolique permettant la synthèse du glycogène dans les familles des *Waddliaceae* et des *Criblamydiaceae*.

Le glucose-6-phosphate (G-6-P) et les nucléotides triphosphates UTP et ATP sont importés dans le cytosol de la *Chlamydiae via* les transporteurs UhpC et NTT. La première étape de la synthèse du glycogène consiste en l'isomérisation du glucose-6-phosphate (G-6-P) en glucose-1-phosphate (G-1-P) par l'activité phosphoglucomutase (MrsA). L'UDP-glucose pyrophosphorylase (UGP3) synthétise l'UDP-glucose à partir de G-1-P et UTP. La tréhalose-6-phosphate synthase (OtsA) et la tréhalose-6-phosphate phosphatase (OtsB) convertissent le nucléotide-sucre et le G-6-P en tréhalose. L'activité bifonctionnelle TreS-Mak fournit le maltose-1-phosphate (M1P) nécessaire à l'activité maltosyltransférase (GlgE). GlgE, de part ses capacités d'initiation et d'élongation des α-glucanes, permet la synthèse d'un α-polysaccharide constitué de liaisons α-1,4 et α-1,6, le glycogène, en coopération avec l'enzyme de branchement (GlgB). L'action synergique de la glycogène phosphorylase (GlgP), de l'enzyme de débranchement (GlgX) et de la 4-α glucanotransférase (MalQ) permet de dépolymériser le glycogène en G-1-P et en courts malto-oligosaccharides (MOS). Le G-1-P alimente à la fois la voie oxydative des pentoses phosphates (OPP) et la voie d'Embden-Meyerhof-Parnas (EMP) qui fournissent aux formes extracellulaires (corps élémentaires) des composés réduits (NADPH, H +) et de l'ATP, respectivement. Les cations divalents Mn^{2+} nécessaires à l'activité TreS-Mak sont probablement importés via le transporteur ABC composé des 3 sous-unités MntA, MntB et MntC identifiées dans les génomes chlamydiens. Les *Waddliaceae* et les *Criblamydiaceae* peuvent manipuler le pool de carbone de l'hôte en absorbant le tréhalose via un transporteur de disaccharide putatif (flèche pointillée / orange) ou en sécrétant les enzymes du métabolisme du glycogène par le biais du système de sécrétion de type III (flèches pointillées / vertes).

II-E. La régulation de l'activité GlgE chez les *Chlamydiae*

Comme la voie de synthèse du glycogène GlgE utilise un intermédiaire toxique, le M1P, cette voie doit être finement régulée afin de ne pas provoquer la mort de la bactérie. De manière surprenante, jusqu'à présent, seule l'activité maltosyltransférase GlgE semble être la cible de mécanismes de régulations. Tout d'abord, chez *Corynebacterium glutamicum*, la transcription de l'opéron *glgE-glgB* augmente quand la bactérie est cultivée en présence de glucose

(Seibold *et al.*, 2011). Deuxièmement, chez *Mycobacterium tuberculosis*, GlgE est modifiée post-traductionnellement, la phosphorylation de résidus sérine et thréonine réduisant son activité (Leiba *et al.*, 2013). Dans cette étude, nous montrons que la GlgE d'*E. lausannensis* est la cible de modifications post-traductionnelles, plus précisément de N^{ε} acétylation sur les résidus lysine. Alors que l'acétylation des lysines est généralement liée à la réduction de l'activité enzymatique chez les bactéries, l'hyper-acétylation de la GlgE d'*E. lausannensis* augmente son activité.

Plus de vingt sites d'acétylation ont été identifiés sur la GlgE d'*E. lausannensis*, certains d'entre eux sur des lysines conservées parmi les maltosyltransférases chlamydiennes. La plupart de ces sites se trouvent également à proximité du site catalytique ou du domaine d'interaction pour la formation d'homodimère, suggérant l'importance fonctionnelle de ces sites.

Nous avons également montré que la GlgE recombinante d'*E. lausannensis* peut être acétylée *in vitro* par incubation avec de l'acétyl-coenzyme A, sans pourtant impacter son activité. Finalement, cette étude indique que la présence d'un métabolisme du glycogène fonctionnel dans la souche d'*E. coli* qui permet de sur-exprimer la GlgE d'*E. lausannensis* est essentielle pour que cette dernière soit hyper-acétylée et au maximum de son activité.

Pour finir cette étude, nous avons effectué une analyse du contenu en gènes associés au métabolisme de l'acétylation des protéines chez les *Chlamydiae*. Nous avons trouvé de nombreuses potentielles acétyltransférases, leur nombre étant bien plus élevé chez les *Chlamydiae* environnementales que chez les *Chlamydiaceae*. Cependant, seules quelques espèces semblent posséder une potentielle déacétylase, ce qui soulève des questions quant à la réversibilité de l'acétylation des lysines dans ces espèces. Parmi les acétyltransférases retrouvées dans le génome d'*E. lausannensis*, deux possèdent des homologues chez *E. coli* : PatZ et YafP. Si l'on suppose que l'acétylation de la GlgE d'*E. lausannensis* est médiée par voie enzymatique, ces deux enzymes sont de bons candidats. Cependant, *E. lausannensis*, comme la plupart des *Chlamydiae* environnementales possède les gènes nécessaires à la synthèse de phosphate d'acétyle, ce qui ne permet pas d'exclure que GlgE est acétylée, et donc régulée, de manière non-enzymatique par le phosphate d'acétyle.

III. Conclusion

L'ensemble de cette étude montre que les familles des *Waddliaceae* et des *Criblamydiaceae*, qu'on pensait incapables de synthétiser du glycogène dû à l'absence de gène encodant une ADP-glucose pyrophosphorylase, ont substitué la voie classique de synthèse de glycogène basée sur l'utilisation de nucléotides-sucres par la voie alternative GlgE basée sur l'utilisation de tréhalose. Durant cette étude, les différentes enzymes composant cette voie ont été caractérisées, permettant de mettre en lumière des particularités de cette voie jusqu'ici ignorées, telle que la capacité de GlgE à initier la synthèse de malto-oligosaccharides *de novo*. De plus, le métabolisme du tréhalose, jusqu'alors ignoré chez les *Chlamydiae*, semble

important chez les *Chlamydiae* environnementales aux vues de la conservation et de la redondance de ce métabolisme. Nous montrons également un mécanisme de régulation particulier de GlgE, qui est activée par acétylation des lysines. De manière surprenante, de nombreuses lysine acétyltransférases sont retrouvées dans les génomes chlamydiens, et notamment quelques-unes chez les *Chlamydiaceae*. Il serait intéressant d'étudier l'impact de ce système d'acétylation des protéines dans un contexte de vie intracellulaire obligatoire.

Finalement, avec l'ensemble de cette étude, nous démontrons que le métabolisme du glycogène est conservé chez toutes les *Chlamydiae,* sans exception, et ce malgré le processus de réduction du génome, soulignant ainsi une fonction essentielle et sous-estimée de ce polysaccharide de réserve. Nous proposons que le catabolisme du glycogène est essentiel chez les *Chlamydiae*, fournissant l'énergie nécessaire au maintien des fonctions métaboliques basales, qui sont indispensables à la survie et à la virulence des formes extracellulaires, également appelées corps élémentaires.

Table of contents

List of Figures

List of Tables

General introduction

I. Diversity and importance of storage polysaccharides

Maintaining energy status in response to a carbon-limiting environment is a key issue for any living organism. As a result, several compounds have emerged during the evolution to store energy and carbon temporarily. Polysaccharides are perhaps the most widely used energy-carbon storage compounds in all three domains of life. They are large carbohydrate molecules made of repetitions of one or few monosaccharides, mostly glucose moieties that may or may not be branched. They are divided in two main groups, α- and β-glucans, based on the type of glycosidic linkages: α-glucans, such as glycogen and starch, are glucose homopolymers linearly linked by α-1,4 and branched through α-1,6 glycosidic bonds. Glycogen is found in *Bacteria*, *Archaea* and most heterotrophic *Eucaryota* while starch is mostly restricted to *Archaeplastida*, organisms originated from primary plastid endosymbiosis as well as to some unicellular diazotrophic cyanobacteria (Suzuki *et al.*, 2013). β-glucans, such as paramylon or laminarin, are found in a large number of protists. For instance, laminarin made of β-1,3 glucose linkages is described in *Stramenopiles* (Becker *et al.*, 2020). In plants, other unusual storage polysaccharides exist, like the β-fructan inulin found in some cultivated plants (e.g. chicory or garlic)(Mystkowska *et al.*, 2018).

Despite their distinct physicochemical properties, storage polysaccharides share common features: (i) they are polymers with a high molecular weight reducing the internal osmotic pressure within cells compared to free glucose (Smith, 1985) (ii) they are synthesized when there is an excess of energy and (iii) they are catabolized when cells must maintain their energy homeostasis in absence of exogenous sources of carbon or energy.

Why are homopolymers of glucose so successful among living organisms? One reasonable hypothesis might be a co-evolution of storage polysaccharide metabolism pathway and central carbon metabolism that includes glycolytic pathways (Embden-Meyerhof-Parnas and Entner-Doudoroff pathways), TCA cycle and oxidative/reductive pentose phosphate pathways, which are universally found in eukaryotes, bacteria and archaea. By selecting a homopolymer of glucose as storage polysaccharide, living cells ensure an efficient way to store carbon with a minimal cost. It is noteworthy that physicochemical properties of storage polysaccharides have evolved in respect to cell physiology. In plants and unicellular diazotrophic cyanobacteria, large and semi-crystalline starch granules are synthesized during the day and broken down at night to fuel the cell. This contrasts with tiny water-soluble glycogen particles, which are synthesized or catabolized quickly depending on the needs of the cells.

In this introduction, our attention will be confined to the glycogen metabolism pathway in prokaryotic and heterotrophic cells. Other energy-carbon storage compounds such as starch, granulose, polyhydroxybutyrate, polyhydroxyalkanoate and polyphosphate will then be

omitted. However detailed reviews are available for those compounds (Albi and Serrano, 2016; Jendrossek and Pfeiffer, 2014). The aim of this introduction is to provide an overview of glycogen pathways in prokaryotes and to some extent in heterotrophic eukaryotic cells, which have converged to form the same storage polysaccharide: glycogen.

II. Glycogen: the most widespread storage polysaccharide

II-A. Structural organization of glycogen: the most widespread storage polysaccharide

First isolated by Claude Bernard in the 1850's, glycogen is a water-soluble polysaccharide (Bernard, 1857). It consists of linear chains (D-glucose bound through α-1,4 linkages) that adopt a helical structure with an average chain length of 8-15 glucose depending on the organism. Every chain with the exception of external ones, harbours two α-1,6 bonds or branching points that account for 7-10% of the glycosidic linkage (Ball *et al.*, 2011; Shearer and Graham, 2002). Inside the glycogen particle, the inner branched chains, called B-chains, are uniformly distributed to form concentric tiers (Figure 1). This branching pattern enables the spherical growth of the glycogen β-particle with an increase in chain density that doubles in each tier. Each successive tier is then more crowded, leading to a theoretical maximum size of 12 tiers due to steric hindrance. According to mathematical modelling, peripheral chains, called A-chains, cannot be enzymatically proceed by branching enzymes and therefore remain unbranched (Meléndez *et al.* 1998). This leads to a theoretical maximum size of 42 nm for the hydrosoluble glycogen β-particle, corresponding to approximately 55 000 glucose units and 1.10^7 Da (Meléndez *et al.* 1997; Prats *et al.* 2018; Cifuente *et al.* 2019). Interestingly, according to mathematical modelling, A-chains that account for 36% of the total chains number, can be catabolized by glycogen phosphorylase, leading to the release of 19 000 glucose molecules in 20 seconds (Meléndez *et al.*, 1997). Hence this structure of 12 concentric tiers is also optimal for the glycogen particle function as it allows rapid remobilisation of glucose without the need for debranching activity (Ball *et al.*, 2011; Meléndez *et al.*, 1998).

In eukaryotic cells, glycogen particles do not entirely consist of carbohydrates, but are much more carbohydrate-protein complexes called glycosomes. Not to be confused with the organelles found in *Kinetoplastida* that share the same name (Opperdoes and Michels, 1993), these protein-glycogen complexes have been identified by electron microscopy in mammalian tissues, especially in the liver (Drochmans, 1962). So far, three levels of structure have been identified: γ-particles, small protein rich structures that are 3 nm wide ; β-particles, already mentioned in the paragraph above, with a mean diameter of 20-30 nm, serve as a rapid energy source and are very unlikely to reach the maximum diameter of 42 nm *in vivo* ; and α-particles, found in liver, constituted of β-particles linked through protein-protein disulfide bonds to form larger particles that can reach 300 nm in diameter (Prats *et al.*, 2018; Rybicka, 1996; Sullivan

et al., 2010). To date such 3-level protein-glycogen structures have not been described in *Bacteria*.

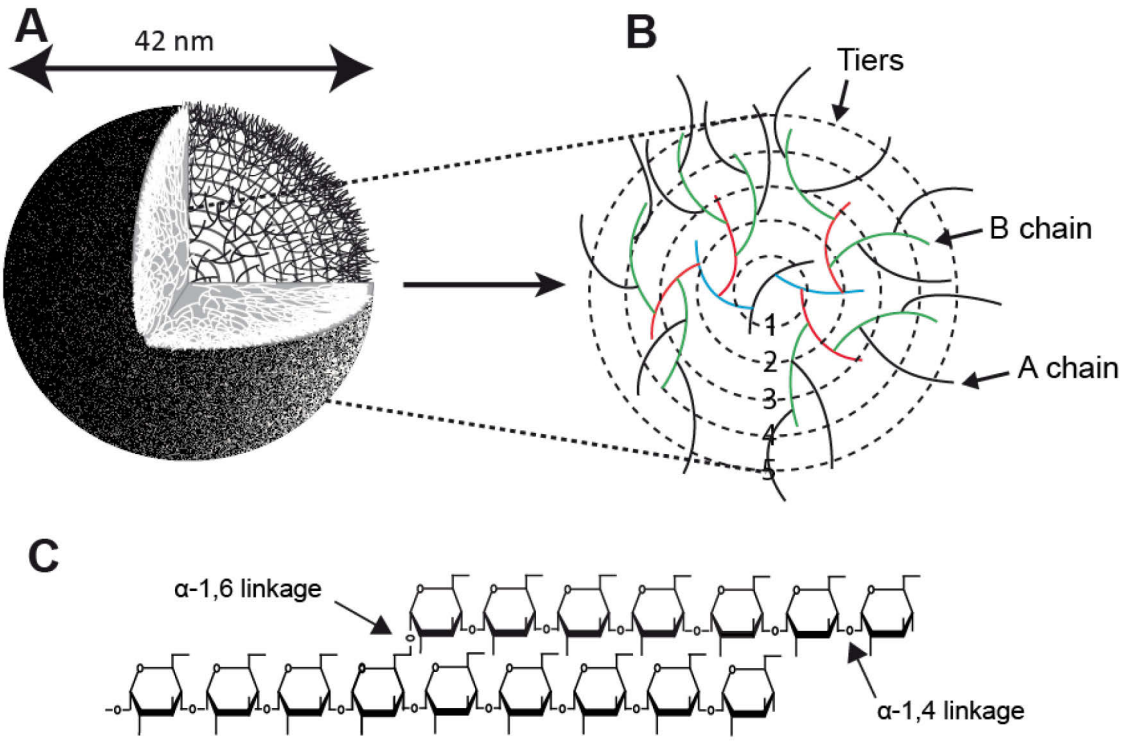

Figure 1: Schematic overview of the structure of a glycogen β-particle.
Inside a glycogen particle, (**A**) steric hindrance increases at each successive tier, resulting in a theoretical maximum size of 12 tiers for a glycogen β-particle, corresponding to a diameter of 42 nm. This increase in steric hindrance is explained by the particular branching pattern inside glycogen particles: (**B**) every chains with the exception of the most external ones (in black), called B chains, harbour two branching points, uniformly distributed to form concentric tiers (chains of the same colour are part of the same tier). Most external chains, called A chains, do not harbour any branching point and can therefore be proceed by enzymatic activities. (**C**) Like starch, glycogen is composed of linear chains of α-1,4 D-glucose, branched through α-1,6 linkages.

Another structural feature of glycogen that is often neglected is its phosphorylation. The first evidence of covalent bound phosphate to glycogen dates back to 1980 when it was shown that radiolabeled phosphate was incorporated into glycogen in rats and *Neurospora crassa* (Fontana, 1980). Since then, this particularity has been studied mainly in relation to Lafora disease (Gentry *et al.*, 2018; Roach, 2015). Humans with Lafora disease synthesize water-insoluble, aberrant glycogen inclusions with hyper-phosphorylated and longer glucose chains (Tagliabracci *et al.*, 2008). While the level of phosphorylation is 10 times higher in patient with Lafora disease, glycogen from a healthy person tends to be phosphorylated at around every 1000 glucose units, with 20% of phosphorylation on C6 and 80% on either C2 or C3 (Contreras *et al.*, 2016; Tagliabracci *et al.*, 2008, 2011). It is noteworthy that phosphorylation of glycogen is not specific to superior eukaryotes: C6 phosphorylation has been described in *E. coli* (Lorberth *et al.*, 1998; Viksø-Nielsen *et al.*, 2002). While mechanisms of glycogen phosphorylation and dephosphorylation begin to be fully understood in humans, they remain unexplained in bacteria, as does the function of the basal level of phosphorylation within the glycogen particles.

II-B. Convergent evolution of glycogen biosynthesis in living cells

Over the past decades, genomic comparison and functional approaches have largely contributed to a better understanding of glycogen biosynthesis in living organisms. The use of nucleotide-sugars as activated substrates predominates in both prokaryotic and eukaryotic cells. In addition, the alternative GlgE-pathway has been evidenced in bacteria and uses maltose-1-phosphate (M1P) as building blocks (Figure 2).

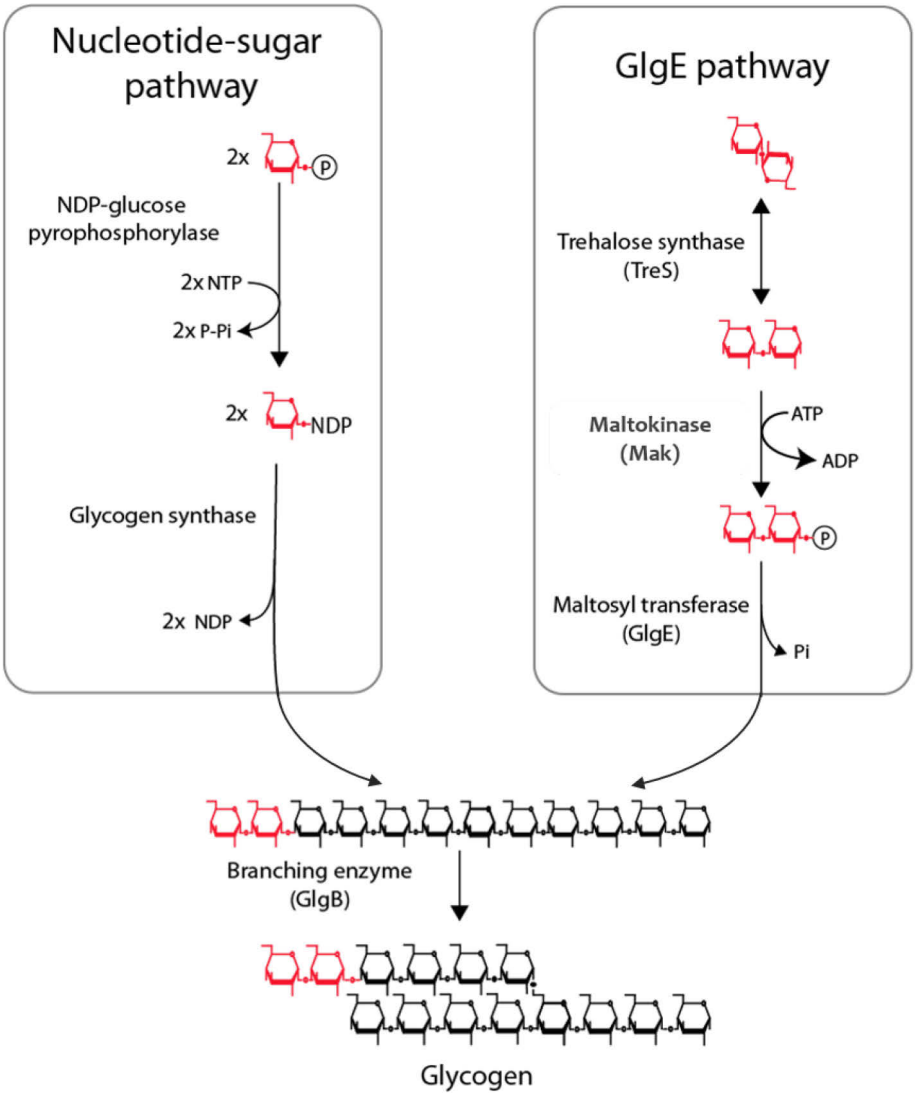

Figure 2 : Two metabolic routes lead to the synthesis of glycogen particles.
The most widespread pathway for the synthesis of glycogen is based on the use of nucleotide-sugar (left panel). This pathway relies on two enzymatic activities. First, an NDP-glucose pyrophosphorylase synthesizes NDP-sugars from NTPs and glucoses-1-phosphate. While heterotrophic eukaryotes only rely on UDP-glucose for the synthesis of glycogen, bacteria use ADP-glucose. Second activity involves a glycogen synthase that catalyses the elongation of α-1,4 glucose chains, transferring the glucose residue of the NDP-glucose molecule to the non-reducing end of a linear chain. The alternative pathway is, for its part, specific to bacteria (right panel). Less studied but nonetheless widespread among most bacterial phyla, GlgE-pathway relies on 3 enzymatic activities. The entry point of this pathway is trehalose, that is reversibly converted into maltose by trehalose synthase TreS. Then, maltose is phosphorylated by the maltokinase Mak into maltose-1-phosphate, the building block for the elongation activity. Maltosyltransferase GlgE finally transfers the maltosyl residue of maltose-1-phosphate onto the non-reducing end of a linear glucose chain. Both pathways end up by sharing a common step: the insertion of branching points by a branching enzyme.

II-B-1) Overview of nucleotide-sugar based Glycogen biosynthesis in Bacteria and Eucaryota

Glycogen synthesis relies on the production of an activated form of glucose: nucleoside-sugar (NDP-glucose). While ADP-glucose (adenosine diphospho-glucose) is the glycosyl donor for the synthesis of glycogen in *Bacteria*, this metabolite is not produced in heterotrophic eukaryotes and is substituted by UDP-glucose (uridine diphospho-glucose) (Ball *et al.*, 2011; Wilson *et al.*, 2010). These compounds are synthesized from α-D-glucose-1-phosphate (G1P) and ATP or UTP by enzymatic reactions catalysed by ATP:α-D-glucose-1-phosphate adenylyltransferase (E.C. 2.7.7.27) and UTP:α-D-glucose-1-phosphate uridylyltransferase (E.C. 2.7.7.9) respectively (Figure 2). As these enzymes generate pyrophosphate (PPi) in addition to NDP-glucose, they are commonly referred to as NTP-glucose pyrophosphorylases (Ballicora *et al.*, 2004; Turnquist *et al.*, 1974).

The elongation of malto-oligosaccharides is then catalysed by glycogen synthases (E.C. 2.4.1.21 with ADP-glucose; E.C. 2.4.1.11 with UDP-glucose). They transfer the glycosyl moiety from the NDP-glucose to the non-reducing end of a pre-existing malto-oligosaccharide to elongate it by one glucose unit (Preiss, 1984). During this process, one NDP is released as a by-product. These glycogen synthases, also known as α-1,4 glycosyltransferases, belong to 2 mains groups according to the CAZy classification: GT3 found in *Animalia* and *Fungi*, and GT5 in the other clades (Buschiazzo *et al.*, 2004; Coutinho *et al.*, 2003). The goal of these enzymatic activities is to generate long enough glucose chains that can serve as a substrate for the branching enzyme.

Branching enzymes (E.C. 2.4.1.18) are glycosylhydrolases that fall into two groups: GH13 and GH57 (Suzuki and Suzuki, 2016; Zhang *et al*., 2019). They catalyse a two-steps enzymatic reaction. First, they cleave an α-1,4 glucosidic bond of a donor malto-oligosaccharide. The oligo-maltosyl group attached to the enzyme is then transferred to the same chain or to another acceptor chain to form an α-1,6 bond or branching point (intra- or inter-chain branching, respectively).

Following these three common enzymatic steps in heterotrophic and prokaryotic cells, the product is a soluble and hyperbranched polysaccharide called glycogen. As my PhD work focused on glycogen biosynthesis in obligate intracellular bacteria, our attention will be mainly focused on the glycogen metabolizing enzymes in prokaryotes. However, since obligate intracellular bacteria tend to hijack the glycogen metabolism of their host, specificities of glycogen metabolizing enzymes of heterotrophic eukaryotes will be quickly overviewed.

II-B-2) ADP-glucose based glycogen biosynthesis in Bacteria

II-B-2(a) Genomic Organization and role of *glg* genes in E. coli

The glycogen metabolism in Bacteria is highly conserved and has been extensively studied in γ-proteobacteria and in particular in *Escherichia coli* (Cifuente *et al.*, 2019; Preiss, 2009). In

E. coli, genes involved in glycogen anabolism and catabolism pathways are clustered in a 15 kb long cluster, organized in two adjacent operons: BX and CAP (Almagro *et al.*, 2015; Preiss, 1984; Wilson *et al.*, 2010). BX operon is constituted of *glgB* and *glgX* genes, coding respectively for the branching enzyme (GlgB) and the debranching enzyme (GlgX). CAP operon encodes the ADP-glucose pyrophosphorylase (GlgC), the glycogen synthase (GlgA) and the glycogen phosphorylase (GlgP). It is noteworthy that glycogen-catabolizing enzymes, GlgP and GlgX, are coproduced with glycogen anabolizing enzymes. Both functions and regulation of GlgP and GlgX are described in the following section Glycogen catabolic pathway.

II-B-2(b) ADP-glucose pyrophosphorylase (GlgC) regulates the amount of glycogen in Bacteria

Bacteria uptake extracellular glucose *via* the carbohydrate phosphotransferase system (PTS). During this transport, glucose is phosphorylated into G6P, which is then transformed by Phosphoglucomutase (PGM) into G1P, one of the two substrates of GlgC. As previously mentioned, the glycogen synthesis in bacteria relies on ADP-glucose, a metabolite not synthesized by heterotrophic eukaryotes. While ADP-glucose is used in glycogen anabolism, but also in glycolipids and glucosylglycerol synthesis in cyanobacteria, GlgC is, to this day, the only known enzyme that supplies bacterial cells in ADP-glucose. While it was thought that the trehalose glucosyltransferase TreT catalyses the formation of ADP-glucose from trehalose and ADP in the archaea *Thermococcus literalis* (Qu *et al.* 2004), characterization of homologous enzymes from *Crenarchaeon Thermoproteus tenax* (Kouril *et al.*, 2008) and *Rubrobacter xylanophilus* (Nobre *et al.*, 2008) showed that this enzyme is physiologically involved in trehalose synthesis. To this day, only one species devoid of *glgC* gene has been shown to synthesize glycogen (Lou *et al.*, 1997). Indeed, *Prevotella bryantii* gene has replaced its endogenous *glgA* gene with a eukaryotic UDP-glucose-dependent glycogen synthase. Despite a large body of evidence showing that glycogen biosynthesis relies on ADP-glucose in most bacteria, the overexpression of endogenous GlgA in *ΔglgCAP E. coli* strain has shown that this strain produced normal amounts of both glycogen and ADP-glucose, suggesting the existence of another source of ADP-glucose (Morán-Zorzano *et al.*, 2007). It is supposed that the UDP-glucose pyrophosphorylase GalU is able to synthesize ADP-glucose in addition to its main activity of UDP-glucose production (Zea and Pohl, 2004). But further studies are needed to confirm this putative activity of GalU.

GlgC activity is tightly regulated at the transcriptional, post-transcriptional and protein levels. The secondary messengers ppGpp (guanosine 3'-bisphosphate 5'-bisphosphate) and CRP protein (cAMP receptor protein) activate the transcription of CAP operon while CsrA protein (Carbon storage regulator A) prevents the translation of *glgC* (Baker *et al.*, 2002; Romeo and Babitzke, 2018; Romeo *et al.*, 1993). In addition, GlgC activity is also regulated by allosteric activators and inhibitors. Depending on their susceptibility to various allosteric regulators, bacterial ADP-glucose pyrophosphorylases can be classified into 8 different groups (Ballicora

et al., 2003). In heterotrophic bacteria, the general scheme of regulation involves metabolic intermediates that reflect either high or low carbon and energy levels, with exception of GlgC from *Bacillus* spp., which are apparently unregulated (Takata *et al.*, 1997). This general scheme also involved a homotetrameric structure of GlgC, with exception of *Bacillus* spp. that form a heterotetramer with two GlgC and two GlgD, another isoform of ADP-glucose pyrophosphorylase. Allosteric activators of GlgC in heterotrophic bacteria are glycolytic intermediates, such as fructose-6-phosphate, fructose-1,6-bisphosphate and pyruvate. Depending on the bacterial origin of GlgC, several sets of metabolites serve as activators. Accumulation of these metabolites occurs in conditions of carbon excess in the medium and acts as sensor for GlgC activation and glycogen biosynthesis (Preiss, 2009). On the other hand, accumulation of low energy level metabolites, like ADP, AMP and orthophosphate (Pi), acts as inhibitors of GlgC activity and therefore as inhibitors of glycogen synthesis. In contrast, activation and inhibition of GlgC in cyanobacteria are only mediated by 3-phosphoglycerate (intermediate of reductive pentose phosphate pathway and of Calvin cycle) and Pi (Iglesias *et al.*, 1991).

II-B-2(c) GlgA initiates the synthesis of malto-oligosaccharides and elongates them

Although most prokaryotes have a *glgA* gene, cyanobacteria genomes encode two isoforms named *glgA1* and *glgA2* (Kadouche, 2016). Surprisingly, two cyanobacteria strains, *Cyanobacterium* sp. CLg1 and *Crocosphaera watsonii*, encode a third *glgA* gene, which is phylogenetically related to Granule Bound Starch Synthase (GBSS) of plants (Deschamps *et al.*, 2008). While it is known for a long time that bacterial glycogen synthase GlgA elongates existing malto-oligosaccharides at their non-reducing ends using ADP-glucose, the mechanism by which these malto-oligosaccharides were synthesized *de novo* remained elusive for a long time (Kawaguchi *et al.*, 1978). However, it has been shown that GlgA from *Agrobacterium tumefaciens* is capable of initiating the synthesis of the primer required for its elongation activity by auto-glycosylation (Ugalde *et al.*, 2003). GlgA catalyses its own glycosylation to form short malto-oligosaccharides of DP 2 (DP: degree of polymerisation; number of glucose units that compose the malto-oligosaccharide) to DP 9 that are then released and act as substrates for GlgA elongation activity (Cifuente *et al.*, 2019). This processive initiation capacity takes place in absence of available α-1,4 glucan. But with its very high affinity for malto-oligosaccharides, GlgA rapidly shifts its activity to a distributive elongation process when a sufficient concentration of glucan primers is reached. It is noteworthy that in contrast to GlgC, bacterial glycogen synthases do not undergo allosteric regulation.

II-B-2(d) GlgB is the last required step for glycogen synthesis

Following the elongation activity of GlgA, the last step of glycogen biosynthesis is catalysed by the branching enzymes GlgB that introduce branching points into the glycogen particle. They play a crucial role as they give a more compact structure to the glycogen particle while

increasing the number of accessible non-reducing ends for glucose storage and recovery. Branching enzymes from various organisms differ by the length of the transferred fragment (i.e., the branching pattern). For example, the GlgB from *E. coli* transfers small glucan segments, preferentially between DP 5 and DP 16 (Cifuente *et al.*, 2019). The length of the N-terminus region of GlgB also seems to influence the size of the malto-oligosaccharide transferred (Binderup *et al.*, 2002; Wang *et al.*, 2015), as truncations result in the transfer of longer chains (Devillers *et al.*, 2003). The rule appears to be that the longer this N-terminus region is, the shorter are the transferred chains.

GlgB is essential to glycogen biosynthesis as *ΔglgB* bacteria exhibit glycogen-less phenotype (Eydallin *et al.*, 2007a). To the contrary, overexpression of GlgB induces lower glycogen accumulation compared to wild type cells (Eydallin *et al.*, 2010). A sweet balance of GlgB expression is then needed to produce optimized glycogen particles.

It is noteworthy that most branching enzymes belong to the GH 13 family, that encompasses a large variety of enzymes (e.g., amylases, debranching enzymes, trehalose synthases). But some of them also belong to the GH 57 family and have been identified in archaea (Murakami *et al.*, 2006), cyanobacteria (Suzuki and Suzuki, 2016) and some bacteria, like *Petrotoga mobilis* and *Mycobacterium tuberculosis* that possess both GH 13 and GH 57 branching enzymes (Garg *et al.* 2007; Zhang *et al.* 2019b). To this day, the role of these GH 57 branching enzymes remains unclear, as deletion of the classical GH 13 branching enzyme in *M. tuberculosis* do not give a viable mutant (Sambou *et al.*, 2008).

II-B-3) Comparison between glycogen biosynthesis is Bacteria and heterotrophic Eukaryotes

In opisthokonts (previously named Metazoa/Fungi), the main difference in glycogen synthesis is the use of UDP-glucose instead of ADP-glucose as activated glucose. Because UDP-glucose, synthesized by UDP-glucose pyrophosphorylase is involved in many metabolic pathways (Ball *et al.*, 2011), the regulation of glycogen biosynthesis occurs at the second step of the metabolic pathway: the elongation of glucose chains by glycogen synthase. While no regulatory mechanism have been found in bacterial GT 5 glycogen synthase, opisthokonts harbour GT 3 glycogen synthases that are regulated by two mechanisms: (i) allosteric activation by G6P and (ii) inhibition by phosphorylation on Ser/Thr residues (Baskaran *et al.*, 2010; Roach and Larner, 1977; Roach *et al.*, 2012).

Another difference can be pointed out in the *de novo* synthesis of malto-oligosaccharide primers. Indeed, priming of glucose chain elongation involves glycogenin, a protein that has no homolog in the Bacteria domain. Glycogenin is a GT 8 that forms a homodimer and catalyses its autoglucosylation using UDP-glucose (Zeqiraj and Sicheri, 2015). Short α-glucans of 8 to 12 glucose residues are formed and remain covalently attached to glycogenin, even after elongation and branching by glycogen synthase and branching enzyme. Glycogenin is then found at the centre of the glycogen particle and was thought to be required

for glycogen biosynthesis (Cao *et al.*, 1993; Smythe and Cohen, 1992). However, a study has shown that some colonies of glycogenin knocked-out mutants of *Saccharomyces cerevisiae* were able to accumulate glycogen, suggesting a dispensable role of glycogenin for the biosynthesis of glycogen (Torija *et al.*, 2005). More recently, it has been shown that glycogenin KO mice not only are capable of synthesizing glycogen particles, but also accumulate larger amount of this polysaccharide without any protein remaining attached to the particle (Testoni *et al.*, 2017). Overall, these findings suggest that glycogenin may regulate both quantity and quality of glycogen by interacting with glycogen synthase (Oldfors, 2017). Indeed, the glycogenin deficiency in humans results in the accumulation of both glycogen and indigestible polyglucosans that are responsible for various pathologies, such as cardiomyopathy (Visuttijai *et al.*, 2019).

II-C. GlgE pathway is a fully functional alternative pathway for the synthesis of glycogen in Bacteria

II-C-1) Discovery of GlgE pathway

In order to identify new pharmaceutical targets against *Mycobacterium tuberculosis*, the etiologic agent of tuberculosis, a genetic forward approach using random mutagenesis was carried out to discover essential genes involved in the virulence (Sassetti *et al.*, 2003). Among them, the *glgE* gene was identified to be mandatory for the synthesis of glycogen. The first study was conducted on a temperature-sensitive mutant of GlgE in *Mycolicibacterium smegmatis* (Belanger and Hatfull, 1999), a non-pathogenic cousin of *M. tuberculosis* often used as a model organism in lab (Tyagi and Sharma, 2002). This mutant exhibits normal growth at low temperature (30°C), but rapidly stops growing at higher temperature (42°C), highlighting the essential function of GlgE in *M. smegmatis*. This phenomenon was correlated with a 17-fold increase in glycogen accumulation at 42°C, in comparison to the wild type strain. It was then proposed that GlgE was a hydrolytic enzyme (i.e. amylase), essential to breakdown glycogen particles and therefore to supply in energy the dividing Mycobacteria (Belanger and Hatfull, 1999). However in 2010, two independent research groups demonstrated that GlgE activity is implicated in the anabolism of glycogen and not, as expected, in its catabolism (Elbein *et al.*, 2010; Kalscheuer *et al.*, 2010).

II-C-2) Overview of GlgE-pathway

The novel glycogen biosynthetic pathway discovered in Mycobacteria, called GlgE pathway includes 4 enzymatic reactions (Figure 2). The first step consists in the conversion of trehalose into maltose by the trehalose synthase TreS. Maltose is then phosphorylated on the available C1 by the maltokinase Mak (also known as Pep2) to produce maltose-1-phosphate (M1P). The latter is the substrate of the α-1,4-glucan:maltose-1-phosphate maltosyltransferase GlgE that transfers the maltosyl moiety onto the non-reducing end of a glucan chain (Kalscheuer *et al.*, 2010). The last step of this pathway shares a common enzymatic activity with the classical GlgC-pathway, which consists in the formation of branching points by a branching enzyme.

In general, the four genes of this pathway are organized into one operon, as in *Streptomyces coelicolor* (Schneider *et al.*, 2000) or into two separate *treS-mak* and *glgE-glgB* clusters, as in *M. tuberculosis* (Chandra *et al.*, 2011). Until now, GlgE-pathway has been fairly deciphered in the *Actinobacteria* phylum with the main objective to discover new drugs against *M. tuberculosis*. A survey of 1045 bacterial genomes on the prevalence of glycogen pathways revealed that GlgE-pathway and GlgC-pathway are present, respectively, in 14% and 32 % of prokaryotes while 6% have both pathways (Chandra *et al.*, 2011). This suggests, on the one hand, that 60% of bacteria do not synthesize glycogen or use an alternative pathway and, on the other hand, that GlgE pathway is not specific to *Actinobacteria* and can be found in several different phyla, including *Proteobacteria*, *FCB group*, *Nitrospirae* or *PVC group*, and even in the *Archaea* superkingdom. It is important to remember that the model *E. coli* does not possess a GlgE pathway, which explains why it has been discovered decades after the GlgC-pathway.

The GlgE-pathway depends on the trehalose synthesis. As seen on Figure 2, the entry molecule for GlgE pathway, trehalose, is a non-reducing disaccharide composed of two glucose units bound through α,α-1,1 linkage. Trehalose is produced by all living organisms except vertebrate (Elbein, 1974). This stable and hydrosoluble molecule acts as a temperature and osmoprotectant, and can be synthesized through five different enzymatic pathways, all of them being present in the Bacteria superkingdom (Figure 3) (Paul *et al.*, 2008).

II-C-3) Different pathways for the synthesis of trehalose

II-C-3(a) The TreS pathway

The trehalose synthase (TreS) catalyses the reversible interconversion of maltose and trehalose. Various TreS homologs have been characterized and shown to be more effective in converting maltose into trehalose (Cai *et al.*, 2019; Gao *et al.*, 2013; Tsusaki *et al.*, 1996; Zhu *et al.*, 2010). However, in *M. tuberculosis*, TreS activity preferably converts trehalose into maltose (Pan *et al.*, 2004), suggesting a role of this enzyme in the synthesis of glycogen by GlgE pathway, which had been later confirmed by physiological studies on *M. smegmatis*.(Kalscheuer *et al.*, 2010).

II-C-3(b) The OtsA-OtsB pathway

The OtsA-OtsB pathway (Ots stands for osmoregulatory trehalose synthesis) is also known as TPS/TPP pathway. The trehalose-phosphate synthase (TPS) OtsA mediates the formation of trehalose-6-phosphate (T6P) by transferring the glucose moiety of NDP-glucose to G6P. Then, the trehalose-phosphate phosphatase (TPP) dephosphorylates the T6P into trehalose (Kaasen *et al.*, 1992). As its name suggests, expression of this pathway is induced by high

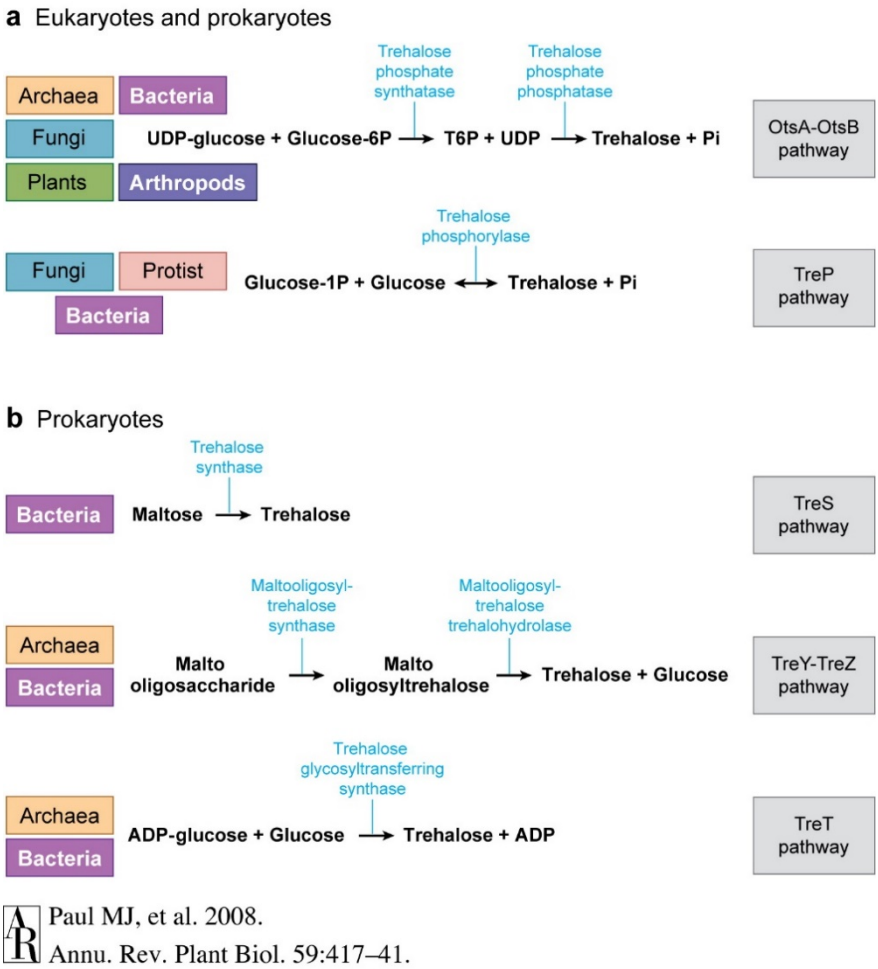

Figure 3 : (from Paul *et al.*, 2008) Metabolic pathways for the synthesis of trehalose.
While only 2 pathways (OtsA-OtsB and TreP) are known for the synthesis of trehalose in Eukaryotes (**a**), 3 additional pathways (TreS, TreY-TreZ, TreT) exist among Prokaryotes (**b**). UDP: uridine diphosphate, Glucose-6P: glucose-6-phosphate, T6P: trehalose-6-phosphate, Glucose-1P, glucose 1-phosphate, ADP: adenosine diphosphate.

osmotic stress in *E. coli*, and monovalent cations, such as K^+ and Na^+, significantly improve OtsA activity (Giaever *et al.*, 1988). The synthesis of trehalose by this pathway is mandatory for survival in a high osmolarity environment, as it was shown by mutant analysis, and can also serve as a way to store carbon and energy (Strøm and Kaasen, 1993). In *E. coli*, this pathway relies only on UDP-glucose production by GalU, as *galU* mutants are defective in trehalose synthesis and in resistance to osmotic stress (Giaever *et al.*, 1988). However, not all OtsA homologs use specifically UDP-glucose as nucleotide-sugar. For instance, OtsA of *M. tuberculosis* can transfer the glucose moiety from either UDP-glucose, GDP-glucose or ADP-glucose (Mendes *et al.*, 2019). In contrast OtsA activity of *Streptomyces venezuelae*, another GlgE pathway-possessing *Actinobacteria,* preferentially uses GDP-glucose (Asención Diez *et al.*, 2017). This pathway is largely found in Bacteria, Archaea and most Eukaryotes, including Fungi, Archaeplastida, Amoebozoa, with the exclusion of vertebrates (Paul *et al.*, 2008). Unexpectedly, TPS/TPP pathway seems to be involved in a variety of regulatory mechanisms in the yeast *S. cerevisiae*, such as the import of extracellular glucose or the glycolysis. Notably, it was hypothesised that TPS/TPP is useful to quickly regenerate

the orthophosphate depleted during the import of extracellular glucose, (Thevelein and Hohmann, 1995).

II-C-3(c) The TreY-TreZ pathway

This pathway involves the two enzymes TreY and TreZ (De Smet *et al.*, 2000). TreY is a maltooligosyl-trehalose synthase found in Bacteria (Nakada *et al.*, 1995) and Archaea (Nakada *et al.*, 1996) that catalyses an intramolecular transglycosylation reaction to convert the α-1,4 glucosidic bond at the non-reducing end of malto-oligosaccharides into α,α-1,1 linkage (Gueguen *et al.*, 2001; Zhao *et al.*, 2018). The maltooligosyl-trehalose (n glycosyl units) is further hydrolysed by maltooligosyl-trehalose trehalohydrolase TreZ into trehalose and malto-oligosaccharide (n-2 glycosyl units) (Fang *et al.*, 2006). As trehalose synthesis by TreY and TreZ needs malto-oligosaccharides as substrate, we can assume that another way to synthesize trehalose should be present in organisms that only rely on GlgE to produce glycogen. Nonetheless, in these organisms, the TreY-TreZ pathway could allow a rapid turnover between trehalose and glycogen.

II-C-3(d) The TreP pathway

This pathway, first discovered in the *Protozoa Euglena gracilis*, involves a unique enzymatic reaction mediated by trehalose phosphorylase TreP (Belocopitow and Maréchal, 1970). The TreP activity catalyses the reversible phosphorolysis of trehalose into glucose and G1P. TreP acts in both directions, with similar activity in the Fungi *Agaricus bisporus* (Wannet *et al.*, 2000), that makes it efficient for either trehalose synthesis or degradation. In addition to *E. gracilis*, this enzyme has been characterized in various Fungi (Kitamoto *et al.*, 1988; Schwarz *et al.*, 2007; Wannet *et al.*, 1998) and Bacteria (Aisaka *et al.*, 1998; INOUE *et al.*, 2002; Kizawa *et al.*, 1995). One slight difference can be pointed out from these studies: fungal TreP only acts on the α-anomer of G1P while TreP from *E. gracilis* and from bacterial origin solely reacts with β-D-glucose-1-phosphate.

II-C-3(e) The TreT pathway

The last known enzymatic pathway for the synthesis of trehalose has been discovered in the Archaea *Thermococcus litoralis* (Qu *et al.*, 2004) and is composed of a unique enzymatic reaction. A trehalose glycosyltransferring synthase, called TreT, transfers the glycosyl moiety of NDP-glucose onto glucose to produce trehalose with the release of NDP. TreT activities, restricted to certain Archaea and Bacteria (Kouril *et al.*, 2008) operate either unidirectionally (Kouril *et al.*, 2008) or in both directions with a better efficiency for the synthesis of trehalose (Nobre *et al.*, 2008; Qu *et al.*, 2004; Ryu *et al.*, 2005) depending on the organism. Various nucleotide-sugars, including ADP-, GDP- and UDP-glucose can be used as substrates for this activity.

To resume, 5 enzymatic pathways guarantee the production of trehalose required for the GlgE pathway. It should be stressed that these pathways are not mutually exclusive. For instance,

OtsA/OtsB, TreY-TreZ and TreS pathways co-exist in *M. tuberculosis*. This also suggests that TreS must act in the direction of maltose production (Miah *et al.*, 2013). Among them, TreY/TreZ pathway is more likely to be involved in a turnover between trehalose and glycogen pools. On the other hand, each of the three other pathways should be sufficient to provide trehalose to GlgE pathway either from nucleotide-sugars (OtsA/OtsB and TreT) or from G1P (probably the β anomer) with the help of TreP.

II-C-4) Maltose-1-phosphate: the building block of GlgE pathway

TreS activity mediates the first step of GlgE pathway with the conversion of trehalose into maltose. Maltose is then phosphorylated on C1 by a maltokinase to produce maltose-1-phosphate (M1P). Discovered in the actinobacteria *Actinoplanes* sp. (Drepper *et al.*, 1996), maltokinase was first supposed to be involved in carbohydrate uptake, but the discovery of GlgE rather suggested its role in glycogen metabolism (Elbein *et al.*, 2010; Kalscheuer *et al.*, 2010). Enzymatic characterization of actinobacterial maltokinases showed these enzymes share similar properties: they preferentially use ATP as phosphate donor even if UTP and GTP can be used to a lesser extent, and they are strictly dependent on divalent cations, Mg^{2+} being the best activator (Fraga *et al.*, 2015; Jarling *et al.*, 2004; Mendes *et al.*, 2010). To fulfil their role in the GlgE pathway, TreS and Mak form heterocomplexes composed of either 4 TreS and 2 Mak subunits or 4 TreS and 4 Mak subunits (Kermani *et al.*, 2019; Roy *et al.*, 2013). However, many of these characteristics may be specific to actinobacterial maltokinases since most Bacteria express a fused TreS-Mak protein (Fraga *et al.*, 2015).

II-C-5) An alternative way to synthesise maltose-1-phosphate

The consecutive action of TreS and Mak activities is not the only way to synthesise M1P. The characterization of *treS* or *mak* mutant strains of *M. tuberculosis* has revealed an alternative biosynthetic pathway. Further investigation pointed out the accumulation of M1P in the mutant strains was due to an enzyme annotated as a glycogen synthase (Koliwer-Brandl *et al.*, 2016). However, this glycogen synthase does not belong to the GT5 CAZy family, but rather to the GT4 family that transfers glycosyl moiety of nucleotide-sugar onto phospho-sugar (Coutinho *et al.*, 2003). Although this enzyme is capable in some extent to transfer the glucose moiety of ADP-glucose onto non-reducing end of glucan, it clearly displays a better activity (1000-folds higher) when G1P is used as an acceptor (Koliwer-Brandl *et al.*, 2016). It was therefore renamed α-maltose-1-phosphate synthase (GlgM; EC 2.4.1.342). In *M. tuberculosis* and *M. smegmatis*, GlgM activities are able to use ADP-glucose and to a lesser extent UDP-glucose. Taking into account the lack of precision in the annotation of glycogen synthase, a recent genome analysis has revealed that bacterial GT4 glycogen synthases (GlgM), found mostly in *Actinobacteria*, but also in some members of the *FCB* group, *Verrucomicrobia*, *Chloroflexi*, *Firmicutes*, *Proteobacteria* and *Acidobacteria* account for one third of annotated GlgA in the database (Syson *et al.*, 2020). Therefore the proportion of bacteria that synthesize glycogen

by the classical GlgC-pathway was then re-evaluated from 32% (Chandra *et al.*, 2011) to 20% (Syson *et al.*, 2020).

To summarize, there are two pathways for M1P synthesis: one from trehalose with TreS and Mak, and the other one from ADP-glucose with GlgM. These two pathways can coexist, as in the case of *M. tuberculosis* (Figure 4), but there is no evidence that this is the norm. It is noteworthy that presence of GlgE, the only known enzyme that consumes M1P, must be associated with a M1P synthesis pathway because its accumulation is toxic (Kalscheuer *et al.*, 2010). This effect can be observed in all *glgE* single mutants with developmental delay in *Streptomyces venezuelae* (Miah *et al.*, 2016), bacteriostatic effect in *M. smegmatis* (Sassetti *et al.*, 2003) or bactericidal toxicity in *M. tuberculosis* (Kalscheuer *et al.*, 2010). Mechanisms underlying M1P toxicity remain elusive but, may imply inhibition of respiration and DNA damages in *M. tuberculosis*.

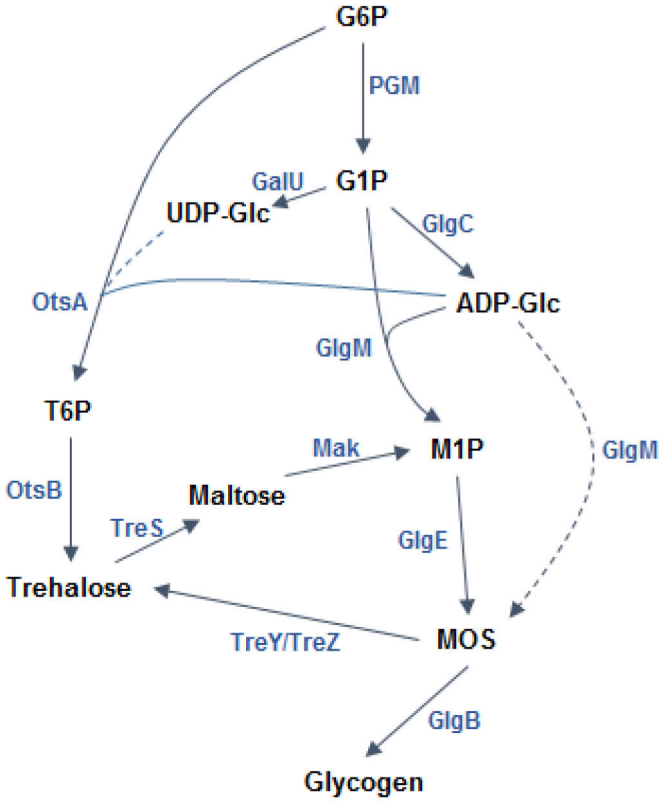

Figure 4 : Schematic representation of glycogen biosynthesis in *M. tuberculosis*.
Full and dotted lines respectively represent favoured and minor enzymatic routes. Even if successive activities of GlgC and GlgM can lead to the synthesis of malto-oligosaccharides, the main route for glycogen synthesis in *M. tuberculosis* involves GlgE. The M1P building block of GlgE is produced through two alternate routes: either by GlgM or from trehalose by TreS and Mak. Trehalose synthesis occurs by successive action of OtsA and OtsB. As ADP-glucose is the favoured NTP-glucose substrate of OtsA, this nucleotide-sugar plays a central role in glycogen biosynthesis. Presence of TreY and TreZ allows a rapid recycling of MOS into trehalose to fuel other metabolic pathways. The last step of glycogen synthesis is shared by GlgC- and GlgE pathways and relies on GlgB to insert branching points. G6P: glucose-6-phosphate ; G1P: glucose-1-phosphate ; UDP-Glc: uridine diphosphoglucose ; ADP-Glc: adenine diphosphoglucose ; T6P: trehalose-6-phosphate ; M1P: maltose-1-phosphate ; MOS: malto-oligosaccharides ; PGM: phosphoglucomutase ; GalU: UDP-glucose pyrophosphorylase ; GlgC: ADP-glucose pyrophosphorylase ; OtsA: trehalose-6-phosphate synthase ; OtsB: trehalose-6-phosphate phosphorylase ; TreS: trehalose synthase ; Mak: maltokinase ; GlgM: maltose-1-phosphate synthase ; GlgE: α-1,4-glucan:maltose-1-phosphate maltosyltransferase ; TreY: maltooligosyl trehalose synthase ; TreZ: maltooligosyl trehalose trehalohydrolase ; GlgB: branching enzyme

II-C-6) GlgE synthesises α-1,4 glucan chains using maltose-1-phosphate

The α-1,4-glucan:maltose-1-phosphate maltosyltransferase GlgE belongs to GH13 subfamily 3 (CAZy annotation) and is currently the only enzyme known to use M1P as substrate. It catalyses the reversible transfer of the maltosyl residue of M1P on non-reducing ends of malto-oligosaccharides following this reaction (Elbein *et al.*, 2010):

$$\textbf{(Glucosyl)}_{n} \textbf{ + M1P = (Glucosyl)}_{n+2} \textbf{ + Pi}$$

However, only ~10 % of Pi is converted to M1P when GlgE activity is incubated with malto-oligosaccharides and orthophosphate (Pi), suggesting that the elongation reaction is favoured (Kalscheuer *et al.*, 2010). The minimum size of substrate for this activity is DP4 that is then elongated by an even number of glucose units. In addition to this elongation activity, GlgE can also disproportionate malto-oligosaccharides, DP4 being also the minimal acceptor and minimal product. In *Actinobacteria*, the GlgE ability to initiate *de novo* synthesis of malto-oligosaccharides without primer was not examined, as GlgM is supposed to do so. However, GlgE1 from *Streptomyces coelicolor* was shown to slowly form short malto-oligosaccharides only from M1P (Syson *et al.*, 2011). This priming is done by slow hydrolysis of M1P to form maltose, which is then slowly elongated to maltotetraose, a good acceptor of GlgE (Rashid *et al.*, 2016). Thus, priming by GlgE seems to be possible, but at a slow pace and is therefore not efficient.

II-C-7) Post-translational modifications control the GlgE activity.

GlgE protein is subjected to post-translational modification (PTM), which consists of Ser/Thr phosphorylation by a specific protein kinase PknB (Leiba *et al.*, 2013). This PTM mechanism occurs in *M. tuberculosis*, but also in *M. smegmatis* as well as in *S. coelicolor*, suggesting it is conserved at least in *Actinomycetales*. Nevertheless, the 7 phosphorylation sites identified on *M. tuberculosis* GlgE are not conserved among *Actinomycetales*. The phosphate groups on Ser/Thr residues of GlgE results in an overall decrease of the catalytic efficiency by 2 orders of magnitude. The relevance of PTM of GlgE is quite puzzling as its downregulation would lead to the accumulation of highly toxic M1P (Leiba *et al.*, 2013). Further controls are likely to take place in the GlgE-pathway to prevent the deleterious effects of M1P.

To resume, GlgE is the key enzyme of this alternative glycogen biosynthetic pathway: it can initiate the *de novo* synthesis of malto-oligosaccharides in addition to elongate and disproportionate them. The branching enzyme GlgB, like in the classical GlgC-pathway, is the last step to produce glycogen.

II-D. Glycogen catabolic pathway

The catabolism of α-1,4 and α-1,6 linkages involves the synergic actions of glycogen phosphorylase (GlgP) and glycogen debranching enzyme (GlgX). GlgP catalyses the reversible phosphorolytic cleavage of α-1,4 glucosidic bonds at the non-reducing ends of the glycogen particle (Kitaoka and Hayashi, 2002). During this process, G1P is produced, then

transformed into glucose-6-phosphate (G6P) by the phosphoglucomutase (PGM) to enter in the glycolysis pathway and provide energy to the cell (Najjar and Pullman, 1954). Action of GlgP generates phosphorylase-limit dextrins: short maltotriose or maltotetraose chains branched to the linear glucose chain that cannot be degraded by GlgP because of the presence of the α-1,6 linkage. The short-branched glucans are specifically trimmed by the GlgX activity. For recall, GlgX does not cleave off the long-branched glucan. The short cleaved malto-oligosaccharides are then disproportionated and catabolized by the combined action of 4-α-glucanotransferase MalQ and maltodextrin phosphorylase (MalP) (Figure 5). As we mentioned previously, the catabolic enzymes, GlgP and GlgX are produced during the glycogen biosynthesis. In order to avoid a futile cycle, GlgP activity is negatively regulated by ADP-glucose. The latter acts as a competitive inhibitor with respect to G-1-P during the biosynthesis of glycogen (Chen and Segel, 1968; Takata *et al.*, 1998). The GlgP activity is also regulated by the formation of a tight complex with the Histidine phosphocarrier protein (Hpr) (Seok *et al.*, 1997). The Hpr protein belongs to the phosphoenol-pyruvate: sugar phosphotransferase system (PTS), which is involved in the transport and the phosphorylation of many sugars (Deutscher *et al.*, 2006). The phosphorylated form of Hpr (P-Hpr) displays a

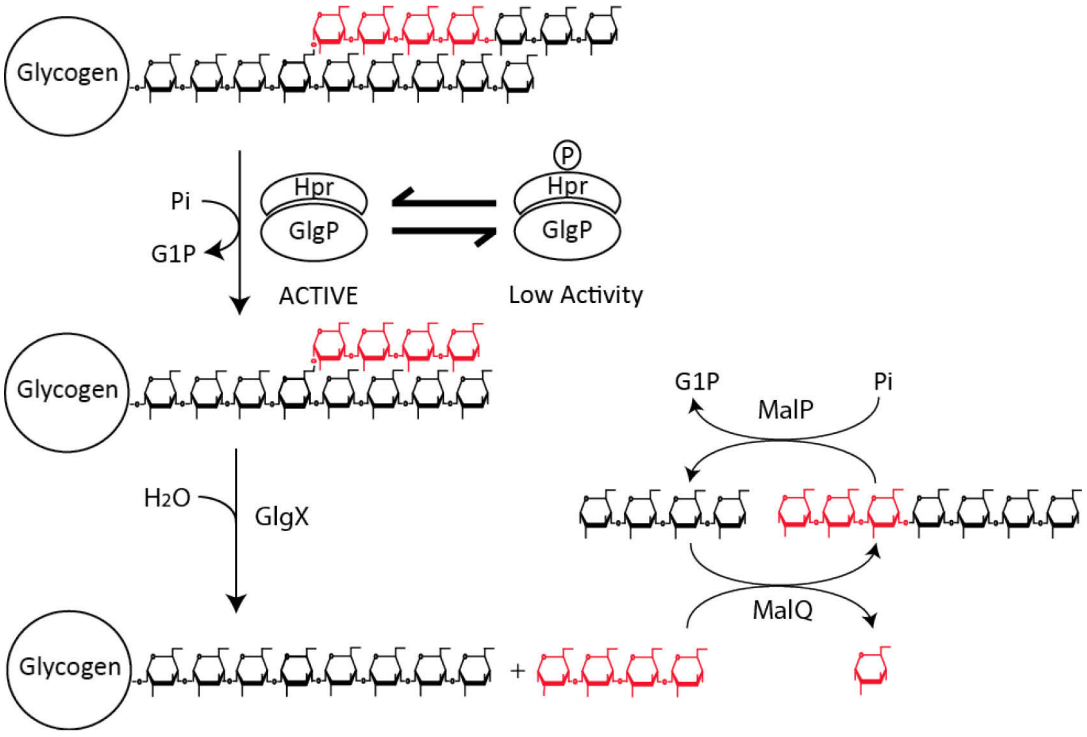

Figure 5 : Glycogen catabolism pathway.
Glycogen phosphorylase (GlgP) and Histidine carrier protein (Hpr) form a stable complex. Hpr proteins favours the formation of dimer, tetramer and octamer of GlgP (not shown here for the sake of simplicity). Both phosphorylated Hpr proteins and competitive inhibitor (i.e. ADP-glucose) reduce drastically the GlgP activity during glycogen biosynthesis. The degradation of glycogen is initiated when Hpr proteins are dephosphorylated. In the presence of phosphate inorganic (Pi), GlgP activities release glucose-1-phosphate (G1P) from the non-reducing of glucan chains of glycogen. The enzymatic reactions stop four units of glucose residues before reaching an α-1,6 linkage or branching point. Debranching enzyme activities (GlgX) recognize and trim specifically short-branched maltotetraosyl residues. The new linear glucan chains produced can be then further digested by GlgP activity. Maltotetraose molecules are metabolized in glucose and G1P via the synergic action of 4-α-glucanotransferase (MalQ) and maltodextrin phosphorylase (MalP).

4-fold higher affinity for GlgP than the un-phosphorylated form (Hpr). However, only the Hpr form allosterically activates GlgP, by 2.5-fold. Interestingly, because the concentration of Hpr is much higher than that of GlgP, this indicates that GlgP is always complexed with either P-Hpr or Hpr (Mattoo and Waygood, 1983). The phosphorylation state of Hpr varies with the physiological state of the cell. Thus, at the onset of stationary phase, which coincides with glycogen operon activation and glycogen synthesis, most of Hpr is found to be phosphorylated. Both the predominant form of P-Hpr and the increase in ADP-glucose level will prevent the dimerization and activity of GlgP, respectively, and therefore glycogen degradation (Chen and Segel, 1968; Seok *et al.*, 2001).

III. Chlamydiae

III-A. Discovery of the *Chlamydiae* phylum

The relationship between Humans and *Chlamydiae* is very ancient, with evidence of trachoma, an ocular infection, among Australian aborigines around 10 000 years ago (Webb, 1990). Mentions of this infection are also found in ancient texts, such as the Bible (Johnson, 2005), Greek literature (Herodotus, Hippocrates) and even in Ebers papyrus (Taborisky, 1952), an Egyptian medical papyrus of herbal knowledge dating back to around 1550 BC. It was not until 1907 that Halberstädter and von Prowazek first directly observed the etiological agent of trachoma (Taylor-Robinson, 2017). They saw intracytoplasmic inclusions in conjunctival epithelial cells draped around the nucleus and therefore suggested to call this agent Chlamydozoa (from Greek khlamús, a cloak) (Subtil *et al.*, 2014). This microorganism was first thought to be a protozoan, then a virus because of its very small size, before it was shown to be an obligate intracellular bacterium (Moulder, 1964). The name was changed to *Chlamydia*, specifically to *Chlamydia trachomatis* to name the etiologic agent of trachoma.

Following the discovery of *Chlamydia trachomatis*, several other *Chlamydiae* species have been reported as agents of various diseases among vertebrates. While *C. trachomatis* is an exclusive pathogen to humans, causing trachoma and genital infection, *Chlamydia abortus* and *Chlamydia pecorum* are the causes of abortion in sheep and cattle, respectively (Fukushi and Hirai, 1992; Szeredi and Bacsadi, 2002). Among pathogens of humans are also reported *Chlamydia psittaci* and *Chlamydia pneumonia* that are respectively widespread among birds or found in a wide range of vertebrates (Frydén *et al.*, 1989). These five species all belong to a family called *Chlamydiaceae*, the most studied family of *Chlamydiae* due to their damages on human health and livestock. We had to wait until the end of XXth century and the improvement of molecular biology to discover an abundance of new *Chlamydiae* species, with more than 60 sequenced species (Pillonel *et al.*, 2018).

III-B. Chlamydiae are obligate intracellular bacteria with various host ranges

The hallmark of all *Chlamydiae* species is an obligate intracellular lifestyle with a biphasic developmental cycle. Species that share at least 90 % 16S rRNA identity with *C. trachomatis*

belong to the *Chlamydiaceae* family, and those between 80 and 90 % identity are classified as chlamydia-like (or environmental *Chlamydiae*) inside different new families (Everett *et al.*, 1999). These environmental *Chlamydiae* have the characteristic to have a broader host range and possess larger genomes (~2.5 Mb) than their pathogenic counterparts (~1 Mb). Indeed, most environmental *Chlamydiae* were described as symbionts of free-living amoebae and other eukaryotic hosts (Horn, 2008). Today, besides *Chlamydiaceae* family, there are five families (*Parachlamydiaceae*, *Waddliaceae*, *Criblamydiaceae*, *Simkaniaceae* and *Rhabdochlamydiaceae*) and ten candidate families (*Candidatus* Parilichlamydiaceae, *Ca.* Novochlamydiaceae, *Ca.* Pelagichlamydiaceae, *Ca.* Enkichlamydiaceae, *Ca.* Limichlamydiaceae, *Ca.* Arenachlamydiaceae, *Ca*. Kinetochlamydiaceae, *Ca.* Clavichlamydiaceae, *Ca*. Piscichlamydiaceae and *Ca*. Motilichlamydiaceae) that all encompass Chlamydia-like bacteria (Figure 6) (Omsland *et al.*, 2014; Pillonel *et al.*, 2018). Even if chlamydia-like are mainly symbionts of *Amoeba*, as these protozoa are ubiquitous and can be found in soil, air, marine and freshwater (Rodríguez-Zaragoza, 1994), the issue of human infection and its impact on health arises. More and more reports suggest a relationship between environmental *Chlamydiae* and pathologies in humans (Taylor-Brown *et al.*, 2015), such as *Waddlia chondrophila* and adverse pregnancy outcomes and infertility (Baud *et al.*, 2014, 2020), *Estrella lausannensis* that replicates inside macrophages and pneumonia (Lienard *et al.*, 2011; Rusconi *et al.*, 2015) or *Protochlamydia naegleriophila* and pneumonia (Casson *et al.*, 2008). Recently, *Chlamydiae* were shown to be very abundant in deep marine sediments, with more than 150 different species found in the Arctic Mid-Ocean Ridge (Dharamshi *et al.*, 2019). Asides from the growing knowledge of the evolution of *Chlamydiae* evolution, the absence of detectable eukaryotic hosts within the community questions the prerequisite of obligate intracellular lifestyle of these newly discovered species.

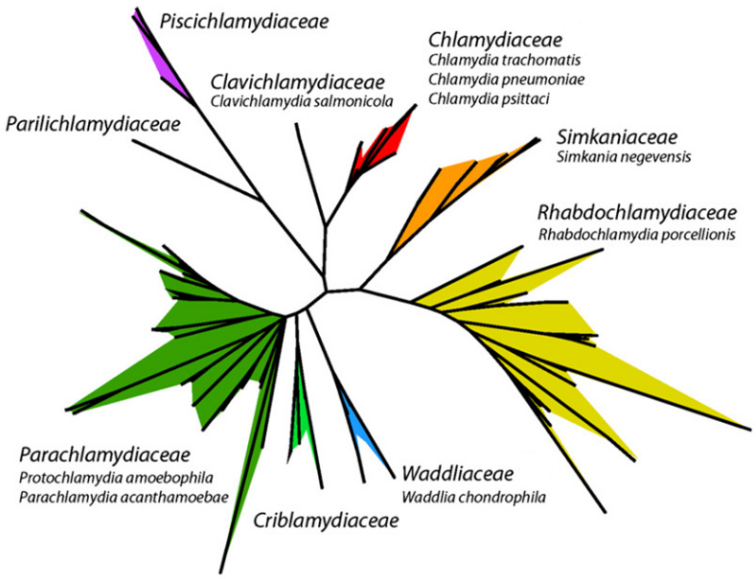

Figure 6 : (adapted from Omsland *et al.*, 2014) Diversity of the Chlamydiae.
The phylogenetic tree shows the relationship of pathogenic *Chlamydiae* (*Chlamydiaceae*) with 8 other families collectively referred to as environmental *Chlamydiae*. Representative species are displayed. For a more complete phylogenetic tree including all available sequenced genomes of *Chlamydiae*, see https://chlamdb.ch/.

III-C. Particularities of the *Chlamydiae* phylum

III-C-1) Developmental cycle of Chlamydiae

As previously stated, one of the hallmarks of all *Chlamydiae* is its biphasic development cycle. During this cycle, *Chlamydiae* alternate between two morphologically distinct states: the infectious form called elementary body (EB) and the reticulate body (RB) which is the replicative form (Figure 7). EBs are less metabolically active than RBs (Cossé *et al.*, 2018) and begin the developmental cycle in the extracellular environment. They are recognizable from RBs by their small size (~300 nm and ~1 µm in diameter for *Chlamydiaceae* EBs and RBs, respectively) and appear darker in transmission electron microscopy due to nuclear material condensation (Friis, 1972). Recognition and attachment to the host cell require two successive steps: a non-specific electrostatic interaction with heparan sulphate moieties followed by an irreversible attachment to a yet still unknown receptor (Hackstadt *et al.*, 1999). Directly following this attachment, EBs secrete by its type three secretion system (T3SS) the effector protein Tarp (Translocated Actin-Recruiting Phosphoprotein) that recruit host's actin cytoskeleton to form an inclusion (Clifton *et al.*, 2004).

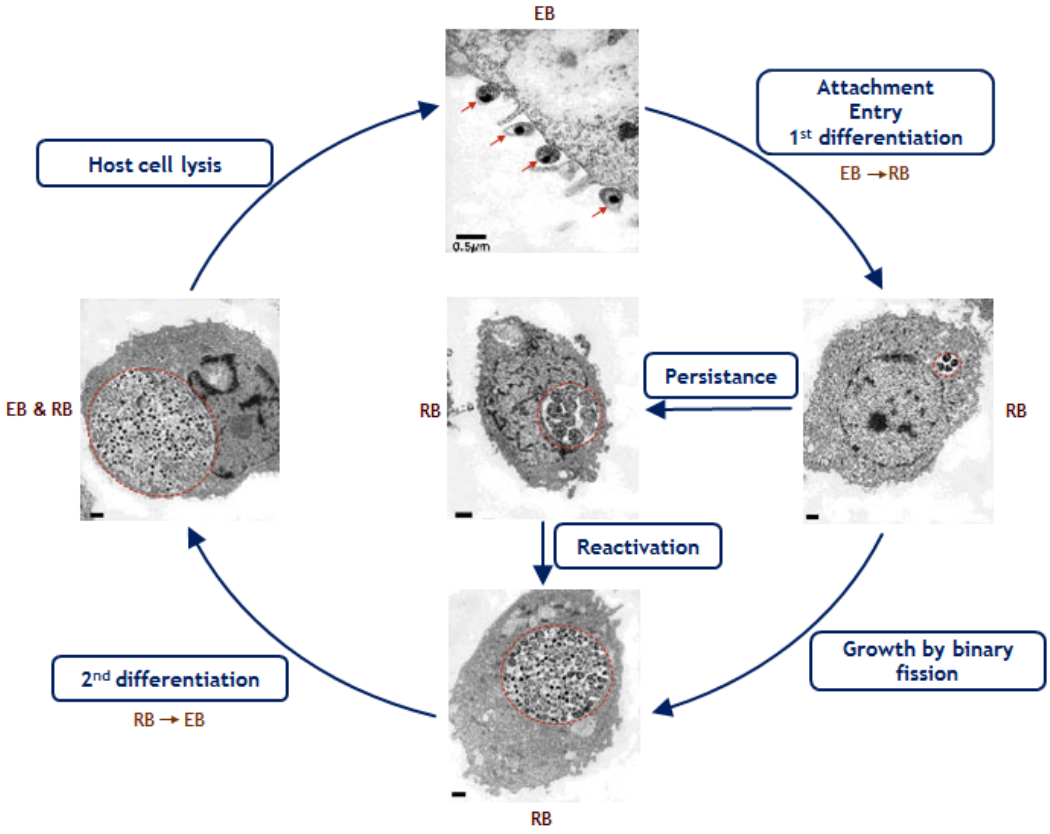

Figure 7 : Biphasic developmental cycle of *Chlamydiae*.
Elementary bodies (or EBs), the extracellular and infectious forms of *Chlamydiae* (red arrows) recognize the cell to infect and enter through an inclusion (red dash circle). EBs will then differentiate into reticulate bodies (or RBs), the metabolically active form. The secretion of virulence factors and various carriers by the type III secretion system allows the *Chlamydiae* to hijack the energy and carbon necessary for growth by binary fusion. RBs will then redifferentiate into EBs, which will be released after cell lysis. RBs may also persist inside host cells when conditions are not ideal and reactivate later on.

Rapidly after the entry into the host cell, EBs differentiate into the more metabolically active RBs (Omsland *et al.*, 2012). While DNA is condensed in EBs due to the two histone-like proteins Hc1 and Hc2 (a.k.a. HctA and HctB, respectively), an antagonist of Hc1 is synthesized after bacterial entry, leading to further gene transcription and differentiation into RBs (AbdelRahman and Belland, 2005). T3SS has been involved since the onset of the infection, and a number of effectors called Inc proteins are rapidly secreted into the inclusion (Fields *et al.*, 2003) to interact and hijack numerous host metabolic pathways (Mirrashidi *et al.*, 2015). During RB state, which can last up to 48 h, the number of proteins expressed increase drastically and cell division takes place. The mechanism of cell division is peculiar due to the missing *ftsZ* orthologue gene that encodes a key protein involved in the bacterial cell division. Instead, MurA, which catalyses the first step of peptidoglycan synthesis, is thought to initiate cell division as it is expressed immediately prior to cell division (AbdelRahman and Belland, 2005; Belland *et al.*, 2003; McCoy *et al.*, 2003).

Following cell division, RBs redifferentiate into EBs. This secondary differentiation is asynchronous and induced by yet unidentified signal. The “late genes” expressed at the end of the RB stage, such as genes encoding histone-like proteins and T3SS, prepare the cell for extracellular life and future infection (Nicholson *et al.*, 2003). Most of the time, the chlamydial developmental cycle ends with host cell lysis.

Alternatively, RBs can persist within host cells due to the incompleteness of this cycle. This mechanism could explain why many chlamydial infections are associated with long term or chronic diseases. However, RBs can escape from persistence and clinical evidence for this reactivation exist (Thygeson, 1963). Persistence is associated with enlarged RBs that neither divide by binary fission nor undergo secondary differentiation, but chromosomes replication continues. This particular state can be induced by various effects, like antibiotic or IFN-γ exposure, amino acid or glucose starvation, monocyte infection or continuous culture (Hogan *et al.*, 2004).

III-C-2) Relevance of glycogen metabolism and type three secretion system in Chlamydiae

At variance with their facultative counterparts, obligate intracellular pathogens undergo a large genome reduction as they specialize into host metabolism hijacking. During this process of genome size reduction, the metabolism of glycogen is lost in almost all cases, except for the notable exception of *Chlamydiae* (Henrissat *et al.*, 2002). Moreover, distinctively from *C. psittaci* and *C. pneumoniae* that do not accumulate visible amount of glycogen during their infection cycle (Moulder, 1991) *C. trachomatis* and *C. muridarum* accumulate a large amount of glycogen particles within the inclusion. The detection of iodine-glycogen complex in infected cells has been used for a long time to diagnose *C. trachomatis* infections (Ripa, 1982). Interestingly, most of *C. trachomatis* strains carry a highly conserved plasmid of 7.5 kbp that encodes eight ORF (named pgp1 to pgp 8). As highlighted, the plasmid plays a significant role

in *C. trachomatis* pathogenesis. A detailed study of pgp4 has indicated that it regulates 20 chlamydial genes, including *glgA* (Song *et al.*, 2013). Yet all *Chlamydiae* species possess genes of the GlgC-pathway except *Estrella lausannensis*, *Criblamydia sequanensis* and *Waddlia chondrophila* that lack a *glgC* gene. Altogether, this indicates that glycogen metabolism plays a central role in the life of *Chlamydiae*, probably to supply the energy needed for the particular biphasic cycle, with slight species-specific differences. It is noteworthy that almost all *Chlamydiae* lack a hexokinase, the enzyme that catalyses the phosphorylation of glucose and imports the host glucose-6-phosphate *via* the specific transporter UhpC (Gehre *et al.*, 2016).

The glycogen metabolism in *C. trachomatis* is very well studied and is particularly interesting. Indeed, glycogen accumulates mainly outside of bacteria, inside the inclusion (Chiappino *et al.*, 1995). While some glycogen is transported in bulk from the host cell to the inclusion, *de novo* synthesis also occurs (Gehre *et al.*, 2016). Actually, SLC35D2, a human transporter, is recruited to the inclusion membrane and imports UDP-glucose from host cytosol. In addition, *C. trachomatis* seems to secrete all its glycogen metabolic enzymes, with the exception of GlgC, to the inclusion. Synthesis of glycogen is then achievable, as *C. trachomatis* GlgA can use both ADP- and UDP-glucose efficiently to elongate α-glucans and is clearly evidenced to be secreted (Gehre *et al.*, 2016; Lu *et al.*, 2013). Furthermore, catabolic enzymes also seem to be secreted inside of the inclusion, allowing a glycogen turnover with the production of G1P, converted into G6P by chlamydial phosphoglucomutase MrsA, that is finally imported into bacterial cytosol by UhpC. This highlights *C. trachomatis* ability to hijack carbon of the infected cell and trap it within the inclusion where it is inaccessible for the host but ready to use for the bacteria.

The *Chlamydiae* propensity to secrete glycogen enzymes by T3SS is not specific to *C. trachomatis*. Some *in vivo* data obtained using *Shigella flexneri* heterologous system (Subtil *et al.*, 2001) suggest that all glycogen metabolizing enzymes (GlgC, GlgA, GlgB, GlgP, GlgX and MalQ), from various *Chlamydiae* species, possess a T3SS signal, except for GlgC of *C. trachomatis* (Table 1) (Ball *et al.* 2013; Kadouche 2016). This highlights both relevance of glycogen metabolism and T3SS in *Chlamydiae* developmental cycle. As mentioned previously, *C. trachomatis* bypasses the lack of GlgC secretion by recruiting SLC35D2, a host's UDP-sugar transporter, on the inclusion (Gehre *et al.*, 2016). UDP-glucose is then incorporated into chlamydial glycogen metabolism, as GlgA from *C. trachomatis* can use both ADP- and UDP-glucose to elongate α-glucans.

	GlgC	GlgA	GlgB	GlgP	GlgX	MalQ
Chlamydia trachomatis	-	+	+	+	+	n.d.
Parachlamydia acanthamoeba	+	+	+	n.d.	n.d.	+
C. Protochlamydia amoebophila	+	+	+	+	+	n.d.
Estrella lausannensis	n.d.	+	n.d.	+	n.d.	+
Waddlia chondrophila	n.d.	+	n.d.	n.d.	n.d.	+
Simkania nevegensis	+	+	+	+	n.d.	n.d.

Table 1 : Most chlamydial glycogen-related enzymes are potentially secreted through type III secretion system. *Shigella flexneri* heterologous system was used to determine which chlamydial glycogen-related enzymes are secreted through T3SS. Tests were performed on enzymes from *Chlamydia trachomatis* (*Chlamydiaceae*), but also from five environmental *Chlamydiae* representing the diversity of the phylum. All tested enzymes were secreted in this system, except for GlgC from *Chlamydia trachomatis*. Until now, only the secretion of GlgA from *Chlamydia trachomatis* was evidenced by *in situ* experiments. GlgC: ADP-glucose pyrophosphorylase, GlgA: glycogen synthase, GlgB: branching enzyme, GlgP: glycogen phosphorylase, GlgX: debranching enzyme, MalQ: 4-α-glucanotransferase. n.d.: not determined.

Asides from their role in glycogen metabolism and in bacterial entry, that has been discussed above, effectors secreted in the host cell by T3SS contribute to subversion and evasion of the host cell during the entire chlamydial developmental cycle (Ferrell and Fields, 2016). More and more effectors are continuously identified (Dai and Li, 2014; Elwell *et al.*, 2016; Kebbi-Beghdadi *et al.*, 2019), some of them being unique to *Chlamydiae* phylum or even specific to one or two species (McKuen *et al.*, 2017).

III-D. Involvement of Chlamydiae in plastidial endosymbiosis: The *Ménage-à-Trois* Hypothesis

It is now widely admitted that the emergence of the three *Archaeplastida* families (*Chloroplastida*, *Rhodophyta* and *Glaucophyta*) arose from a primary endosymbiotic event between a photosynthetic cyanobacterium and a phagotrophic eukaryote. This single event (Rodríguez-Ezpeleta *et al.*, 2005) occurred 0.9 to 1.6 billion years ago (McFadden, 2014; Shih and Matzke, 2013; Yoon *et al.*, 2004) and likely involved an amoeba and a freshwater cyanobacterium (Ponce-Toledo *et al.*, 2017; de Vries and Archibald, 2017). Dysfunctional phagocytosis of a cyanobacterium led to the establishment of an endosymbiosis link and provided a supplementary source of carbon from photosynthetic origin for the host. But this bipartite scenario badly explained how this unique endosymbiotic event took place, and a tripartite scenario was therefore proposed (Ball *et al.*, 2011, 2013).

During an endosymbiotic event, whether for plastid or mitochondria, a large number of genes are transferred from the symbiont to the host cell (Timmis *et al.*, 2004). While these genes are lost from the symbiont's genome, proteins encoded by their nuclear counterparts have to be addressed to the symbiont to exert their function. During the endosymbiotic process, most symbiont's genes are lost, as they do not give a selective advantage for the host. In the end, the symbiont has lost most of its genome and becomes an organelle inside the host cell, the plastid in this case (Bonen and Doolittle, 1975; Keeling *et al*., 2015).

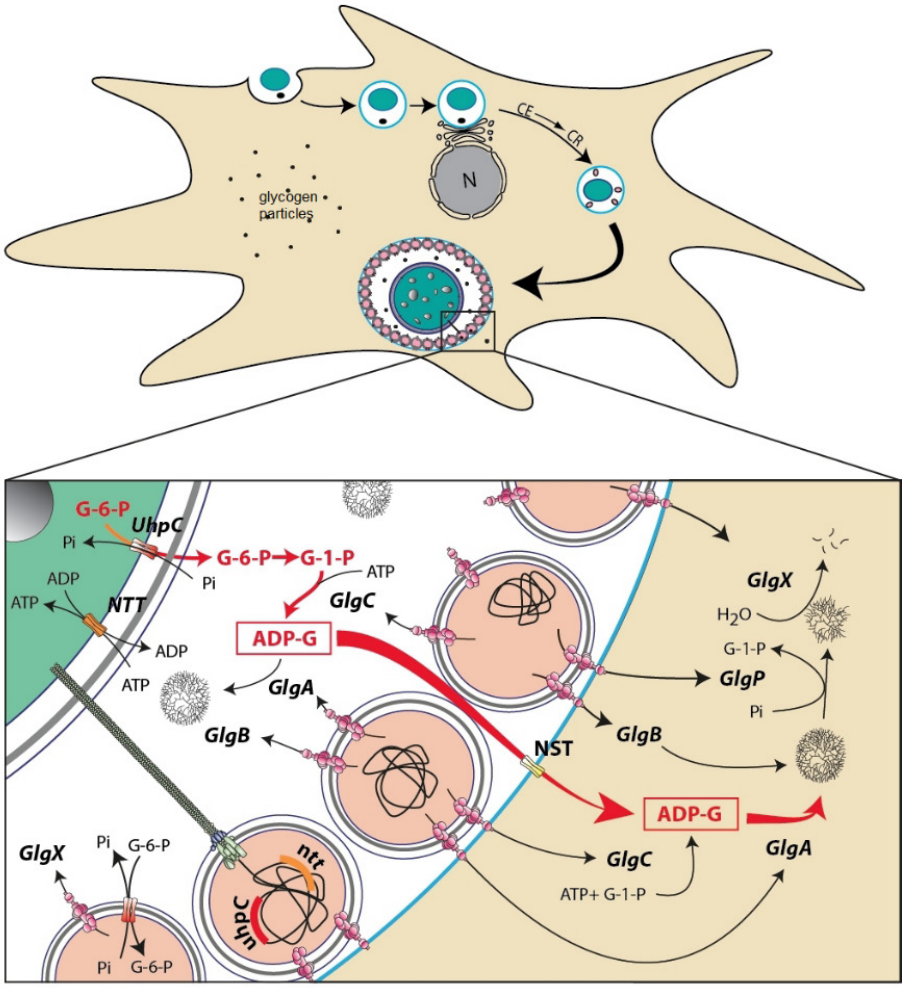

Figure 8 : MATH model of the metabolic link at the onset of plastidial endosymbiosis.
In this model, endosymbiosis was achieved through the simultaneous entry of a cyanobacterium (in green, with starch granules in white) and an environmental *Chlamydiae* (in pink) inside an ancestral amoeba (in beige) through a common inclusion (in blue). The inclusion is derived from the endocytosis of the elementary body (EB) at the surface of the amoeba. Glycogen particles are displayed as black dots. Following this entry, *Chlamydiae* EBs differentiate into reticulate bodies (RBs) that grow by binary fission.
A section of the cyanobiont and the RBs sharing the same inclusion inside the host cell is enlarged. Proposed metabolic link involving storage polysaccharides is displayed. A lateral gene transfer mediated by type IV secretion system (in gray) is depicted, transferring two chlamydial genes, *uhpC* and *ntt* (in red and orange respectively), to the cyanobiont through conjugation-related mechanism. Thus, both UhpC and NTT are expressed by the cyanobiont and targeted to the membrane. UhpC, a glucose-6-phophate (G-6-P) / orthophosphate (Pi) antiporter, induces the channelling of the cyanobiont photosynthetic carbon (G-6-P) to the inclusion lumen. To balance the outflow of G-6-P during non-photosynthetic periods, it is proposed that the cyanobiont imported ATP *via* the ATP/ADP antiporter NTT. While a fraction of the photosynthetic G-6-P is imported in *Chlamydiae* cytosol by UhpC, the remaining is metabolised inside the inclusion lumen by chlamydial effectors secreted through the type III secretion system (in pink). First, phosphoglucomutase MrsA transforms G-6-P into glucose-1-phosphate (G-1-P), used by the ADP-glucose pyrophosphorylase GlgC to produce ADP-glucose (ADP-G). Subsequent secretion of chlamydial GlgA (glycogen synthase), GlgB (branching enzyme), in addition to GlgP and GlgX (glycogen phosphorylase and debranching enzyme, respectively; not depicted) into the inclusion leads to an intravesicular glycogen metabolism orchestrated by the bacteria. *Chlamydiae* also secretes its glycogen-metabolising enzymes inside the host cytosol, allowing the synthesis of glycogen from ADP-glucose whereas glycogen metabolism in eukaryotes only relies on UDP-glucose (not depicted). The recruitment of a nucleotide-sugar transporter (NST) of eukaryotic origin on the inclusion allows the host to get the overflow of ADP-G. This creates an early endosymbiotic link (red arrows) as photosynthates are, in the end, incorporated into the metabolism of the host.

The primary plastid endosymbiotic event therefore leaves evidence inside archaeplastidal genomes. Aside from the cyanobacterial signal, a large amount of genes of different origins are found in *Archaeplastida*, with a high prevalence for *Chlamydiae* (Qiu *et al.*, 2013). As

Chlamydiae are unable to pass through plant cell wall and that chlamydial signal is found in the three archaeplastidal lineages, it is more likely that chlamydial genes were horizontally transferred to the common ancestor of *Archaeplastida* than by multiple lateral genes transfer during *Archaeplastida* diversification (Subtil *et al.*, 2014). Hence, the involvement of an ancient *Chlamydiae* during the primary plastidial endosymbiosis was suggested in a tripartite scenario called *Ménage-à-trois* hypothesis (MATH).

The simultaneous entry of the cyanobiont and the ancient chlamydia in a common inclusion inside the eukaryotic host could have provided protection with the escape from phagocytosis. The establishment of a rapid metabolic link was crucial at the onset of plastidial endosymbiosis (Figure 8). In the MATH model, the cyanobiont exported its photosynthetic carbon in the form of G6P in the inclusion by UhpC, a G6P/Pi transporter of chlamydial origin (Facchinelli *et al.*, 2013). The loss of cyanobiont energy store is therefore compensated by the import of ATP during darkness by a nucleotide transporter (NTT), also of chlamydial origin (Cenci *et al.*, 2017; Linka *et al.*, 2003). With the secretion of chlamydial glycogen metabolizing enzyme by T3SS, glycogen is therefore synthesized inside the lumen of the inclusion. A fraction of ADP-glucose, an intermediate of this synthesis is imported into host cytosol by a nucleotide-sugar transporter (NST) of eukaryotic origin. This bacterial-specific intermediate cannot be metabolized by glycogen synthases of eukaryotic origin. The last major event for the establishment of the endosymbiotic link is consequently the transfer of chlamydial *glgA* gene to the host genome. Cyanobiont's photosynthate is then accessible and ready to use by the host, leading to the stabilization of the endosymbiotic link.

Following the early lateral gene transfers for the establishment of endosymbiosis, various other chlamydial genes were transferred to the eukaryote, notably genes involved in menaquinone synthesis (Cenci *et al.*, 2018), tryptophan synthesis (Cenci *et al.*, 2016) and glycogen metabolism that led to the formation of starch (Cenci *et al.*, 2014).

IV. Protein acetylation in bacteria

IV-A. Relevance and role of post-translational modifications in Bacteria

Bacteria have survived and evolved over billions of years to adapt to their various environments. In their respective niches, bacteria have to face numerous environmental changes and stresses, some of which compromise their survival. These conditions can change unexpectedly and there is no other choice for Bacteria to adapt quickly for their survival. It is well known that bacteria adapt to their environment by changes in their transcriptional and translational programs (Gottesman, 2017). Nonetheless, these two processes are energy- and time-consuming. On the other hand, post-translational modifications (PTMs) allow for rapid changes in the cellular physiology by modifying pre-existing proteins (Christensen *et al.*, 2019a). PTMs consist of the addition of diverse covalently-bound chemicals on proteins, some of which are reversible, some others are not (Aksnes *et al.*, 2015; VanDrisse and Escalante-Semerena, 2019). To date, more than 650

types of PTMs have been identified (https://www.uniprot.org/docs/ptmlist) in the tree of life, and the most preeminent are considered to be phosphorylation, N-linked glycosylation, acetylation, O-linked glycosylation, ubiquitination, methylation, SUMOylation, hydroxylation, carboxylation, palmitoylation, sulfation, nitrosylation and C-linked glycosylation (Minguez *et al.*, 2012). Thus, PTMs can range from minor chemical modifications such as acetylation, to the linkage of complete proteins in the case of ubiquitination. PTMs can influence the features of a protein in a variety of ways, such as changes in the activity, folding, protein stability, or even localization and interactions with other proteins (Soppa, 2010). While PTMs have been extensively studied in eukaryotes, our understanding of their relevance among prokaryotes has arisen over the last two decades (Yu *et al.*, 2008). PTMs in bacteria occur in relatively low abundance and on less proteins than in eukaryotes, making them more challenging to detect and analyse (Macek *et al.*, 2019). Among the different types of PTMs, protein acetylation, either on the N^{α}-terminus of the protein or on the N^{ε} residue of lysine residues, is abundant in the three domains of life (Drazic *et al.*, 2016; Soppa, 2010) and involved in a wide range of cellular processes (Choudhary *et al.*, 2009; Kim and Yang, 2011).

IV-B. Discovery of protein acetylation

While protein phosphorylation was extensively studied after its discovery in 1959 (Fischer *et al.*, 1959), the mechanisms and relevance of protein acetylation, discovered just a few years later (Phillips, 1963), remained largely unknown over the next decades (Verdin and Ott, 2015). Nonetheless, and quickly after its discovery, histone acetylation was proposed to be a dynamic and reversible mechanism for activation and repression of RNA synthesis (Allfrey *et al.*, 1964). We had to wait more than three decades for the almost concomitant identifications of the first histone acetyl-transferase (HAT) and the first histone deacetylase (HDAC). Former, identified in the protozoan *Tetrahymena thermophila*, was an orthologue of yeast's transcription regulator Gcn5 (Brownell and Allis, 1995; Brownell *et al.*, 1996) while the second was identified as a bovine orthologue of the yeast transcription regulator Rpd3 (Taunton *et al.*, 1996). In the years that followed, few other HATs and HDACs were found, but we had to wait until 2006 for the next major leap, which consisted of the first proteomic survey of protein acetylation. It led to the discovery of 388 acetylation sites in 195 human proteins (Kim *et al.*, 2006). A few years later, another human acetylome identified 3 600 sites of lysine acetylation in 1750 proteins (Choudhary *et al.*, 2009) involved in a wide range of cellular processes, placing protein acetylation under the spotlights. As it became evident that histones were not the only targets of protein acetylation, HATs were renamed protein acetyltransferases (PATs), or lysine acetyltransferases (KATs) for homologs of yeast Gnc5 that specifically acetylate the N^{ε} residues of lysine (Allis *et al.*, 2007).

IV-C. Two types of protein acetylation: N^{α} and N^{ε} acetylation

Protein acetylation occurs by two distinct mechanisms: acetylation on ε-amino group of internal lysines (N^{ε} lysine acetylation) and N-terminal protein acetylation (N^{α} acetylation) (Drazic *et al.*, 2016; Christensen *et al.*, 2019a). While 80-90 % of human proteins are co-translationally acetylated to their N^{α} termini (Brown and Roberts, 1976; Arnesen *et al.*, 2009), this PTM is unusual is bacteria, as only 145 and 31 proteins harbouring N^{α} acetylation have been identified in *Acinetobacter baumannii* (Kentache *et al.*, 2016) and in *E. coli* (Schmidt *et al.*, 2016), respectively. This type of modification (Figure 9A), catalysed by Nt-acetyltransferases (NATs) (Aksnes *et al.*, 2015), usually occurs co-translationally in eukaryotes (Polevoda and Sherman, 2003), but post-translationally in bacteria, mitochondria and plastids. However, post-translational N^{α} acetylation can occur for several eukaryotic proteins (Helbig *et al.*, 2010). This usually irreversible acetylation is observed either on the N-terminal methionine or on the exposed amino acid after cleavage of the N-terminal methionine (Helsens *et al.*, 2011). In *E. coli*, RimI, RimJ and RimL, the three known NATs, mainly target ribosomal proteins S5, L12 and S18, respectively (Yoshikawa *et al.*, 1987; Tanaka *et al.*, 1989; Lapteva *et al.*, 2020). In addition, it has been shown that acetylation of the L12 subunit of the ribosomal stalk complex significantly improved overall ribosomal stability in response to nutrient depletion (Gordiyenko *et al.*, 2008).

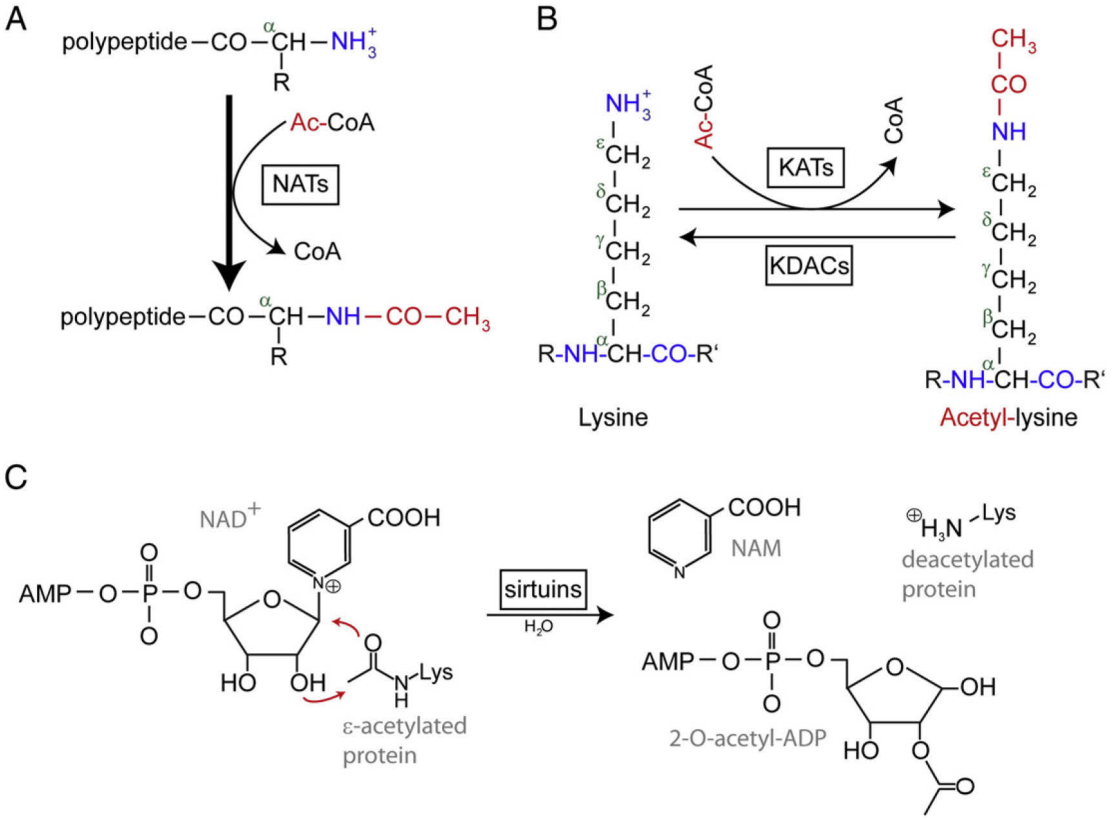

Figure 9 : (From Drazic *et al.*, 2016) Mechanisms of enzymatic protein acetylation and deacetylation. Irreversible N^{α} acetylation (**A**) is catalysed by N-terminal acetyltransferases (NATs) through the transfer of an acetyl group from AcCoA to the N-terminal amino-group of a protein. On the other hand, reversible N^{ε} lysine acetylation (**B**) is catalysed by lysine acetylases (KATs) and lysine deacteylases (KDACs). Class III KDACs, also known as sirtuins (**C**) have the specificity to use NAD^{+} as a cofactor during the deacetylation reaction, leading to the release of NAM. NAD^{+}: nicotinamide adenine dinucleotide, NAM: nicotinamide.

Protein acetylation also occurs on internal residues of proteins. Until recently, internal lysine residues were thought to be the only ones subjected to acetylation (N^{ε} lysine acetylation), but some pathogenic bacteria are also able to acetylate histidine, serine and threonine residues (O-acetylation on serine and threonine) (Birhanu *et al.*, 2017; VanDrisse and Escalante-Semerena, 2018). This is the case in several *Yersinia* species, with YopJ catalysing the acetylation of serine and threonine residues of many host's kinases to escape the immune system (Mittal *et al.*, 2010; Mukherjee *et al.*, 2006; Paquette *et al.*, 2012). However, we will further focus on N^{ε} lysine acetylation.

IV-D. Mechanisms of reversible N^{ε} lysine acetylation in bacteria

IV-D-1) Enzyme-driven lysine acetylation

The first identified and most studied targets of N^{ε} lysine acetylation are eukaryotic histones, modified by the action of HATs. Nevertheless, N^{ε} lysine acetylation is not limited to histones, and HATs were renamed lysine acetyltransferases (KATs). In contrary to N^{α} acetylation, N^{ε} lysine acetylation is reversible and is tightly regulated by the opposite action of KATs which catalyse the transfer of an acetyl moiety from acetyl-coenzyme A (AcCoA) to the ε-amine of a lysine residue, and lysine deacetylases (KDACs) (Figure 9B). Several families of KATs have been identified, the two major families being the Gcn5-related N-acetyltransferases (GNATs) and the MYST family (Berndsen *et al.*, 2007; Vetting *et al.*, 2005). GNAT family is the only one conserved in the three domains of life, and in fact, all known bacterial KATs belong to this family (Hentchel and Escalante-Semerena, 2015; Ren *et al.*, 2017; Thao and Escalante-Semerena, 2011). It should be remembered that in addition to protein acetylation, members of the GNAT family also exert their activity on small molecules and metabolites. The first identified bacterial KAT was the protein acetyltransferase Pat in *Salmonella enterica* (known as PatZ or YfiQ in *E. coli*) (Starai and Escalante-Semerena, 2004). Pat was shown to directly acetylate the K609 residue of the AMP-forming acetyl-CoA synthetase Acs, leading to a substantial decrease of this enzymatic activity (Castaño-Cerezo *et al.*, 2014). As Acs catalyses the activation of acetate into AcCoA, its inhibition by N^{ε} lysine acetylation can be considered as a negative feedback in acetate metabolism (Castaño-Cerezo *et al.*, 2015). This regulation mechanism tends to be conserved in most bacteria but with some variations of GNAT proteins: PatZ is replaced in *Mycolicibacterium smegmatis* and *Staphylococcus aureus* by the non-homologous KATs called PatA and AcuA, respectively, to acetylate Acs (Hayden *et al.*, 2013; Burckhardt *et al.*, 2019). Notably, PatA possesses an additional feature, as its activity is allosterically enhanced by cyclic adenosine monophosphate (cAMP) (Noy *et al.*, 2014), the main virulence factor among *Mycobacteria* (Nambi *et al.*, 2010).

Besides PatZ and its homologs, four additional KATs have been identified in *E. coli*: RimI, YiaC, YjaB and PhnO (Christensen *et al.*, 2018), and many others among the bacterial diversity. The growing number of known GNATs has led Christensen *et al.* (2019c), to propose a classification based on domain organization, summarized in Figure 10. Three classes,

depending on sequence length and number of GNAT domains, and five types (I to V) of KATs based on domain arrangement, are proposed. Class I KATs consist of large multidomain enzymes with a single GNAT domain while class II KATs are small enzymes with only a single GNAT domain. Finally, class III KATs encompass mid-sized proteins harbouring multiple GNAT domains. Type I and II harbour an ADP-forming acetyl-CoA synthetase domain and a single GNAT domain at the C- or N-terminus respectively. Nonetheless, the ADP-forming acetyl-CoA synthetase domain of these KATs is inactive as the catalytic histidine has been substituted (Starai and Escalante-Semerena, 2004). This large domain (700-900 amino acids) seems to rather be involved in the oligomerization of the enzyme. Indeed, the autoacetylation of this domain by AcCoA triggers the formation of octamers, and 5 residues were identified as critical for the function of the enzyme (Thao and Escalante-Semerena, 2012). Nevertheless, the requirement of octameric state for *in vivo* activity has not yet been confirmed. Type III KATs have a C-terminal GNAT domain and a N-terminal regulatory domain. PatA from *Mycolicibacterium smegmatis*, which is allosterically regulated by cAMP, is part of this group. Type IV KATs are the most abundant and do not exhibit any regulatory domains. They are thought to acetylate a wide range of protein substrates, but also small non-protein molecules (VanDrisse *et al.*, 2017). This characteristic is also found for the only one characterized KAT that belongs to the type V: Eis from *Mycobacterium tuberculosis* (Zaunbrecher *et al.*, 2009; Ghosh *et al.*, 2016; Kim *et al.*, 2012), which is nonetheless larger.

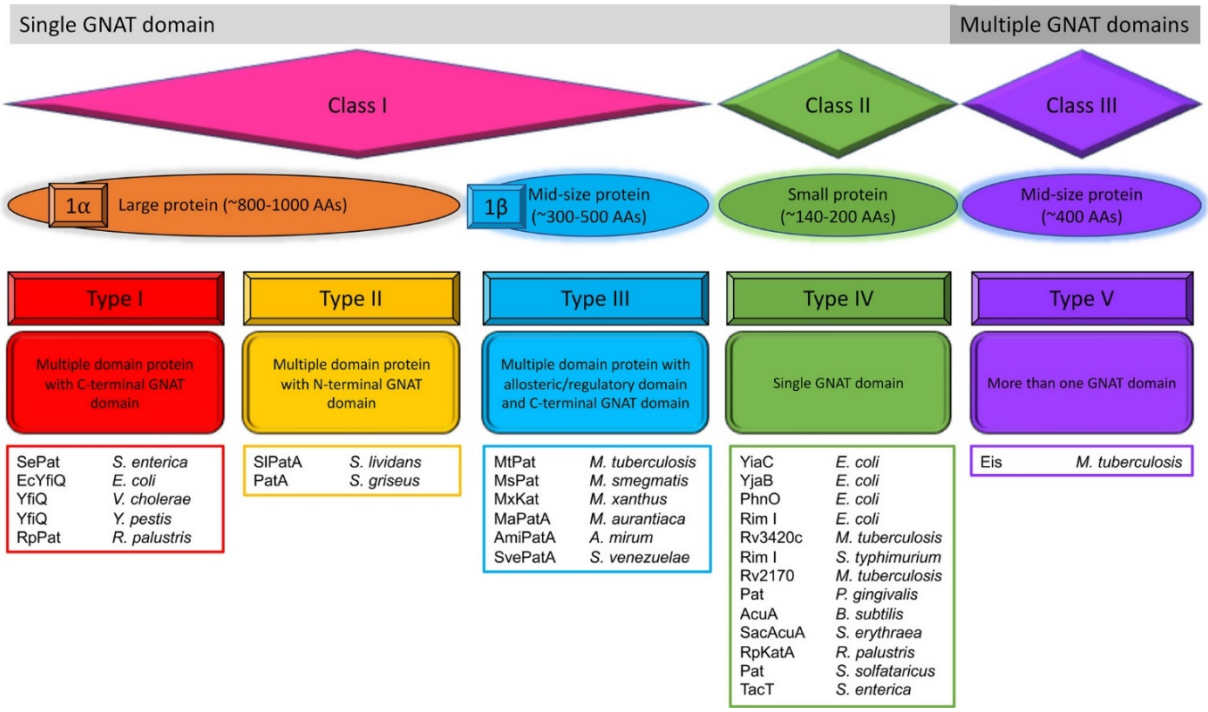

Figure 10 : (From Christensen *et al.*, 2019c) Classification of KATs among bacteria.
Bacterial KATs are currently categorized into three classes (I, II and III) depending on their size, and subdivided into five types (I to V) depending on the type and arrangement of domains they are made of. For each type, characterized representatives are displayed.

Chemical mechanism of enzymatic N^{ε} lysine acetylation involves three steps: (i) deprotonation of the target lysine, (ii) nucleophilic attack of the carbonyl carbon of the lysine on the acetyl group of AcCoA, and (iii) protonation and dissociation of CoA (Vetting *et al.*, 2005). In the catalytic pocket of KATs, a base, generally a glutamate (E), deprotonates the target lysine (Trievel *et al.*, 1999). This deprotonated lysine then performs a nucleophilic attack on the AcCoA, bound to the KAT *via* positive charge. As a result, acetylated lysine can be dissociated from the KAT, and finally, CoA must be protonated, mostly by a tyrosine residue from KAT's catalytic pocket, prior its release (Lin *et al.*, 1999; Christensen *et al.*, 2019a). Basics of this enzymatic N^{ε} lysine acetylation remain unchanged, even when lysine acetylation is non-enzymatically mediated.

IV-D-2) Non-enzymatic protein acetylation

In addition to KAT-mediated acetylation, a large body of evidence for non-enzymatic acetylation of N^{ε} lysine has grown the past few years. Both AcCoA and the bacterial metabolite acetyl-phosphate (AcP) have been shown to acetylate lysine residues of a wide variety of proteins *in vitro* (Ramponi *et al.*, 1975). Recently, acetylome studies even indicated that AcP is the predominant acetyl donor among some bacterial species, such as *E. coli* (Weinert *et al.*, 2013) and *B. subtilis* (Kosono *et al.*, 2015). Indeed, mutants impaired in the synthesis or degradation of AcP displayed an overall alteration in the acetylome profile (Kuhn *et al.*, 2014). While AcP naturally hydrolyses inside the water (Koshland, 1952) to non-enzymatically acetylate proteins, this phenomenon is favoured in high pH conditions for AcCoA. Furthermore, concentrations of AcCoA and AcP required to acetylate lysine residues *in vitro* appear to be similar or even lower than their physiological concentrations in *E. coli* (i.e. 20-600 µM for AcCoA and 3 mM for AcP) (Takamura and Nomura, 1988; Klein *et al.*, 2007). However, the non-enzymatic acetylation of lysine residues varies drastically from one lysine to another, and also depending on the acetyl donor (Baeza *et al.*, 2015). While certain lysine residues are specifically acetylated by AcCoA and not by AcP, or *vice versa*, acetylation rates differ strongly from one site to another one on the same protein. Overall, acetylation rates were higher for lysine residues clustered with basic residues whereas they are reduced on lysines interacting with acidic residues, suggesting that non-enzymatic acetylation depends on the immediate environment of the lysine.

AcP-mediated N^{ε} lysine acetylation appears to be essential for the translational machinery in *E. coli*. Indeed, AcP acetylates most ribosomal subunits, aminoacyl-tRNA ligases and elongation factors. However, the effect of these PTMs on the translational rate or fidelity remains elusive to this day. Central metabolism (i.e. Embden–Meyerhof–Parnas and Pentose Phosphate pathways, TriCarboxylic Acid cycle) appears to be another major target of the AcP-dependant acetylation and some functional consequences have been identified in this case (Nakayasu *et al.*, 2017). Thus, AcP-dependant acetylation of enolase from *E. coli* and *B. subtilis*, as well as glyceraldehyde 3-phosphate dehydrogenase and L-lactate dehydrogenase

from *Borrelia burgdorferi* (Bontemps-Gallo *et al.*, 2018) leads to the inhibition of their respective activities. At variance, malate dehydrogenase from *E. coli*, to our knowledge, is the only reported enzyme with enhanced activity when acetylated by AcP (Venkat *et al.*, 2017).

As previously stated, the chemical mechanisms for non-enzymatic acetylation of lysine are similar to those mediated by KATs. The major difference is that in the absence of KAT, a nearby glutamate performs the lysine deprotonation, while AcP or AcCoA binds to a neighbouring positively charged amino-acid, such as arginine or lysine. The follow-up remains the same as in KAT-mediated acetylation: the deprotonated lysine performs a nucleophilic attack on AcP or AcCoA, and orthophosphate or CoA are released, respectively (Christensen *et al.*, 2019a). Even if non-enzymatic acetylation mostly occurs on surface-exposed lysine, the small size of AcP and AcCoA allow them to act on internal residues, inaccessible from KATs (Kuhn *et al.*, 2014), emphasizing the relevance of this non-enzymatic mechanism to the regulation of important metabolic pathways.

IV-E. Deacetylation of lysine in Bacteria

N^{ε} lysine acetylation is a dynamic and reversible process for the quick activation and repression of a vast variety of proteins. This reversibility is performed by lysine deacetylases (KDACs), primarily called histone deacetylases (HDACs) as histones were the first identified targets of these newly discovered activities (Vidal and Gaber, 1991; Taunton *et al.*, 1996; Imai *et al.*, 2000). Currently, KDACs are categorized into 2 large families and 4 classes: the Zn^{2+}-dependant deacetylases family (Classes I, II and IV) (Yang and Seto, 2008) and the NAD^{+}-dependant sirtuin family (class III) (Blander and Guarente, 2004; Hodawadekar and Marmorstein, 2007). Overall, bacterial genomes tend to encode one or two sirtuin homologs, while most of them, with the notable exception of *E. coli* also encodes Zn^{2+}-dependant deacetylases (VanDrisse and Escalante-Semerena, 2019).

The Zn^{2+}-dependant deacetylases are simple hydrolases, which do not need any cofactor, and cleave the acetyl group of the targeted lysine to release acetate (Figure 9B). Activity requires a conserved histidine and Zn^{2+} to attack the acetyl group. While no such enzyme has been identified in *E. coli*, some Zn^{2+}-dependant deacetylases were identified in other species, such as AcuC in *Bacillus subtilis* (Gardner *et al.*, 2006) and LdaA in *Rhodopseudomonas palustris* (Crosby *et al.*, 2010).

Class III KDACs, or sirtuins, deacetylate lysine residues using NAD^{+} as a cofactor, releasing nicotinamide, a strong inhibitor of sirtuins (Schmidt *et al.*, 2004), and 2′-*O*-acetyl-ADP-ribose (Figure 9C). Since intracellular NAD^{+} level is linked to nutritional status and therefore energy homeostasis, we can assume that sirtuins are essential for the adaptation of the cell to these changes (Frye, 2000). According to this assumption, defective sirtuins in Human led to severe diseases, such as neurodegenerative or cardiovascular diseases (Ren *et al.*, 2017). The first identified and best studied sirtuin among bacteria is CobB from *Salmonella enterica* (Starai *et*

al., 2002). Several CobB homologs were further identified in various species, including *E. coli* (Zhao *et al.*, 2004). CobB is active on a broad range of substrates that may be enzymatically or non-enzymatically acetylated on lysines (AbouElfetouh *et al.*, 2015). Whereas sirtuins are classically annotated as deacetylases, it turns out that they can perform additional hydrolytic activities on post-translational modified lysines, notably on acyl groups, such as desuccinylation (Colak *et al.*, 2013), deproprionylation (Sun *et al.*, 2016) and debutyrylation activities (Xu *et al.*, 2018). In addition to these deacylase activities, an additional class of sirtuins, called SirTMs, has been reported in *Staphylococcus aureus* and has been shown to rather catalyses the ADP-ribosylation of certain aspartate residues (Rack *et al.*, 2015).

However, the number of deacetylases encoded in bacterial genomes may be underestimated, as some exotic proteins which do not fit into either Zn^{2+}-dependant KDAC or sirtuins, possess a KDAC activity. This is the case with YcgC in *E. coli*, recently identified as a functional KDAC (Tu *et al.*, 2015). Interestingly, YcgC, which belongs to the serine hydrolase family, deacetylates various substrates that differ from those of CobB.

IV-F. Production of AcCoA and AcP

Acetyl-CoA, the only acetyl donor for the enzymatic N^{ε} lysine acetylation, is produced from several metabolic pathways in bacteria. Glucose metabolism (Embden-Meyerhof-Parnas pathway) and short-chain fatty acids account for a large part of AcCoA production. Furthermore, the deamination and oxidation of free amino acids accumulation during proteolysis lead to an additional source of AcCoA (Figure 11). This high energy metabolic is then used by the cell for a variety of purposes, such as synthesis of fatty acids for membrane production, production of reducing equivalents *via* TCA cycle, or protein acetylation (VanDrisse and Escalante-Semerena, 2019). In addition, AcCoA is generated by the AMP-forming acetyl-CoA synthetase Acs from acetate under low acetate conditions (approx. 10 mM), when no better carbon source is available. However, under high acetate conditions (approx. 50 mM), the PTA-AckA pathway takes over the consumption of acetate: acetate is activated in AcP by the acetate kinase AckA, which is then converted into AcCoA by the phosphotransacetylase PTA.

Action of this PTA-AckA pathway is however reversible. In high concentration of available carbon in the environment, the flux of carbon through glycolysis depletes the limiting pool of AcCoA faster than it can be recycled. In this context, and even in aerobic conditions, *E. coli* will ferment acetate from AcCoA *via* PTA-AckA pathway, releasing free CoA, in a process called overflow metabolism (Peebo *et al.*, 2014; Wolfe, 2005). During this process, production of AcP by PTA is faster than its dephosphorylation by AckA, leading to the accumulation of AcP (Keating *et al.*, 2008; Klein *et al.*, 2007). Thus, when *E. coli* grows in the presence of excess carbon nutriment, AcP accumulates during acetate fermentation, and overall level of

protein acetylation increases (Kuhn *et al.*, 2014). It is noteworthy that acetate and AcP can respectively be produced directly from pyruvate by pyruvate dehydrogenase PoxB in *E. coli* (Dittrich *et al.*, 2005; Wolfe, 2005) and by pyruvate oxidase SpxB in *Streptococcus* spp (Spellerberg *et al.*, 1996).

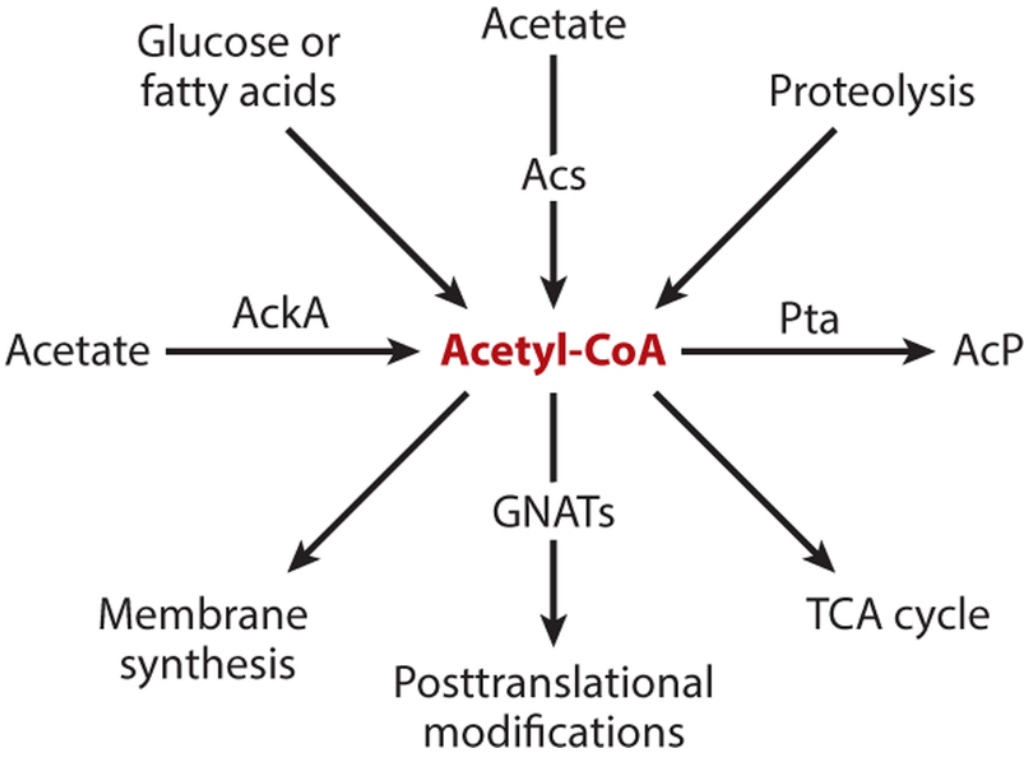

Figure 11 : (from VanDrisse and Escalante-Semerena, 2019) Sources and purposes of AcCoA in Bacteria. Metabolism of glucose and short chain fatty acids, as well as proteolysis, leads to the production of AcCoA. In addition, under low-acetate conditions, acetate is converted into AcCoA by the AMP-forming acetyl-CoA synthetase Acs, while under high-acetate conditions, acetate is activated into AcCoA by the acetate kinase AckA and further converted into AcP by the phosphotransacetylase PTA. Accumulated AcCoA is useful for various metabolic processes, like membrane synthesis, production of reducing equivalent *via* TCA cycle and enzymatic protein acetylation. Regarding AcP, its accumulation in Bacteria leads to the non-enzymatic acetylation of numerous protein targets.

Finally, in some lactic acid bacteria, AcP is produced through heterolactic pathway, also known as phosphoketolase pathway. In this metabolic route, glucose-6-phosphate is catabolised to form lactate, as an end product (Arsköld *et al.*, 2008). In *Lactobacillus* spp., the intermediate metabolite xylulose-5-phosphate is cleaved into glyceraldehyde-3-phosphate and AcP by xylulose-5-phosphate phosphoketolase XpkA (Posthuma *et al.*, 2002). On the other hand, *Bifidobacterium* spp. possess a unique glycolytic pathway involving the xylulose-5-phosphate/fructose-6-phosphate phosphoketolase XFP that produces AcP from both fructose-6-phosphate and xylulose-5-phosphate intermediates (Meile *et al.*, 2001). Nonetheless, the impact of this pathway on AcP accumulation and overall level of protein acetylation is yet to be figured out.

Objectives of the thesis

For many years, my laboratory has been interested in the role of *Chlamydiae* in the establishment of primary plastid endosymbiosis. This interest led my laboratory to propose the *Ménage à trois* hypothesis. According to this hypothesis, presence of an ancestral *Chlamydiae* would have facilitated the establishment of a symbiotic link between the cyanobiont and the ancestral heterotrophic eukaryote during this unique event which led to the emergence of photosynthetic eukaryotes (Ball *et al.*, 2011). In particular, metabolism of storage polysaccharides is supposed to be a major driver in the establishment of this symbiotic link. In this context, particular interest was brought on the enzymes involved in the glycogen metabolism of *Chlamydiae*, and my lab demonstrated that the chlamydial genes *glgA* and *glgX*, coding for a glycogen synthase and a direct debranching enzyme, respectively, were transferred to the ancestor of *Archaeplastida* (Ball *et al.*, 2011, 2015; Facchinelli *et al.*, 2013). However, during this survey of chlamydial glycogen metabolism, we noticed a peculiarity within the *Waddliaceae* (*Waddlia chondrophila*) and *Criblamydiaceae* (*Estrella lausannensis* and *Criblamydia sequanensis*) families: no gene coding for ADP-glucose pyrophosphorylase (*glgC*) was detected within their genome. However, despite the genome streamlining process due to their obligate intracellular lifestyle, all *Chlamydiae* species have retained functional glycogen metabolism. This raises the question: Could *Waddliaceae* and *Criblamydiaceae* be exceptions within the *Chlamydiae* phylum?

Objectives of my thesis are therefore: (i) to ensure that GlgC is not functional in these two families, (ii) to figure out if these environmental *Chlamydiae* are still able to accumulate glycogen particles. In the scenario of glycogen accumulation despite a functional defect in the GlgC activity, objectives will then be to (iii) identify an alternative activity for the synthesis of ADP-glucose, or an alternative pathway for the synthesis of glycogen in these species.

Results

I. State of art of glycogen metabolism in the *Chlamydiae* phylum

I-A. Not all *Chlamydiae* possess an entire classical GlgC-pathway

Chlamydiae have this particularity, as obligate intracellular bacteria, to synthesize glycogen particles during their developmental cycle. In *Chlamydiaceae*, like *Chlamydia trachomatis*, synthesis of storage polysaccharides relies on the GlgC-pathway. Environmental *Chlamydiae* also possess genes of this pathway with the exception of two families, *Waddliaceae* and *Criblamydiaceae* that include three species (*Waddlia chondrophila* in *Waddliaceae* family, *Criblamydia sequanensis* and *Estrella lausannensis* in *Criblamydiaceae* family). A survey of gene content showed that these three species lack a *glgC* gene and have a fused *glgA-glgB* gene (Table 2).

	glgC	*glgA*	*glgA-glgB*	*glgB*	*glgP/malP*	*malQ*	*galU*	*glgX*
Chlamydia trachomatis	1	1	-	1	1	1	-	1
Parachlamydia acanthamoeba UV7	1	1	-	1	2	1	-	1
Parachlamydia sp. C2	1	1	-	1	2	1	-	1
Protochlamydia massiliensis	2	1	-	1	1	1	-	2
Protochlamydia naegleriophila	1	1	-	1	1	1	-	3
Waddlia chondrophila	-	-	1	1	1	1	-	1
Criblamydia sequanensis	-	-	1	1	1	1	-	1
Estrella lausannesis	-	-	1	1	1	1	-	1
Simkania negevensis	1	1	-	1	1	2	-	1

Table 2 : Summary of genes involved in the classical glycogen metabolism found in 9 *Chlamydiae* species. A schematic tree represents the phylogeny of these species at the left of the figure. The number of each gene found in the genome of the nine different species is indicated. *W.* chondrophila, *C. sequanensis* and *E. lausannensis* lack a *glgC* gene while their *glgA* and *glgB* gens are fused, with the presence of a premature stop codon into the *glgA-glgB* gene of *E. lausannensis*. *glgC*: ADP-glucose pyrophosphorylase ; *glgA*: glycogen synthase ; *glgA-glgB*: fused glycogen synthase with branching enzyme ; *glgB*: branching enzyme ; *glgP/malP*: glycogen/maltodextrin phosphorylase ; *malQ*: 4-α-glucanotransferase ; *galU*: UDP-glucose pyrophosphorylase ; *glgX*: debranching enzyme.

Furthermore, a premature stop codon in the *glgA-glgB* gene of *E. lausannensis* leads to the expression of a truncated protein that lacks the GH13 (branching) domain and some highly conserved residues in the GT5 (synthase) domain that are part of the nucleotide binding and catalytic sites (Figure 12). The finding that some chlamydial glycogen synthases, notably in *Chlamydiaceae* are able to use either ADP-glucose or UDP-glucose to elongate malto-oligosaccharides, prompt us to carry out blast searches to identify *galU* gene, coding the bacterial UDP-glucose pyrophosphorylase. However, no *galU* was identified in *Chlamydiae* genomes, suggesting that no synthesis of nucleoside-sugars occurs in *W. chondrophila*, *C. sequanensis* and *E. lausannensis*.

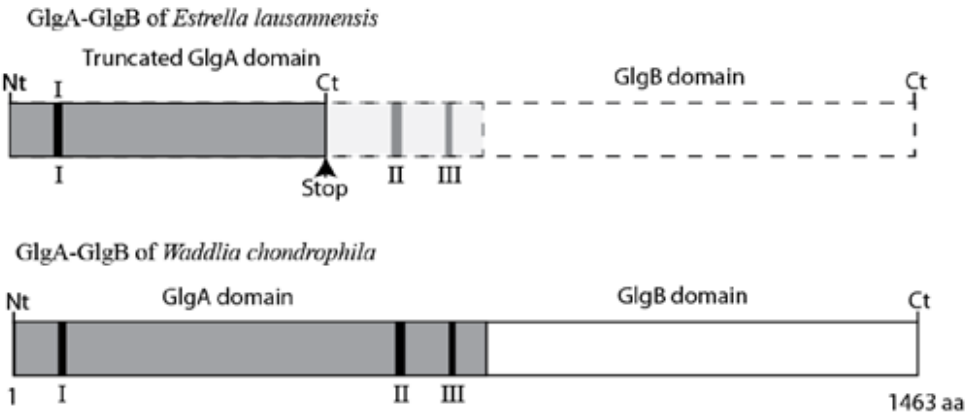

Figure 12 : Domain organization of the fused GlgA-GlgB proteins of *E. lausannensis* and *W. chondrophila*. GT 5 Glycogen synthase domain (gray box) and GH 13 branching enzyme domain (white box) are respectively located at the N- (Nt) and C-termini (Ct) respectively. The insertion of one-nucleotide in *E. lausannensis* sequence results in a frame shift leading to the truncation of GlgA-GlgB protein. Regions I, II and III represent highly conserved sequences of GT5 family glycogen synthases that include amino acid residues involved in the catalytic site and nucleotide binding sites.

To further investigate whether GlgA-GlgB of *E. lausannensis* and *W. chondrophila* arbour a functional glycogen synthase domain, his-tagged recombinant proteins were expressed in a *ΔglgA* BW25113 *E. coli* strain lacking endogenous glycogen synthase activity. Their activity was assayed by measuring the incorporation of labelled ^{14}C-glucosyl moieties from ADP- or UDP-^{14}C-glucose onto glycogen and by performing a specific zymogram (or native PAGE) to visualize glycogen synthase activities (Figure 13). These experiments were performed by a previous Ph.D. student in my lab: Mathieu Ducatez (Ducatez, 2015). Recombinant GlgA-GlgB proteins were separated on native PAGE containing 0.6% glycogen and gels were incubated overnight in the presence of 1.2 mM ADP- or UDP-glucose. After soaking gels in iodine solution, elongation of glucose chains by glycogen synthase activity is visualised as dark bands.

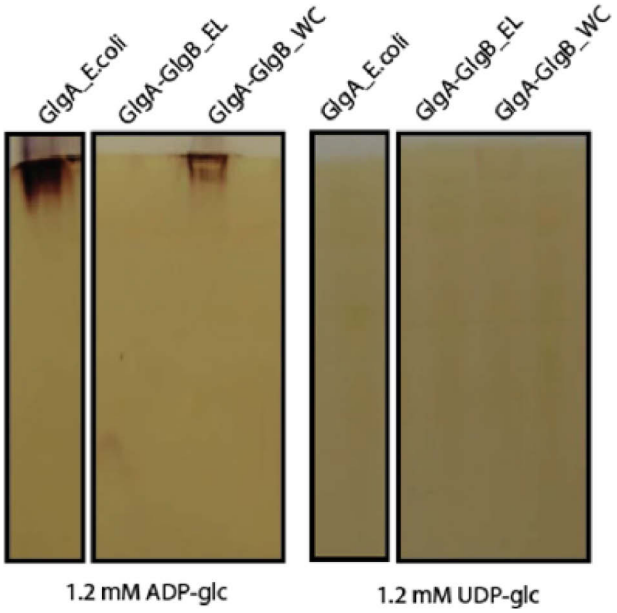

Figure 13 : (from Ducatez, 2015) Zymogram analysis of recombinant glycogen synthases. Recombinant his-tagged glycogen synthase from *E. coli* (GlgA_Ecoli) and chimeric glycogen synthase – branching enzymes from *E. lausannensis* (GlgA-GlgB_EL) and *W. chondrophila* (GlgA-GlgB_WC) were expressed in *ΔglgA* BW25113 *E. coli* derivative. Crude extracts were separated on native PAGE containing 0.6% glycogen and gels were further incubated overnight in the presence of 1.2 mM ADP glucose (left panel) or 1.2 mM UDP-glucose (right panel). Gels were then soaked into an iodine solution to visualize elongation of glucose chains as dark bands. Glycogen synthase domain of GlgA-GlgB_WC is functional with ADP-glucose, whereas no activity was observed for GlgA-GlgB_EL. Like GlgA_Ecoli, both chimeric enzymes are not able to use UDP-glucose as a substrate.

Both enzymatic assays and zymogram analyses showed that GlgA-GlgB of *W. chondrophila* has a functional glycogen synthase activity that is highly specific for ADP-glucose with little or no activity with UDP-glucose. Consistent with the presence of a premature stop codon, no glycogen synthase activity was observed with GlgA-GlgB of *E. lausannensis*.

We further investigated whether the branching activity domain at the carboxy-terminus of the chimeric GlgA-GlgB protein of *W. chondrophila* was also functional. To do so, the recombinant enzyme was incubated overnight with ADP-glucose (3 mM) and maltoheptaose (10 mg.ml^{-1}) by a previous Ph.D. student in my lab: Derifa Kadouche. Subsequently, the formation of branching points (i.e. α-1,6 linkages) on malto-oligosaccharides can be specifically observed by the resonance of protons onto carbon 6 at 4.95 ppm using proton-NMR analysis. However, no signal was observed at 4.95 ppm (Figure 14), suggesting that no branching point was formed by GlgA-GlgB_WC. This result is consistent with other studies (Binderup *et al.*, 2000, 2002) that indicate that long extension on the amino-terminus of branching enzymes lowers their activity.

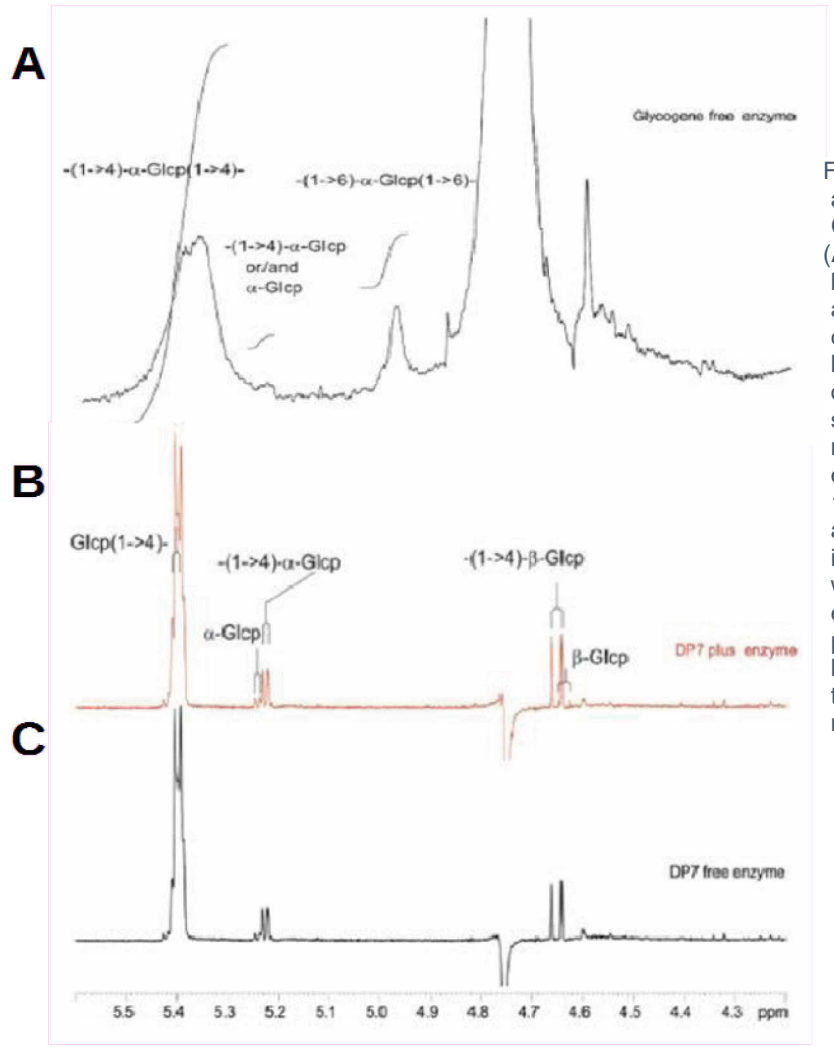

Figure 14 : Proton NMR analysis to assess the branching activity of GlgA-GlgB of *W. chondrophila*. (**A**) Analysis of glycogen from rabbit liver. Protons that resonate at 5.4 and 4.95 ppm respectively correspond to α-,1.4 and α-1,6 linkages. Protons in α and β position on the reducing ends generate signals at 5.23 and 4.65 ppm respectively. To assess branching enzyme activity of GlgA-GlgB_WC, 10 mg.ml^{-1} of maltoheptaose (DP7) and 3 mM ADP-glucose were incubated overnight with (**B**) or without (**C**) the recombinant enzyme. Absence of signal at 4.95 ppm strongly suggests that no branching point was formed and therefore that GlgA-GlgB_WC does not possess any branching activity.

Altogether, these data strongly suggest that the classical GlgC-pathway for glycogen synthesis is not functional in both *Waddliaceae* and *Criblamydiaceae* families (Figure 15).

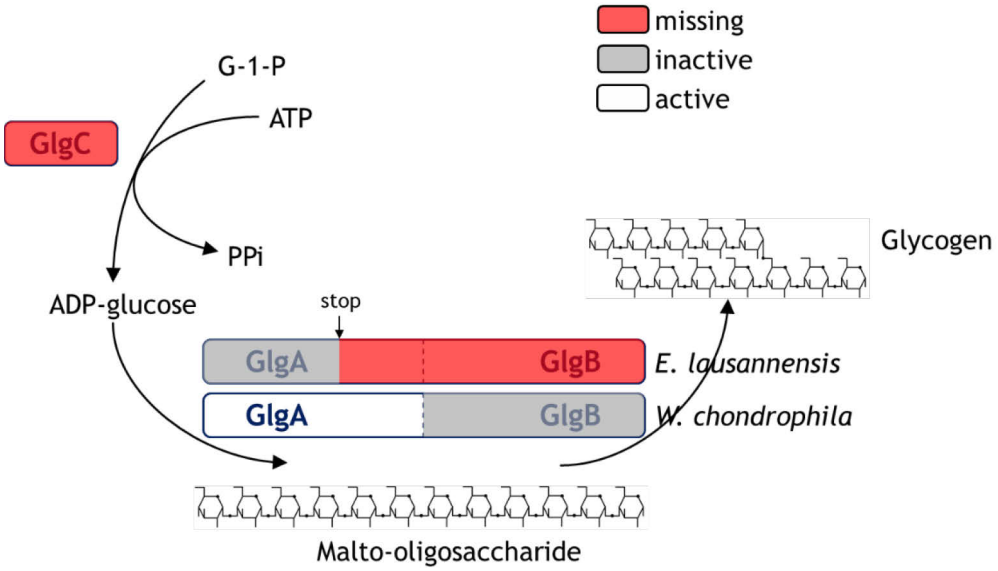

Figure 15 : Schematic representation of the glycogen-synthesizing GlgC-pathway in *E. lausannensis* and *W. chondrophila*.
Both species lack a functional ADP-glucose pyrophosphorylase (GlgC) and their glycogen synthases (GlgA) are fused with their branching enzymes (GlgB). This synthase activity is still functional in *W. chondrophila*, but a premature stop codon in the chimeric gene of *E. lausannensis* leads to the expression of a truncated and inactive enzyme.

I-B. *Estrella lausannensis* and *Waddlia chondrophila* accumulate glycogen particles

Since the GlgC-pathway is not functional in *E. lausannensis* and *W. chondrophila*, we decided to confirm that these species are exceptions within the *Chlamydiae* phylum, and are unable to synthesize glycogen particles. To do so, we infected the amoeba *Acanthamoeba castellanii* with either *E. lausannensis* or *W. chondrophila* and checked for the accumulation of glycogen particles within the cytosol of *Chlamydiae*. At twenty-four hours post infection, thin sections of infected *Acanthamoeba castellanii* (Figures 16A and 16C) and purified elementary bodies (Figures 16B and 16D) were subjected to specific glycogen staining based on the periodic acid method (PATAg staining) and observed in transmission electron microscopy. Glycogen particles appear as electron-dense particles (white head arrows) in the cytosol of elementary bodies of *E. lausannensis* and *W. chondrophila.* Therefore, *Criblamydiaceae* and *Waddliaceae* families, like all other families, accumulate glycogen particles within their cytosol. However, GlgC-pathway, the only way to synthesize glycogen that has been described in *Chlamydiae* is not functional in these two families. The next objective is therefore to explain how these two families are able to accumulate glycogen particles.

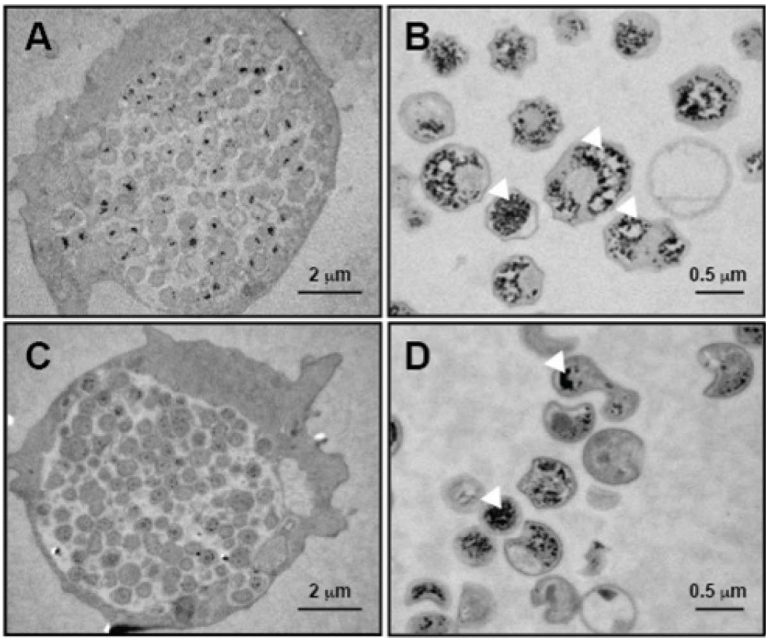

Figure 16 : Accumulation of glycogen particles within the cytosol of *Estrella lausannensis* (**A**, **B**) and *Waddlia chondrophila* (**C**, **D**).
Glycogen particles (white arrowed heads) were observed by transmission electronic microscopy after PATAg (periodic acid – thiocarbohydrazide – silver proteinate) staining of ultrathin sections of *Acanthamoeba castellanii* 24 h post infection (**A**, **C**) or purified bacteria (**B**, **D**). Both species accumulate electron-dense glycogen particles within their cytosol.

I-C. Two different glycogen metabolic pathways are identified in *Chlamydiae* phylum

As we mentioned, *Criblamydiaceae* and *Waddliaceae* families accumulate glycogen particles without a functional GlgC-pathway. In order to get some insight, we analysed 220 genomes (including some genomes assembled from metagenomic data) from 47 different chlamydial species that represent the currently known chlamydial diversity. The genomic database used in this study (https://chlamdb.ch/) includes genomes from both cultured and uncultured *Chlamydiae* species that cover the diversity of the *Chlamydiae* phylum (Figure 17B). A complete GlgC-pathway was found in most species, notably in all *Chlamydiaceae* (letter “d” on the figure), pathogens of vertebrates that underwent a large genome reduction, but also in some deeply branching families such as Candidatus *Parilichlamydiaceae* (“b”). As expected, *glgC* gene is lacking in *Waddliaceae* (“l”) and *Criblamydiaceae* (“m”) families, but also in Candidatus *Enkichlamydia* sp. (“i”), in Candidatus *Pelagichlamycidiaceae* (“a”), and one *Motilichlamydiaceae* sp. (“k”). It should be stressed out that genome coverage is quite incomplete in the last two (see percentages in brackets on Figure 17B), and *glgC* could be in a yet unsequenced genome region. However, in Candidatus *Enkichlamydia* sp., *glgC* gene is missing from 6 independent draft genomes estimated to be 71% to 97% complete, suggesting either the loss of *glgC* gene or that *glgC* is located in a particular genomic region (e.g., next to repeated sequences) that systematically led to its absence from genome assemblies.

More strikingly, GlgE-pathway, a set of enzymes producing glycogen from trehalose (Figure 17A), was found in *Criblamydiaceae*, *Waddliaceae*, and in some *Parachlamydiaceae*, including *Protochlamydia phocaeensis* (syn. *Parachlamydia* sp. C2), *Protochlamydia*

naegleriophila KNic (syn. Candidatus *Protochlamydia naegleriophila*) and *Protochlamydia naegleriophila* Diamant (syn. Candidatus *Protochlamydia massiliensis*).

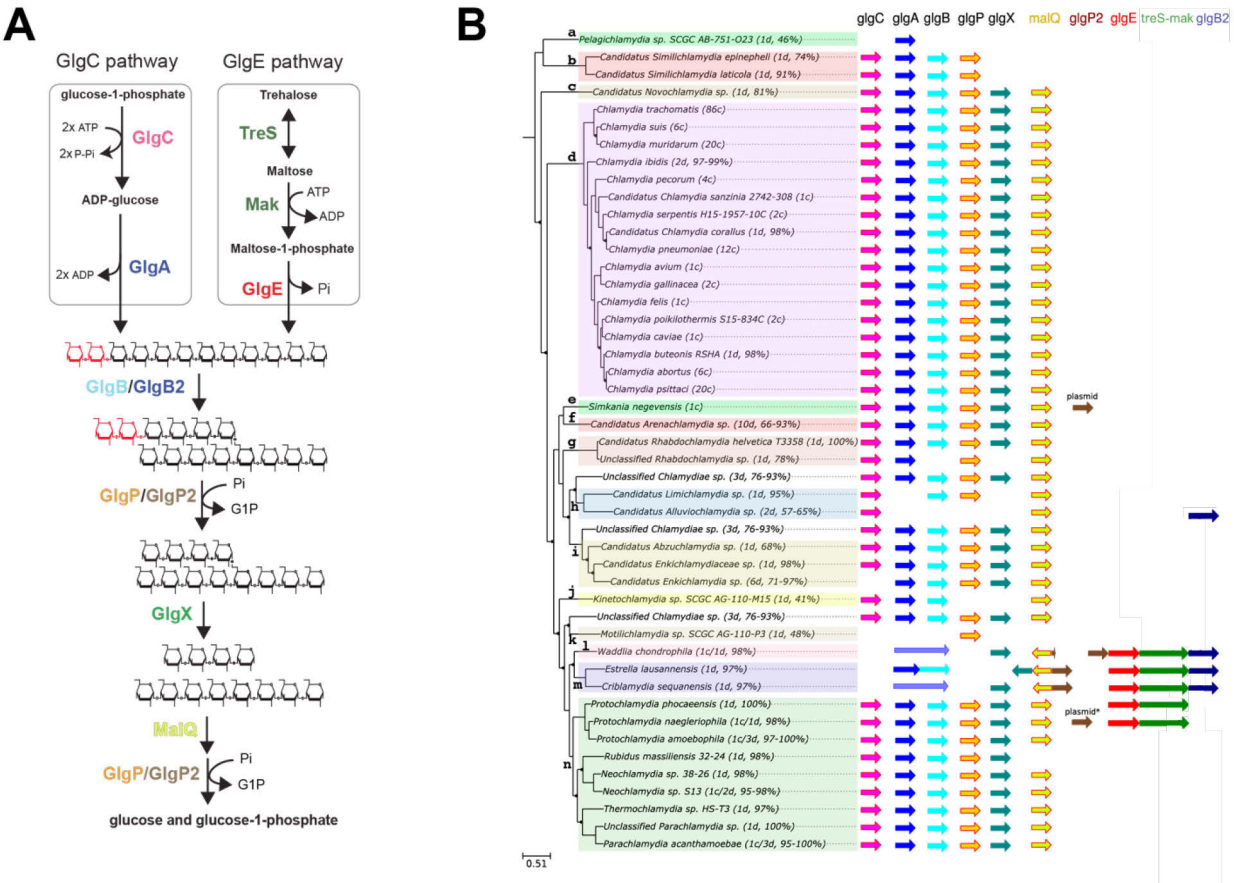

Figure 17 : Comparative genomic analysis of glycogen metabolizing genes among *Chlamydiae* phylum.
(**A**) GlgC- and GlgE-pathways represent the two main currently known routes for glycogen biosynthesis in bacteria. The formation of linear (α-1,4 linked) glucose chains relies on the successive actions of ADP-glucose pyrophosphorylase (GlgC) and glycogen synthase (GlgA) in GlgC-pathway while it depends on successive actions of trehalose synthase (TreS), maltokinase (Mak) and maltosyltransferase (GlgE) in the GlgE-pathway (more details in the introduction). Formation of branching points (α-1,6 linkages) is catalysed by one of the two branching isoforms: GlgB that is highly conserved in the entire *Chlamydiae* phylum and GlgB2, which is part of the GlgE operon (Figure 18) except in *Parachlamydiaceae* family where it is absent. The branched polysaccharide formed by either GlgC- or GlgE- pathway is then catabolized by the synergic actions of glycogen phosphorylase isoforms (GlgP and GlgP2), debranching enzyme (GlgX) and a-1,4 glucanotransferase (MalQ) to produce glucose-1-phosphate and glucose. (**B**) Phylogenetic tree of cultured and uncultured *Chlamydiae* species. For each species of the families: a, Ca. *Pelagichlamydiaceae*; b, Ca. *Parilichlamydiaceae*; c, Ca. *Novochlamydiaceae*; d, *Chlamydiaceae*; e, *Simkaniaceae*; f, Ca. *Arenachlamydiaceae*; g, *Rhabdochlamydiaceae*; h, Ca. *Limichlamydiaceae*; i, Ca. *Enkichlamydiaceae*; j, Ca. *Kinetochlamydiaceae*; k, Ca. *Motilichlamydiaceae*; l, *Waddliaceae*; m, *Criblamydiaceae*; n, *Parachlamydiaceae*, the number of draft (d) or complete (c) genomes and genome completeness expressed in percentage are indicated between brackets. Homologous genes of the GlgC- and GlgE-pathways are symbolized with coloured arrows.

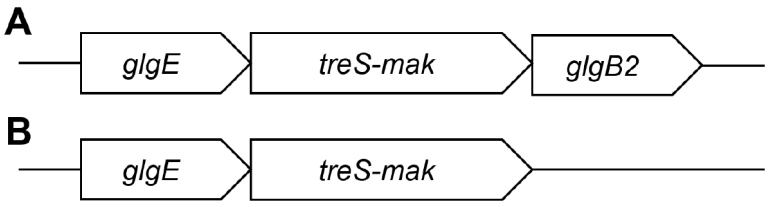

Figure 18 : Organisation of the *glgE* operon in *Chlamydiae* phylum.
In *Criblamydiaceae* and *Waddliaceae* families (**A**), the three genes involved in the GlgE-pathway form an operon with the succession of *glgE*, the fused *treS-mak* gene, and the *glgB2* isoform of branching enzyme. Same organisation is present in *Parachlamydiaceae* family (**B**), but *glgB2* is missing.

GlgE-pathway relies on trehalose synthase (TreS), maltokinase (Mak) and α-1,4-glucan:maltose-1-phosphate maltosyltransferase (GlgE) to produce malto-oligosaccharides that are then branched by one of the two isoforms of branching enzyme (GlgB/GlgB2) to form a glycogen particle (Figure 17A). As GlgC-pathway is not fully functional in *Criblamydiaceae* and *Waddliaceae* families, presence of the GlgE-pathway in these two families could explain the accumulation of glycogen observed on Figure 16. It is noteworthy that some *Parachlamydiaceae* possess two sets of genes to synthesize glycogen from both GlgC- and GlgE-pathways.

During our analysis, we noticed that the *glg* genes of the GlgC-pathway are at least 10 kbp apart with a notable exception for *glgP* and *glgC*, which are mostly separated by one or two genes. On the contrary, genes of the GlgE-pathway are arranged in an operon similar to what is found in *Mycobacteria* (Figure 18), with the notable fusion of *treS* and *mak* genes in chlamydial genomes, and the absence of *glgB2* gene in parachlamydial GlgE operons. This indicates that in each *Chlamydiae*, only one branching enzyme isoform is functional: GlgB2 in *Criblamydiaceae* and *Waddliaceae*, and GlgB in all other families. Furthermore, the occurrence of GlgE pathway restricted to *Parachlamydiaceae*, *Waddliaceae* and *Criblamydiaceae* families arises questions about its origin in *Chlamydiae*.

I-D. On the origin of GlgE-pathway in *Chlamydiae*

In order to get some insight on the origin of the GlgE operon in *Chlamydiae*, phylogenetic trees of GlgE (Figure 19A) and TreS-Mak (Figure 19B) were inferred using the phylobayes method. Even if *W. chondrophila* is split from other *Chlamydiae* sequences, GlgE seems to be monophyletic within the phylum, as the only strongly supported node (marked as red star) with a posterior probability (pp) higher than 0.95 (pp = 0.99) unifies all *Chlamydiae* sequences. This phylogeny analysis also highlights the presence of two distant phylogenetic groups of GlgE, named class I and class II GlgE, indicated on the right side of the tree. *Chlamydiae* and other PVC GlgE sequences belong to the class I while class II encompasses sequences of *Actinobacteria* (i.e., *Mycobacteria*, *Streptomyces*). To date, only a few actinobacterial maltosyltransferases have been characterized, and class II GlgE, including chlamydial ones, could potentially present yet unknown characteristics. More than that, GlgE is part of the glycoside hydrolase family 13 (CAZy - GH13) that encompasses a wide range of functions, and some class I GlgE sequences should be characterized before we could assume that they possess the same activities that class II GlgEs. Concerning TreS-Mak phylogeny, all chlamydial sequences cluster together, but with a relatively low statistical support (pp=0.93). However, GlgE and TreS-Mak seem to be monophyletic within the *Chlamydiae* phylum, excluding multiple lateral gene transfers. Even if the origin of GlgE operon cannot be pinpointed, 2 scenarios could explain its presence in *Chlamydiae*. First, GlgE may have been acquired in the common ancestor of *Parachlamydiaceae*, *Waddliaceae* and *Criblamydiaceae*,

and then lost in some *Parachlamydiaceae* species. The second possibility could be that GlgE operon reflects vestigial metabolic function of the ancestral *Chlamydiae* and then has been lost in most families while the genes of the classical GlgC-pathway were retained through genome streaming process. This is consistent with the loss of *glgB2* gene in *Parachlamydiaceae* (Figure 17B). However, in *Criblamydiaceae* and *Waddliaceae*, conservation of GlgE operon was favoured, leading to the loss of *glgC* as well as some rearrangements between *glgA* and *glgB* genes.

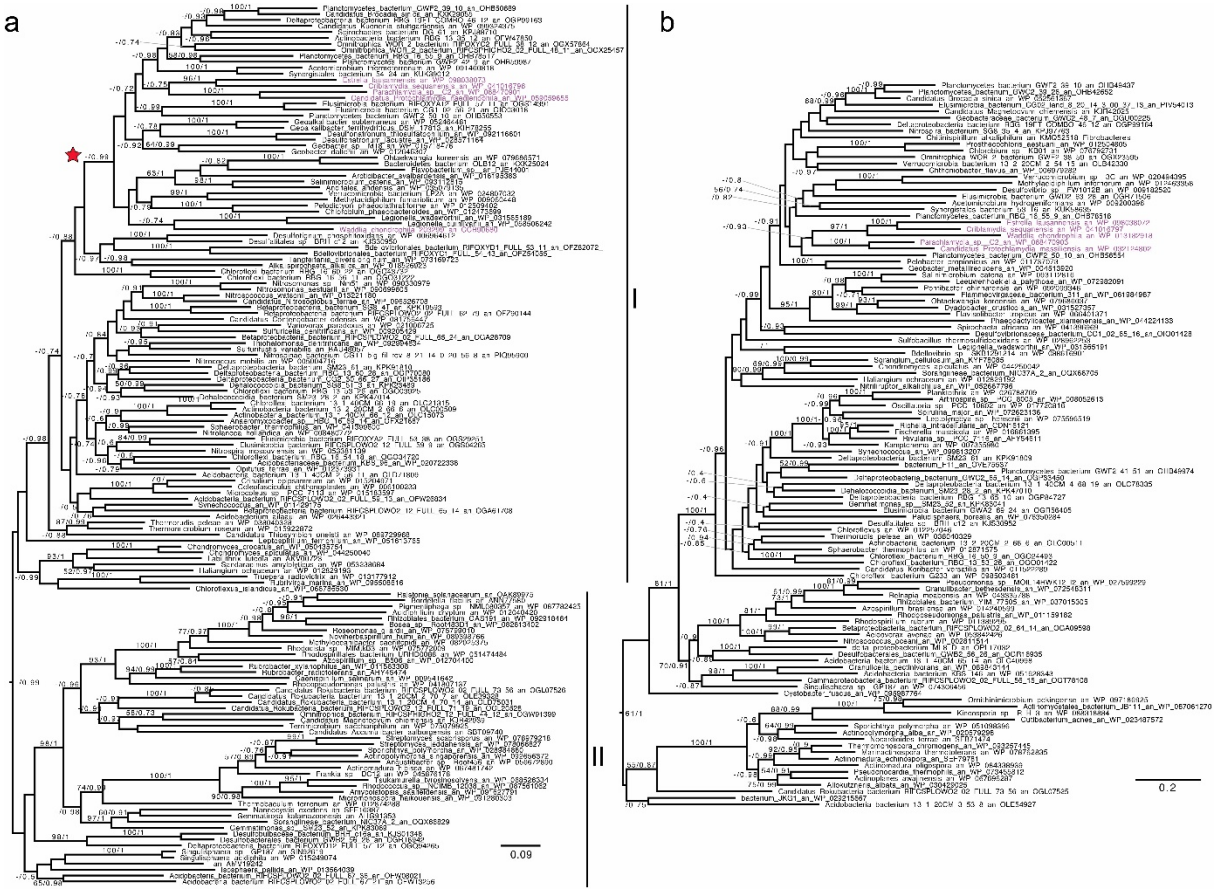

Figure 19 Phylogenetic analysis of GlgE (A) and TreS-Mak (B).
Trees displayed were obtained with Phylobayes under the C20+poisson model. We then mapped onto the nodes ML bootstrap values obtained from 100 bootstrap repetitions with LG4X model (left) and Bayesian posterior probabilities (right). Bootstrap values >50% are shown, while only posterior probabilities >0.6 are shown. The trees are midpoint rooted. The scale bar shows the inferred number of amino acid substitutions per site. *Chlamydiae* are in purple.

Nevertheless, acquisition of GlgE appears to be ancient, as, for example, *E. lausannensis* GlgE has a low sequence identity with other chlamydial sequences (55% with *C. sequanensis*, 49-51% with the rest), not so far from its identity with *Mycobacterium tuberculosis* (43%). It also must be stressed out that, although phylogeny of GlgE split sequences into two distinct classes, no specific signal (e.g., gaps, block sequences) can differentiate a class I protein from a class II protein directly from the sequence.

To resume these first data, comparative genomic analysis of glycogen metabolizing enzymes in *Chlamydiae* unravelled the presence of GlgE-pathway in *Criblamydiaceae*, *Waddliaceae* and in some *Parachlamydiaceae*. While GlgC-pathway is not complete in *Criblamydiaceae* and *Waddliaceae*, the existence of this alternative glycogen pathway may explain our observations in transmission electron microscopy (Figure 16). However, GlgE is part of the large GH 13 family, and phylogenetic analysis pinpoints that actinobacterial and chlamydial GlgE belong to two distinct groups, with potentially different characteristics and functions.

Our next objectives are then to ensure that sequences annotated as maltosyltransferases in *Chlamydiae* encode functional GlgE activities and to determine whether GlgE-pathway is sufficient to explain the accumulation of glycogen particles observed within the cytosol of *E. lausannensis* and *W. chondrophila*.

Moreover, despite its large occurrence in the *Bacteria* lineage (at least 14% of bacterial genomes ; (Chandra *et al*., 2011; Syson *et al*., 2020) GlgE-pathway has only been studied and characterized in *Actinobacteria*, more specially in *Mycobacterium tuberculosis*. New characterization of a phylogenetically distant GlgE-pathway could contribute to a greater understanding of its relevance and of the mechanisms that lead to the synthesis of glycogen. More than that, as depicted in Figure 4, glycogen metabolism pathway is complex in *Mycobacterium tuberculosis*, with the co-occurrence of both GlgC- and GlgE-pathways and the presence of a particular enzyme, GlgM, that possess both a maltose-1-phosphate producing activity and a glycogen synthase activity, acting as a bridge between the two pathways. In this context, *W. chondrophila*, and especially *E. lausannensis*, in which GlgC-pathway is totally impaired (Table 3), could be better models than *M. tuberculosis* to study GlgE-driven glycogen synthesis. Notably, absence of a glycogen synthase activity in *E. lausannensis* could help us to assess if GlgE-pathway is sufficient to produce a glycogen particle without the priming activity of GlgA.

Therefore, characterization of the enzymes of the GlgE-pathway, especially in *E. lausannensis*, is also part of the objectives of this thesis, as it could lead to further insight into the role and the physiological relevance of this pathway in bacteria.

	glgC	*glgA*	*glgA-glgB*	*glgB/glgB2*	*treS-mak*	*glgE*	*glgM*
Chlamydia trachomatis	1	1	-	1	-	-	-
Parachlamydia acanthamoeba UV7	1	1	-	1	-	-	-
Parachlamydia sp. C2	1	1	-	1	1	1	-
Candidatus Protochlamydia massiliensis	2	1	-	1	1	1	-
Candidatus Protochlamydia naegleriophila	1	1	-	1	1	1	-
Waddlia chondrophila	-	-	1	1	1	1	-
Criblamydia sequanensis	-	-	1	1	1	1	-
Estrella lausannesis	-	-	1*	1	1	1	-
Simkania negevensis	1	1	-	1	-	-	-

Table 3 : Summary of GlgC- and GlgE-pathways-related genes found in 9 Chlamydiae species.
The number of each gene found in the genome of the different species is indicated. *E. lausannensis* is a good model to study GlgE-pathway, as its genome only harbour genes of this pathway, and a *glgA-glgB* gene encoding an inactive enzyme. GlgM, the main producer of maltose-1-phosphate in *M. tuberculosis* is lacking in chlamydial genomes. *glgC*: ADP-glucose pyrophosphorylase ; *glgA*: glycogen synthase ; *glgA-glgB*: fused glycogen synthase with branching enzyme ; *glgB/glgB2*: branching enzyme ; *treS-mak*: fused trehalose synthase with maltokinase ; *glgE*: α-1,4-glucan:maltose-1-phosphate maltosyltransferase ; *glgM*: α-maltose-1-phosphate synthase. The asterisk for the *glgA-glgB* gene of *E. lausannensis* signals the presence of a premature stop codon leading to the expression of a truncated and not functional protein.

II. Characterization of GlgE homologs of *E. lausannensis* and *W. chondrophila*

II-A. Genes annotated as GlgE of *E. lausannensis* and *W. chondrophila* encode α-1,4-glucan:maltose-1-phosphate maltosyltransferases

II-A-1) Expression of recombinant GlgE homologs

Homologs of GlgE from *E. lausannensis* and *W. chondrophila* (accession numbers CRX38224.1 and CCB90680.1, respectively called GlgE_EL and GlgE_WC in the rest of the study) were cloned using Gateway™ technology in pET15b plasmid. A 6x-His tag was added at the amino-terminus to purify recombinant proteins using nickel affinity chromatography. Recombinant proteins were expressed in Rosetta™ *E. coli* strain and overexpression induced with 0.5 mM IPTG at the mid-log phase. After one night under agitation at 30°C, cells were harvested and proteins were extracted then purified on a nickel affinity column. Expression and purification were assessed by SDS-PAGE (Figure 20). While these conditions lead to a good level of expression for the recombinant protein from *E. lausannensis* (Figure 20A), little to no expression of GlgE_WC was observed. We therefore used an auto inducible medium (see material and methods) to express GlgE_WC and the conditions that lead to the maximal level of expression were kept during the rest of the study (Figure 20B).

For both recombinant proteins, purified enzymes appear as a doublet on SDS-PAGE, with denser upper bands that migrate as proteins of 76 kDa and 72 kDa, respectively, a few kDa less than the predicted molecular weights of GlgE_EL (81 kDa) and GlgE_WC (80 kDa).

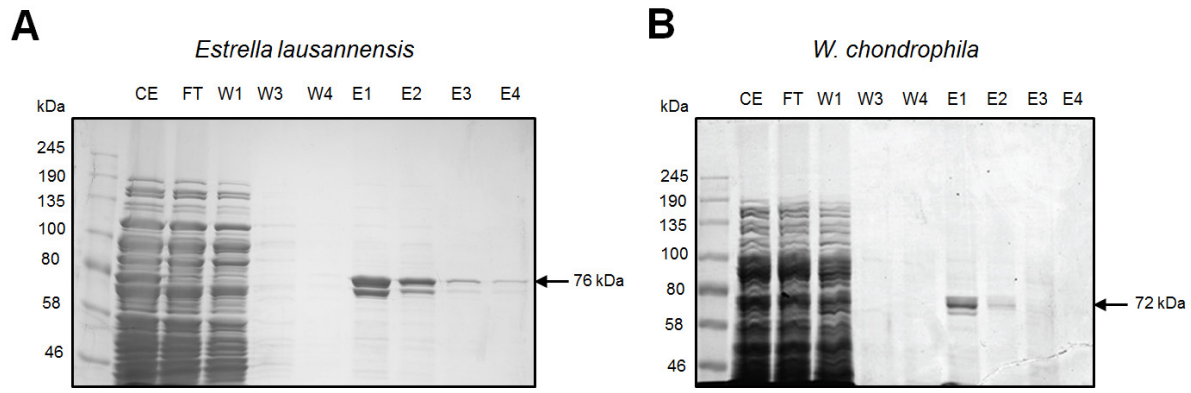

Figure 20 : SDS-PAGE analysis of purified recombinant GlgE_EL and GlgE_WC .
6xHis-tagged GlgE of *E. lausannensis* (**A**) and *W. chondrophila* (**B**) were expressed in Rosetta™ *E. coli* strain. After induction at mid-log phase with IPTG for GlgE_EL and culture in auto-inducible medium for GlgE_WC, the overnight cultures were harvested by centrifugation. Cell pellets were suspended into a buffer containing 25 mM Tris-acetate pH 7.5 and then subjected to sonication. After centrifugation, crude extracts (CE) were incubated on nickel affinity column at 4°C for one hour. Total proteins in both CE and affinity purification fractions - flow-through (FT), washing steps (W1 to W4) and elution (E1 to E4) fractions - were separated on 7.5% SDS-PAGE. Based on standard molecular weights, the apparent molecular weights of GlgE were estimated to be 76 kDa and 72 kDa for *E. lausannensis* and *W. chondrophila*, respectively. A doublet was observed for both purified enzymes.

II-A-2) Test of maltosyltransferase activities in the direction of glycogen degradation

GlgE activity transfers the maltosyl moiety of maltose-1-phosphate (M1P) to the non-reducing end of an α-1,4-linked glucose chain. Nevertheless, this reaction is defined as reversible (Kalscheuer *et al.*, 2010). In order to check whether chlamydial recombinant proteins were active and produce M1P after an overnight incubation with glycogen and orthophosphate, reaction products were separated on thin layer chromatography and revealed with orcinol-sulphuric acid (Figure 21A). This experiment indicates the presence of a new compound that migrates between maltopentaose (DP5) and maltotetraose (DP4). The incubation experiments conducted with GlgE_WC yielded little or no synthesis of this new compound. Purified GlgE_WC was concentrated 20 times, and then incubated under the same conditions as described above to clearly produce this compound (Figure 21B), suggesting a lower specific activity than GlgE_EL.

II-A-3) Both recombinant proteins can produce maltose-1-phosphate

To further characterize this compound, that we supposed to be M1P, time course analysis of alkaline phosphatase (PAL) treatment was performed on the purified reaction product obtained from sample E1 of GlgE-EL (see Material and methods on M1P purification). After 180 min of incubation, the initial product is completely converted into a compound with a similar mobility than maltose (DP2) (Figure 22A), which supports the idea that the maltose is derived from the dephosphorylation of M1P. The compound produced by GlgE_EL in presence of glycogen and orthophosphate was further characterized through mass spectrometry and proton-NMR analyses (Figures 22B-D). The combination of these approaches confirms that GlgE of *E. lausannensis*, as well as *W. chondrophila* (S1 Figure), catalyses the formation of a compound of 422 Da corresponding to α-maltose-1-phosphate.

The production of pure M1P (i.e., free of both orthophosphate and glucans) was scaled up in order to perform the enzymatic characterization of GlgE activities.

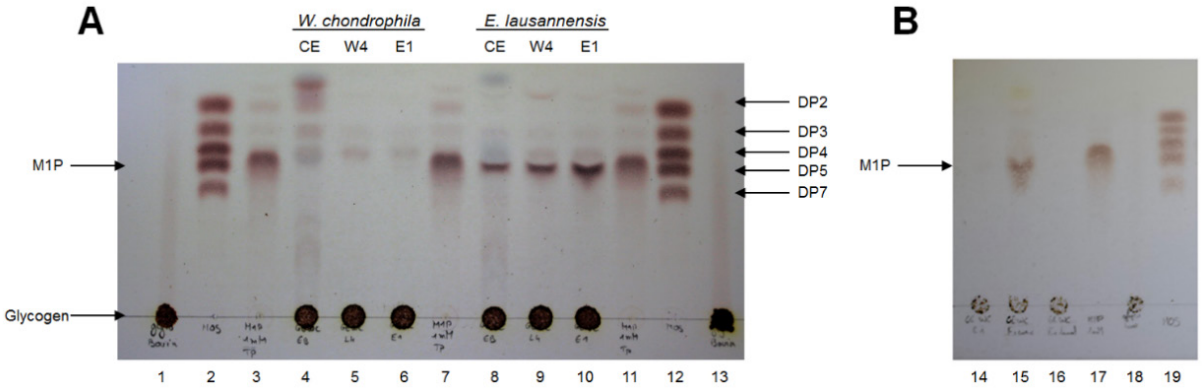

Figure 22 : Activity of GlgE_EL and GlgE_WC on thin layer chromatography.
(**A**) Cellular extract (CE), last washing step (W4) and first elution fraction (E1) of GlgE_WC (lanes 4, 5 and 6) and GlgE_EL (lanes 8, 9 and 10) were incubated overnight at 30°C with 5 mg.ml^{-1} glycogen and 20 mM orthophosphate in 20 mM Tris-HCl pH 6.8. Reaction products were separated on silica plate and carbohydrates were visualized after vaporisation of orcinol (0.2 %) sulphuric (20 %). A new compound that migrates between maltotetraose and maltopentaose appears in large quantities in the samples of *E. lausannensis*, especially with purified enzyme. As little to no activity was observed with GlgE_WC, (**B**) the purified enzyme (lane 14) was concentrated 20 times (lane 15) to repeat the experiment in the same conditions and the formation of a new compound was observed. Lanes 1, 13 and 18: glycogen. Lanes 2, 12 and 19: mix of maltose (DP2), maltotetraose (DP3), maltotetraose (DP4), maltopentaose (DP5) and maltoheptaose (DP7). Lanes 3, 7 and 11: maltose-1-phosphate (M1P) controls.

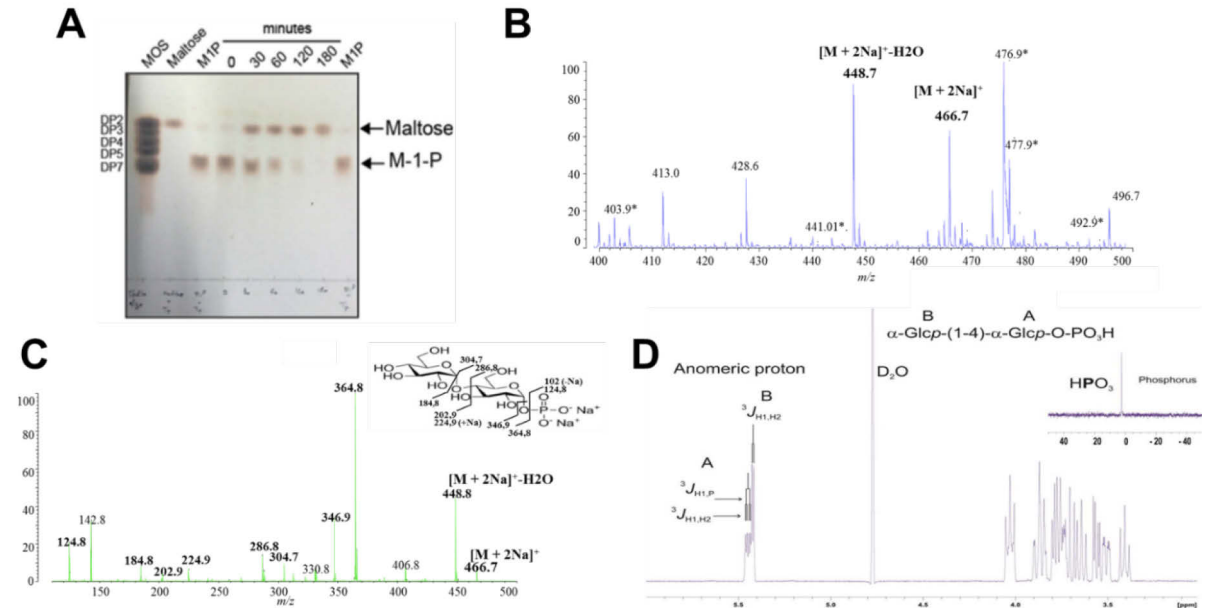

Figure 21 : GlgE_EL produces M1P from glycogen orthophosphate.
(**A**) After purification, the compound produced by GlgE_EL was incubated in presence of 1U alkaline phosphatase (PAL). Times course analysis (0 to 180 minutes) shows a complete conversion of this unknown compound into maltose. (**B**) MALDI-QIT-TOF-MS profile of the purified compound obtained in the positive mode. Peaks at m / z = 448.7 and 466.7 correspond respectively to a maltose-phosphate with 2 sodium ions and the loss of a water molecule or not, respectively. The peaks marked with a star (*) correspond to the matrix. (**C**), MS-MS sequencing profile of M1P. The molecular ion [M + 2Na]+ at m/z 466,7 was fractionated in different ions. Peak assignments were determined according to panel incrusted on the top right. (**D**) ^{1}D-^{1}H-NMR spectrum of maltose-1-phosphate. α-anomer configuration of both glucosyl residues were characterized by their typical homonuclear vicinal coupling constants ($^{3}J_{H1A,H2A}$ and $^{3}J_{H1B,H2B}$) with values of 3.5 Hz and 3.8 Hz respectively. A supplementary coupling constant was observed for α-anomeric proton of residue A as shown the presence of the characteristic doublet at 5.47 ppm. This supplementary coupling constant is due to the heteronuclear vicinal correlation ($^{3}J_{H1A,P}$) between anomeric proton of residue A and phosphorus atom of a phosphate group, indicating that phosphate group was undoubtedly O-linked on the first carbon of the terminal reducing glucosyl unit A. The value of this $^{3}J_{H1A,P}$ was measured to 7.1Hz. Sum of these experiments clearly demonstrated that GlgE_EL is able to produce α-maltose-1-phosphate.

II-A-4) GlgE_EL elongates α-1,4 glucans using maltose-1-phosphate

The maltosyltransferase activities of GlgE_EL and GlgE_WC were assessed in the elongation direction and analyzed on native polyacrylamide gel (i.e., zymogram). Cellular extract and purified GlgE_EL were loaded onto a native-PAGE containing 0.3 % bovine liver glycogen. After migration, the gel is cut and incubated in 3 different buffers overnight: one containing maltose-1-phosphate (M1P), another with orthophosphate (Pi), and the last one neither of the two (Ø). The gels are then stained with iodine solution to observe structural changes within glycogen molecules (Figure 23). The glycogen then turns orange - light brown. Darker staining indicates lengthening of the α-glucans, while weaker staining indicates degradation.

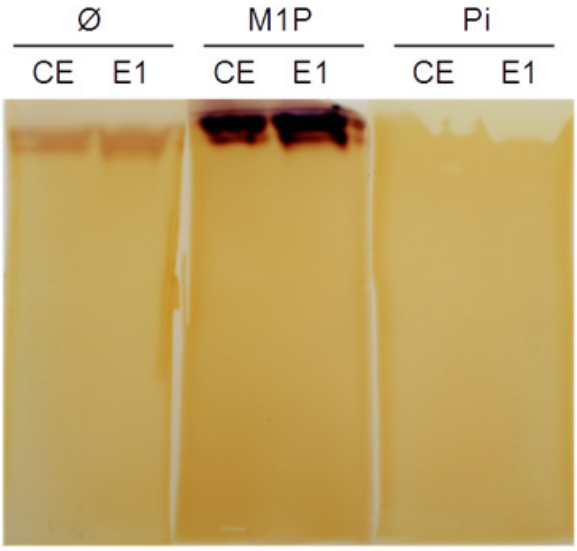

Figure 23 : Zymogram analysis of the GlgE activity of *E. lausannensis*.
Cellular extract (CE) and purified enzyme (E1) were loaded onto a native-PAGE containing 0.3 % glycogen. After migration, gels are soaked overnight in 25 mM Tris-acetate buffer (Ø), 25 mM Tris-acetate buffer supplemented with 1 mM M1P (M1P), or in 25 mM Tris-acetate buffer supplemented with 20 mM orthophosphate (Pi). Staining with iodine solution allows the visualization of structural changes in glycogen.

Incubated in the presence of M1P, dark bands appear at the entrance of the gel, which means that GlgE_EL catalyses the lengthening of glucose chains and has a strong affinity for glycogen. Conversely, in the presence of orthophosphate, the enzyme degraded glycogen enough so that no coloration was visible. More surprisingly, bands slightly darker than the glycogen are visible when the enzyme was only incubated in the presence of Tris-acetate buffer, suggesting slight structural rearrangement of glycogen. It must be pinpointed that several close bands (at least two) are visible, even with the pure enzyme. This strongly suggests that GlgE_EL has at least two functionally active forms that could be linked either to homodimerization of the enzyme or to the presence of post-translational modifications (Leiba *et al.*, 2013).

II-B. Determination of biochemical characteristics of GlgE from *E. lausannensis* and *W. chondrophila*

II-B-1) Substrate specificity of chlamydial maltosyltransferases

GlgE activity of *Mycobacterium tuberculosis* can elongate malto-oligosaccharides with maltosyl groups (DPn + 2) from M1P molecules with similar specificity from maltotetraose to maltoheptaose (Kalscheuer *et al.*, 2010). Here, the substrate specificity of chlamydial

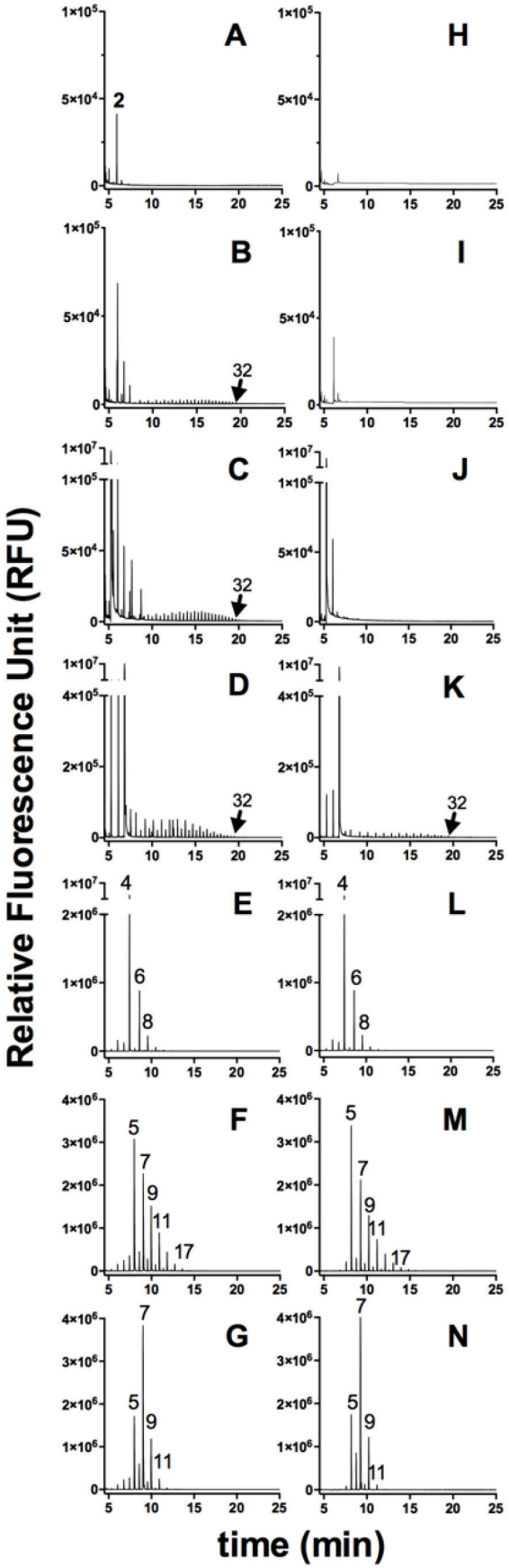

maltosyltransferases was assessed by incubating either purified GlgE_EL or GlgE_WC with 5 mM of malto-oligosaccharides ranging from DP0 (negative control) to DP7 (maltoheptaose) and 1.6 mM of M1P. In addition to its elongation activity, GlgE from *M. tuberculosis* appears to catalyse the disproportionation of DP4 and longer malto-oligosaccharides. To ensure whether the chlamydial GlgE activities possess this additional activity, strongly suggested by rearrangement of glycogen on Figure 23, incubations in the absence of M1P were also carried out. Incubation experiments were conducted at pH 6.8 and 30°C, for 1 hour or overnight, and reaction products were separated according to their degree of polymerization by capillary electrophoresis (Fluorophore Assisted Carbohydrates Electrophoresis, or FACE) (Figure 24, S2 Figure and S3 Figure).

Figure 24 : FACE analyses of enzymatic reaction products of GlgE_WC (**A** to **G**) and GlgE_EL (**H** to **N**).
Reactions were conducted overnight at 30°C and pH 6.8. Spontaneous dephosphorylation of M1P during overnight incubation was estimated by incubating denatured GlgE enzymes in buffer containing 1.6 mM M1P (**A** and **H**). The transfer of maltosyl moieties from M1P (1.6 mM) onto non-reducing ends of glucan acceptors (5 mM) were determined in absence of glucan acceptor (**B**, **I**) or in presence of glucose, (**C**, **J**), maltotriose (**D**, **K**), maltotetraose (**E**, **L**) and maltoheptaose (**F**, **M**). 4-α-glucanotransferase activities of GlgE were assessed by incubation of GlgEs with 5 mM of maltoheptaose, in absence maltose-1-phosphate (**G**, **N**). Numbers on the top of fluorescence peaks represent the degree of polymerizations of glucan chains.

The amount of maltose released from M1P due to spontaneous dephosphorylation during the experiment was appreciated by performing incubations with denatured

enzymes (Figures 24A and 24H). Incubation experiments showed that both GlgE_EL and GlgE_WC possess either maltosyltransferase or 4-α-glucanotransferase activities depending on the presence of M1P. When M1P is omitted, GlgE activities catalyse the disproportionation of malto-oligosaccharides composed of six or seven glucose units (DP6 or DP7). Interestingly, after one hour or overnight incubation, DP6 or DP7 are disproportionated with one or two maltosyl moieties leading to the release of shorter (DPn-2) and longer glucans (DPn+2) (Figures 24G and 24N and S2, S3 Figures). The limited number of transfers probably emphasizes a side reaction of GlgE activities. It is noteworthy that this side reaction was also observed on zymogram (Figure 23). However, both recombinant enzymes elongate malto-oligosaccharides constituted of at least 4 glucose units (Figures 24E and 24L), with better efficiency on DP6 and DP7 (Figures 24F and 24M). Moreover, after 1h reactions (S2 and S3 Figures), the elongation activity was clearly the main activity of both GlgE of *E. lausannensis* and *W. chondrophila*.

Another interesting result is the production of a small amount of long malto-oligosaccharides, up to DP32, when enzymes are incubated with only M1P or with M1P and DP≤3 (Figures 24B-D and 24K). This suggests that both enzymes possess a second side activity, probably a processive activity, to synthesize long malto-oligosaccharides only from M1P. The mechanism underlying the switch between the processive (on DP<4) and the distributive (on DP≥4) elongation activities probably reflects a competition of glucan primers for the glucan binding site in the vicinity of the catalytic site. Thus, we can hypothesize that the low affinity of short glucan primers (DP<4) for glucan binding site probably favours iterative transferase reactions onto the same acceptor glucan (i.e., processive mode) resulting in the synthesis of long glucan chains whereas glucan primers containing at least 4 glucose units compete strongly for the binding site, leading to the distributive mode.

II-B-2) Kinetic parameters of GlgE_EL

To further characterize GlgE_EL and GlgE_WC activities, kinetic parameters were determined in the biosynthetic direction, using malachite green assay to follow the liberation of orthophosphate. Specific activities for GlgE_EL and GlgE_WC are respectively 10 and 0.2 µmoles of released orthophosphate per minute and per mg of proteins. Because the specific activity of GlgE_WC is 50-fold lower than GlgE_EL, kinetic parameters were determined only for GlgE_EL.

II-B-2(a) Temperature and pH optimum

Prior to further characterization, we determined the optimum temperature and pH of the GlgE_EL (Figure 25). The enzyme appears to have optimal activity between 30°C and 40°C (Figure 25A). While activity slowly decreases at lower temperatures, it drops drastically above 40°C. In addition, GlgE_EL appears to reach its optimum activity under slightly acidic conditions, at pH 6 (Figure 25B). However, it will not be subsequently characterized at this pH to avoid the spontaneous hydrolysis of maltose-1-phosphate that occurs in acidic conditions.

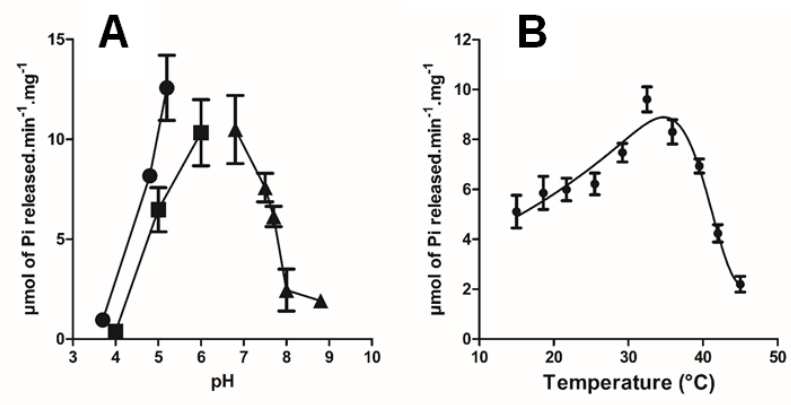

Figure 25 : Determination of the optimum temperature (**A**) and pH (**B**) of the GlgE of *E. lausannensis*.
The optimum temperature is determined by incubating the purified enzyme in a range of temperature from 15°C to 45°C in the presence of 5 mM DP7 and 1 mM M1P in a 50 mM Tris-HCl buffer pH 6.8. The optimum pH is determined at 30°C, with the same substrate concentrations as for temperature. The buffers used are 25 mM sodium acetate (●) at pH 3.7 ; 4.8 ; 5.2, 25 mM sodium citrate (■) pH 3 ; 4 ; 5 ; 6 and 25 mM Tris-HCl (▲) pH 6.8 ; 7 ; 7.5 ; 7.8 ; 8 ; 8.8).

II-B-2(b) Enzymatic constants

Kinetic constants of GlgE_EL were determined (Figure 26) and are resumed in Table 4.

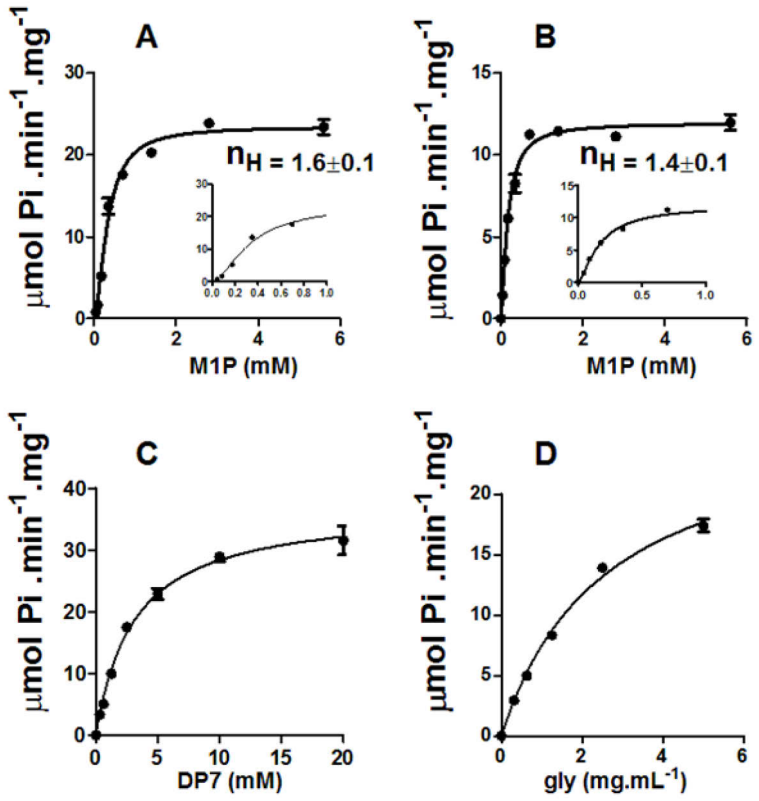

Figure 26 : Determination of the kinetic parameters of the GlgE_EL in the elongation direction.
Maltosyltransferase activity was assayed in triplicate, at 30°C and pH 6.8, by measuring the release of orthophosphate by malachite green assay. M1P saturation graphs were determined in the presence of 10 mM maltoheptaose (**A**) or 10 mg.ml^{-1} glycogen (**B**). The boxes show the behaviour of the enzyme at low concentrations of M1P. The DP7 (**C**) and glycogen (**D**) saturation graphs were obtained in the presence of 2 mM M1P. Hill's constant (n_H) is indicated when its value differs from 1. Activities are expressed in µmoles of orthophosphate produced per minute per mg of protein.

In the presence of a saturating concentration of M1P, the enzyme exhibits a michaelian behaviour towards DP7 and glycogen (Figures 26C and 26D). While GlgE from *Mycolicibacterium smegmatis* has a K_m ($K_m = S_{0.5}$ under michaelian conditions) of 35 ± 8 mM for maltohexaose (Kalscheuer *et al.*, 2010), the K_m for maltoheptaose is about 10 times lower for GlgE_EL, reflecting a strong affinity for malto-oligosaccharides. Since the concentration of glycogen is expressed in mg.ml^{-1}, it is difficult to determine whether the enzyme is more affine for glycogen or for DP7. However, with close k_{cat} (Table 4), the enzyme acts with a similar

efficiency on both substrates (k_{cat} = number of products formed per second per enzyme). In such experimental conditions, the apparent K_m values for glycogen and DP7, 2.5 ± 0.2 mg.ml^{-1} and 3.1 ± 0.2 mM, respectively were similar to the apparent K_m value of glycogen synthase (GlgA) that synthesizes α-1,4 linkages from ADP-glucose (Wayllace *et al.*, 2012).

Thus, under variable M1P concentrations and using fixed concentrations of glycogen or maltoheptaose, the GlgE-EL activity displays allosteric behaviour (Figures 26A and 26B), indicating a positive cooperativity, which has been corroborated with Hill coefficients (n_H) that are above 1. This behaviour can notably be explained if several enzymes interact to form functional homocomplexes. However, the affinity of the enzyme for M1P appears to be very high, with $S_{0.5}$ values of 0.332 ± 0.020 and 0.170 ± 0.011 mM in the presence of 10 mM of DP7 or 10 mg.ml^{-1} of glycogen respectively (Table 4). This value is close to the K_m of the GlgE of *Mycobacterium tuberculosis* for M1P, determined to be 0.25 ± 0.05 mM in the presence of 1 mM of maltohexaose. The catalytic constant (k_{cat}) rises to 185 ± 13 s^{-1} in the presence of M1P and a fixed concentration of 10 mM of maltoheptaose, indicating a high efficiency of the enzyme under these conditions.

Variable substrate	Fixed substrate	Vmax (M.s^{-1})	$S_{0.5}$ (mM)	n_H	K_{cat} (s^{-1})	$K_{cat}/S_{0.5}$ (M^{-1}.s^{-1})
M1P	DP7	3,45.10^{-7} ± 0,08.10^{-7}	0,332 ± 0,020	1,69 ± 0,14	185 ± 13	5,58.10^{5} ± 0,73.10^{5}
	glycogen	1,76.10^{-7} ± 0,04.10^{-7}	0,170 ± 0,011	1,41 ± 0,11	21,6 ± 1,8	1,28.10^{5} ± 0,19.10^{5}
DP7	M1P	2,19.10^{-7} ± 0,07.10^{-7}	3,10 ± 0,27	1,18 ± 0,12	48,2 ± 3,5	1,56.10^{4} ± 0,25.10^{4}
glycogen		2,83.10^{-7} ± 0,13.10^{-7}	2,58 ± 0,24 [a]	1,13 ± 0,10	34,8 ± 3,8	1,35.10^{4} ± 0,27.10^{4} [b]

Table 4 : Table 4 : Kinetic parameters of the GlgE_EL on different substrates.
The substrates tested are maltose-1-phosphate, DP7 and bovine liver glycogen. For glycogen, $S_{0.5}$ is expressed in mg.ml^{-1} ([a]) and kcat / $S_{0.5}$ in L.g^{-1}.s^{-1} ([b]).

II-B-3) Determination of molecular weight

The molecular weight of native GlgE_EL was determined either by size exclusion chromatography or by using native-PAGE (Figure 27) containing different polyacrylamide concentrations (5 %, 7.5 %, 10 % and 12.5 %). In agreement with the cooperativity behaviour observed previously, both techniques indicate an apparent molecular weight of 140 to 180 kDa, respectively, corresponding to the formation of dimer species while no monomer species of around 76 kDa were observed.

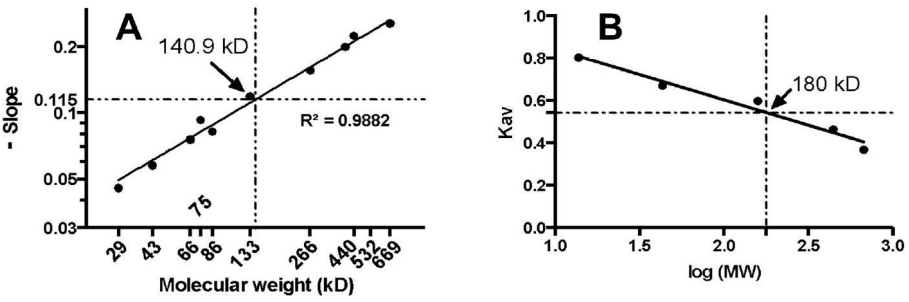

Figure 27 : Determination of the apparent molecular weight of GlgE_EL.
Apparent molecular weight was determined by native PAGE (**A**) and size exclusion chromatography (Superose 6 Increase GL 10/300) (**B**) to be 140.9 kDa and 180 kDa, respectively, suggesting a homodimerization of GlgE (76 kDa).

II-C. *De novo* glycogen synthesis: GlgE activity enables the initiation and elongation of glucan.

II-C-1) GlgE_EL is able to initiate the synthesis of long malto-oligosaccharides

Prokaryotic glycogen synthases (GlgA) do not require the presence of a short α-1,4 glucan or primer to initiate glycogen biosynthesis (Ugalde *et al.*, 2003). In absence of GlgA and GlgC activity in *E. lausannensis* and in the absence of GlgC in *W. chondrophila*, this raised the question of the ability of GlgE activities to substitute for GlgA with respect to the priming of glycogen biosynthesis. We previously demonstrated that GlgE_WC is able of synthesising long malto-oligosaccharides (up to DP32) when incubated only with M1P or with M1P supplemented with glucose, maltose or maltotriose (Figure 24), whereas GlgE of *E. lausannensis* appears to be able to do so only when maltotriose is used as a substrate. As this result was puzzling, another experiment was conducted to visualize the initiation capability of GlgE_EL directly in native-PAGE (Figure 28).

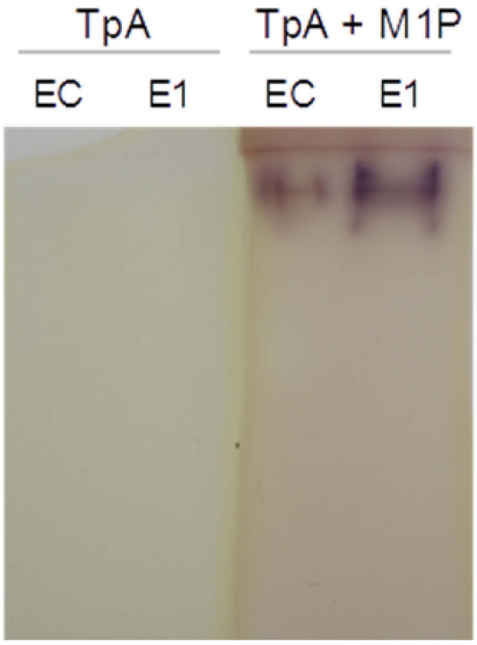

Figure 28 : Zymogram analysis of GlgE_EL shows its ability to initiate malto-oligosaccharide synthesis.
Cellular extract (EC) and purified recombinant GlgE (E1) of *E. lausannensis* were loaded on a native-PAGE containing no added carbohydrate substrate. After migration, gel was soaked overnight in a buffer containing 25 mM Tris-acetate buffer and 5 mM DTT supplemented with 1 mM of M1P (TpA + M1P) or not (TpA). Gel was then rinsed and soaked into iodine solution to visualise the activities. Only with M1P, GlgE_EL is able to synthesise long-enough malto-oligosaccharides to be visualised as dark bands.

Purified GlgE_EL was loaded onto a native polyacrylamide gel containing no carbohydrate substrate. After migration, the gel was incubated overnight in a buffer containing 1 mM of M1P. After soaking the gel in iodine solution, the synthesis of long chains of glucose (DP≥15) can be visualized as dark-blue bands due to iodine-glucan complex. As depicted on Figure 28, such coloration is observed with crude extract and purified GlgE_EL, which means that GlgE_EL is able to produce long malto-oligosaccharides only from M1P. Altogether, these results suggest that GlgE activities are, like GlgA in the classical GlgC-pathway, able to initiate the biosynthesis of glycogen. However, we cannot exclude the role of maltose in the initiation process of glucan synthesis since spontaneous dephosphorylation of M1P is unavoidable.

II-C-2) *De novo* glycogen synthesis by GlgE and GlgB

We further carried out a series of experiments that consisted of synthesising *in vitro* high molecular branched glucans by incubating both glycogen branching enzyme and GlgE_EL in the presence of M1P. As we have failed to express and purify branching enzyme encoded on the GlgE-operon (GlgB2) of *E. lausannensis*, we decided to use GlgB2 of *W. chondrophila*, after making sure that the recombinant enzyme is functional on zymogram (S4 Figure). We therefore conducted reactions by incubating GlgE_EL, GlgB2_WC, M1P, and a malto-oligosaccharide substrate (DP7) and analysed reactions products by thin layer chromatography (Figure 29).

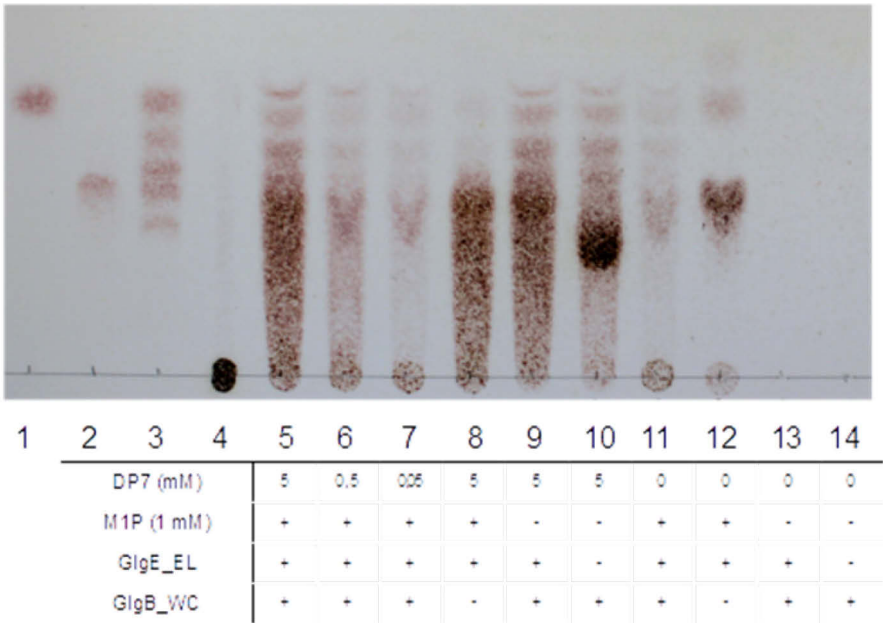

	1	2	3	4	5	6	7	8	9	10	11	12	13	14
DP7 (mM)					5	0,5	025	5	5	5	0	0	0	0
M1P (1 mM)					+	+	+	+	-	-	+	+	-	-
GlgE_EL					+	+	+	+	+	-	+	+	+	-
GlgB_WC					+	+	+	-	+	+	+	-	+	+

Figure 29 : High-mass polysaccharide synthesis by GlgE from *Estrella lausannensis* and GlgB2 from *Waddlia chondrophila*.
Different reactions (composition summarized in the table) are incubated overnight at 30°C (lanes 5 to 14). 3 µl of reactions products were separated and analysed by thin layer chromatography. Lane 1: maltose; 2: maltose-1-phosphate; 3: mix of malto-oligosaccharides (DP2, 3, 4, 5 and 7); 4: bovine liver glycogen. The reactions were carried out in a volume of 50 µl. 1.5 µg and 10 µg of GlgE_EL and GlgB_WC, respectively, were used per reaction. As commercial DP7 is contaminated by small malto-oligosaccharides, these contaminants are more or less visible depending on the amount of DP7 present in each sample. Protocol used for this thin layer chromatography was the same as previously described.

When both recombinant enzymes are incubated in the presence of DP7 and M1P (lanes 5 to 7), maltosyltransferase activity is more or less visible depending on the amount of DP7. High molecular weight glucans, branched or not, are visible at the level of the deposit line. In absence of DP7, GlgE_EL synthesizes long malto-oligosaccharides that therefore do not migrate on the silica gel and stay at the level of the deposit line (lane 12). The addition of GlgB2_WC (lane 11) results in a higher consumption of M1P as well as a significant accumulation of high molecular weight polysaccharides on the deposit line, which are associated with a trail of malto-oligosaccharides. This preliminary experiment confirmed that GlgE_EL is capable of initiating the synthesis of long malto-oligosaccharides. These malto-oligosaccharides appear to be long enough to be taken over by the branching enzyme to form branched polysaccharides.

To ensure that the combination of GlgE_EL and GlgB2_WC is sufficient to synthesize glycogen from M1P alone, the previous reaction (Figure 29, lane 11) was scaled up by incubating 2 mg M1P with 30 µg GlgE_EL and 200 µg GlgB2_WC. Reaction product was directly submitted to NMR spectroscopy to detect the presence of α-1,6 linkages, with M1P and glycogen as controls (Figure 30A). Signals at 5.6 ppm and 4.9 ppm, involved in α-1,4 and α-1,6 linkages, were detected in the incubation products, meaning that a branched polysaccharide was produced. This branched polysaccharide material was further purified and incubated with commercial isoamylase and pullulanase to trim branching points. Released linear glucan chains were analysed through capillary electrophoresis analysis (i.e., FACE). The chain length distribution of synthesized polysaccharides (Figure 30B) was compared with glycogen from bovine liver (Figure 30D). As control, the amount of free linear glucans was estimated by analysing the APTS-labelled samples not submitted to debranching activities (Figures 30C and 30E). The *in vitro* synthesized polysaccharide possesses a typical chain length distribution of glycogen, with a monomodal distribution and maltohexaose as most abundant glucan chain. Altogether, these results confirm that GlgE activities display similar functions than GlgA: they are able to initiate the synthesis to initiate and elongate the growing glycogen particles.

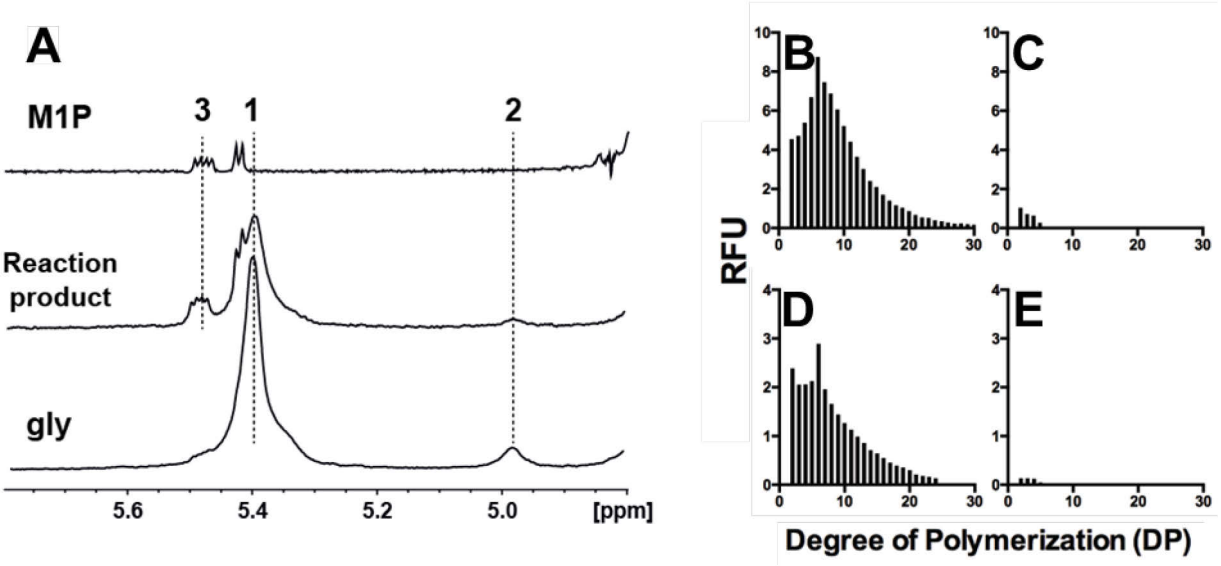

Figure 30 : *De novo* synthesis of branched polysaccharides.
(**A**) Part of ^{1}H-NMR spectra of maltose-1-phosphate (M1P), non-purified reaction mixture and glycogen (gly) from bovine liver in D2O. Peak 1 (5.45 to 5.3 ppm) and 2 (4.98 ppm) correspond to signals of protons involved respectively into α-1,4 and α-1,6 linkages while peak 3 (5.47 ppm) represents the characteristic doublet of α-anomeric proton located on C1 of maltose-1-phosphate. As both peaks 1 and 2 appear in the incubation product, this indicates the formation of branched polysaccharide composed of α-1,4 and α-1,6 linkages. However, M1P was not totally consumed as there is also a signal for peak 3. Branched polysaccharide was then purified (see materials and methods) and incubated overnight with both amylase and pullulanase to cut off all branching points. Chain length distribution of the purified product (**B**) and of a glycogen from bovine liver (**D**) control were then assessed by fluorophore-assisted carbohydrate electrophoresis (FACE). In order to estimate the content of free malto-oligosaccharides, the enzymatic product (**C**) and the control glycogen (**E**) were both analysed by FACE analysis without being submitted to debranching.

So far, we showed that chlamydial GlgEs are able to initiate the synthesis of malto-oligosaccharides, and to elongate them to form a glycogen-like particle with the help of the GlgB2. Still, the question of maltose-1-phosphate synthesis arises, as it is mandatory for maltosyltransferase activities. Currently, only two enzymes have been described as M1P producers: the maltose-1-phosphate synthase GlgM and the maltokinase Mak (syn. Pep2 in *Mycobacteria*) (Koliwer-Brandl *et al.*, 2016). GlgM is a GT4 glycogen synthase-like, that is not encoded in chlamydial genomes, in contrast to GT5 GlgA (Table 3). Furthermore, in *E. lausannensis*, GlgA is truncated and inactive (Figures 12, 13 and 15), suggesting that Mak is the only way to synthesize M1P in *Chlamydiae*. Furthermore, trehalose synthase TreS is fused to Mak in the 6 chlamydial species that possess the GlgE-pathway, and to our knowledge, the characterization of a bifunctional TreS-Mak activity has not yet been reported in the literature yet.

New objectives are then to ensure that TreS-Mak is able to synthesize the M1P mandatory for maltosyltransferase activity from trehalose and ATP. Furthermore, characterization of this bifunctional enzyme will be a first and should help us to completely reconstruct the glycogen biosynthetic metabolism found in *Criblamydiaceae* and *Waddliaceae*.

III. Characterization of TreS-Mak from *Estrella lausannensis*

III-A. Cloning and expression of the *treS-mak* gene of *Estrella lausannensis* shows off M1P toxicity

III-A-1) Cloning of *treS-mak* on VCC1 expression plasmid

As we have more information on the GlgE of *Estrella lausannensis*, we decided to focus here on the TreS-Mak fusion protein of *Estrella lausannensis* (TreS-Mak_EL). As a reminder, trehalose synthase TreS catalyses the reversible conversion of trehalose into maltose while maltokinase Mak catalyses the phosphorylation of maltose into maltose-1-phosphate from a nucleoside triphosphate.

The *treS-mak* gene of *E. lausannensis* was cloned into the VCC1 expression vector, using Gateway technology. The Rosetta strain of *E. coli* was transformed by VCC1 - *treS-mak_EL* and plated on LB medium without any inductor. This does not yield to any colony after an overnight incubation at 37°C (Figure 31). We presumed that a basal transcription of *treS-mak* gene leads to the synthesis of highly toxic maltose-1-phosphate. Indeed, various reports indicate that accumulation of M1P is toxic (Sassetti *et al.*, 2003; Miah *et al.*, 2016; Kalscheuer *et al.*, 2010), and trehalose, the substrate of TreS-Mak alongside ATP, reaches a concentration of 8.5 mM in *E. coli* in this conditions (Hayner *et al.*, 2017; Kretschmer *et al.*, 2016), as the 10 $g.l^{-1}$ NaCl concentration in LB medium is sufficient to induce trehalose synthesis *via* OtsA-OtsB pathway (Figure 3 , Giaever *et al.*, 1988). By analyzing global gene expression in *M. tuberculosis*, Kalscheuer *et al.* have shown that M1P inhibits the respiration machinery and severely damages DNA. It is therefore not surprising that even without

induction, basal expression of TreS-Mak_EL in *E. coli* results in severe toxicity, since no endogenous GlgE consumes M1P. Two strategies were then put in place to avoid this toxicity in *E. coli*.

The first one was to prevent the synthesis of trehalose in *E. coli*, as no TreS-Mak substrate means no M1P accumulation. As the trehalose synthesising OtsA-OtsB pathway in *E. coli* is induced by NaCl, we decided to spread our transformed cells on Terrific Broth (TB) plates, a medium devoided of NaCl (Figure 31B). On this medium, we observed the growth of many small colonies after 16 h incubation at 37°C. We believe that this growth delay could be explained by small amounts of trehalose or NaCl in the yeast extract used to prepare TB medium (Mosser *et al.*, 2015).

Second strategy was to reduce the level of basal expression of recombinant proteins by using the BL21 AI *E. coli* strain. While the *treS-mak_EL* gene is under the control of a T7 RNA polymerase-inducible promoter, expression of T7 RNA polymerase is itself placed under the control of an arabinose promoter. After plating on LB medium, numerous colonies are observed without any growth delay (Figure 31A). To express TreS-Mak during the rest of the study, a combination of both approaches (i.e., culture of BL21 AI cells transformed with VCC1-*treS-mak_EL* in TB medium) was chosen.

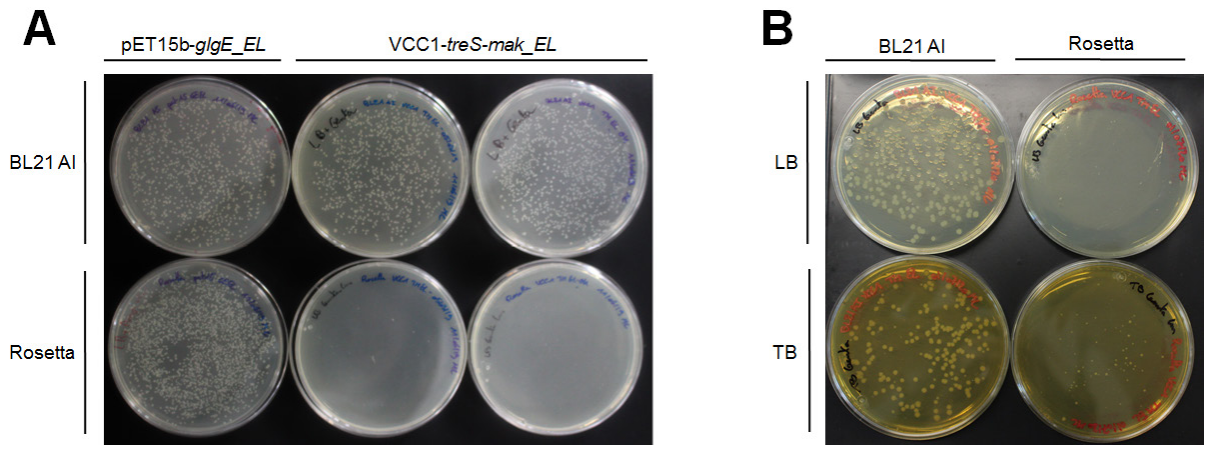

Figure 31 : Toxicity of TreS-Mak_EL after transformation with the VCC1-*treS-mak_EL* plasmid.
(**A**) BL21 AI and Rosetta *E. coli* strains were transformed with pET15b-*glgE_EL* and VCC1-*treS-mak_EL* to respectively express GlgE_EL and TreS-Mak_EL, and then plated on LB medium. After one night at 37°C, plates were photographed to assess the number of colonies. pET15b-*glgE_EL* serves as control. Basal expression of TreS-Mak_EL is highly toxic in Rosetta, as little to no colonies were observed. To the contrary, in BL21 AI, as basal expression is repressed, no toxicity was observed. (**B**) BL21 AI and Rosetta *E. coli* strains were transformed with VCC1-*treS-mak_EL* and plated on Lysogeny Broth (LB) or Terrific Broth (TB). After one night at 37°C, plates were photographed to assess the number of colonies. While the number of BL21 AI colonies was quite similar on LB and TB, a notable difference occurred with Rosetta: little to no colonies were observed on LB, whereas a significant amount of small colonies was visible on TB. This suggests that the absence of NaCl in TB medium reduces the toxicity induced by basal expression of TreS-Mak_EL.

III-A-2) Expression of recombinant TreS-Mak_EL

As the recombinant protein has a 6xHis-tag at the N-terminus, we purified TreS-Mak_EL by nickel affinity chromatography, using the same protocol as we did for recombinant GlgEs. As depicted on Figure 32, purified TreS-Mak appears a single band with an apparent molecular weight of 115 kDa, less than the 130 kDa predicted.

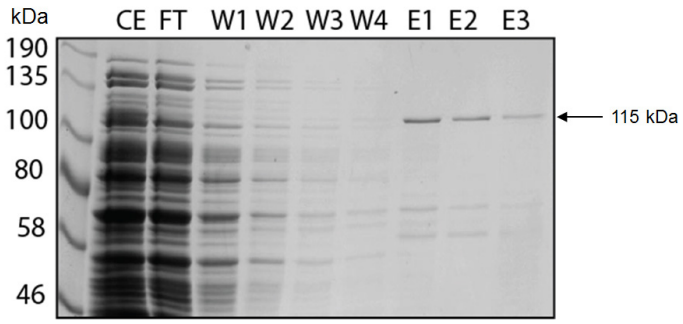

Figure 32 : Expression and purification of TreS-Mak_EL.
TreS-Mak_EL was expressed in BL21 AI cells cultured at 37°C in liquid Terrific Broth. Expression was induced at mid exponential growth phase with addition of 1 mM IPTG and 0.2 % L-arabinose. After an overnight incubation at 30°C, cells were harvested, proteins extracted, recombinant TreS-Mak_EL purified by Ni^{2+} affinity chromatography and separated on 7,5 % SDS-PAGE. CE : cellular extract; FT : flow-through ; W1 to W4 : washing steps 1 to 4 ; E1 to E3 : elution steps 1 to 3. Purified TreS-Mak_EL appears to have a molecular weight of 115 kDa whereas it is predicted to weight 130 kDa.

III-A-3) About TreS-Mak-induced toxicity

As indicated previously, basal expression of TreS-Mak_EL produces sufficient amount of highly toxic M1P to yield no *E. coli* colony after transformation (Figure 31). The toxicity of M1P accumulation has been confirmed in different ways: (i) it has been demonstrated in other species, (ii) the level of toxicity depends on the synthesis of trehalose by *E. coli* and (iii) no toxicity was observed when TreS-Mak_EL was co-expressed with GlgE_EL. To gain more insights on this induced toxicity of TreS-Mak_EL, we followed the growth and death of BL21 AI cells transformed with VCC1-*treS-mak_EL* and cultivated in LB (Figure 33). Surprisingly, we did not observe any toxicity in these conditions when expression of TreS-Mak was induced at the mid-log phase.

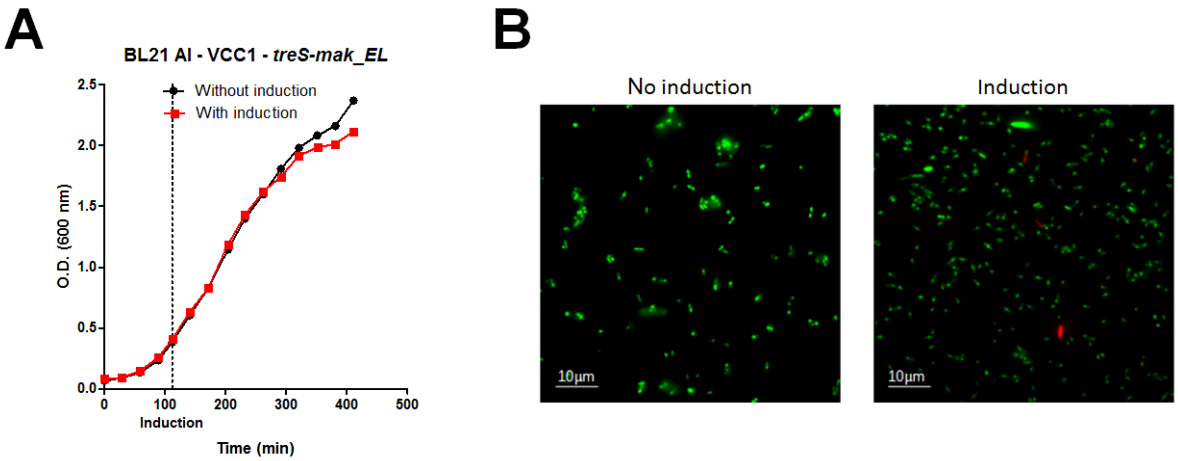

Figure 33 : Overexpression of TreS-Mak_EL is not toxic in BL21 AI cells.
(**A**) BL21 AI cells transformed with VCC1-*treS-mak_EL* were cultivated at 30°C in liquid LB. At O.D. (600 nm) ≈ 0.4, overexpression of TreS-Mak was induced by addition of 1 mM IPTG and 0.2 % L-arabinose and growth (red curve) was compared with a non-induced control (black curve). No significant growth difference was observed during the five first hours following the induction. (**B**) At T = 4h after induction, some cells were harvested and fluorescently stained using LIVE/DEAD BacLight Bacterial Viability kit to assess cell viability in both conditions. SYTO®9 (in green) diffuses through membranes and interacts with DNA, whereas propidium iodide (in red) requires damaged membranes to enter et stain cells. Dying cells then appear as orange.

No growth delay and no significant cell death (Figure 33A and 33B) were observed, suggesting that expression of TreS-Mak, and therefore M1P accumulation were not toxic in these conditions. This result is quite puzzling when we consider the severe toxicity observed on plates (Figure 31). In a way to reconcile these two contrary observations, we propose that an enzyme that catabolizes or inactivates the M1P may be produced during the exponential growth, which it is not present or active after the transformation of competent cells to prevent the toxicity of M1P.

III-B. Biochemical characterization of TreS-Mak_EL

III-B-1) Test of potential TreS-Mak activities

Trehalose synthase (TreS) activity of *Mycolicibacterium smegmatis* catalyses the interconversion of trehalose into maltose (Pan *et al.*, 2004). Because this activity is strongly inhibited by Tris, Tris-free buffers were used during the enzymatic characterization of TreS-Mak activity. In addition, TreS of *Mycolicibacterium tuberculosis* has been reported to harbour an amylase-like activity, which in some extent can degrade glycogen into maltose and trehalose (Pan *et al.*, 2008). Finally, maltokinase (Mak) activity of *Mycobacterium bovis* BCG requires the presence of both nucleoside triphosphate (ATP) and divalent cation (Mg^{2+}) in order to phosphorylate the maltose at the reducing-end (Mendes *et al.*, 2010). Based on the characterizations of TreS and Mak activities of *M. bovis*, first incubation experiments were carried out by incubating on the fused TreS-Mak_EL, with maltose or trehalose and in the presence of ATP and Mg^{2+}. After an overnight incubation, reactions products were analysed by thin layer chromatography (Figure 34, S5 Figure).

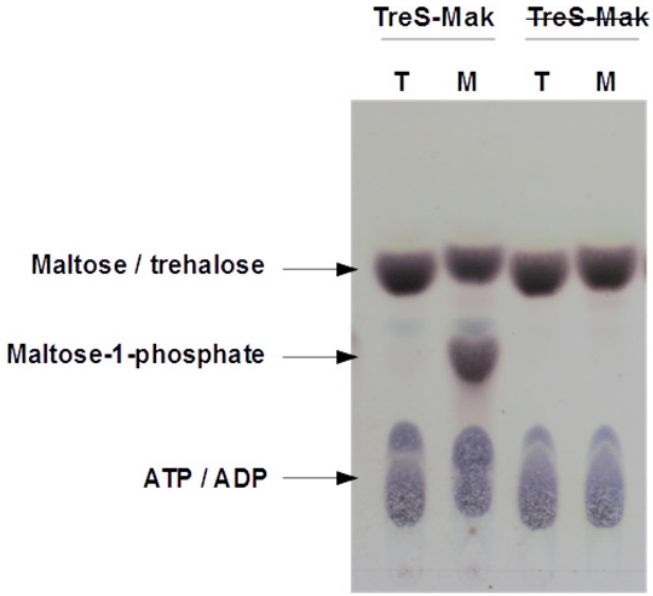

Figure 34 : Recombinant TreS-Mak enzyme from *E. lausannensis* is functional and catalyses the synthesis of maltose-1-phosphate from nucleoside triphosphate and trehalose or maltose.
Purified TreS-Mak_EL was incubated overnight at 30°C with either 20 mM trehalose (T) or maltose (M), 20 mM ATP and 10 mM $MgCl_2$. Control reactions were performed using heat-denatured TreS-Mak_EL (5 min at 95°C). All reactions were buffered at pH 7 with 25 mM imidazole, 30 mM NaCl and 5 mM sodium acetate. Reaction products were separated on thin layer chromatography. We observed that TreS-Mak catalyses the synthesis of maltose-1-phosphate from ATP and maltose (M), but also directly from trehalose (T) in very small quantities.

Production of M1P was clearly observed when recombinant TreS-Mak_EL was incubated with maltose, ATP and $MgCl_2$ while it was barely visible with trehalose (Figure 34). Recombinant TreS-Mak from *E. lausannensis* therefore seems to possess both trehalose synthase and

maltokinase activities, even if conditions have to be improved to further characterize trehalose synthase activity.

III-B-2) Characterization of the maltokinase activity of TreS-Mak_EL

III-B-2(a) Determination of optimal divalent cation and nucleoside triphosphate

As maltokinase activity of TreS-Mak_EL was clearly visible on TLC, we initiated the biochemical characterization of recombinant TreS-Mak_EL. The maltokinase activity was enzymatically monitored by measuring the release of nucleosides diphosphate *via* pyruvate kinase assay. First, maltokinase activity of TreS-Mak_EL was inferred in the presence of various divalent cations (Figure 35A and 35C). As expected, the recombinant TreS-Mak was strictly dependent on divalent cations, in particular, with the best stimulatory effect for Mn^{2+}.

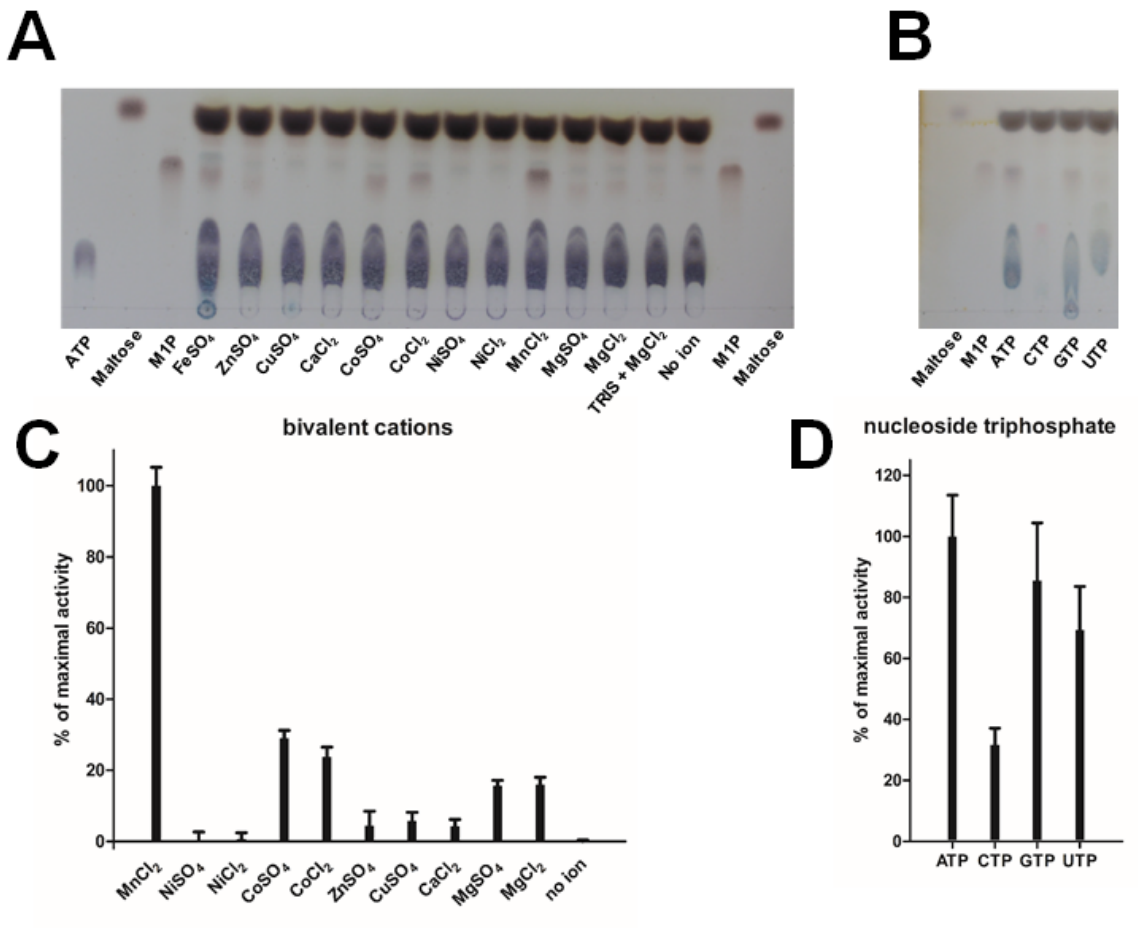

Figure 35 : Determination of the optimal divalent cation and nucleotide triphosphates for maltokinase activity. Optimal divalent cation (**A**,**C**) and nucleoside triphosphate (**B**,**D**) were inferred by incubating 1h at 30°C 10 µg.ml^{-1} of recombinant TreS-Mak_EL with 20 mM maltose, 20 mM ATP or other nucleosides phosphate (CTP, GTP or UTP) and 10 mM $MnCl_2$ or other divalent cations ($FeSO_4$, $ZnSO_4$, $CuSO_4$, $CaCl_2$, $CoSO_4$, $CoCl_2$, $NiSO_4$, $NiCl_2$ or $MgCl_2$). Enzymatic reactions were analyzed by thin layer chromatography (**A**,**B**). For each reaction, maltokinase activity was also measured by enzymatic assay of ADP. Results are reported in percentage of maximum activity. While Mn^{2+} is the best activator of the maltokinase activity, ATP, GTP and UTP are efficient phosphate donors.

Others tested divalent cations, such as Co^{2+}, Mg^{2+}, Fe^{2+}, Ca^{2+} and Cu^{2+} activated Mak activity as well, but to a lower extent, while no effect was observed in presence of Ni^{2+}. Interestingly, at variance with Mak activity of *Mycobacterium bovis* BCG, which prefers Mg^{2+}, the catalytic

site of the Mak activity domain of TreS-Mak_EL binds preferentially Mn^{2+} over Mg^{2+}, the latter showing only 16 % of the activity measured with Mn^{2+}. No difference was observed by using SO_4^{2-} or Cl^- as a counter-ion. Then, nucleosides triphosphate ATP, CTP, GTP and UTP were tested as phosphate donors by measuring the amount of nucleosides diphosphate released (Figure 35B and 35D). The data expressed in percentage of maximal activity showed that ATP (100%), GTP (85%), UTP (70%) and to a lower extent CTP (31%) are efficient phosphate donors. Furthermore, through the characterization of TreS-Mak_EL, we evidenced that Mak activity is strongly dependent on a high concentration of imidazole (S6 Figure). We hypothesized that this compound may enhance the *in vitro* stability of TreS-Mak_EL protein. In addition, lower concentrations of $MnCl_2$ than 10 mM decrease maltokinase activity (S7 Figure).

III-B-2(b) Determination of optimal pH and temperature for the maltokinase activity of TreS-Mak_EL

After the determination of the best divalent cations and nucleoside tri-phosphates, both pH and temperature optima were determined for the enzyme. Purified TreS-Mak_EL was therefore incubated for 30 min in the presence of 20 mM of maltose, 20 mM of ATP, 10 mM of MnCl2, in 32.5 mM sodium acetate, 97.5 mM NaCl and 162.5 mM imidazole buffers ranging from pH 4 to 9, or in the same buffer at pH 7 of 15 and 45°C.

Both temperature and pH optima for maltokinase activity were inferred in range of temperatures (from 15 to 45°C) and of pH (from 4 to 9). In comparison with GlgE_EL, TreS-Mak_EL shows maximum activity at a higher temperature, around 42°C (Figure 36B), and prefers a basic pH (around pH 8). As no activity was measured at low pH (4 to 6) (Figure 36A), these data were withdrawn from the graph. Furthermore, the drop of Mak activity at low pH may be correlated with the protonation of imidazole into imidazolium. Indeed, high concentration of imidazole seems to stabilize TreS-Mak (S6 Figure), and around 90 % of solubilized imidazole gets protonated at pH 6 (≥ 99 % at pH ≤ 5 ; Thomason *et al.*, 2015). Therefore, change of imidazole speciation in acidic environment could explain the huge gap of enzyme activity observed between pH ≥ 7 and pH ≤ 6.

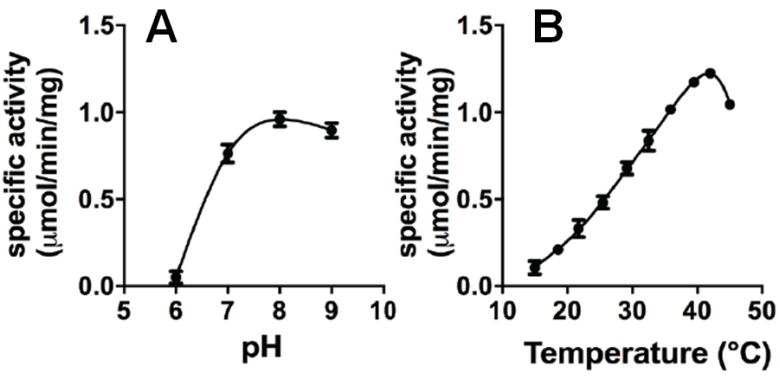

Figure 36 Determination of optimal pH (**A**) and temperature (**B**) for the maltokinase activity of TreS-Mak_EL. 25 µg.ml^{-1} of purified TreS-Mak_EL were incubated for 40 min in the presence of 20 mM maltose, 20 mM ATP, 10 mM of $MnCl_2$, in 32.5 mM sodium acetate, 97.5 mM NaCl and 162.5 mM imidazole buffers ranging from pH 4 to 9 at 30°C, or in the same buffer at pH 7 from 15 to 45°C, respectively. TreS-Mak_EL seems to be the most efficient at pH 8 and at 42°C. Points at pH 4 et 5 were withdrawn from graph (**A**) as measured activity was null.

It is noteworthy that specific maltokinase activity of TreS-Mak_EL stands between 1 and 1.5 µmol of ADP produced per minute per mg of proteins under optimal conditions. This activity is much lower than those of *Mycobacterium bovis* BCG (21.05 ± 0.89 µmol.min^{-1}.mg^{-1}; Mendes *et al.*, 2010) and of *Streptomyces coelicolor* (144.8 µmol.min^{-1}.mg^{-1}; Jarling *et al.*, 2004), but also lower than the specific activity measured for the GlgE_EL (10 µmol.min^{-1}.mg^{-1}), which prevents the accumulation of toxic M1P inside bacterial cytosol.

III-B-3) Characterization of the trehalose synthase activity of TreS-Mak_EL

The TreS activity at the N-terminus domain of TreS-Mak_EL was inferred by measuring the interconversion of trehalose into maltose. The amount of maltose was enzymatically quantified using the amyloglucosidase assay that specifically hydrolyses the α-1,4 glucosidic linkages. Previous reports indicated that TreS activities are overall strongly inhibited with 10 mM of divalent cation while a concentration of 1 mM can slightly enhance their activity (Pan *et al.*, 2008; Yue *et al.*, 2009; Filipkowski *et al.*, 2012). The effect of Mn^{2+} cation on the activity of TreS domain was inferred at 200 mM of trehalose. As depicted on Figure 37A, trehalose synthase activity increases only slightly by 1.1-fold from 0 mM to 1 mM of Mn^{2+} (from 0.34 to 0.37 µmol maltose. min^{-1}.mg^{-1}) whereas a noticeable decrease of TreS activity (0.24 µmol maltose. min^{-1}.mg^{-1}, 72 % of residual activity) is obtained at 10 mM of Mn^{2+}. Contrary to previous reports (Pan *et al.*, 2008), TreS domain is not associated with an amylase activity, as no short carbohydrate was produced by incubating TreS-Mak_EL with glycogen (S5 Figure). Nonetheless, conversion of trehalose into maltose is associated with the release of small amounts of glucose (Figures 37A and 37B).

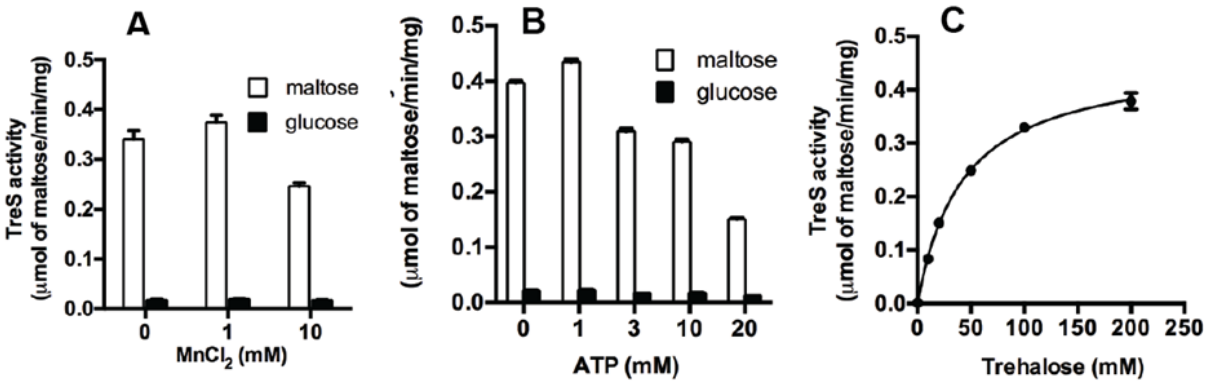

Figure 37 : Kinetic parameters of the trehalose synthase activity of TreS-Mak_EL.
The interconversion of trehalose into maltose and subsequent release of glucose were inferred by using amyloglucosidase assay method (see material and methods). Effect of Mn^{2+} (**A**) and ATP (**B**) on TreS activity were assessed at 30°C and pH 8, in the presence of 125 mM imidazole, 150 mM NaCl, 25 mM sodium acetate, 200 mM trehalose and 0 mM ATP or 1 mM $MnCl_2$ respectively. While 1 mM $MnCl_2$ and ATP slightly enhance TreS activity, higher concentrations show inhibitory effects. Saturation plot for trehalose (**C**) was inferred at 30°C and pH 8 by incubating TreS-Mak_EL with 125 mM imidazole, 150 mM NaCl, 25 mM sodium acetate, 1 mM $MnCl_2$ and varying concentrations of trehalose (0, 10, 20, 50, 100 and 200 mM). Apparent Km value is 42.3 ± 2.7 mM under these conditions.

Because TreS activity is fused with the Mak domain in *E. lausannensis*, the effect of a wide range of concentration of ATP concentration on the interconversion of trehalose was tested (Figure 37B). Although no significant effect of ATP was observed on TreS activity at 1mM (0.40 and 0.43 µmol maltose.min^{-1}.mg^{-1} at 0 and 1 mM respectively), TreS activity decreased by 1.5-fold at 3 or 10 mM ATP (0.29 µmol maltose. min^{-1}.mg^{-1}) and dropped by 2.7-fold when the ATP concentration reaches up to 20 mM (0.15 µmol maltose. min^{-1}.mg^{-1}). Finally, the apparent K_m value for trehalose was determined at 42.3 ± 2.7 mM in the presence of 1 mM $MnCl_2$ and 0 mM ATP (Figure 37C). This is quite consistent with the apparent K_m values for trehalose (50 to 150 mM) reported in the literature for TreS activity in various species (Chen *et al.*, 2006; Zhang *et al.*, 2011; Wang *et al.*, 2012).

III-B-4) Determination of the molecular weight of TreS-Mak_EL.

We also determined the molecular weight of His-tagged recombinant TreS-Mak_EL protein purified on nickel affinity columns. While it displays a molecular weight of 115 kDa on SDS-PAGE (S7B Figure), in native conditions, recombinant TreS-Mak_EL appears as a homodimer with an apparent molecular weight of 256 kDa when analysed by Superose 6 column chromatography (Figure 38). No monomer was observed. This contrasts with the hetero-octameric complex composed of 4 TreS and 4 Mak subunits (≈490 kDa) observed in *Mycolicibacterium smegmatis* in which homotetramers of TreS forms a platform to recruit dimers of Mak via specific interaction domain (Roy *et al.*, 2013; Kermani *et al.*, 2019).

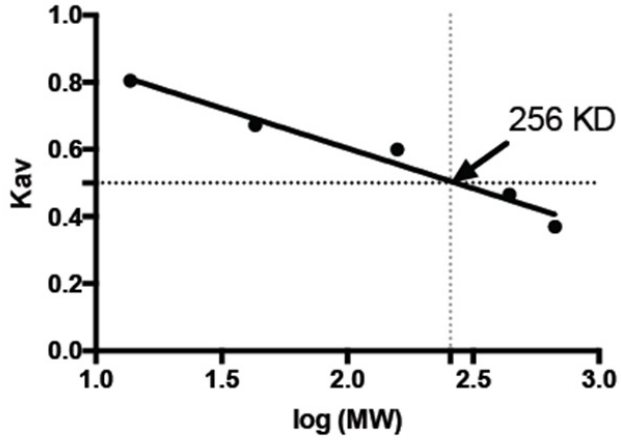

Figure 38 : Molecular weight of TreS-Mak_EL by size exclusion chromatography.
Superose 6 Increase 10-300 GL column (GE-Healthcare) pre-equilibrated with 140 mM NaCl, 10 mM orthophosphate pH 7.4 was calibrated with standard proteins (669; 440; 158; 43 and 13.7 kDa) and Blue Dextran. The determination of a partition coefficient (Kav) of 0.5 suggests an apparent molecular weight of 256 kDa.

Altogether, we demonstrated that TreS and Mak domains are functional in the fused TreS-Mak protein of *E. lausannensis*. The reversible interconversion of trehalose combined with the irreversible phosphorylation of maltose drives the synthesis of M1P to the further synthesis of glycogen particles.

Thus far, we demonstrated that enzymes of the GlgE-pathway are fully functional in *Estrella lausannensis* and probably in *Waddlia chondrophila* as well. This GlgE-pathway relies on a source of trehalose or maltose, nucleoside triphosphate and manganese for synthesizing glycogen particles (Figure 35). In the case of obligate intracellular bacteria, such as *Chlamydiae*, which come along with the loss of numerous metabolic pathways, a question

arises on how GlgE-pathway is fuelled. Are precursors synthesized by the bacteria, imported from the host cell, or a mix of both? To answer this question, a survey of gene content for trehalose biosynthesis and putative transporter was carried out on chlamydial species that possess the GlgE-pathway.

IV. Reconstruction of the GlgE-associated glycogen metabolism in *Chlamydiae*

IV-A. Environmental *Chlamydiae* can synthesize trehalose

During our investigation of chlamydial genomes, no gene encoding a specific transporter of either trehalose or maltose was found among PTS (phosphotransferase system) and ABC (ATP-binding cassette) transport systems. Maltose is generally a catabolic product, except in the case of GlgE-pathway, where it is produced from trehalose by TreS. We then focused on the presence of another trehalose-synthesis pathway (Figure 3) in the 6 chlamydial species that possess the GlgE-pathway. Surprisingly, all four other trehalose-synthesizing pathways (i.e., OtsA/OtsB, TreY/TreZ, TreT and TreP) are found in various species of the *Chlamydiae* phylum (Table 5).

	treS-mak	*glgE*	*otsA*	*otsB*	*βPGM-otsB*	*treY*	*treZ*	*treT*	*treP*	*Trehalase*
Chlamydia trachomatis	-	-	-	-	-	-	-	-	-	-
Parachlamydia acanthamoeba UV7	-	-	1	1	-	-	-	1	-	-
Parachlamydia sp. C2	1	1	-	-	-	1	2	-	-	-
Candidatus Protochlamydia massiliensis	1	1	-	-	-	1	1	-	-	-
Candidatus Protochlamydia naegleriophila	1	1	-	-	-	1	1	-	-	-
Waddlia chondrophila	1	1	1	-	1	-	-	-	1	-
Criblamydia sequanensis	1	1	1	1	-	1	1	-	-	-
Estrella lausannesis	1	1	1	1	-	-	-	-	-	-
Simkania negevensis	-	-	-	-	-	-	-	-	-	1

Table 5 : Trehalose-related genes in *Chlamydiae*.
Presence of trehalose-related genes in 9 *Chlamydiae* species was inferred from ChlamDB database. *treS-mak* and *glgE* are part of the GlgE-pathway. Genes of the four other pathways of trehalose synthesis are *otsA/otsB*, *treY/treZ*, *treT* and *treP*. *otsB* gene in *W. chondrophila* is fused with another gene encoding a βPGM (β-phosphoglucomutase) that catalyses the interconversion between D-glucose-6-phosphate and β-D-glucose-1-phosphate. Trehalase, that hydrolyses trehalose into two glucose molecules was not encoded inside chlamydial genomes except in *Simkania negevensis*. Activities encoded by other genes are described in the introduction. *otsA*: trehalose-6-phosphate synthase; *otsB*: trehalose-6-phosphate phosphatase; *treY*: maltooligosyl-trehalose synthase; *treZ*: maltooligosyl-trehalose trehalohydrolase; *treT*: trehalose glucosyltransferase; *treP*: trehalose phosphorylase.

First, presence of GlgE-pathway in *Chlamydiae* is always associated with the co-occurrence of at least one trehalose synthesis route. In chlamydial species defective for GlgC-pathway (i.e., *W. chondrophila*, *C. sequanensis* and *E. lausannensis*), synthesis of trehalose seems to mainly be mediated by OtsA and OtsB, thus relying on the presence of NDP-glucose and glucose-6-phosphate. Interestingly, in *W. chondrophila*, *otsB* is fused with a β-

phosphoglucomutase, that catalyses the interconversion of glucose-6-phosphate into β-D-glucose-1-phosphate. This is associated with the presence of TreP that mediates the synthesis of trehalose from glucose and β-D-glucose-1-phosphate. To the contrary, in species that possess both GlgC- and GlgE-pathways (i.e., *Parachlamydia.* sp C2, Ca. *P. massiliensis* and Ca. *P. naegleriophila*), only the TreY/TreZ route is retrieved. This route uses glycogen as a substrate to produce trehalose, and could then potentially create a bridge between GlgC- and GlgE-pathways.

Furthermore, the occurrence of trehalose biosynthetic pathways is not always correlated with the presence of the GlgE-pathway. Some other species, including *P. acanthamoeba* UV7, may accumulate trehalose through OtsA/OtsB and TreT pathways. Nonetheless, the physiological role of this trehalose remains elusive, as no *Chlamydiae*, except *S. negevensis*, that cannot synthesise trehalose, encodes a trehalase to ensure its catabolism. However, it is noteworthy that no trehalose-related genes are encoded into genomes of the *Chlamydiaceae* family. As a remainder, members of this family harbour a host range limited to vertebrates. This is particularly interesting as capacity to synthesize trehalose is ubiquitous in the tree of life, with exceptions made for vertebrates (Elbein, 1974; Argüelles, 2014).

In *E. lausannensis*, OtsA/OtsB is the only pathway to produce trehalose. OtsA activity condenses glucose-1-phosphate and NDP-glucose into trehalose-6-phosphate. However, no *glgC* or *galU* genes, encoding respectively ADP- and UDP-glucose pyrophosphorylases are found in its genome (Table 6). We rather evidenced a homolog of UGP3, a chloroplastic UDP-glucose pyrophosphorylase activity dedicated to sulfolipid biosynthesis in plants (Okazaki *et al.*, 2009). Interestingly, UGP3 is only specific to some *Archaeplastida* species and environmental *Chlamydiae* and belongs to a set of 50 to 90 chlamydial genes identified as lateral gene transfers in the genomes of *Archaeplastida* (Ball *et al.*, 2013).

	glgC	*galU*	*cugP*	*ugp3*
Chlamydia trachomatis	1	-	-	-
Parachlamydia acanthamoeba UV7	1	-	-	1
Parachlamydia sp. C2	1	-	-	1
Candidatus Protochlamydia massiliensis	2	-	-	1
Candidatus Protochlamydia naegleriophila	1	-	-	1
Waddlia chondrophila	-	-	-	1
Criblamydia sequanensis	-	-	-	1
Estrella lausannesis	-	-	-	1
Simkania negevensis	1	-	-	1

Table 6 : Genes related to NDP-glucose synthesis in *Chlamydiae*.
glgC, that encodes the bacterial ADP-glucose pyrophosphorylase, is absent from *Criblamydiaceae* and *Waddliaceae* families. Chlamydial genomes also lack a bacterial (*galU*) or cyanobacterial (*cugP*) UDP-glucose pyrophosphorylase, but rather possess a homolog of plants *ugp3*, encoding a chloroplastic UDP-glucose pyrophosphorylase

IV-B. Import of other metabolites from the host cell

Bacteria from the *Chlamydiae* phylum express various carriers to hijack energetic metabolites from their host. The first example is the hexose phosphate transporter UhpC, which imports host's glucose-6-phosphate in exchange of orthophosphate (Schwöppe *et al.*, 2002; Gehre *et al.*, 2016). The second well known example encompasses the nucleotides transporters (NTT). Several NTTs are encoded in chlamydial genomes, each of them harbouring a particular specificity to import ATP, CTP, GTP, UTP or NAD^+ (Tjaden *et al.*, 1999; Haferkamp *et al.*, 2006; Trentmann *et al.*, 2007). Like UhpC, NTTs are ubiquitous among *Chlamydiae*; only their number varies from one species to another one (Table 7).

	UhpC	*NTT*	*MntA*	*MntB*	*MntC*	*MntH*
Chlamydia trachomatis	1	2	1	1	1	-
Parachlamydia acanthamoeba UV7	2	4	1	1	1	-
Parachlamydia sp. C2	1	4	1	1	1	1
Candidatus Protochlamydia massiliensis	1	4	1	1	1	-
Candidatus Protochlamydia naegleriophila	1	4	1	1	1	-
Waddlia chondrophila	1	3	1	1	1	-
Criblamydia sequanensis	1	5	1	1	1	-
Estrella lausannesis	1	5	1	1	1	-
Simkania negevensis	1	4	1	1	1	-

Table 7 : Some genes involved in the import of metabolites in *Chlamydiae*.
Glucose-6-phosphate is imported by *Chlamydiae* using UhpC in the exchange of orthophosphate. *ntt* genes encodes nucleotides transporters. Each NTT specifically imports either ATP, CTP, GTP, UTP NAD^+ or several of them. MntABC is a manganese transporter from the ABC (ATP-binding cassette) family, while MntH belongs to the NRAMP (natural resistance-associated macrophage protein) family and imports several divalent cations including Mn^{2+}.

As the presence of divalent cations is mandatory for maltokinase activity, with Mn^{2+} being by far the best activator (Figure 35), we also took a look at the presence of genes involved in the import of manganese in *Chlamydiae* to found out that an ATP-binding cassette (ABC) manganese transporter MntABC (Kehl-Fie *et al.*, 2013; Radin *et al.*, 2019) is encoded in all chlamydial genomes. In addition, another manganese transporter MntH is encoded solely in *Parachlamydia* sp. C2 genome.

Based on this work and taking into account the current genome analysis, we propose that glycogen metabolism pathway in *Waddliaceae* and *Criblamydiaceae* families occurs as depicted on Figure 39.

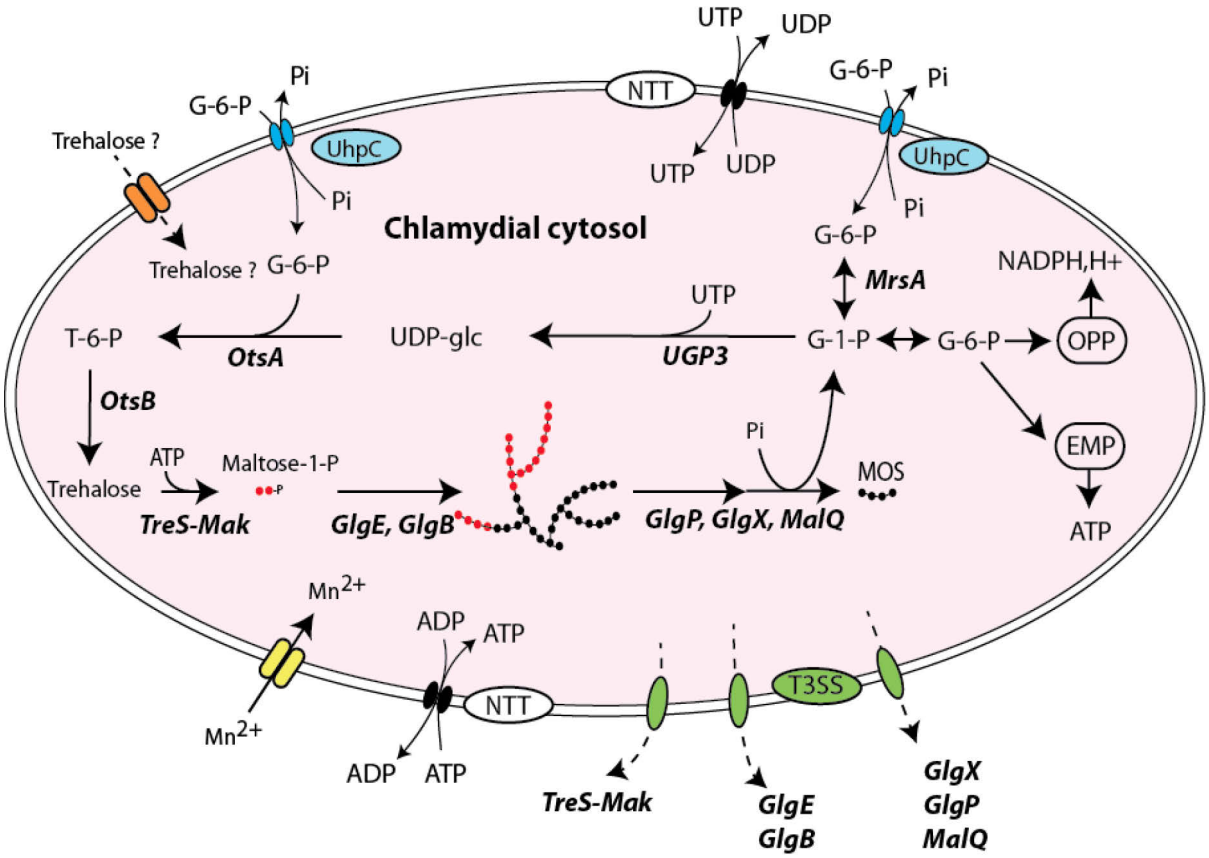

Figure 39 : Glycogen metabolism network in *Waddliaceae* and *Criblamydiaceae* families.
Glucose-6-phosphate (G-6-P) and UTP/ATP are transported in the cytosol via UhpC and NTT translocators. The first committed step consists into the isomerization of glucose-6-phosphate (G-6-P) into glucose-1-phosphate (G-1-P) catalysed by the phosphoglucomutase activity (*MrsA*). UDP-glucose pyrophosphorylase (*UGP3*) synthesizes UDP-glucose from G-1-P and UTP. Both trehalose-6-phosphate synthase (OtsA) and trehalose-6-phosphate phosphatase (OtsB) convert nucleotide-sugar and G-6-P into trehalose. The bifunctional TreS-Mak activity supplies the maltosyl transferase activity (GlgE) in maltose-1-phosphate (M1P). *De novo* glucan initiation and elongation properties of GlgE and branching enzyme activity (GlgB) allow the appearance of α-polysaccharide (*i.e.* glycogen) made of α-1,4 and α-1,6 linkages. The synergic action of glycogen phosphorylase (GlgP), debranching enzyme (GlgX) and 4-α-glucanotransferase (MalQ) depolymerize glycogen into G-1-P and short malto-oligosaccharides (MOS). The former fuels both oxidative pentose phosphate (OPP) and Embden-Meyerhof-Parnas (EMP) pathways that supply the extracellular forms (elementary bodies) in reduced power ($NADPH,H^+$) and ATP, respectively. Divalent cations Mn^{2+} required for TreS-Mak activity are probably imported *via* ABC transporter composed of MntA, MntB and MntC 3 sub-units identified in chlamydial genomes. *Waddliaceae* and *Criblamydiaceae* may manipulate the carbon pool of the host by uptaking trehalose through a putative disaccharide transporter (orange/dash arrow) or by secreting glycogen-metabolizing enzymes through type three-secretion system (green/dash arrow). In order to improve visibility, only the OtsA-OtsB route of trehalose synthesis is represented.

IV-C. Potential secretion of enzymes of the GlgE pathway by the type III secretion system

In *Chlamydiae*, many proteins involved in the glycogen metabolism act as effectors, and are therefore secreted through or into the inclusion *via* the type III secretion system (T3SS; Gehre *et al.*, 2016b; Kadouche, 2016). To test if chlamydial GlgE and TreS-Mak enzymes are also

secreted by T3SS, we decided to use a previously validated heterologous *in vivo* assay (Subtil *et al.*, 2001, 2005) based on the recognition of type III secretion signals in *Shigella flexneri*. As secretion signals are located at the amino-terminus of proteins, the 30 first amino acids of GlgE and TreS-Mak from *E. lausannensis* and *W. chondrophila* were fused to a reporter (calmodulin-dependent adenylate cyclase of *Bordetella pertussis* Cyc). The four chimera were expressed in two mutant strains of *S. flexneri*: one with a constitutively active T3SS (*ipaB*), and the other one with a defective T3SS (*mxiD*). After a 4 h culture, presence of the chimeric Cyc in the pellets and supernatants is analysed by Western blot. IpaD is a protein secreted by T3SS which serves as a positive control and must therefore be present in the supernatant of the IpaB strain and the pellet of MxiD. Conversely, the cAMP receptor protein CRP is not secreted, therefore only found in the pellets of the two strains, and serves as a negative control.

Chimeric adenylate cyclases were detected in the supernatant of the IpaB strain, and only in the pellet of the MxiD strain (Figure 40). These results suggest that GlgE and TreS-Mak from *E. lausannensis* and *W. chondrophila* harbour a signal of T3S at their amino-termini. Like many other chlamydial enzymes involved in glycogen metabolism, enzymes of GlgE pathway also appear to be secreted by the T3SS in order to hijack the host's carbohydrates metabolism. However, direct evidence of these enzymes inside the inclusion lumen or host cell are needed to conclude on their effector nature.

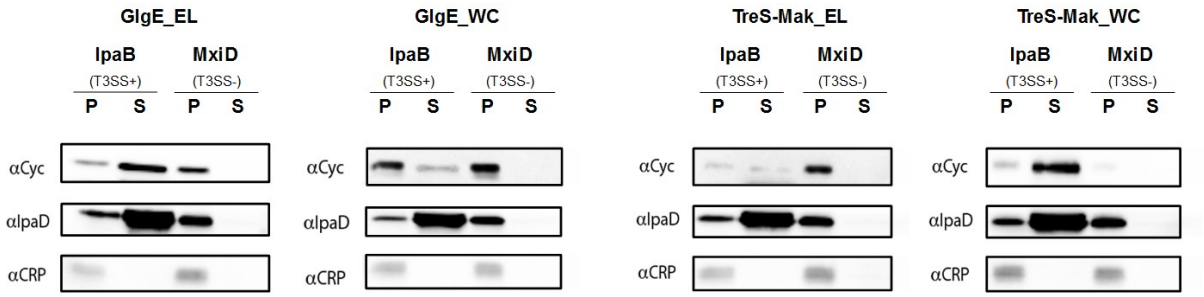

Figure 40 : Heterologous secretion assay in *Shigella flexneri* of GlgE and TreS-Mak proteins.
The first thirty amino acids at N-terminus extremity of each protein were fused with the reporter protein adenylate cyclase from B. pertussis (Cyc). Fused proteins were expressed in IpaB (T3SS+) and MxiD (T3SS-) strains of *S. flexneri* possessing a functional and a defective type-three secretion system, respectively. Western blot analyses were performed on both cell pellets (P) and supernatants (S) using anti-adenylate cyclase antibodies (αCyc). In parallel, a secreted (IpaD) and a non-secreted protein (CRP) were selected as positive and negative controls, respectively. Both proteins were detected in cell pellets or supernatants using αCRP and αIpaD antibodies. Those preliminary results suggest that both GlgE and TreS-Mak proteins of *Estrella lausannensis* (EL) and *Waddlia chondrophila* (WC) are secreted by the type-three secretion system. Assay was repeated twice.

V. Regulation of GlgE activity

Foreword: This part of my Ph.D. work is still in progress. Preliminary results regarding the regulation of GlgE_EL will be presented, and future experiments will be discussed in the afterword.

V-A. Differential expression and activity of GlgE_EL depending on the strain used

Unexpectedly, the expression of GlgE_EL in the commercial Rosetta *E. coli* strain and its glycogen-free mutant ΔCAP (*ΔglgC ΔglgA ΔglgP*) resulted in a change in the quantity and quality of the synthesis of recombinant protein. As depicted on Figures 20A and 41A, two polypeptides with apparent molecular weights of 76 and 72 kDa were purified from Rosetta strain, close from the expected molecular weight of GlgE of *E. lausannensis* (81 kDa), while a single polypeptide was observed in the ΔCAP strain (Figure 41A). Because chaperone proteins are usually co-purified with the recombinant proteins, polypeptides purified from wild-type and ΔCAP Rosetta strains were subjected to mass spectrometry analysis. Interestingly, all polypeptides correspond to the full-sized recombinant GlgE_EL. According to these results, we excluded the presence of chaperone protein or a partially cleaved GlgE_EL. In addition, we also noticed that the specific activity of GlgE_EL is 17-times lower when expressed in ΔCAP (0.33 ± 0.02 µmol.min^{-1}.mg^{-1}) rather than in Rosetta (5.69 ± 0.44 µmol.min^{-1}.mg^{-1}) (Figure 41B). Because the ΔCAP strain was originally derived from the commercial Rosetta strain, this suggests that glycogen in Rosetta cells may enhance both the expression and specific activity of GlgE_EL. In order to clarify the effect of glycogen on the expression of GlgE, the glycogen biosynthesis was induced in the ΔCAP strain by supplementing the culture medium with maltose. As reported by Park *et al*. (2011), the 4-α-glucanotransferase activity (MalQ) can disproportionate short glucans and allow the synthesis of polysaccharide in *E. coli* strain impaired in GlgC and GlgA activity. As control, various carbon sources were tested as well.

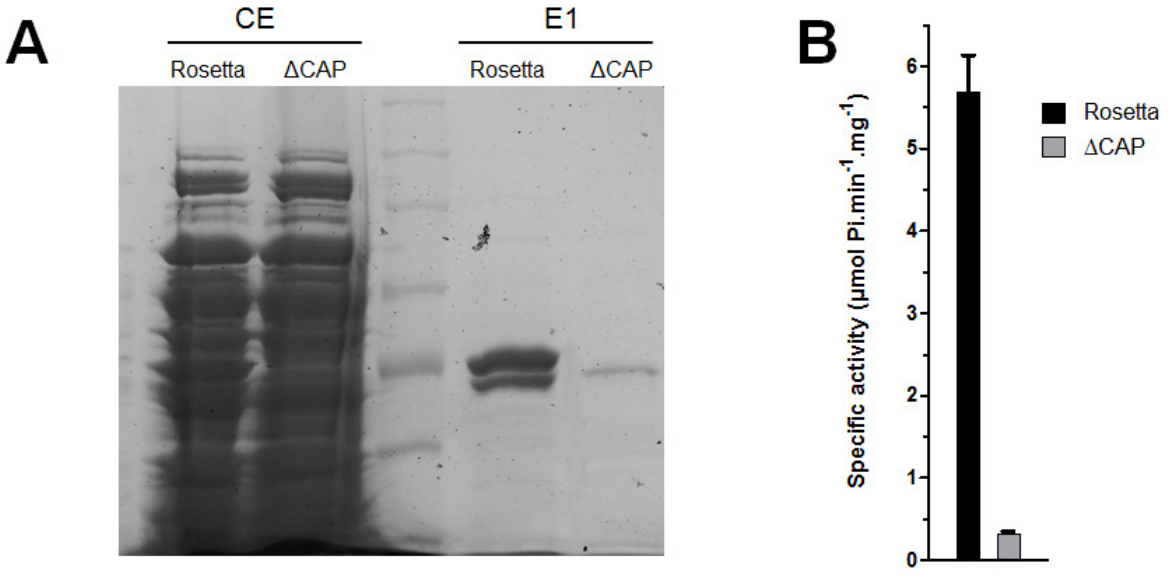

Figure 41 : Differences in expression and activity of GlgE_EL produced in Rosetta or ΔCAP cells.
(**A**) GlgE_EL was expressed in wild-type and ΔCAP (mutant impaired in glycogen synthesis) Rosetta *E. coli* strains and the level of expression was assessed on SDS-PAGE. From the same amount of cellular extract (CE), His-tagged GlgE_EL was purified by nickel affinity chromatography, and equivalent volumes of purified enzymes (E1, for Elution n°1) were loaded onto the gel. Two polypeptides were obtained for GlgE_EL expressed in Rosetta, while only one was visible when expressed in ΔCAP. Furthermore, when expressed in wild-type Rosetta, level of expression was orders of magnitude more important than in the mutant strain, (**B**) and specific activity was also 17 times higher (5.69 ± 0.44 µmol of Pi.min^{-1}.mg^{-1} in Rosetta, 0.33 ± 0.02 µmol.min^{-1}.mg^{-1} in ΔCAP).

V-B. Impact of the carbon source on GlgE_EL expression and activity

As the only difference between Rosetta and its ΔCAP derivative is the ability to synthesize glycogen, both the level of expression and specific activity of GlgE activity were measured by purifying the recombinant GlgE from Rosetta and ΔCAP strains cultivated in the absence (H2O) or in the presence of 25mM maltose, glucose, glycerol or sodium acetate (Figure 42).

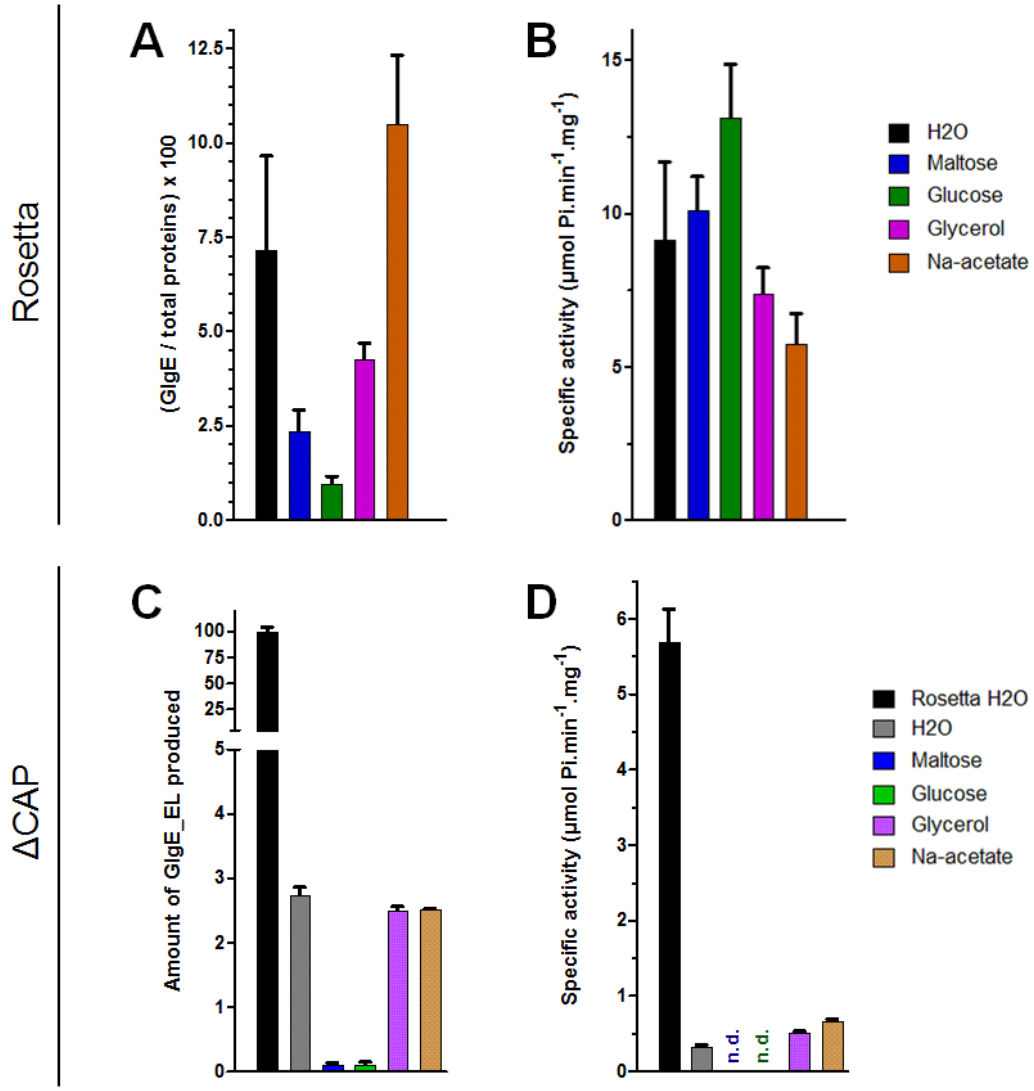

Figure 42 : Impact of the carbon source on the expression and activity of GlgE in Rosetta and ΔCAP.
Wild-type and ΔCAP Rosetta *E. coli* strains were transformed with pET15-*glgE_EL* and cultivated in LB medium supplemented with various carbon sources (25 mM of glucose, glycerol, maltose or sodium acetate) prior to induction of expression with 0.5 mM IPTG. The same volume of H_2O was added for one sample as a control. After extraction of proteins in a volume of 1 ml, His-tagged recombinant proteins were purified on Ni^{2+} affinity columns, and the amount of purified GlgE_EL was quantified by densitometry on SDS-PAGE. Level of GlgE_EL expression in Rosetta (**A**) for the different carbon sources are expressed in percentage of the total amount of proteins, while in ΔCAP (**C**) values are expressed in percentage of the expression level observed in the Rosetta control. For both strains, addition of glucose or maltose in the culture medium significantly decreased the expression of GlgE_EL in comparison with the other conditions. Specific activity of GlgE_EL expressed in Rosetta (**B**) and ΔCAP (**D**) (in µmol of orthophosphate produced per minute and per mg of proteins) was determined by malachite green assay for each condition. Condition Rosetta-H2O was used as a control for ΔCAP samples. Impact of the carbon source on GlgE_EL activity is weak in comparison with the impact of the strain. Nevertheless, in Rosetta, the specific activity slightly increases for GlgE-glucose while it slightly decreases for GlgE-glycerol and GlgE-acetate in comparison with GlgE-H2O. Even if GlgE_EL was functional when expressed in ΔCAP with glucose and maltose, expression was too low to quantify the corresponding specific activities (n.d.: not determined).

As previously observed, both the level of expression and specific activity of GlgE_EL were significantly lower in ΔCAP than in the Rosetta *E. coli* strain (Figures 42C and 42D). The presence of maltose or glucose as carbon source has a negative effect on the level of expression of GlgE in ΔCAP strain that precludes the determination of the specific activity of GlgE, while no significant effect in comparison with GlgE purified from ΔCAP strain cultivated without carbon source (H20) has been observed in the presence of both glycerol and sodium acetate. Although the various carbon sources also have negative effects on the level of expression of GlgE purified from Rosetta cells, except for sodium acetate (Figure 42A), the specific activity increases for GlgE-glucose and decreases slightly for GlgE-glycerol and GlgE-acetate in comparison with GlgE-H2O (Figure 42B). Overall, these results emphasize the unforeseen effects of carbon sources on the synthesis and specific activity of GlgE.

V-C. GlgE from *E. lausannensis* undergoes post-translational modifications

In *Mycobacterium tuberculosis*, activity of GlgE is negatively regulated by phosphorylation on multiple sites (Leiba *et al*., 2013). Therefore, the recombinant GlgE proteins previously purified were analysed by mass spectrometry for any post-translational modifications. Data obtained are resumed on Table 8 and Figure 43.

Strain	Carbon source added	Band on SDS-PAGE	Coverage (%)	Peptides	Acetylated peptides
WT Rosetta	None	Upper band	78	95	37
		Lower band	77	79	17
ΔCAP Rosetta	None	Unique	46	31	5
	Glucose	Unique	77	47	4
	Glycerol	Unique	59	45	1
	Maltose	Unique	54	39	4
	Na-acetate	Unique	67	45	0

Table 8 : Resume of mass spectrometry analysis on GlgE_EL expressed in different conditions.
GlgE_EL was expressed in wild-type and ΔCAP Rosetta *E. coli* strains. For ΔCAP, 25 mM of several carbon sources (glucose, glycerol, maltose or sodium acetate) were added in the LB medium. After purification of GlgE_EL by Ni^{2+} affinity chromatography and migration on SDS-PAGE, a doublet and a unique band were observed for GlgE_EL expressed in Rosetta or ΔCAP respectively (cf. Figure 41). Proteins were extracted from the gel and analysed on Orbitrap Q-Exactive plus mass spectrometer. Number of recovered peptides corresponding to the amino-acids sequence of recombinant GlgE_EL (S8 Figure) and sequence coverage are indicated. Among these peptides, some of them were acetylated. For GlgE_EL expressed in Rosetta, more acetylated peptides were found in the upper band than in the lower band. When expressed in ΔCAP, GlgE_EL was hypo-acetylated, especially when glycerol and sodium acetate were added in the culture medium.

These first preliminary results have shown that GlgE_EL is subjected to two kinds of post-translational modifications: acetylation on lysine residues, and phosphorylation on serines, threonines, but also on one tyrosine residue. Concerning phosphorylation, 7 sites were identified, 4 from Rosetta samples, 3 from ΔCAP maltose sample (Figure 43). It is important to remember that, in *M. tuberculosis*, 7 phosphorylation sites were identified to be involved in the negative regulation of GlgE. Only one of these 7 sites is conserved on chlamydial maltosyltransferases: T370 (T382 for *E. lausannensis*) that is not among phosphorylated

residues identified in our study. This strongly suggests that regulation mechanisms on chlamydial GlgEs strikingly differ from those that take place in *M. tuberculosis*. Indeed, the main PTM identified in this study is lysine-acetylation, especially on Rosetta's upper band sample (Table 8). In total, 24 acetylation sites were identified with probability ≥ 99 %, 17 of them within Rosetta samples.

Altogether, these results suggest that lysine acetylation is the main PTM observed on GlgE_EL, which is more prominent on GlgE_EL expressed in Rosetta than in ΔCAP. In addition, the specific activity appears to be higher for GlgE-Rosetta than for GlgE-ΔCAP, suggesting that this PTM may have a positive effect on GlgE_EL activity. It is still not clear why GlgE proteins are globally hypo-acetylated in ΔCAP strains. Could endogenous glycogen participate indirectly to the acetylation of protein?

V-D. Identified and probable acetylation sites on GlgE_EL are located at proximity of the homodimer interface and of the active site.

In order to understand the potential impact of acetylation on GlgE_EL activity, the acetylation sites were indicated on the tri-dimensional model of the enzyme. Modelization of the 3D-structure of GlgE_EL was obtained using the Phyre2 suite of tools. Structure from residues 65 to 699 (88 % coverage) was modelled with a 100 % confidence. As depicted on Figure 44A, five domains and two inserts were identified by sequence homology from *Mycobacterium thermoresistibile* and *Streptomyces coelicolor* maltosyltransferases (Mendes *et al.*, 2015; Syson *et al.*, 2011). Domains N, S, B and A have previously been shown to be involved in the homodimer interactions (to recall, GlgE_EL forms homodimers (Figure 27)), with domains A and B from one protomer interacting respectively with domains N and S of the second protomer. Domains A and B, in addition to inserts 1 and 2 form, for their part, the catalytic unit. Finally, domain C, at the C-terminal, is thought to help stabilize domain A. Specific residues involved in the active site and the homodimer interface that were predicted by InterPro are highlighted in red and blue respectively on Figure 44B. Acetylated lysine residues identified by mass spectrometry with probability ≥ 99 % and lysines conserved among all chlamydial maltosyltransferases that are potentially acetylated (identified in mass spectrometry with a probability > 0 %) are respectively highlighted in green on Figures 44C and 44D. Overall, identified and potential acetylation sites are located at proximity of the active site and of the homodimer interface. Acetylation of GlgE_EL could then potentially modulate its activity by acting on the interaction between protomers or by slight modifications of the active site. Furthermore, among acetylated lysines identified by mass spectrometry (probability ≥ 99 %), one draws our attention: Lysine 392, as this residue, conserved among all six chlamydial GlgE sequences, is predicted to be part of the active site, and was only identified on GlgE_EL expressed in the wild-type Rosetta *E. coli* strain.

Rosetta H2O – upper band

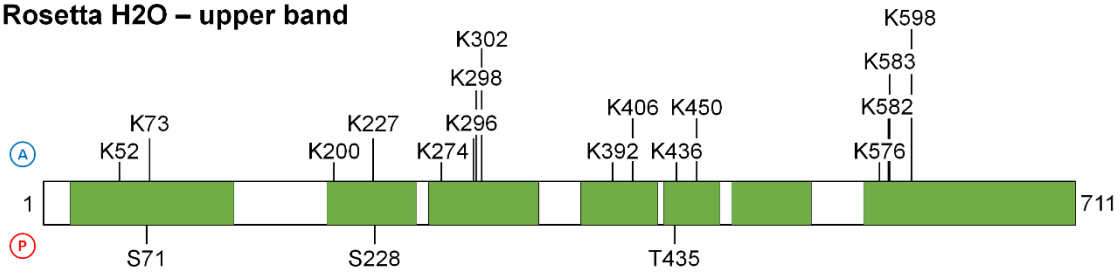

Rosetta H2O – lower band

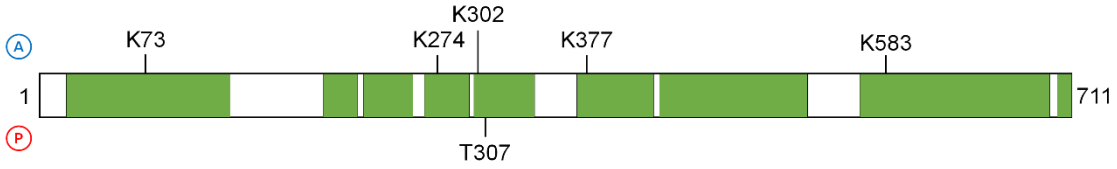

ΔCAP H2O

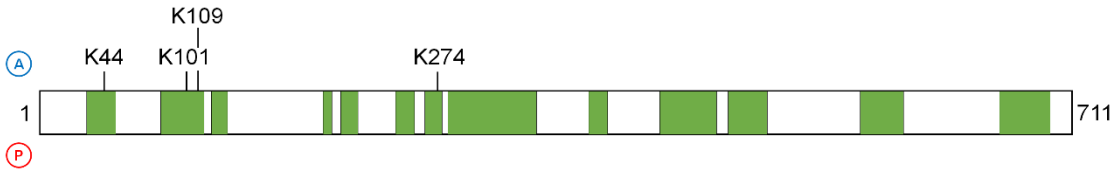

ΔCAP Glucose

ΔCAP Glycerol

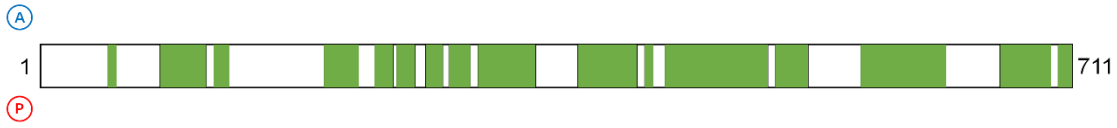

ΔCAP Maltose

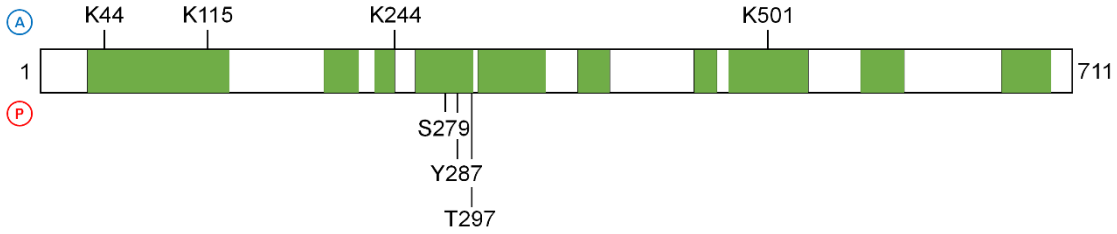

ΔCAP Sodium acetate

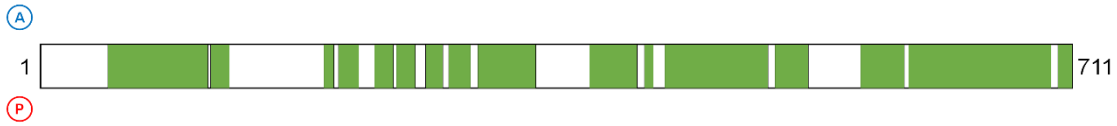

Figure 43 : Acetylation and phosphorylation sites identified on GlgE_EL.
GlgE_EL was expressed in wild-type and ΔCAP Rosetta *E. coli* strains. For ΔCAP, 25 mM of several carbon sources (glucose, glycerol, maltose or sodium acetate) were added in the LB medium. After purification of GlgE_EL by Ni^{2+} affinity chromatography and migration on SDS-PAGE, a doublet or a unique band were observed for GlgE_EL expressed in Rosetta or ΔCAP respectively (cf. Figure 41). Proteins were extracted from the bands and analysed on Orbitrap Q-Exactive plus mass spectrometer. Green boxes correspond to peptides coverage of the total His-tagged recombinant GlgE_EL sequence (S8 Figure). Peptides obtained were analysed using Proteome Discoverer software, and several peptides were identified with post-translational modifications (PTMs). Acetylation (Ⓐ) and phosphorylation (Ⓟ) sites identified with a probability ≥ 99 % are indicated for each GlgE_EL sample. 24 lysine residues (K) were found to be acetylated, with the vast majority of them (16) on the upper band of GlgE expressed in the wild-type Rosetta strain. 7 phosphorylation sites were also identified: 3 on serine (S), 3 on threonine (T) and one on tyrosine (Y) residues. This clearly evidences that GlgE_EL is the target of PTMs, including acetylation and phosphorylation.

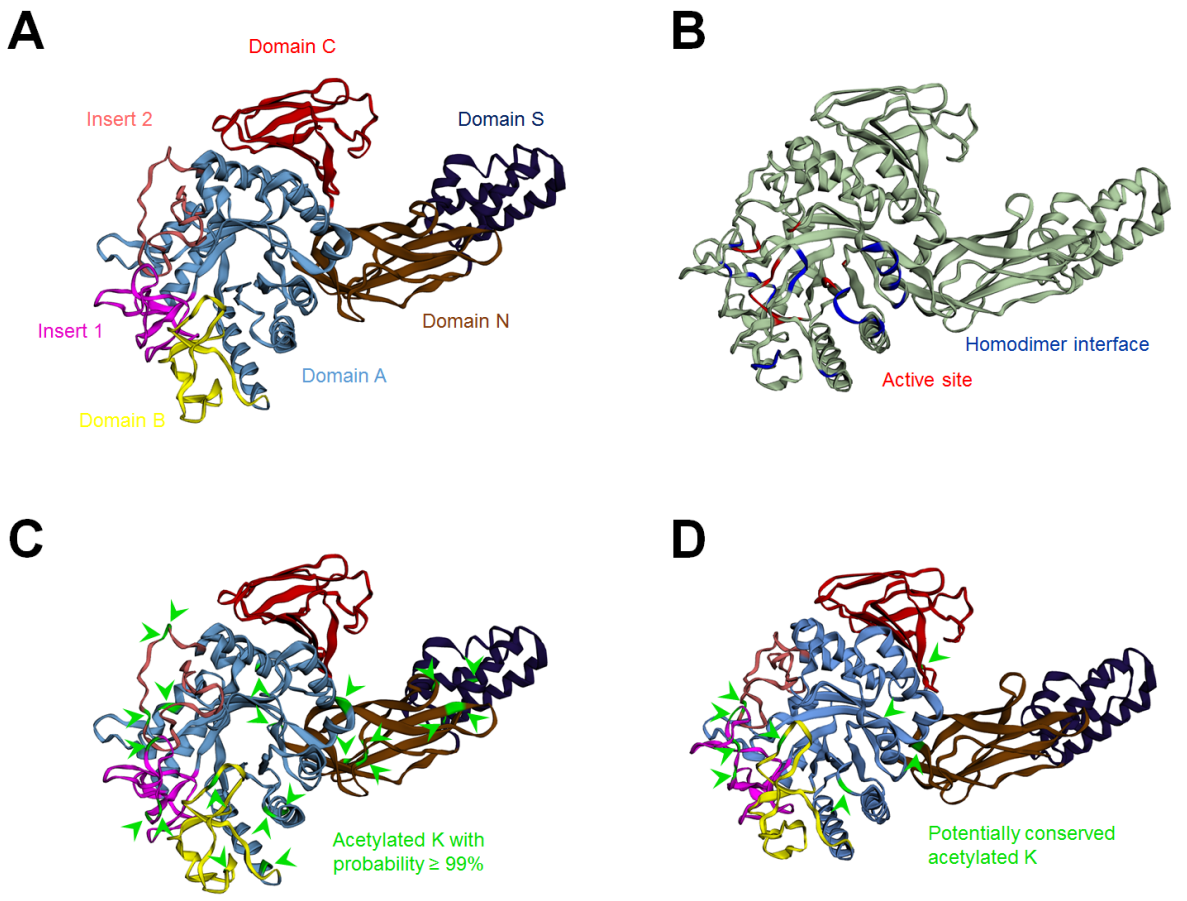

Figure 44 : Predicted structure of GlgE_EL
Cartoon representation of the three-dimensional structure of GlgE_EL was predicted using Phyre2 suite of tools. 3D structures of GlgE homologs from *Mycobacterium thermoresistibile* and *Streptomyces coelicolor* were used as models. Structure was modelled from residues 65 to 699. Figures were prepared with EzMol - Molecular display wizard. (**A**) The five domains of GlgE_EL were determined by homology. Domains N (brown) consists of residues 37-149 and 230-242, domain S (dark blue) 150-229, domain A (light blue) 243-289, 336-358, 404-551 and 587-607, domain B (yellow) 359-403, domain C (dark red) 608-699, insert 1 290-335 (magenta) and insert 2 (light red) 552-586. (**B**) Residues involved in the homodimer interface (in blue: residues 378-380, 387-389, 402, 434-437, 439, 442, 464, 466, 467, 470 and 474) and in the active site (in red: residues 300, 304, 315, 317, 360, 392, 393, 395, 396, 429, 431, 432, 460, 518, 572 and 573) were predicted using InterPro. These residues seem to be closely located, on domains A and B. (**C**) Acetylation sites identified previously by mass spectrometry (Figure 40) with a probability ≥ 99 % (K73, 101, 109, 115, 194, 200, 227, 244, 274, 296, 298, 302, 377, 392, 406, 436, 450, 501, 576, 582, 583 and 598), coloured in green, and pinpointed by green arrowheads, are located on all domains and inserts, except for domain C, with a majority of them being close to homodimer interface and active site. (**D**) Potential acetylation sites identified with a probability ranging from 0-25 % to ≥ 99 %, and conserved among the six chlamydial maltosyltransferase homologs (K81, 245, 298, 300, 302, 392, 436, 576 and 624) are highlighted in green and pinpointed by green arrowheads. Most of these residues are also closely located from residues involved in homodimer interface and active site, with K392 being part of the active site.

V-E. *In vitro* acetylation of GlgE_EL

In Bacteria, proteins can be non-enzymatically acetylated by acetyl-coenzyme A (AcCoA) or acetyl-phosphate (AcP) (Christensen *et al.*, 2019; Wang *et al.*, 2017). We therefore conducted an *in vitro* acetylation assay of purified recombinant GlgE_EL expressed in ΔCAP (hypo-acetylated form) to observe whether it is possible to improve its specific activity. As high concentrations of AcP or AcCoA are required to acetylate proteins *in vitro*, we have carried out this experiment only with AcCoA since AcP strongly interacts with the malachite green and consequently, preclude the assay of maltosyltransferase activity. We incubated 15 µg of purified GlgE_EL at 30°C with increasing concentrations of AcCoA (0, 34.2, 136.8 and 684 µM), adding 5 $mg.ml^{-1}$ of glycogen in the incubation mixtures to stabilize GlgE. After 2h, 5 µg of GlgE_EL were loaded onto SDS-PAGE (Figure 45B) and the level of protein acetylation was inferred by Western Blot using anti-N-acetyl-lysine antibody (Figure 45A and 45C). The level of protein acetylation clearly correlates with increasing AcCoA concentrations. Nonetheless, as shown on Figure 45D, the level of acetylation has no significant effect on the

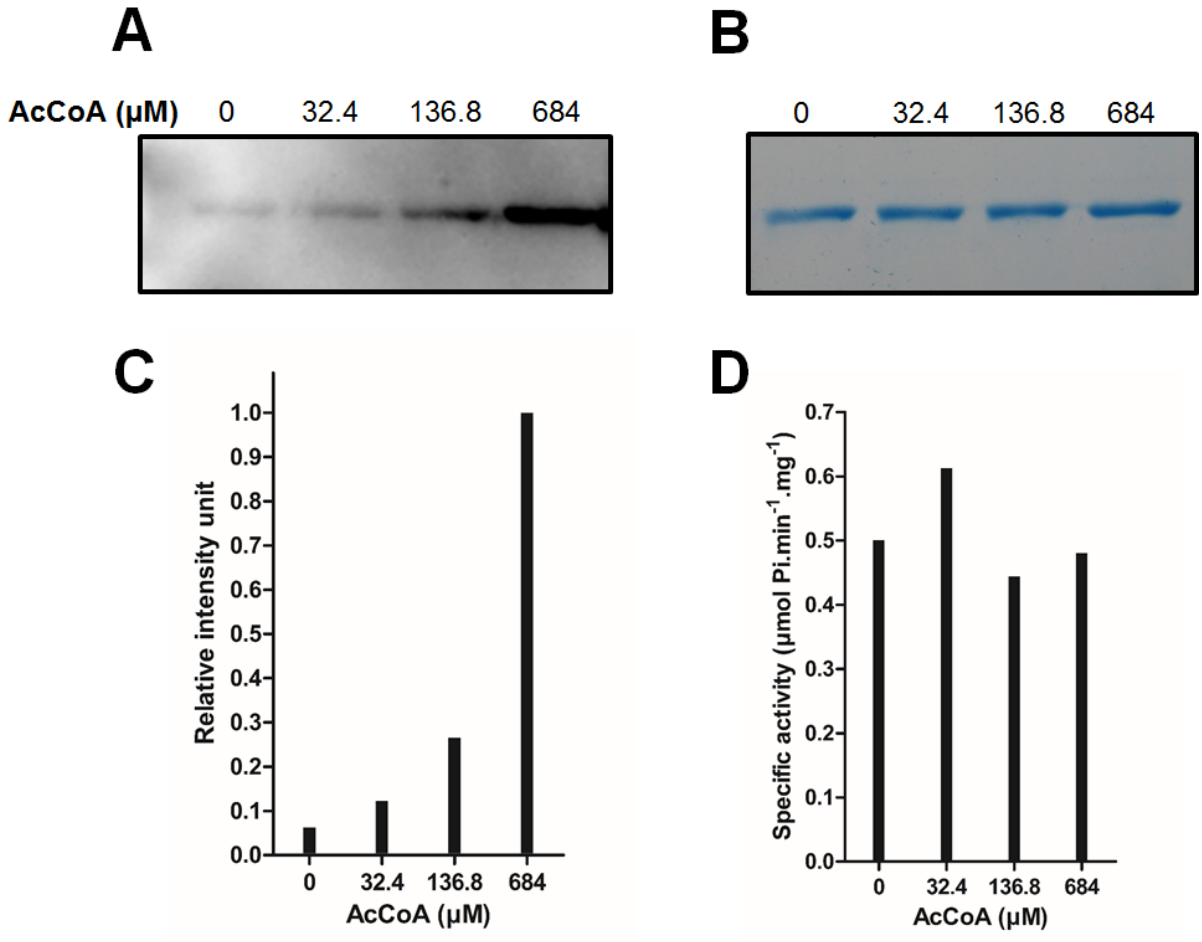

Figure 45 : *In vitro* acetylation of GlgE_EL with acetyl-coenzyme A has no impact on the specific activity.
GlgE_EL expressed in ΔCAP *E. coli* strain was purified and incubated 2h with growing concentrations of acetyl-coenzyme A (AcCoA; 0, 32.4, 136.8 and 684 µM) at 30°C. 5 $mg.ml^{-1}$ of glycogen from bovine liver were added to the incubation mixtures in order to stabilize GlgE at this temperature. (**B**) 5 µg of treated GlgE_EL were loaded on 7.5 % SDS-PAGE prior to (**A**) Western Blot using antibodies targeted against N-acetyl lysines. (**C**) While blotting signal increased with growing concentrations of AcCoA, (**D**) specific maltosyltransferase activity remains around 0.5 µmol of Pi produced per minute and milligram of proteins.

specific activity of GlgE_EL that remained around 0.5 µmol of $Pi.min^{-1}.mg^{-1}$. However, this rather surprising result may be explained by the different specificity of acetylation sites between enzymatic and non-enzymatic acetylation (Wang *et al.*, 2017; You *et al.*, 2017). Indeed, this *in vitro* acetylation with AcCoA can target other sites than the one or few that may have an effect on GlgE_EL activity.

V-F. Content of genes associated with protein acetylation in chlamydial genomes

In order to gain more insight into how protein acetylation could occur in *Chlamydiae*, we carried out a genomic survey of genes that encode proteins related to post-translational modification and AcP/AcCoA metabolisms among diverse chlamydial species (Table 9). First, we found out that most chlamydial species possess several genes encoding putative N-acetyltransferases with GNAT (Gcn5-related N-acetyltransferase) domain. The number of GNAT domain-containing proteins strongly varies from one species to another, with an overall greater number of candidates in environmental *Chlamydiae* in comparison to *Chlamydiaceae*. Indeed, 10 and 4 GNAT domain-containing proteins are respectively encoded in *E. lausannensis* and *W. chondrophila* genomes (environmental *Chlamydiae*), while only one is present in *Chlamydia pneumoniae* (*Chlamydiaceae*). While most of these genes appear to be specific and unique for one species (for instance, 3 on the 4 putative KATs of *W. chondrophila* have no homolog on NCBI nr database) or only few species, one was conserved in almost all *Chlamydiae* phylum (Table 9). As no homolog of this protein has been characterized, we decided to arbitrarily call it PG7, for Putative GNAT protein 7, as it was the 7th GNAT domain-containing protein discovered during our analysis without any characterized homolog. Furthermore, homologs of characterized *E. coli* PatZ (Castaño-Cerezo *et al.*, 2011) and partially characterized YafP acetyltransferases (Gutierrez *et al.*, 2011; Christensen *et al.*, 2018) are encoded in some chlamydial genomes, including genome of *E. lausannensis*. According to the classification of (Christensen *et al.*, 2019b), PatZ is a Type I KAT (i.e. protein of ~800-1000 amino acids, with multiple domains, one of them being the GNAT domain, at the C-terminus) while both YafP and PG7 belong to the type IV (i.e. protein of ~140-200 amino acids with a single GNAT domain). As acetylated recombinant GlgE_EL are expressed in *E. coli*, PatZ and YafP, conserved in both *E. coli* and *E. lausannensis*, are potential candidates to explain this heterologous protein acetylation. As N^{ε}-acetylation is a dynamic process, protein deacetylases are encoded in all domains of life to remove this PTM. In *E. coli*, the only known protein deacetylase is the sirtuin deacetylase CobB (Blander and Guarente, 2004; Weinert *et al.*, 2017) that is dependant of NAD^+. But in *Chlamydiae*, the only deacetylases identified during our genomic survey were Zn^{2+}-dependent class II protein deacetylases, homologs of yeast Rpd3 and *Bacillus subtilis* AcuC (Gardner *et al.*, 2006; Yang and Grégoire, 2005; Yang and Seto, 2008), which are independent from NAD^+. Nonetheless, it is striking to observe that some *Chlamydiae*, expressing putative N^{ε}-acetyltransferases, do not possess any gene encoding a deacetylase.

	PatZ - Type I	YafP - Type IV	Putative GNAT 7 - Type IV	CobB	Class II deacetylase	PTA	EutD	AckA	Acs	SpxB	PoxB	XpkA
Chlamydia trachomatis	-	-	1	-	-	-	-	-	-	-	-	-
Parachlamydia acanthamoeba UV7	-	1	1	-	1	-	-	1	1	-	1	1
Parachlamydia sp. C2	1	1	1	-	-	-	-	1	1	-	-	1
Candidatus Protochlamydia massiliensis	1	1	1	-	-	-	-	2	2	-	-	2
Candidatus Protochlamydia naegleriophila	-	1	1	-	-	-	-	1	2	-	-	1
Waddlia chondrophila	-	-	1	-	1	-	-	-	1	-	-	-
Criblamydia sequanensis	1	1	1	-	2	-	-	2	1	-	-	2
Estrella lausannesis	1	1	1	-	1	-	-	1	2	-	-	1
Simkania negevensis	-	-	2	-	-	1	-	1	-	-	-	1

Table 9 : Summary of genes encoding proteins involved in the acetylation process in some *Chlamydiae* species. From *Estrella lausannensis* genome, 10 putative protein N-acetyltransferases, containing a GNAT domain (Gcn5-related N-acetyltransferase), were found to be encoded. 3 of them are specific to *E. lausannensis*, and 4 others specific to *E. lausannensis* and few other chlamydia-like species (data not shown). The remaining 3 are more ubiquitous and consist of *E. coli* PatZ and YafP homologs and of an unknown GNAT domain containing protein retrieved in almost all *Chlamydiae* species (called PG7 for Putative GNAT domain containing protein 7, ELAC_1488 in UniProtKB database). Type of acetyltransferases are indicated according to the classification of Christensen. No orthologue of CobB, the main lysine deacetylase of *E. coli* was identified, but a class II deacetylase (Zn^{2+}-dependant) seems to be encoded in some chlamydial species. Other genes encode proteins involved in acetate, AcCoA and AcP synthesis, as depicted in Figure 46. Phosphotransacetylases PTA and EutD interconvert AcCoA in AcP, acetate kinase AckA interconverts AcP in acetate, acetyl-coenzyme A synthetase converts acetate into AcCoA, pyruvate oxidase SpxB converts pyruvate into AcP and pyruvate dehydrogenase PoxB converts pyruvate into acetate. Xylulose-5-phosphate phosphoketolase XpkA is involved is heterolactic acid pathway and catalyses the degradation of xylulose-5-phosphate into glyceraldehyde-3-phosphate and AcP.

Concerning proteins involved in both AcCoA/AcP biosynthesis and enzymatic/non-enzymatic acetylation, a summary of those proteins encoded in the genome of *E. lausannensis* is displayed on Figure 46. First, only the acetate kinase AckA and the acetyl-CoA synthetase Acs seem to be conserved in most of environmental *Chlamydiae*. These two enzymes catalyse the synthesis of AcCoA and AcP from acetate, respectively. The absence of any gene encoding a phosphotransacetylase (PTA or EutD) is quite surprising since in many bacteria, PTA and AckA form a major pathway for the synthesis of AcP. Presence of a gene encoding an ADP-forming acetyl-CoA synthetase AcdA, that converts AcCoA into acetate, is unclear, as the only putative protein that possesses such a predicted domain happens to be the acetyl-transferase PatZ. Nonetheless, in addition to acetate, the entry metabolite for the synthesis of both AcP and AcCoA appears to be glucose-6-phosphate (G6P). First, AcP can be produced directly from G6P by the phosphoketolase pathway (a.k.a heterolactic acid pathway), with the action of the xylulose-5-phosphate phosphoketolase XpkA (Table 9). This pathway, found in heterolactic bacteria, seems to be surprisingly conversed among environmental *Chlamydiae*. On the other hand, AcCoA is produced with the successive action of the Embden-Meyerhof-Parnas pathway (glycolysis) and the pyruvate dehydrogenase (PDH) complex. It is noteworthy that pyruvate oxidase SpxB and pyruvate dehydrogenase

PoxB are lacking in most chlamydial genomes, preventing a bridge for the production of AcP and AcCoA from either pyruvate and acetate.

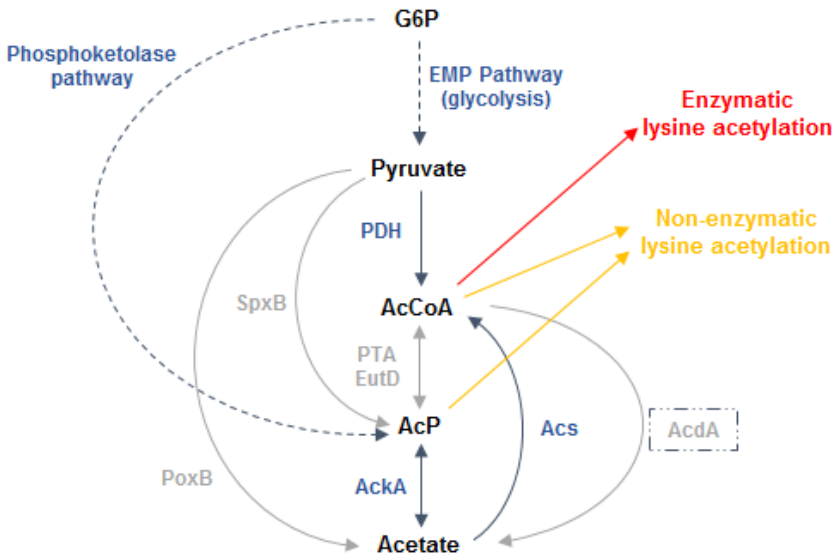

Figure 46 : Acetyl-CoA and acétyl-phosphate biosynthesis pathways in *E. lausannensis*.
In dark blue: putative enzymes encoded in *E. lausannensis* genome; in grey: not encoded. While the presence of AcCoA is mandatory for enzymatic protein acetylation, both AcCoA and AcP are able to non-enzymatically acetylate proteins. In *E. lausannensis*, these two metabolites seem to be produced independently from G6P, through phosphoketolase and EMP pathways or from acetate with the action of acetate kinase and acetyl-CoA synthetase. G6P: glucose-6-phosphate ; AcCoA: acetyl-coenzyme A ; AcP: acetyl-phosphate ; EMP pathway: Embden-Meyerhof-Parnas pathway ; PDH: pyruvate dehydrogenase complex ; PTA & EutD: phosphotransacetylases ; AckA: acetate kinase ; Acs: acetyl-CoA synthetase (AMP-forming) ; AcdA: acetyl-CoA synthetase (ADP-forming) ; SpxB: pyruvate oxidase ; PoxB: pyruvate dehydrogenase. Presence of a gene encoding AcdA is unclear, as the only putative protein that harbour such a predicted domain happens to be the acetyl-transferase PatZ.

V-G. Impact of glycogen on the activity of GlgE_EL

To confirm that the effect of endogenous glycogen metabolism on expression, PTMs and activity of recombinant GlgE_EL in the BL21-derivative Rosetta *E. coli* strain (Figure 41) is not associated to the intensive genetic engineering of this strain, we decided to repeat our experiments another genetic background: the K12-derivative BW25113 strain. A ΔglgC BW25113 strain, impaired in glycogen synthesis, was generated by insertion of a kanamycin resistance cassette inside the gene encoding ADP-glucose pyrophosphorylase. Both wild-type and mutant strains were further lysogenized with λDE3 phage to introduce the T7 RNA polymerase gene under lac promoter. After transformation with pET15b-*glgE_EL*, the expression of His-tagged recombinant enzyme was induced by adding 0.5 mM IPTG at mid exponential growth phase. After overnight incubation at 30°C, recombinant GlgE was purified on Ni^{2+} affinity chromatography. Like in the Rosetta cell background, the expression of recombinant GlgE_EL was significantly lower in the ΔglgC mutant strain impaired in glycogen synthesis than in the BW25113 wild-type strain (data not shown). But a major difference with Rosetta was observed on SDS-PAGE, since GlgE_EL purified from both wild-type (BW25113) and ΔglgC mutant strains appears as a doublet (Figure 47A). Specific activity of GlgE_EL was twice lower from ΔglgC (6.6 µmol $Pi.min^{-1}.mg^{-1}$) than from wild-type (13.3 µmol $Pi.min^{-1}.mg^{-1}$).

Although we noticed a lowest specific activity of GlgE purified from ΔCAP (below 1 µmol $Pi.min^{-1}.mg^{-1}$), a significant effect remains observable when GlgE is expressed in a glycogen-free background. It is important to keep in mind that, in addition to the differences in regulation of the acetate metabolism between BL21 and K12 *E. coli* strains (Castaño-Cerezo *et al.*, 2015), a ΔglgC strain strongly differs from a ΔCAP (ΔglgCΔglgAΔglgP) strain in terms of glycogen metabolism. Indeed, previous studies have shown that ΔglgC *E. coli* strains are still able to synthesize small amounts of glycogen (Eydallin *et al.*, 2007b; Morán-Zorzano *et al.*, 2007).

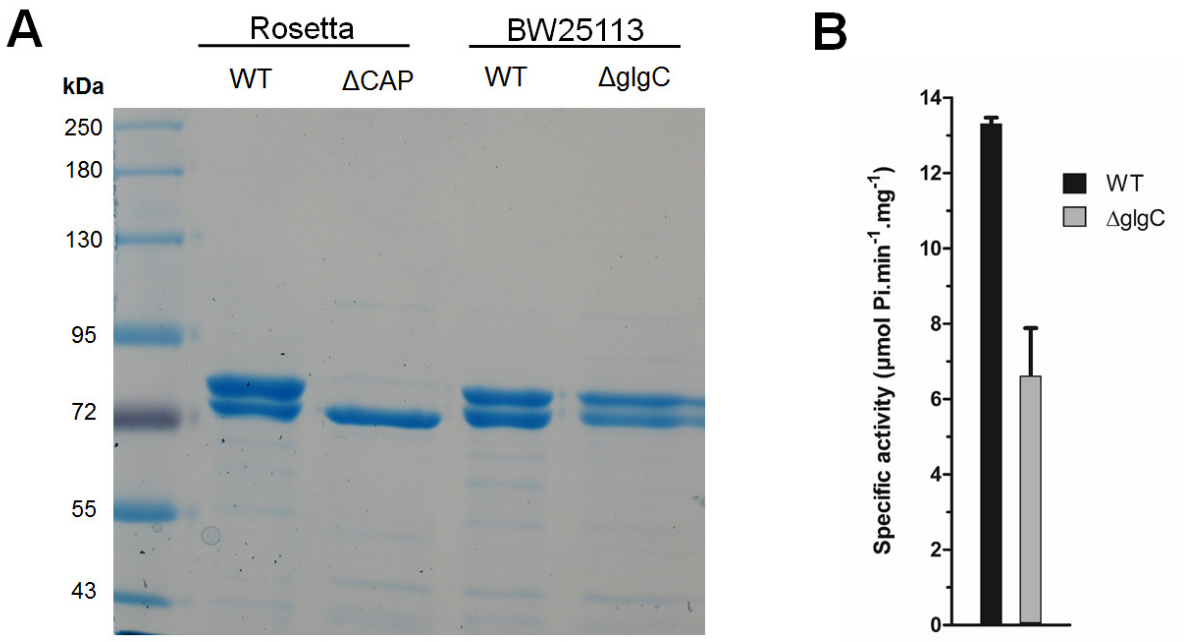

Figure 47 : Expression of recombinant GlgE_EL in isogenic *E. coli* strains impaired or not in glycogen biosynthesis and effects on the specific activity of GlgE_EL.
GlgE_EL was expressed in wild-type and ΔglgC BW25113 *E. coli* strains. Mutant strain is impacted in the glycogen synthesis as no ADP-glucose can be synthesized by the ADP-glucose pyrophosphorylase GlgC. After purification on Ni^{2+} column, His-tagged recombinant GlgE_EL from both BW25113 strains were loaded on SDS-PAGE (**A**). GlgE_EL expressed in WT and ΔCAP Rosetta strains were sued as controls. In contrast to GlgE_EL expression profile in Rosetta, a doublet was observed in both wild-type and mutant BW25113. (**B**) Specific activity of GlgE_EL expressed in WT and ΔCAP was measured by malachite green assay after incubation of the recombinant enzyme with 2 mM M1P and 5 $mg.ml^{-1}$ glycogen from bovine liver. Activity was approximately two times lower in the mutant than in the wild-type BW25113 strain.

V-H. Afterword

As previously mentioned, data presented in this part are preliminary results. Future experiments are planned to fully elucidate the mechanism regulating the maltosyltransferase activity of *E. lausannensis*. First, we are planning to confirm some of the preliminary results that we obtained. A mass spectrometry analysis of GlgE_EL expressed in the BW25113 strain would confirm that this enzyme is the target of N^{ε} lysine acetylation. Moreover, it would give us more information to determine which acetylation sites are involved in the regulation of GlgE activity. We also intend to confirm that the overall acetylation level of GlgE varies between the

four strains used (Rosetta, ΔCAP, wild-type and ΔglgC BW25113) by western blot against N-acetyl lysines.

In addition, a few questions remain unanswered. What is the exact acetylation mechanism involved to enhance GlgE activity? Which acetylation sites have the greatest impact on GlgE activity?

In order to answer these questions, it is important to recall the three known mechanisms of N^{ε} lysine acetylation: enzymatic acetylation by a specific KAT and non-enzymatic acetylation by either AcCoA or AcP. We have already shown that non-enzymatic acetylation of GlgE_EL by AcCoA has no impact on its activity (Figure 45). To determine which of the two remaining mechanisms is involved in the regulation of GlgE activity, we are currently planning to express GlgE in BW25113 *E. coli* strains impaired in the synthesis of AcP (*ΔptaΔackA*) or in acetyltransferase activity (*ΔpatZ*). In addition, three genes of *E. lausannensis*, encoding putative KATs (the homologs of *E coli patZ* and *yafP*, as well as *pg7*) are cloned for their future co-overexpression with GlgE_EL. Determination of GlgE specific activity, of acetylation level by western blot, and of acetylated sites by mass spectrometry, for each condition, should allow us to demonstrate by which mechanism GlgE_EL is regulated. Finally, substitution of a few selected lysine residues by glutamine should help us to pinpoint which acetylation sites have the greatest impact on GlgE activity.

Discussion

The present study examined the glycogen metabolism pathway in *Chlamydiae* phylum. Unlike other obligate intracellular bacteria, *Chlamydiae* have been documented to retain their capacity to synthesize and degrade storage polysaccharide with the notable exception of the *Criblamydiaceae* and *Waddliaceae* families, for which the key enzyme of glycogen biosynthesis pathway, ADP-glucose pyrophosphorylase GlgC activity is missing. In bacteria, all mutants deficient in GlgC activity are associated with glycogen-less phenotypes. While it has been shown that *E. coli* strains lacking a functional GlgC still synthesize small amounts of glycogen (Eydallin *et al.*, 2007b; Morán-Zorzano *et al.*, 2007), so far, no alternative ADP-glucose-producing activity has been identified among prokaryotes (Preiss, 2014; Wilson *et al.*, 2010). To our knowledge, only two cases have been documented for which GlgC activity has been bypassed in the classical GlgC-pathway. The ruminal bacterium *Prevotella bryantii* that does not encode an ADP-glucose pyrophosphorylase (*glgC*) gene has replaced the endogenous *glgA* gene with an eukaryotic UDP-glucose-dependent glycogen synthase (Lou *et al.*, 1997). The second case reported concerns the GlgA activity of *Chlamydia trachomatis* which has evolved to polymerize either UDP-glucose from the host or ADP-glucose produced by its own GlgC activity (Gehre *et al.*, 2016). In order to get some insight in *Criblamydiaceae* and *Waddliaceae* families, a survey of glycogen-related enzymes involved in the classical GlgC-pathway and in the recently described GlgE-pathway was carried out over 47 chlamydial species representing the diversity of *Chlamydiae* phylum (Figure 17). As expected, we found a complete GlgC-pathway in most chlamydial families and the most striking finding was the occurrence of GlgE-pathway in three phylogenetically related families: *Parachlamydiaceae*, *Waddliaceae* and *Criblamydiaceae*. Our genomic analysis also pinpointed a systematic lack of *glgC* gene in 6 draft genomes of Candidatus *Enkichlamydia* sp. Those genomes are derived from metagenomic studies and were estimated to be 71 to 97% complete. If we assume that Candidatus *Enkichlamydia* sp lost *glgC*, the characterization of glycogen synthase with respect to nucleotide sugars should shed light on the glycogen pathway, and may provide another example of GlgC bypass in the classical GlgC-pathway. In addition to the occurrence of GlgE-pathway, a detailed genomic analysis of *Waddliaceae* and *Criblamydiaceae* families has revealed a large rearrangement of *glg* genes of GlgC-pathway, which had led to the loss of *glgP* gene and a fusion of *glgA* and *glgB* genes. This fusion appears exceptional in all three domains of life and no other such examples have been reported. In *E. lausannensis* (*Criblamydiaceae* fam.), the fusion of *glgA-glgB* genes is associated with a non-sense mutation resulting in a premature stop codon in the open reading frame of the GlgA domain, precluding the presence of the fused branching enzyme (Figure 13). We have shown that the glycogen synthase domain of chimeric GlgA-GlgB of *W. chondrophila* was active and remained ADP-glucose dependent while its branching enzyme domain already appears to be non-functional due to the presence of GlgA domain at the N-terminal extremity that prevents

branching activity (Figure 14). In line with these observations, at variance with *Parachlamydiaceae* which have only maintained the *glgB* gene of GlgC-pathway, both *Waddliaceae* and *Criblamydiaceae* have conserved *glgB2* gene in GlgE operon, further suggesting that the glycogen branching activity domain is indeed defective or impaired in all GlgA-GlgB fusions. Overall, this study clearly implies that GlgC-pathway does not operate in both the *Waddliaceae* and *Criblamydiaceae* families. In addition it appears possible that the genes required for the presence of a functional GlgC-pathway are at different stages of disappearance from these genomes, as suggested by the non-sense mutation in glgA-glgB gene of *E. lausannensis* (Andersson and Kurland, 1998).

We further investigated the GlgE glycogen biosynthesis pathway in *Chlamydiae*. A series of biochemical characterizations have shown that GlgE activities are capable of transferring maltosyl residue of maltose-1-phosphate onto linear chains of glucose. More remarkably, GlgE activities fulfil the priming function of glycogen biosynthesis as described for GlgA activity in GlgC-pathway (Ugalde *et al.*, 2003). We have shown that the GlgE activities switch between the processive-like or distributive modes of polymerization depending on the initial presence of glucan chains. Thus the “processive mode” of GlgE activity yields long glucan chains (up to DP 32) and is favoured in their absence or in the presence of short glucan primers (DP<4). This “processive mode” of GlgE activity fulfills the critical function of initiating long glucan chains that will be taken in charge by the branching enzyme in order to initiate the formation of glycogen particles. *In vitro* incubation experiments performed in the presence of M1P and/or branching enzyme activity further confirmed that GlgE activity alone is sufficient to synthesize *de novo* a branched polysaccharide with high molecular weight. At variance with *Mycobacteria* and *Streptomyces*, trehalose synthase (TreS) and maltokinase (Mak) activities of *Chlamydiae* form a bifunctional enzyme composed of TreS and Mak domains at the N- and C-terminus, respectively, which has never been reported to our knowledge. The fused TreS-Mak activity is functional and mediates the trehalose conversion into maltose and the phosphorylation of maltose into maltose-1-phosphate in the presence of ATP, GTP or UTP as phosphate donors. In contrast to *Mycobacteria*, the maltokinase domain requires preferentially manganese rather magnesium as divalent cation (Mendes *et al.*, 2010). Interestingly, and in contrast to what the fusion between TreS and Mak activities could let us suppose, maltose produced by TreS is not funnelled to the catalytic site of Mak, providing the opportunity to use either free trehalose or free maltose to produce M1P.

The fact that occurrence of GlgE-pathway is limited to a few chlamydial families has led us to wonder about the origin of this operon. Our phylogeny analyses suggest that GlgE operons identified in *Chlamydiae* species share a common origin but are only distantly related to the GlgE operon from *Actinobacteria* (i.e., *Mycobacteria*). We could not determine whether the presence of the GlgE pathway predated the diversification of *Chlamydiae* or whether the operon was acquired by lateral gene transfer by the common ancestor of the *Criblamydiaceae*,

Waddliaceae and *Parachlamydiaceae* from another member of the PVC superphylum. One fair inference is that the genome of common ancestor of *Waddliaceae, Criblamydiaceae* and *Parachlamydiaceae* families encoded both GlgC- and GlgE-pathways. The loss of both *glgP* and *glgC* and fusion of *glgA* and *glgB* occurred before the emergence of *Waddliaceae* and *Criblamydiaceae* and may involve one single deletion event if we presume a *glgA/glgC/glgP/glgB* gene arrangement in the common ancestor. While GlgE pathway was maintained in *Waddliaceae* and *Criblamydiaceae* due to the mandatory function of glycogen in *Chlamydiae*, most members of *Parachlamydiaceae* retained only the GlgC-pathway except for three species. The redundancy of glycogen metabolism pathways in these *Parachlamydiaceae* species is quite surprising and goes against the general rule of genome optimization of obligate intracellular bacteria. It is worthy to note that *P. naegleriophila* species was originally isolated from a protist *Naegleria* sp. *N. fowleri,* the etiological agent of deadly amoebic encephalitis in humans (Casson *et al.*, 2008; Michel *et al.*, 2000), that stores carbon exclusively in the form of trehalose and is completely defective for glycogen gene network (Opperdoes *et al.*, 2011). Therefore, it is tempting to hypothesize that *P. naegleriophila* use the retained GlgE-pathway to effectively mine the trehalose source of its host either by uptaking trehalose from its host through a putative disaccharide transporter or by secreting enzymes of GlgE pathway *via* type three secretion system. Our preliminary experiments based on heterologous secretion assay in *Shigella flexneri* suggested that GlgE and TreS-Mak could be secreted by the type three-secretion system (Figure 40). In this context, further infection experiments of a *Naegleria* sp. with *P. naegleriophila* could fulfil two purposes: (i) figure out whether the presence of GlgE-pathway gives an advantage in infecting this particular protist, and (ii) to provide indirect *in situ* evidence of the putative secretion of TreS-Mak and GlgE. Indeed, as *Naegleria* sp. are unable to synthesise glycogen, the observation of glycogen particles within the lumen of the inclusion or inside the host's cytosol during the infection would imply the secretion of chlamydial enzymes involved in glycogen metabolism. Like in *Chlamydiaceae*, the secretion of chlamydial glycogen metabolism pathway may be a strategy for manipulating the carbon pool of the host (Gehre *et al.*, 2016). As reported for *P. amoebophila* with respect to D-glucose (Sixt *et al.*, 2013), the uptake of host's trehalose or maltose may provide an important advantage in terms of energy costs. In comparison with GlgC-pathway, only one molecule of ATP is required to incorporate two glucose residues onto growing polysaccharide with GlgE-pathway; at the scale of one glycogen particle synthesis this may represent a significant amount of ATP saving. The uptake of radiolabelled trehalose or maltose by host-free elementary bodies may or not support this hypothesis.

The preservation of the glycogen metabolism pathway through the bottleneck of genome reduction process suggests an unexpected function of glycogen that has been hitherto underestimated within *Chlamydiae*. As a result, the question arises as to why *Chlamydiae* have maintained a glycogen metabolism pathway, making them unique among obligate intracellular bacteria. It is worthy to note that most of obligate intracellular bacteria, like

Anaplasma spp., *Ehrlichia* spp., *Wolbachia* spp., *Rickettsia* spp. do not experience environmental stresses like *Chlamydiae* and *Coxellia burnetii* (Otten *et al.*, 2018). They thrive in nutrient rich environments either in animal or insect hosts. Losses of metabolic functions such as carbon storage metabolism in obligate intracellular bacteria are balanced by the expression of a wide variety of transporters for the uptake metabolites from the host. Except for ultra-resistant spore-like forms of *C. burnetii* named small cell variants, over the last decade, our perception of EBs has switched from an inert spore-like form to metabolic active form capable of transcription and translation activities (Haider *et al.*, 2010; Sixt *et al.*, 2013). The combination of different "omic" approaches performed on purified RBs and EBs of *C. trachomatis* and *P. amoebophila* have shown that genes involved in glycogen and energy metabolism pathways are upregulated in the late stage of development (Cossé *et al.*, 2018; König *et al.*, 2017; Skipp *et al.*, 2016) and most remarkably, the uptake of glucose and glucose-6-phosphate by EBs of *P. amoebophila* and *C. trachomatis* improves significantly the period of infectivity (Coulon *et al.*, 2012; Sixt *et al.*, 2013). Consequently, it seems reasonable to argue that the primary function of cytosolic glycogen in EBs is to fuel metabolic processes (i.e., Embden–Meyerhof–Parnas and Pentose Phosphate pathways) when EBs are facing up the poor nutrient environment (Figure 39). Future investigations should provide new opportunities to delineate the function of glycogen in *Chlamydiae* especially with the development of forward genetic approaches (Labrie *et al.*, 2019; Mueller *et al.*, 2017). Furthermore, the use of GlgE inhibitors initially designed against mycobacterial infections (Kalscheuer and Jacobs, 2010; Veleti *et al.*, 2014) and to some extent the use of inhibitors of chlamydial glycogen metabolizing enzymes might define new attractive drugs to treat *W. chondrophila,* since this *Chlamydia*-related bacteria has been increasingly recognized as a human pathogen (Baud *et al.*, 2008; Lamoth *et al.*, 2015).

In addition, this study provides new insights on GlgE-driven glycogen biosynthesis. In contrary to the classical GlgC-pathway that has been extensively studied in various species, including the model *E. coli*, GlgE pathway has been characterized only in *Actinobacteria*, especially in *Mycobacteria* and *Streptomyces*, with a particular attention for *Mycobacterium tuberculosis*. While an initial study reported that 32% and 14% of bacteria possess the GlgC- and GlgE-pathways, respectively (Chandra *et al.*, 2011), the large occurrence of GT 4 glycogen synthases among bacteria suggests that this disparity is smaller than expected (Syson *et al.*, 2020). Indeed, the characterization of the GT 4 glycogen synthase from *Mycolicibacterium smegmatis* evidences that it mainly produces M1P from ADP-glucose and glucose-1-phosphate, and hence this enzyme has been renamed maltose-1-synthase GlgM (Koliwer-Brandl *et al.*, 2016). As approximately one third of GlgA homologs actually belong to the GT 4 family, the occurrence of GlgC-pathway was revised down to 20 %, whereas the occurrence of GlgE-pathway using GlgM for the synthesis of M1P may be underestimated (Syson *et al.*, 2020). In contrast to *Chlamydiae*, all *Mycobacteria* and *Streptomyces* species harbour a maltose-1-phosphate synthase. Thus, this study is, to our knowledge, the first characterization

of a GlgE-pathway that does not involve a GlgM activity, and therefore relies solely on trehalose metabolism. In addition to providing the first characterization of a fused TreS-Mak enzyme, this study also emphasizes the role of trehalose metabolism in the *Chlamydiae* phylum. With exceptions for *Chlamydiaceae*, most chlamydial species (i.e., environmental *Chlamydiae*) possess at least one metabolic pathway for the synthesis of trehalose. Apart from its role in the GlgE-pathway, relevance and function of trehalose among *Chlamydia*-like is still to be determined.

As the accumulation of maltose-1-phosphate intermediate is toxic, the GlgE-pathway should be tightly regulated to prevent cytopathic effects. While maltokinase activity should be the wisest target, only regulation mechanisms on GlgE have been reported. First, the translation of the *glgE-glgB* operon of *Corynebacterium glutamicum* was shown to be slightly enhanced when glucose was added in the culture medium (Seibold *et al.*, 2011). Second, the GlgE activity of *M. tuberculosis* was reported to be negatively regulated by Ser/Thr phosphorylation (Leiba *et al.*, 2013). Seven phosphorylation sites were identified, and phosphorylation on each of them led to a reduction in maltosyltransferase specific activity by a 2 to 3 orders of magnitude. But these sites are not conserved on chlamydial GlgEs, suggesting another mechanism. Instead, we are reporting a post-translational regulation on GlgE of *Estrella lausannensis* involving N^{ε} lysine acetylation. While lysine acetylation in bacteria is generally associated with a decrease of the targeted enzymatic activity, hyper-acetylation of GlgE was correlated with an enhanced maltosyltransferase activity. More than twenty acetylation sites were identified, suggesting the importance of this yet not studied post-translational modification among *Chlamydiae*. However, the exact mechanism leading to GlgE acetylation still remains obscure. Recombinant GlgE was non-enzymatically acetylated *in vitro* by acetyl-coenzyme A, but with no impact on maltosyltransferase activity, suggesting that sites involved in GlgE regulation are not targeted by this mechanism. As enzymatic acetylation mediated by lysine acetyltransferases but also non-enzymatic acetylation by acetyl-CoA and acetyl-phosphate all target different lysine residues (Baeza *et al.*, 2015), we inferred that GlgE regulation relies either acetylation by acetyl-phosphate or lysine acetyltransferases. Genomic analysis revealed that both mechanisms are suitable, as metabolic routes for the synthesis of AcCoA and AcP, as well as some acetyltransferases are encoded in chlamydial genomes. Notably, homologs of *E. coli* acetyltransferases PatZ and YafP are encoded in the genome of *E. lausannensis*. This could explain how GlgE is acetylated in a heterologous system. In order to unravel which one of the two mechanisms is involved in GlgE acetylation, we are currently planning to express GlgE in *E. coli* strains impaired in the synthesis of AcP (*ΔptaΔackA*) or in acetyltransferase activity (*ΔpatZ*). In addition, few acetyltransferases genes of *E. lausannensis* are being cloned for their further co-overexpression with GlgE in order to place the finger on the enzyme involved in this regulation mechanism.

On the other hand, by expressing GlgE of *E. lausannensis* in *E. coli* strains with various genetic backgrounds, we observed that impairment in endogenous glycogen metabolism was correlated with both a decrease in acetylation and maltosyltransferase activity. This effect might be explained by a reduced pool of AcCoA and AcP, as both of them are mainly produced through glycolytic pathways. However, questions arise on the regulation of GlgE, but also on the role of protein acetylation in the context of an obligate intracellular lifestyle. As a further study, it would be interesting to assay if chlamydial acetyltransferases are virulence effectors secreted by the type III secretion system to rapidly modulate metabolism of the host upon their entry or if, on the contrary, protein acetylation allows the bacteria to quickly adapt to an environmental variation in an energy efficient way.

Material and methods

I. General material and methods

I-A. Strains and culture conditions

Escherichia coli Rosetta™ (DE3; pRARE) strain was purchased from Merck, Top 10 and BL21 AI strains from ThermoFisher and BW25113 from *E. coli* Genetic Stock Center. Single knocked-out *ΔglgA* and *ΔglgC* strain are BW25113 derivatives whereas *ΔCAP* (*ΔglgC*, *ΔglgA*, *ΔglgP*) strain is Rosetta™ derivative. The inducible T7 RNA polymerase gene was introduced in wild-type and mutant BW25113 stains using ΔDE3 lysogenization kit (Novagen). Strains were cultivated at 37°C under agitation in Lysogeny Broth (LB ; 1% bacto-tryptone, 0.5% yeast extract, 1% NaCl) or Terrific Broth (TB ; 2% bacto-tryptone, 1% yeast extract, 0.4% glycerol, 17 mM KH_2PO_4 and 72 mM K_2HPO_4) or plated on similar solid media (addition of 1.2% agarose). Media were supplemented with proper concentration of antibiotics: 50 µg/ml of kanamycin (Kan), 100 µg/ml of ampicillin (Amp), 25 µg/ml of chloramphenicol (Cm) or 15 µg/ml of gentamicin (Gent).

I-B. Gene cloning

Genes to overexpress were cloned using Gateway® technology (ThermoFisher). Genes were amplified using primers listed in S1 Table from *Chlamydiae* genomic DNA kindly provided by Dr. A. Subtil from Pasteur Institute (Paris, France) or from *E. coli* BW25113 genomic DNA. *attB* sequences were added at each extremity of the primers to transfer amplicon into pDONR™221 entry vector by BP cloning. Genes of interest were then transferred to pET15b (ColE1 replicon) or VCC1 (p15A replicon) plamsids by LR cloning, both vectors adding a 6xHis tag at the amino terminus of the recombinant protein.

I-C. Recombinant proteins expression

Expression of recombinant proteins was carried out at 37°C in liquid LB ou TB. At at the mid-logarithmic phase growth (A600 = 0.45), expression of recombinant proteins was induced by addition of 0.2% L-arabinose and 1 mM isopropyl β-D-1-thiogalactopyranoside (IPTG) for BL21 AI cells, or with 0.5 mM IPTG in all other *E. coli* strains.]. After 18h of incubation at 30°C, cells were harvested at 4000g at 4°C during 15 minutes. Cell pellets were stored at -80°C until purification step on Ni 2+ affinity column.

I-D. Purification of 6xHis-tagged recombinant proteins

Cell pellets from 100 mL of culture medium were suspended in 1.5 mL of cold buffer (25 mM Tris-acetate, pH 7.5). After sonication (three times 30 s), proteins were purified on Ni^{2+} affinity column (Roth) equilibrated with washing buffer (300 mM NaCl, 50 mM sodium acetate and 60 mM imidazole, pH 7) and eluted with a similar buffer containing 300 mM NaCl, 50 mM sodium acetate and 250 mM imidazole, pH 7. Purification steps were followed by SDS-PAGE and purified enzymes were quantified by Bradford method (Bio-Rad).

II. State of art of glycogen metabolism in the *Chlamydiae* phylum

II-A. Determination of glycogen synthase activities

Fused *glgA-glgB* genes of *E. lausannensis* and *W. chondrophila* were amplified using primer couples harbouring *attB* sites as described in the S1 table. PCR products were then cloned in the pET15b (Novagen) plasmid, modified to be compatible with the Gateway™ cloning strategy. Expression of his-tagged recombinant GlgA-GlgB protein was performed in the derivative BW25113 strain impaired in the endogenous glycogen synthase activity (*ΔglgA*).

Glycogen synthase assays were performed in the synthesis direction. 40 µl of crude extracts were incubated 15 min at 35°C in the presence of 50 mM HEPES-NaOH pH 7, 10 $mg.ml^{-1}$ glycogen, 100 mM $(NH_4)_2SO_4$, 10 mM Dithiothreitol (DTT), 0.5 $mg.ml^{-1}$ BSA, 8 mM $MgCl_2$ and a mix of either 3 mM ADP-glucose + 2 µM ADP-^{14}C-glucose or 3 mM UDP-glucose + 2 µM UDP-14C-glucose. After incubation of the 100 µl reactions, glycogen was precipitated by addition of 1 ml methanol-KCl (75% v/v; 1% m/v) during 10 min at -20°C, then centrifuged 5 min at 3 000 g and 4°C. This washing step was repeated 2 more times before suspension of the pellet in 200 µl of ultrapure water. Finally, 2.5 ml of scintillation cocktail were added to count scintillation of incorporated radiolabelled glucose into glycogen particles. Radiolabelled nucleotide-sugars were purchased from Amersham-Biosciences.

Zymogram analysis was performed in 7.5% acrylamide-bisacrylamide native gels containing 0.6% of glycogen from bovine liver (Sigma Aldrich). Crude extracts were loaded and migration was performed in ice-cold Tris (25 mM) glycine (192 mM) DTT (1 mM) buffer, during 2 h at 120 V and 15 mA per gel, using MiniProtean II (Biorad) electrophoresis system. Gels were then incubated overnight, at room temperature and under agitation, in a specific buffer to induce glycogen synthase activity (70 mM glycyl-glycine pH 9, 135 mM $(NH_4)_2SO_4$, 8 mM $MgCl_2$, 0,7 $mg.ml^{-1}$ BSA, 67 mM β-mercaptoethanol and either 1,2 mM ADP- or UDP-glucose. Gels were rinsed 3 times with ultrapure water prior staining with iodine solution (1% KI, 0.1% I_2). Elongation of glucose chains by glycogen synthase activity is visualized as a dark band.

II-B. Transmission electron microscopy analysis

Fresh cultures of *Acanthamoeba castellanii* grown in 10 mL YPG (Yeast extract, peptone, glucose) were infected with one-week-old 5 µm-filtered suspension of *E. lausannensis* or *W. chondrophila* (105 $cells.ml^{-1}$), as previously reported in Thomas *et al.*, 2008. Samples of time course infection experiments were harvested at 0, 7, 16 and 24 hours post-infection by centrifuging the infected *A. castellanii* cultures at 116 g. Pellets were then fixed with 1 ml of 3 % glutaraldehyde for four hours at 4°C and prepared as described in Rusconi *et al.*, 2013.

II-C. Comparative genomic analysis of glycogen metabolic pathways

In order to gain insight into *Chlamydiae*'s glycogen metabolism, homologs of proteins part of the glycogen pathway of *E. coli* and of *M. tuberculosis* were searched with BLASTp in 220 genomes and metagenome-derived genomes from 47 different chlamydial species available

on the ChlamDB database (https://chlamdb.ch/, Pillonel *et al.*, 2020). The completeness of metagenome-derived and draft genomes was estimated with checkM based on the identification of 104 nearly universal bacterial marker genes (Pillonel *et al.*, 2018). The species phylogeny has also been retrieved from ChlamDB website.

II-D. Phylogeny analysis

Homologous sequences of TreS-Mak and GlgE were carried out by BLAST against the nr database from NCBI with respectively WP_098038072.1 and WP_098038073.1 sequences of *Estrella lausannensis*. We retrieved the top 2000 homologs with an E-value cut off ≤ 10^{-5} and aligned them using MAFFT (Katoh and Standley, 2013) with the fast alignment settings. Block selection was then performed using BMGE (Criscuolo and Gribaldo, 2010) with a block size of four and the BLOSUM30 similarity matrix. Preliminary trees were generated using Fasttree (Price *et al.*, 2010) and 'dereplication' was applied to robustly supported monophyletic clades using TreeTrimmer (Maruyama *et al.*, 2013) in order to reduce sequence redundancy. For each protein, the final set of sequences was selected manually. Proteins were re-aligned with MUSCLE (Edgar, 2004) and block selection was carried out using BMGE with a block size of four and the matrix BLOSUM30. Phylogenetic trees were inferred using Phylobayes (Lartillot *et al.*, 2009) under the catfix C20 + Poisson model with the two chains stopped when convergence was reached (maxdiff<0.1) after at least 500 cycles, discarding 100 burn-in trees. Bootstrap support values were estimated from 100 replicates using IQ-TREE (Minh *et al.*, 2020) under the LG4X model and mapped onto the Bayesian tree.

III. Characterization of GlgE homologs of *E. lausannensis* and *W. chondrophila*

III-A. Expression of GlgE_WC in auto inducible medium

Expression of GlgE_WC was performed in auto inducible medium as described in Fox and Blommel, 2009. Varying concentrations of glucose (0, 0.05, 0.075 and 0.1 %), glycerol (0, 0.0375, 0.075, 0.15, 0.225, 0.3 %) and lactose (0, 0.0375, 0.075, 0.15, 0.225, 0.3 %) were tested to express GlgE_WC in liquid medium at 23°C, 30°C and 37°C, under agitation. The best condition to express GlgE_WC was at 30°C with 0.1% glucose, 0.225% lactose and 0.0375% glycerol. After 18h at 30°C, cells were harvested at 4000 g at 4°C during 15 minutes. Cell pellets were stored at -80°C until purification step on Ni^{2+} affinity column.

III-B. Evidence of maltosyltransferase activities by thin layer chromatography.

Maltosyltransferase activities of GlgE_EL and GlgE_WC were first evidenced by incubating the purified recombinant enzymes overnight at 30°C with 10 $mg.ml^{-1}$ glycogen from rabbit liver (Sigma-Aldrich) and 20 mM inorganic phosphate in 20 mM Tris-HCl buffer (pH 6.8). Reaction products were separated on thin layer chromatography Silica gel 60 W (Merck) using the solvent system n-butanol/ethanol/water (5/4/3 v/v/v) before spraying orcinol (0.2%)-sulphuric

(20%) solution to visualize carbohydrates. GlgE_WC was concentrated using Amicon® Ultra-4 filtration system.

III-C. Production and purification of maltose-1-phosphate

Maltose-1-phosphate (M1P) was enzymatically produced from 20 ml of reaction mixtures containing 1 mg of GlgE-EL, 10 $mg.ml^{-1}$ of potato amylopectin and 20 mM of orthophosphate in 20 mM Tris-HCl pH 6.8. After overnight incubation at 30°C, M1P and over left polysaccharide were separated according to their molecular weight on size exclusion chromatography (TSK-HW 50 (Toyopearl), column size: length 48 cm, diameter 2.3 cm) equilibrated with 1% ammonium acetate at the flow rate of 1 $ml.min^{-1}$. In the second step, M1P and orthophosphate were separated by using anion exchange chromatography (Dowex 1 X 8 100-200 mesh acetate form (Bio-Rad), column size: length 28 cm, diameter 1.6 cm) equilibrated with 0.5 M potassium acetate pH 5 at the flow rate of 0.75 $ml.min^{-1}$. M1P containing fractions were then neutralized with an ammoniac solution (30%). Finally, M1P was desalted using cation exchange chromatography (Dowex 50 W X 8 50-100 mesh H^+ form (Bio-Rad), column size: length 10 cm, diameter 1 cm) equilibrated with water. Around 10 mg of maltose-1-phosphate were recovered from a reaction mixture of 20 mL, with a yield of approximately 5%. Maltose-1-phosphate was also produced by incubating overnight at 30°C recombinant TreS-Mak protein from E. lausannensis with 20 mM ATP, 20 mM maltose, 10 mM MnCl2, 125 mM imidazole and 150 mM NaCl. Following an anion exchange chromatography step as described above, maltose-1-phosphate was purified from remaining maltose and salts using Membra-cell MC30 dialysis membrane against ultrapure water. This purification procedure leads to a better yield (around 10 % of initial maltose was recovered in the form of purified M1P) of highly pure M1P (≥ 98 %).

III-D. MALDI-TOF MS Analysis.

P-maltose was analysed by a MALDI-QIT-TOF Shimadzu AXIMA Resonance mass spectrometer (Shimadzu Europe; Manchester, UK) in the positive mode. The sample was suspended in 20 µL of water. 0.5 µL sample was mixed with 0.5 µL of DHB matrix on a 384-well MALDI plate. DHB matrix solution was prepared by dissolving 10 mg of DHB in 1 mL of a 1:1 solution of water and acetonitrile. The low mode 300 (mass range m/z 250-1300) was used and laser power was set to 100 for 2 shots each in 200 locations per spot.

III-E. Proton-NMR analysis of maltose-1-phosphate

Sample was solubilized in D2O and placed into a 5mm tube. Spectra were recorded on 9.4T spectrometer (1H resonated at 400.33 MHz and 31P at 162.10MHz) at 300K with a 5 mm TXI probehead. Used sequences were extracted from Bruker library sequence. Delays and pulses were optimized for this sample.

III-F. Zymogram analysis of maltosyltransferase activity

Crude protein extracts (2 µg) or purified recombinant enzymes were loaded onto 7.5% acrylamide-bisacrylamide native gels containing 0.3% glycogen from bovine liver (Sigma-Aldrich) or 0.3% potato starch (w/v). Electrophoresis was performed in ice-cold running buffer (25 mM Tris, 192 mM glycine, 1 mM DTT) during 2 h at 120 V (15 mA per gel) using MiniProtean II (Biorad) electrophoresis system. Native gels were then soaked at room temperature and under agitation in 10 ml of incubation buffer (25 mM Tris-acetate pH 7.5, 0.5 mM DTT) supplemented with 1 mM maltose-1-phosphate or 20 mM orthophosphate. After overnight incubation, gels were rinsed 3 times with ultrapure water prior staining with iodine solution (1% KI, 0.1% I_2).

III-G. Determination of chlamydial GlgE substrate specificity by FACE

GlgE activity was qualitatively monitored using fluorophore-assisted carbohydrates electrophoresis (FACE). Reactions of 100 µl with 5 mM of malto-oligosaccharides ranging from glucose to maltoheptaose, 1.6 mM M1P and an activity of 3.51 nmol of orthophosphate produced per minute for GlgE_EL and 1.38 $nmol.min^{-1}$ for GlgE_WC, were performed at 30°C during 1h and 16h. Reactions were stopped at 95°C for 5 min and supernatants recovered after centrifugation. Samples were dried out and solubilized in 2 µL of 1 M sodium cyanoborohydride (Sigma-Aldrich) in THF (tetrahydrofurane) and 2 µL of 200 mM ATPS (8-aminopyrene-1,3,6-trisulfonic acid trisodium salt, Sigma-Aldrich) in 15% acetic acid (v/v). Samples were then incubated overnight at 42°C. After addition of 46 µL ultrapure water, samples were again diluted 300 times in ultrapure water prior to injection in a Beckman Coulter PA800-plus Pharmaceutical Analysis System equipped with a laser-induced fluorescence detector. Electrophoresis was performed in a silicon capillary column (inner diameter: 50 µm; outer diameter: 360 µm; length: 60 cm) rinsed and coated with carbohydrate separation gel buffer-N (Beckman Coulter) diluted 3 times in ultrapure water before injection (7 s at 10 kV). Migration was performed at 10 kV during 1 h.

III-H. Kinetic parameters of GlgE_EL

GlgE activity was monitored quantitatively in the elongation direction by the release of orthophosphate using the Malachite Green Assay Kit (Sigma-Aldrich) following the manufacturer's instructions. The concentration of released free phosphate was estimated from a standard curve. The absorbency was monitored at 620 nm with Epoch microplate spectrophotometer (Biotek) after incubating with the malachite green reagent for 30 minutes. For determination of kinetic parameters, reactions were conducted in triplicate during 30 min at 30°C in 15 mM Tris-HCl pH 6.8 and 0.5 $µg.ml^{-1}$ of GlgE_EL. Reactions were stopped at 95°C during 2 min 30. Saturation plots for maltose-1-phosphate (0.044, 0.088, 0.175, 0.35, 0.7, 1.4, 2.8 and 5.6 mM) were obtained with 10 mM of maltoheptaose or 10 $mg.ml^{-1}$ of glycogen from bovine liver (Sigma-Aldrich), whereas 2 mM maltose-1-phosphate were used to get saturation plots for maltoheptaose (0.313, 0.625, 1.25, 2.5, 5, 10 and 20 mM) and

glycogen from bovine liver (0.313, 0.625, 1.25, 2.5 and 5 mg.ml^{-1}). Kinetic curves were fitted according to Michaelis-Menten ($v = \frac{V \max S}{Km + S}$) and allosteric ($v = \frac{V \max S^h}{S_{0.5}^h + S^h}$) models of GraphPad Prism version 5. Optimal temperature and pH were assayed with 1 mM maltose-1-phosphate and 5 mM maltoheptaose, respectively in 25 mM Tris-HCl pH 6,8 and at 30°C. Temperature was tested in the range of 15°C to 45°C and pH between 3 and 8.8 with different buffers: 25 mM sodium acetate at pH 3.7, 4.8 and 5.2 ; 25 mM sodium citrate at pH 3, 4, 5 and 6 ; 25 mM Tris-HCl at pH 6.8, 7, 7.5, 7.8, 8 and 8,8.

III-I. Determination of the apparent molecular weight of GlgE and TreS-Mak

The apparent molecular weight of recombinant GlgE_EL and TreS-Mak_EL were determined using native PAGE and gel filtration. For native PAGE, 5%, 7.5%, 10% and 15% acrylamide: bisacrylamide (37.5:1) gels (20 cm x 18.5 cm x 1 mm) were loaded with 6 µg of protein of interest and some standard proteins of known mass: 15 µg carbonic anhydrase (29 kDa), 20 µg ovalbumin (43/86 kDa), 15 µg BSA (66.5/133/266/532 kDa), 15 µg conalbumin (75 kDa), 1.5 µg ferritin (440 kDa) and 25 µg thyroglobulin (669 kDa). Log10 of migration coefficient was plotted against the acrylamide concentration in the gel. Negative slopes were then plotted against molecular weights of standard proteins and the apparent molecular weight of proteins of interest was determined using slope equation. Gel permeation chromatography, Superose™ 6 10/300 GL resin (30 cm x 1 cm; GE Healthcare) was equilibrated in PBS buffer (10 mM orthophosphate, 140 mM NaCl, pH 7.4) at 4°C and with a flow rate of 0.3 ml.min^{-1}. Void volume was determined using Blue Dextran 2000. Standard proteins used were ribonuclease A (13.7 kDa, 3 mg.ml^{-1}), ovalbumin (43 kDa, 4 mg.ml^{-1}), aldolase (158 kDa, 4 mg.ml^{-1}), ferritin (440 kDa, 0.3 mg.ml^{-1}) and thyroglobulin (669 kDa, 5 mg.ml^{-1}). All standard proteins used were from GE's Gel Filtration Low Molecular Weight Kit and GE'S Gel Filtration High Molecular Weight Kit (GE Healthcare), except for BSA (Sigma Aldrich).

III-J. Structural analysis of the branched polysaccharide synthesized *in vitro*

1 mg glycogen from bovine liver (Sigma) and *de novo* polysaccharide produced from overnight incubation of 2 mg maltose-1-phosphate with 30 µg GlgE_EL and 200 µg GlgB2_WC were purified by size exclusion chromatography on TSK-HW 50 (Toyopearl, 48 x 2.3 cm, flow rate of 0.5 ml.min^{-1}) equilibrated with 1% ammonium acetate. Remaining maltose-1-phosphate was dephosphorylated with 10 U of alkaline phosphatase (Sigma-Aldrich) overnight at 30°C and samples were dialyzed using Membra-Cel MC30 dialysis membrane against ultrapure water. The chain length distribution of samples was then analysed following protocol described just above, with slight differences. Prior to APTS labelling, samples were debranched overnight at 42°C in 50 mM sodium acetate pH 4.8 by 2 U of isoamylase from *Pseudomonas* sp. (Megazyme) and 3.5 U of pullulanase M1 from *Klebsiella planticola* (Megazyme), then desalted with AG® 501X8(D) Mixed Bed Resin. Samples were then treated as previously

stated to undergo FACE analysis, the only difference being that labelled samples were diluted 10 times in ultrapure water before injection.

IV. Characterization of TreS-Mak from *Estrella lausannensis*

IV-A. Bacterial viability by fluorescence microscopy

BL21 AI cells transformed with VCC1-*treS-mak_EL* were cultivated at 30°C in liquid LB. At A600 = 0.45, overexpression of TreS-Mak was induced by addition of 1 mM IPTG and 0.2 % L-arabinose. After 4h, 25 ml of culture were harvested, centrifuged 10 min at 4 000 g and pellets suspended in 2 ml of wash buffer (0.85 % NaCl). 19 ml of wash buffer were added to 1 ml of resuspended cells, and were then incubated at room temperature with intermittent mix for 1h. Two supplementary washes of 2 minutes were performed prior to staining. 5 µM SYTO®9 and 30 µM propidium iodine (excitation/emission of 480/500 and 490/635 nm respectively, LIVE/DEAD® BacLight™ Bacterial Viability Kit, Thermofisher) were added to 1 ml of suspended cells, mixed thoroughly and incubated 15 min in the dark prior to observation with an AF6000X fluorescent microscope (Leica Microsystems). Figures were reconstructed using Fiji software (ImageJ).

IV-B. Kinetic parameters of the maltokinase domain of TreS-Mak_EL

Maltokinase activity of TreS-Mak protein was monitored following the amount of nucleoside bi-phosphate released. 20 µL of reaction mixtures were added to 80 µl of pyruvate kinase buffer (75 mM Tris-HCl pH 8.8, 75 mM KCl, 75 mM $MgSO_4$, 2 mM phosphoenolpyruvate, 0.45 mM reduced NADH). The amount of nucleoside diphosphate was estimated from a standard curve of ADP, measuring the decrease in absorbance at 340 nm 30 min after addition of 5 U of L-lactic dehydrogenase and 4 U of pyruvate kinase (both from rabbit muscle, Sigma-Aldrich). Optimal divalent cation and nucleoside triphosphate were inferred by incubating 1h at 30°C 10 $\mu g.ml^{-1}$ of recombinant TreS-Mak_EL with 20 mM maltose, 20 mM ATP or other nucleosides phosphate (CTP, GTP or UTP) and 10 mM $MnCl_2$ or other divalent cations ($FeSO_4$, $ZnSO_4$, $CuSO_4$, $CaCl_2$, $CoSO_4$, $CoCl_2$, $NiSO_4$, $NiCl_2$ or $MgCl_2$) in 97.5 mM imidazole, 120 mM NaCl and 20 mM sodium acetate buffered at pH 7. To determine pH and temperature optima, 25 $\mu g.ml^{-1}$ of purified TreS-Mak_EL were incubated for 30 min in the presence of 20 mM maltose, 20 mM ATP, 10 mM of $MnCl_2$, in 32.5 mM sodium acetate, 195 mM NaCl and 162.5 mM imidazole buffers ranging from pH 4 to 9 at 30°C, or in the same buffer at pH 7 from 15 to 45°C respectively.

IV-C. Kinetic parameters of the trehalose synthase domain of TreS-Mak_EL

Trehalose synthase activity of His-tagged TreS-Mak_EL recombinant protein was monitored following the interconversion of trehalose into maltose and glucose using Epoch spectrophotometer (Biotek). 15µl of reaction sample were incubated 30 min at 58°C with 30 µl of 100 mM sodium citrate pH 4.6 containing in the presence or absence of 0.4 U of amyloglucosidase from *Aspergillus niger* (Megazyme) to respectively quantify the amount of

maltose or free glucose released after addition of 100 µl of a working buffer (500 mM triethanolamine hydrochloride, 3.4 mM $NADP^+$, 5 mM $MgSO_4$ and 10 mM ATP, pH 7.8). The increase in absorbance at 340 nm after the supplementary addition of 1.2 U of hexokinase and 0.6 U of glucose-6-phosphate dehydrogenase (Megazyme) allowed us to estimate the amount of glucose units from a standard curve. Unless otherwise stated, enzymatic reactions were performed 40 min at 30°C, pH 8, with 125 mM imidazole, 150 mM NaCl, 200 mM trehalose, 1 mM $MnCl_2$ and approximately 130 $\mu g.ml^{-1}$ of TreS-Mak_EL and were stopped at 95°C for 2 min 30. To obtain saturation plot for trehalose, 130 $\mu g.ml^{-1}$ of TreS-Mak_EL were incubated 40 min at 30°C and pH 8 with 125 mM imidazole, 150 mM NaCl, 25 mM sodium acetate, 1 mM $MnCl_2$ and varying concentrations of trehalose (10, 20, 50, 100 and 200 mM). Enzymatic activities were fitted to Michaelis-Menten curve using GraphPad Prism 5 to obtain values of kinetic parameters.

V. Reconstruction of the GlgE-associated glycogen metabolism in *Chlamydiae*

V-A. Heterologous secretion assay in *Shigella flexneri* of GlgE and TreS-Mak proteins

First 30 codons of candidate genes were amplified by PCR and inserted using T4 DNA ligase in pUC19cya plasmid, upstream of the calmodulin-dependent adenylate cyclase of *Bordetella pertussis* reporter gene to obtain a chimeric gene. pUC19cya constructs were transformed in *ipaB* and *mxiD* strains of *Shigella flexneri*. 30 ml of LB medium were inoculated with 1 ml of an overnight culture for each transformed strain. After 4h at 37°C, 1 ml were harvested, centrifuged 5 min at 16 000 g, and pellets were suspended in 500 µl of Laemmli buffer (4 % SDS, 120 mM Tris-HCl pH 6.8, 5 % glycerol, 200 mM DTT, 0.02 % bromophenol blue) prior to boiling (5 min at 95°C). Concomitantly, 25 ml were harvested and centrifuged 20 min at 4 000 g. Supernatants were filtered using syringe filter with a 0.22 µm pore size (Merck) to remove remaining cells. 3 ml of 100 % trichloroacetic acid were added to precipitate proteins. After 30 min incubation on ice, supernatants were centrifuged 15 min at 10 000 g. Then, new supernatants were removed and proteins pellets were allowed to dry a room temperature for 1 hour, prior to addition of 500µl Laemmli buffer. pH was neutralized by addition of 5 µl 10 M NaOH, and samples incubated 5 min at 95°C. Samples containing cytosolic (pellet) and secreted proteins (supernatant) were then analysed by Western Blot. 35 µl of each sample were loaded on 12 % SDS-PAGE. Migration was performed in Tris (25 mM) glycine (192 mM) SDS (0.1 %) buffer, during 2 h at 120 V and 20 mA per gel, using MiniProtean II (Biorad) electrophoresis system. After separation, proteins were electrotransferred on PVDF (Polyvinylidene fluoride) membrane (Bio-Rad) using Trans-Blot® Turbo™ Transfer System (Bio-Rad) at 25 V and 1.3 A during 7 min. Membrane was first incubated in blocking buffer for 1h (5 % milk in TBS) and then incubated 1h in a fresh blocking buffer containing the primary antibodies against the calmodulin-dependent adenylate cyclase (Cyc) of *Bordetella pertussis*

(1:1000, mouse), IpaD (1:500, mouse) and the cAMP receptor protein (CRP) of *Shigella flexneri* (1:500, rabbit). Membrane was washed 2 times 10 min in TTBS (20 mM Tris-HCl pH 7.5, 500 mM NaCl, 0.05 % Tween 20) and 1 time in TBS (10 mM Tris-HCl pH 7.5, 150 mM NaCl) prior soaking with HRP-conjugated anti-mouse and anti-rabbit secondary antibodies diluted at 1:10 000 in blocking buffer for 1h. After 4 washes of 10 min in TTBS, membrane was revealed using Thermo Scientific™ Substrat chimiluminescent SuperSignal™ West Pico PLUS.

VI. Regulation of GlgE activity

VI-A. Measurement of GlgE_EL expression

Rosetta and ΔCAP cells transformed with pET15-*glgE_EL* were cultivated under agitation at 37°C in LB medium supplemented when stated with 25 mM glucose, glycerol, maltose or sodium acetate. At mid-logarithmic phase growth (A600 = 0.45), expression of recombinant GlgE_EL was induced by addition of 0.5 mM IPTG. After an overnight incubation under agitation at 30°C, cells were collected to further purification on Ni^{2+} affinity column (as described above). 50 and 100 ml of cultures were used to respectively purified GlgE_EL expressed in Rosetta and ΔCAP. Quantity of GlgE expressed in Rosetta cells without addition of a carbon source was measured by Bradford assay. This protein was loaded on a 7.5 % polyacrylamide SDS-PAGE in a range going from 33 ng to 14 µg. After migration and staining of proteins by InstantBlue™ (Merck), gel was subjected to densitometry on Model GS-800 Calibrated Imaging Densitometer (Bio-Rad) and data were analysed with Quantity One® software. Densitometry values were fitted on the known amount of GlgE_EL using the non-linear regression “Log-log line -- X and Y both log” fit on GraphPad Prism 5. The resulting standard curve allowed us to quantity the amount of GlgE_EL produced in all other conditions after SDS-PAGE and analysis in the densitometer.

VI-B. Determination of specific maltosyltransferase activity

Reactions (50 µl final volume) containing 5 $mg.ml^{-1}$ glycogen from bovine liver, 2 mM M1P, 175 mM imidazole, 105 mM NaCl, 35 mM sodium acetate and 1 $µg.ml^{-1}$ or 15 $µg.ml^{-1}$ of recombinant GlgE_EL expressed in Rosetta or ΔCAP strains, respectively, were performed at 30°C and pH 7 for 40 minutes. Reactions were stopped with a 2min30 incubation at 95°C prior to determination of specific maltosyltransferase activity. Orthophosphate produced by GlgE_EL in each condition was measured by malachite green assay, as described before. Specific activity of GlgE_EL expressed in ΔCAP and subjected to *in vitro* acetylation with acetyl-coenzyme A was determined using similar protocol, as well as GlgE expressed in both wild-type and ΔglgC BW25113 strains.

VI-C. Sample preparation for mass spectrometry

Purified His-tagged recombinant GlgE_EL expressed in wild-type and ΔCAP Rosetta *E. coli* strains were purified and separated on 7.5% polyacrylamide SDS-PAGE. Bands of interest

were cut, discoloured by successive washes in 1 ml 50 % acetonitrile (ACN) and 50 mM ammonium bicarbonate and rinsed two times 10 min in 1 ml H_2O prior to bands' dehydration (2 times 5 min in 1ml 100 % ACN). Bands were then completely desiccated using SpeedVac Vacuum Concentrator. Disulfide bonds were reduced by covering the bands with 10 mM DTT during 45 min at 56°C and free cysteines alkylated in the dark for 45 min and at room temperature by covering the bands with 1 % (w/v) iodoacetamide and 50 mM ammonium bicarbonate. Bands were then washed 15 min, under agitation, in 50 mM ammonium bicarbonate, following by three 10 minutes-long washes in 100 % ACN. Bands were then dried out prior to peptide digestion with 200 ng trypsin in 50 mM ammonium bicarbonate at 37°C overnight. Digestion products were conserved, and peptides still in the polyacrylamide gel extracted by two successive 15 minutes-long incubations at 30°C with 45 % ACN / 10 % formic acid and one last incubation at room temperature with 95 % ACN / 5 % formic acid for 15 min. Digestion and extraction products were finally pooled together and dried out on SpeedVac. This method has successively been used to identified acetylation sites in previous study (Fraiberg *et al.*, 2015).

VI-D. Mass spectrometry analysis

A nanoflow HPLC instrument (U3000 RSLC Thermo Fisher Scientific™) was coupled on-line to a Q Exactive plus (Thermo Scientific™) with a nanoelectrospray ion source. 1 µg of gel-band peptide extracts were loaded onto the preconcentration trap (Thermo Scientific™, Acclaim PepMap100 C18, 5 µm, 300 µm i.d × 5 mm) using partial loop injection, for 5 min at a flow rate of 10 µl.min^{-1} with buffer A (5% acetonitrile and 0.1% formic acid) and separated on a reversed phase column (Acclaim PepMap100 C18, 3 µm, 75 mm i.d. × 500 mm) with a linear gradient of 5–50% buffer B (75% acetonitrile and 0.1% formic acid) at a flow rate of 250 nl.min^{-1} and temperature of 45°C. Gradient length was 125 min. MS data was acquired on Q Exactive plus Orbitrap mass spectrometer (Thermo Fisher Scientific) using a data-dependent top 20 method, dynamically choosing the most abundant precursor ions from the survey scan (350–1600 m/z) for HCD fragmentation. Dynamic exclusion duration was 60 s. Isolation of precursors was performed with a 1.6 m/z window and MS/MS scans were acquired with a starting mass of 80 m/z. Survey scans were acquired at a resolution of 70,000 at m/z 400 while resolution for HCD spectra was set to 35,000 at m/z 200. MS data were then analysed using Proteome Discoverer™ Software (Thermo Fisher Scientific). Searches were performed against His-tagged GlgE_EL sequence and a database composed of protein sequences of *Escherichia coli* extracted from UniProt. Search for post-translational modifications identified lysine acetylation, cysteine carbamidomethylation, glutamine and asparagine deamination, methionine and proline oxidation, serine threonine and tyrosine phosphorylation and N-terminal glutamine cyclisation into pyroglutamate. For each PTM, site probability was calculated using ptm*RS* node. Results were filtered in order to obtain a false discovery rate of less than 1%.

VI-E. Modelization of the 3D-structure of GlgE_EL

Modelization of GlgE_EL structure was obtained on Phyre2 web portal (Kelley *et al.*, 2015), using GlgE from *Streptomyces coelicolor* and *Mycobacterium tuberculosis* as templates. Residues 65 to 699 were modelled (88 % coverage) with a 100 % confidence. Visualisation of 3D structure was displayed using EzMol 2.1 (Reynolds *et al.*, 2018). Determination of structural domains was performed by homology from structures of maltosyltransferases of *Mycobacterium thermoresistibile* and *Streptomyces coelicolor*. Residues involved in homodimer interface and actives sites were predicted using InterPro database (Mitchell *et al.*, 2019).

VI-F. *In vitro* non-enzymatic acetylation assay with AcCoA

GlgE_EL was expressed in ΔCAP *E. coli* strain, then purified by Ni^{2+} affinity chromatography. 10 µg of purified GlgE_EL were incubated at 30°C with various concentrations of AcCoA (0, 34.2, 136.8 or 684 µM) and 5 $mg.ml^{-1}$ of glycogen from bovine liver in a buffer containing 217 mM imidazole, 260 mM NaCl and 43 mM sodium acetate at pH 7 for 2h. Following the acetylation reaction, samples were analysed by SDS-PAGE, anti-acetyl lysine Western Blot and measurement of the specific maltosyltransferase activity.

VI-G. Anti-acetyl lysine Western Blot

Following *in vitro* acetylation with AcCoA, 2.5 µg of purified GlgE_EL were loaded on SDS-PAGE. After separation, proteins were electrotransferred on PVDF membrane (Bio-Rad) using Trans-Blot® Turbo™ Transfer System (Bio-Rad) at 25 V and 1.3 A during 7 min. Membrane was first incubated in a blocking buffer constituted of 5 % milk in TTBS (20 mM Tris-HCl pH 7.5, 500 mM NaCl, 0.05 % Tween 20) prior four successive 5 min long washing steps in TTBS. Blot was then incubated overnight at 4°C in TTBS supplemented with 5 % BSA and anti-acetylated lysine antibody (rabbit, Cell Signaling #9441) diluted at 1:1000. Blot was washed 4 times for 5 min each with TTBS and then incubated with HRP-conjugated anti-rabbit secondary antibody at a 1:2500 dilution in 5% milk in TTBS for 1 hour at room temperature. After 4 washes for 10 min each in TTBS, membrane was revealed using Thermo Scientific™ Substrat chimiluminescent SuperSignal™ West Pico PLUS. Quantification of acetylation was performed by densitometry using ImageJ software.

Supplementary data and methods

Name	Sequence	Hybridation temperature	Destination vector	Accesion number
F_glgE_EL	GGGGACAAGTTTGTACAAAAAAGCAGGCTTCATGATGAGTGTTTCTGCTGCCGAA	56,9 °C	pDONR 221	WP_098038073.1
R_glgE_EL	GGGGACCACTTTGTACAAGAAAGCTGGGTCTCATATAAAGTAATCGAAATTGTTTTCCCTCAGCATC			
F_glgE_WC	GGGGACAAGTTTGTACAAAAAAGCAGGCTTCATGGGACAAAATCGAGTCGTCA	61,5 °C	pDONR 221	WP_013182917.1
R_glgE_WC	GGGGACCACTTTGTACAAGAAAGCTGGGTCTCACATGAAATAGTCGAATTGTTG			
F_treS-mak_EL	GGGGACAAGTTTGTACAAAAAAGCAGGCTTCATGAAACAAGATCCGCTCTGGT	56,0 °C	pDONR 221	WP_098038072.1
R_treS-mak_EL	GGGGACCACTTTGTACAAGAAAGCTGGGTCTTAACGCATCTCCTTGAGGATATT			
F_glgB_WC	GGGGACAAGTTTGTACAAAAAAGCAGGCTTCATGAAAGAAGCAGTCGCCGTT	56,9 °C	pDONR 221	WP_013182919.1
R_glgB_WC	GGGGACCACTTTGTACAAGAAAGCTGGGTCCTATTCCGGGGACAGACAAA			
F_glgA_Ecoli	GGGGACAAGTTTGTACAAAAAAGCAGGCTTCATGATGCAGGTTTTACATGTATGTTCAG	59,8 °C	pDONR 221	CP009273.1
R_glgA_Ecoli	GGGGACCACTTTGTACAAGAAAGCTGGGTCCTATTTCAAGCGATAGTAAAGCTCA			
F_glgA-glgB_EL	GGGGACAAGTTTGTACAAAAAAGCAGGCTCGATGAAAATATTTAATATTGAAAGCAAATG	56,9 °C	pDONR 221	WP_098037869.1
R_glgA-glgB_EL	GGGGACCACTTTGTACAAGAAAGCTGGGTATTAGCCAAAGATTTTTTTTGATG			
F_glgA-glgB_WC	GGGGACAAGTTTGTACAAAAAAGCAGGCTCGATGACCGTTTCCGCCATT	61,0 °C	pDONR 221	WP_013181537.1
R_glgA-glgB_WC	GGGGACCACTTTGTACAAGAAAGCTGGGTACTAACCATGATGGACCTCCT			
F_sec_glgE_EL	AGTCAAGCTTGTAATAGTTTTGTTTTTATGAGTGTTTCTGCTGCCGAAAAG	59,8 °C	pUC19cya	WP_098038073.1
R_sec_glgE_EL	AGTCTCTAGAAACGATAGAGTGCAAAGTATTGGTATACAT			
F_sec_glgE_WC	AGTCAAGCTTGTAATAGTTTTGTTTTTATGGGACAAAATCGAGTCGTCA	58,0 °C	pUC19cya	WP_013182917.1
R_sec_glgE_WC	AGTCTCTAGAGATAGACTCTCCTAAGGTTCGTT			
F_sec_treS-mak_EL	AGTCAAGCTTGTAATAGTTTTGTTTTTATGAAACAAGATCCGCTCTGGTTTAAACACG	59,8 °C	pUC19cya	WP_098038072.1
R_sec_treS-mak_EL	AGTCTCTAGATCCGATGCCGTCGTGATTG			
F_sec_treS-mak_WC	AGTCAAGCTTGTAATAGTTTTGTTTTTATGATGCACAACTGGTATAAAGACGCAAT	59,8°C	pUC19cya	WP_013182919.1
R_sec_treS-mak_WC	AGTCTCTAGAGAAATCGCCGATGCCGTCTT			

S1 Table: List of primers used during this study. These primers were used to clone genes involved in glycogen metabolism of *E. lausannensis* and *W. chondrophila* and also for heterologous secretion assay. Underlined nucleotides represent the *attB* sites added to the amplified genes that allow cloning into pDONR 221 vectors following the recommendation of Thermofisher (Gateway™) for BP cloning. Genes were then transferred from the entry pDONR 221 vectors to pET15b or VCC1 expression vectors to overexpress recombinant proteins.

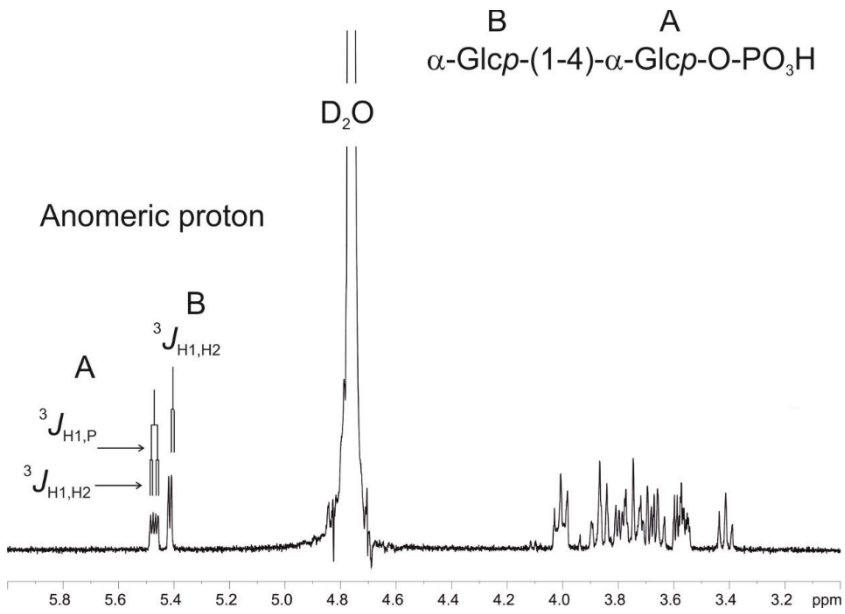

S1 Figure : 1D-1H-NMR spectrum of maltose-1-phosphate produced with GlgE_WC, glycogen and orthophosphate. α-anomer configuration of both glucosyl residues were characterized by their typical homonuclear vicinal coupling constants ($^3J_{H1A,H2A}$ and $^3J_{H1B,H2B}$) with values of 3.5 Hz and 3.8 Hz respectively. A supplementary coupling constant was observed for α-anomeric proton of residue A as shown the presence of the characteristic doublet at 5.47 ppm. This supplementary coupling constant is due to the heteronuclear vicinal correlation ($^3J_{H1A,P}$) between anomeric proton of residue A and phosphorus atom of a phosphate group, indicating that phosphate group was undoubtedly O-linked on the first carbon of the terminal reducing glucosyl unit A. The value of this $^3J_{H1A,P}$ was measured to 7.1Hz.

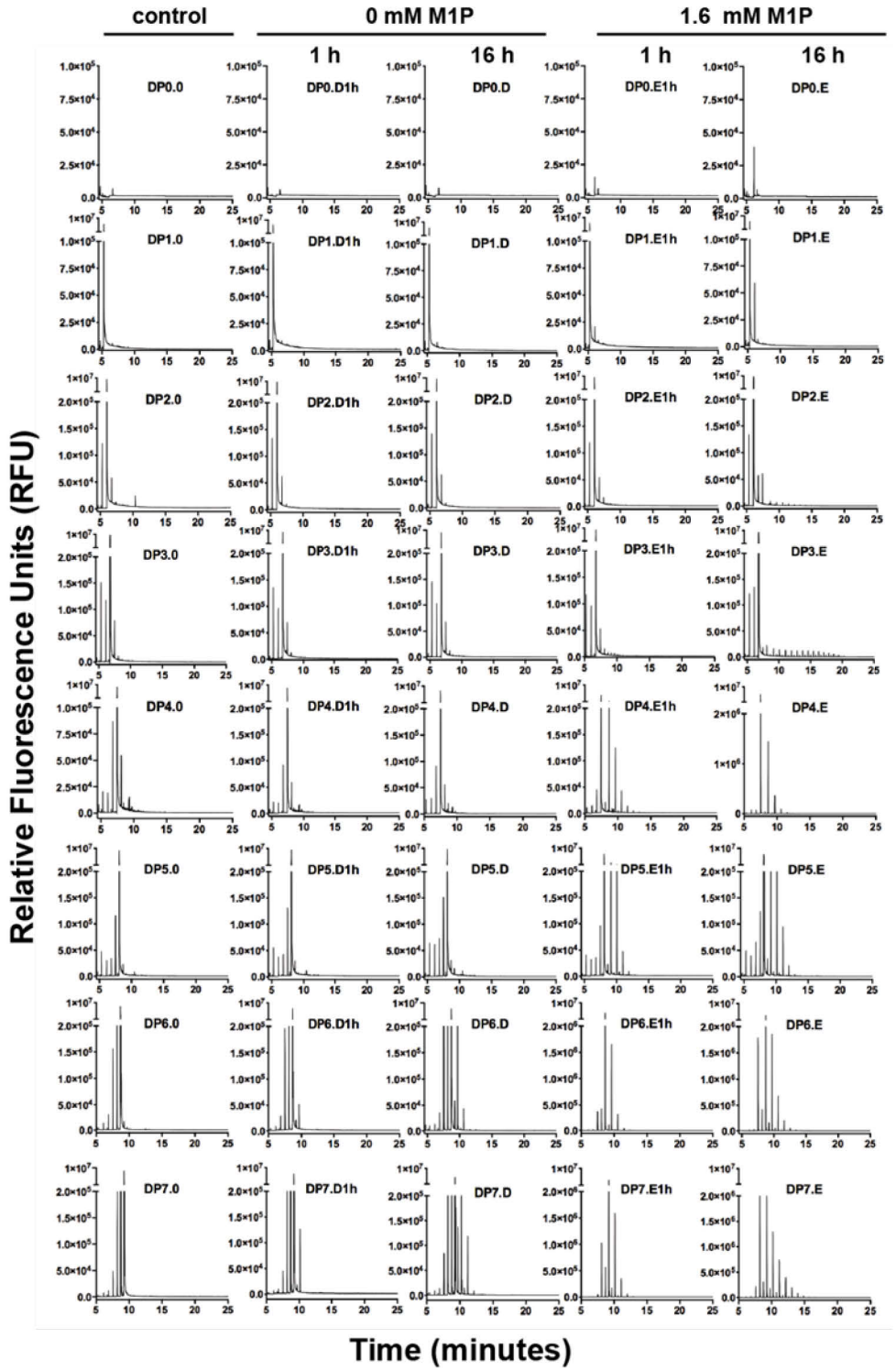

S2 Figure : FACE analysis of GlgE activity from *E. lausannensis*.
Purified recombinant GlgE (3.5 nmol Pi.min^{-1}) was incubated 1 (lanes 2 & 4) or 16 hours (lanes 1, 3 & 5) at 30°C with 5 mM of malto-oligosaccharides ranging from DP0 (nothing) to DP7 (maltoheptaose) and in absence (lanes 2 & 3) or presence (lanes 4 & 5) of 1.6 mM of maltose-1-phosphate (M1P). After incubation, enzymatic reactions are stopped 5 min at 95°C. Malto-oligosaccharides are fluorescently labelled with APTS and then separated according to their DP using capillary electrophoresis. Fluorescence is monitored as relative fluorescence units (RFU). As control, heat denatured GlgE activity was incubated 16 hours at 30°C with M1P and malto-oligosaccharides (lane 1).

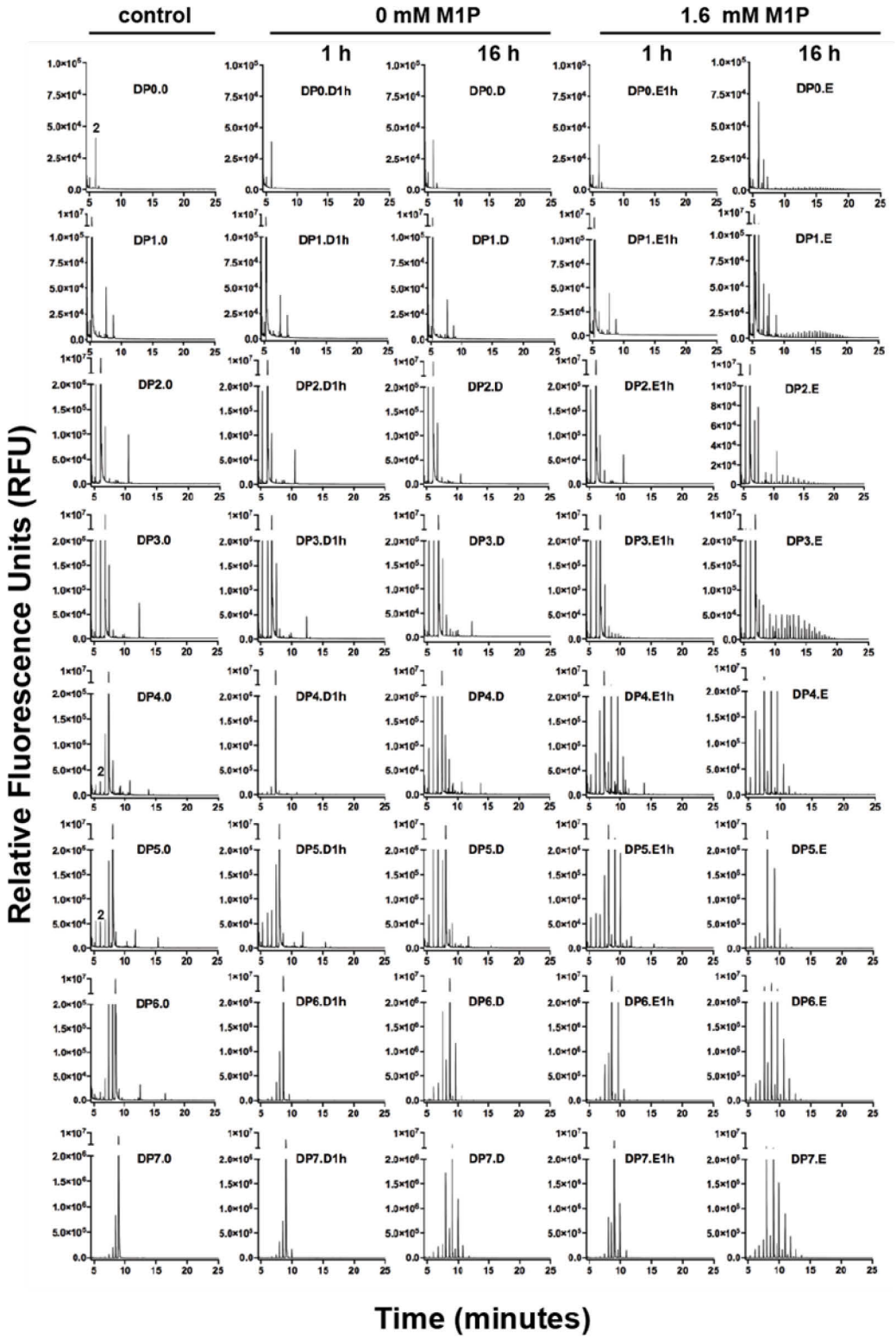

S3 Figure : FACE analysis of GlgE activity from *W. chondrophila*.
Purified recombinant GlgE (1.38 nmol Pi.min^{-1}) was incubated 1 (lanes 2 & 4) or 16 hours (lanes 1, 3 & 5) at 30°C with 5 mM of malto-oligosaccharides ranging from DP0 (nothing) to DP7 (maltoheptaose) and in absence (lanes 2 & 3) or presence (lanes 4 & 5) of 1.6 mM of maltose-1-phosphate (M1P). After incubation, enzymatic reactions are stopped 5 min at 95°C. Malto-oligosaccharides are fluorescently labelled with APTS and then separated according to their DP using capillary electrophoresis. Fluorescence is monitored as relative fluorescence units (RFU). As control, heat denatured GlgE activity was incubated 16 hours at 30°C with M1P and malto-oligosaccharides (lane 1).

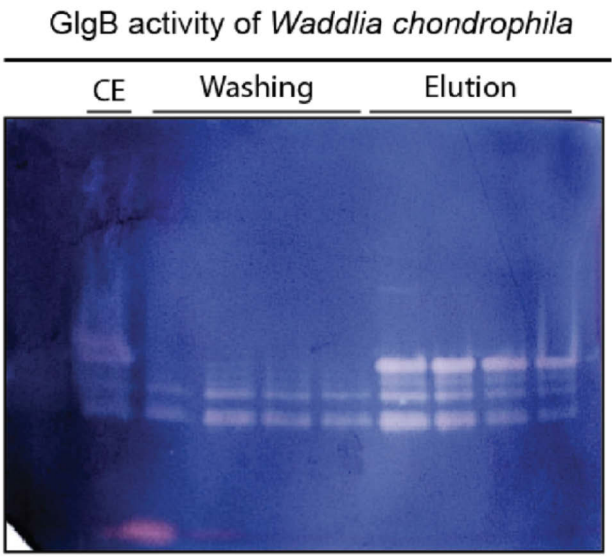

S4 Figure : Purification of the branching enzyme (GlgB2) of *Waddlia chondrophila*.
The plasmid expression pET15b-GlgB2_WC was transferred in *ΔglgB* Rosetta™ *E. coli* strain impaired in endogenous branching enzyme. After induction, crude extract (CE) was incubated for one hour with Ni-NTA-agarose beads at 4°C. Unbound proteins were eluted with 50 mM sodium acetate, 300 mM NaCl and 60 mM imidazole pH 7. After four washing steps, His-GlgB2 was eluted with 50 mM sodium acetate, 300 mM NaCl and 250 mM imidazole pH 7. Proteins in the flow through and elution fractions were separated for 2 hours on native-PAGE (7.5%) at 4°C (120 V, 15 mA). After electrophoresis, proteins were electrotransferred against a native-PAGE containing 0.3% (w/v) of potato starch using TransBlot® Turbo™ transfer system (Bio-Rad). Native-PAGE was then incubated overnight in 25 mM Tris-acetate buffer pH 7.5 at room temperature. Branching enzyme activity is revealed as clear pinkish bands in blue background after soaking the gel in iodine solution (1% KI, 0.1% I_2).

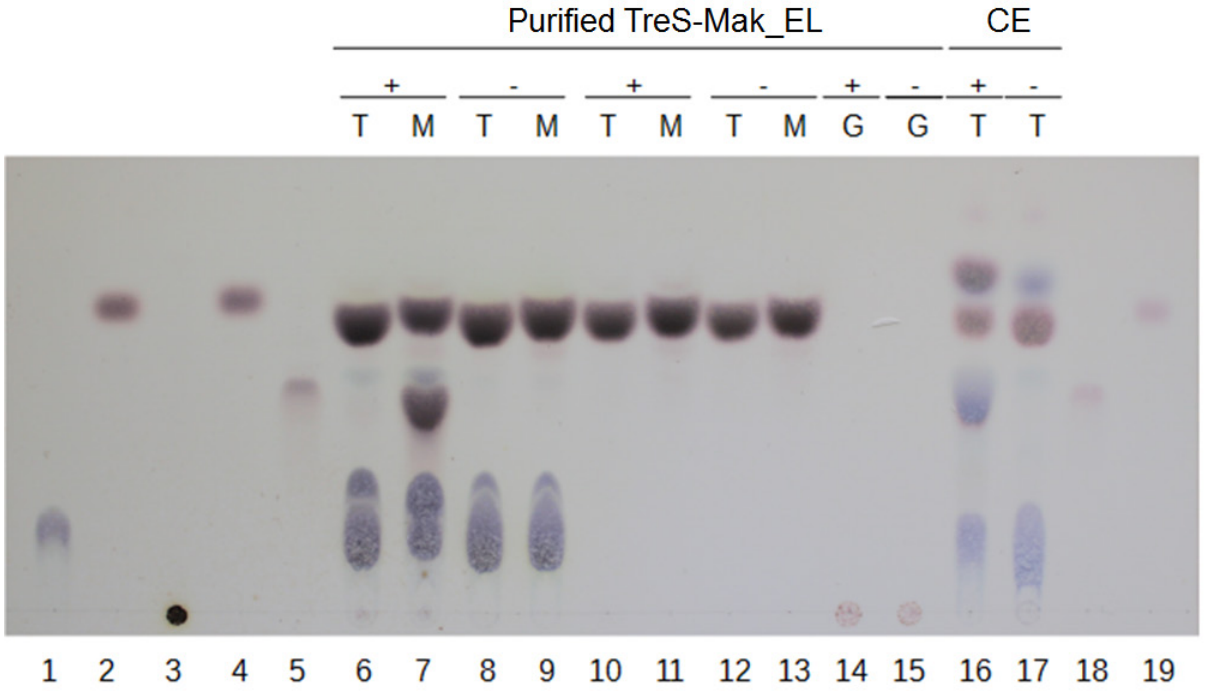

S5 Figure : Test of recombinant TreS-Mak from *E. lausannesis* activity.
Reactions (lanes 6 to 17) were carried out by incubating purified enzyme (lanes 5 to 15) or cellular extract (lanes 16 and 17; EC) in the presence of 20 mM of trehalose (T), 20 mM of maltose (M) or 10 $mg.ml^{-1}$ of glycogen from bovine liver (G) overnight at 30°C. These reactions were carried out with active (+) or heat-inactivated enzyme (-). Reactions 6 to 9 contain 20 mM ATP and 10 mM $MgCl_2$, but not reactions 10 to 15. Control lanes 1: ATP; 2: trehalose; 3: glycogen from bovine liver; 4 and 19: maltose; 5 and 18: Maltose-1-phosphate (M1P). Reaction products were separated on thin layer chromatography Silica gel 60 W (Merck) using the solvent system n-butanol/ethanol/water (5/4/3 v/v/v) before spraying orcinol (0.2%)-sulphuric (20%) solution to visualize carbohydrates in brown and nucleoside derivatives in blue. TreS-Mak_EL is not able to degrade glycogen in either maltose or trehalose (lane 14). However, we observed that TreS-Mak_EL catalyses the synthesis of M1P from ATP and maltose (lane 7), but also directly from trehalose (lane 6) in very small quantities.

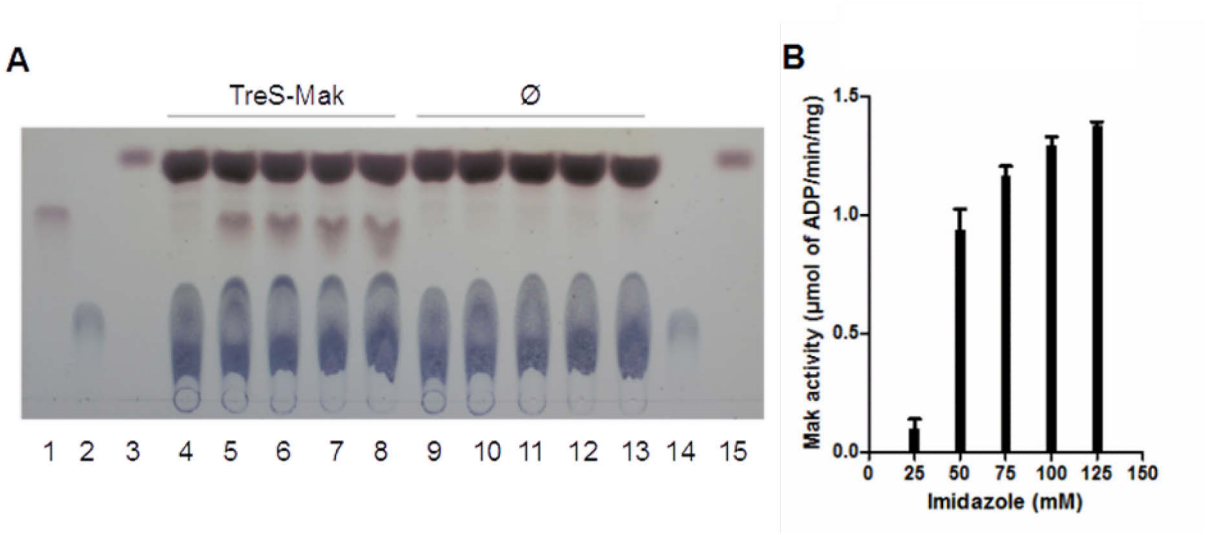

S6 Figure : Impact of imidazole on maltokinase activity.
(**A**) Reactions were carried out by incubating 10 µg.ml^{-1} of active (lanes 4-8) TreS-Mak or heat-inactivated (lanes 9-13) TreS-Mak with 20 mM ATP, 20 mM maltose and 10 mM $MnCl_2$ at 42°C during 40 min. Each reaction was buffered at pH 8 with 150 mM NaCl, 25 mM sodium acetate and various concentrations of imidazole (lanes 4 and 9: 25 mM ; lanes 5 and 10: 50 mM ; lanes 6 and 11: 75 mM ; lanes 7 and 12: 100 mM ; lanes 8 and 13: 125 mM) Reaction products were analysed by thin layer chromatography. Lanes 1 and 15: M1P ; 2 and 14: ATP ; 3 and 15: maltose. (**B**) In addition, specific maltokinase activity, expressed in µmol of ADP produced per minute per milligram of protein was measured for each condition by pyruvate kinase assay. Reactions were performed three times independently. High concentration of imidazole strongly (≥ 50 mM) enhances Mak activity.

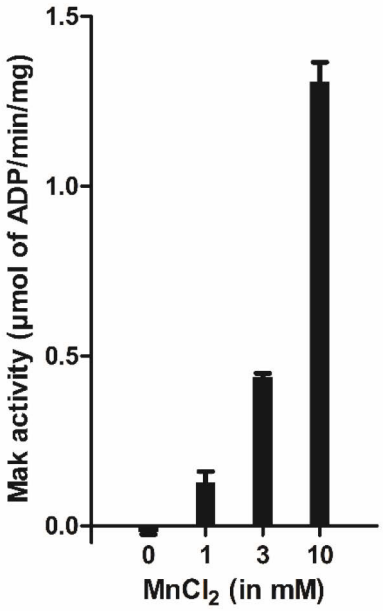

S7 Figure : Impact of Mn^{2+} concentration on maltokinase activity of TreS-Mak_EL.
Reactions were carried out by incubating 10 µg.ml^{-1} of recombinant TreS-Mak_EL with 20 mM ATP, 20 mM maltose and various amounts of $MnCl_2$ (0, 1, 3 and 10 mM) at 42°C during 40 min. Reactions were buffered at pH 8 with 150 mM NaCl, 25 mM sodium acetate and 125 mM imidazole. Specific maltokinase activity, expressed in µmol of ADP produced per minute per milligram of protein was measured for each condition by pyruvate kinase assay. Reactions were performed three times independently. Increasing amounts of Mn^{2+} enhance maltokinase activity, at least up to 10 mM.

```
        10         20         30         40         50         60
MGSSHHHHHH SSGLVPRGSH MLEDHQTSLY KKAGFMMSVS AAEKRQLLTQ VKASGSMYTN

        70         80         90        100        110        120
TLHSIVIQNI SPKPEPFGPA KRVLLEQVEV EADIFTDPHT KLEADLIVKA PGLRKTTRIP

       130        140        150        160        170        180
FHPLVNDRFK AVFVPDTPGT YSFFVEAWVN PAALWQEDLR KKQEARLDLT VDLQIGAALL

       190        200        210        220        230        240
VEVADLLPPE ESVKLLQIAK KLREQKGAEA VAFDPEIARL GRLARPKSRQ GVCSQEQEVF

       250        260        270        280        290        300
VTRKKALFST WYELFPRSCS GTMRHGTFND VVAKLPRISR MGFDVLYLPP IHPIGKTKRK

       310        320        330        340        350        360
GKNNALTALP DDPGSPWAVG SHEGGHDAIQ RELGTLADFE RLVKEAESLG IEIALDIALQ

       370        380        390        400        410        420
CSPDHPYLKE HPEWFLKRPD GTYQYAENPP KKYEDIIPFH FTEDNKDTLF REILRIFLFW

       430        440        450        460        470        480
MKRGVRIFRV DNPHTKPFAL WEYVIGEVRK VDSGVIFLAE AFTRPKIMHH LARIGFDQSY

       490        500        510        520        530        540
TYFTWRNTKW ELTEYLTELT KTEARNYLRP NFFVNTPDIL PESLQWGGRA AFLTRLILAA

       550        560        570        580        590        600
TLSSSYGIYG PAFEQMLSEA VPGKEDYIDS EKYEIKPWDF EKKGTISETI EIVNRIRKEN

       610        620        630        640        650        660
PALQATGNLE FYATDNDYLL AYGKQGPQGE SLLIVVNLDH YHTQSGYVTL PLMHLGIQEK

       670        680        690        700        710
EPYLVDDLLS GERYIWEGER NYIQLSPHLV PAHIFRIRPK MLRENNFDYF I
```

S8 Figure : Amino acids sequence of recombinant His-tagged GlgE_EL.
Amino acids underscored correspond to the His-tag and a short amino-acids linker upstream of GlgE sequence. UniProt accession number of GlgE_EL sequence is A0A0H5DRC6.

Bibliography

AbdelRahman, Y.M., and Belland, R.J. (2005). The chlamydial developmental cycle. FEMS Microbiol. Rev. *29*, 949–959.

AbouElfetouh, A., Kuhn, M.L., Hu, L.I., Scholle, M.D., Sorensen, D.J., Sahu, A.K., Becher, D., Antelmann, H., Mrksich, M., Anderson, W.F., et al. (2015). The E. coli sirtuin CobB shows no preference for enzymatic and nonenzymatic lysine acetylation substrate sites. MicrobiologyOpen *4*, 66–83.

Aisaka, K., Masuda, T., Chikamune, T., and Kamitori, K. (1998). Purification and characterization of trehalose phosphorylase from Catellatospora ferruginea. Biosci. Biotechnol. Biochem. *62*, 782–787.

Aksnes, H., Hole, K., and Arnesen, T. (2015). Chapter Seven - Molecular, Cellular, and Physiological Significance of N-Terminal Acetylation. In International Review of Cell and Molecular Biology, K.W. Jeon, ed. (Academic Press), pp. 267–305.

Albi, T., and Serrano, A. (2016). Inorganic polyphosphate in the microbial world. Emerging roles for a multifaceted biopolymer. World J. Microbiol. Biotechnol. *32*, 27.

Allfrey, V.G., Faulkner, R., and Mirsky, A.E. (1964). ACETYLATION AND METHYLATION OF HISTONES AND THEIR POSSIBLE ROLE IN THE REGULATION OF RNA SYNTHESIS*. Proc. Natl. Acad. Sci. U. S. A. *51*, 786–794.

Allis, C.D., Berger, S.L., Cote, J., Dent, S., Jenuwien, T., Kouzarides, T., Pillus, L., Reinberg, D., Shi, Y., Shiekhattar, R., et al. (2007). New Nomenclature for Chromatin-Modifying Enzymes. Cell *131*, 633–636.

Almagro, G., Viale, A.M., Montero, M., Rahimpour, M., Muñoz, F.J., Baroja-Fernández, E., Bahaji, A., Zúñiga, M., González-Candelas, F., and Pozueta-Romero, J. (2015). Comparative genomic and phylogenetic analyses of Gammaproteobacterial glg genes traced the origin of the Escherichia coli glycogen glgBXCAP operon to the last common ancestor of the sister orders Enterobacteriales and Pasteurellales. PloS One *10*, e0115516.

Andersson, S.G., and Kurland, C.G. (1998). Reductive evolution of resident genomes. Trends Microbiol. *6*, 263–268.

Argüelles, J.-C. (2014). Why Can't Vertebrates Synthesize Trehalose? J. Mol. Evol. *79*, 111–116.

Arnesen, T., Van Damme, P., Polevoda, B., Helsens, K., Evjenth, R., Colaert, N., Varhaug, J.E., Vandekerckhove, J., Lillehaug, J.R., Sherman, F., et al. (2009). Proteomics analyses reveal the evolutionary conservation and divergence of N-terminal acetyltransferases from yeast and humans. Proc. Natl. Acad. Sci. U. S. A. *106*, 8157–8162.

Arsköld, E., Lohmeier-Vogel, E., Cao, R., Roos, S., Rådström, P., and van Niel, E.W.J. (2008). Phosphoketolase pathway dominates in Lactobacillus reuteri ATCC 55730 containing dual pathways for glycolysis. J. Bacteriol. *190*, 206–212.

Asención Diez, M.D., Miah, F., Stevenson, C.E.M., Lawson, D.M., Iglesias, A.A., and Bornemann, S. (2017). The Production and Utilization of GDP-glucose in the Biosynthesis of Trehalose 6-Phosphate by Streptomyces venezuelae. J. Biol. Chem. *292*, 945–954.

Baeza, J., Smallegan, M.J., and Denu, J.M. (2015). Site-specific reactivity of nonenzymatic lysine acetylation. ACS Chem. Biol. *10*, 122–128.

Baker, C.S., Morozov, I., Suzuki, K., Romeo, T., and Babitzke, P. (2002). CsrA regulates glycogen biosynthesis by preventing translation of glgC in Escherichia coli. Mol. Microbiol. *44*, 1599–1610.

Ball, S., Colleoni, C., Cenci, U., Raj, J.N., and Tirtiaux, C. (2011). The evolution of glycogen and starch metabolism in eukaryotes gives molecular clues to understand the establishment of plastid endosymbiosis. J. Exp. Bot. *62*, 1775–1801.

Ball, S.G., Subtil, A., Bhattacharya, D., Moustafa, A., Weber, A.P.M., Gehre, L., Colleoni, C., Arias, M.-C., Cenci, U., and Dauvillée, D. (2013). Metabolic effectors secreted by bacterial pathogens: essential facilitators of plastid endosymbiosis? Plant Cell *25*, 7–21.

Ball, S.G., Colleoni, C., Kadouche, D., Ducatez, M., Arias, M.-C., and Tirtiaux, C. (2015). Toward an understanding of the function of Chlamydiales in plastid endosymbiosis. Biochim. Biophys. Acta *1847*, 495–504.

Ballicora, M.A., Iglesias, A.A., and Preiss, J. (2003). ADP-Glucose Pyrophosphorylase, a Regulatory Enzyme for Bacterial Glycogen Synthesis. Microbiol. Mol. Biol. Rev. *67*, 213–225.

Ballicora, M.A., Iglesias, A.A., and Preiss, J. (2004). ADP-Glucose Pyrophosphorylase: A Regulatory Enzyme for Plant Starch Synthesis. Photosynth. Res. *79*, 1–24.

Baskaran, S., Roach, P.J., DePaoli-Roach, A.A., and Hurley, T.D. (2010). Structural basis for glucose-6-phosphate activation of glycogen synthase. Proc. Natl. Acad. Sci. *107*, 17563–17568.

Baud, D., Regan, L., and Greub, G. (2008). Emerging role of Chlamydia and Chlamydia-like organisms in adverse pregnancy outcomes. Curr. Opin. Infect. Dis.

Baud, D., Goy, G., Osterheld, M.-C., Croxatto, A., Borel, N., Vial, Y., Pospischil, A., and Greub, G. (2014). Role of Waddlia chondrophila placental infection in miscarriage. Emerg. Infect. Dis. *20*, 460–464.

Baud, D., Vulliemoz, N., Zapata, M.V.M., Greub, G., Vouga, M., and Stojanov, M. (2020). Waddlia chondrophila and Male Infertility. Microorganisms *8*.

Becker, S., Tebben, J., Coffinet, S., Wiltshire, K., Iversen, M.H., Harder, T., Hinrichs, K.-U., and Hehemann, J.-H. (2020). Laminarin is a major molecule in the marine carbon cycle. Proc. Natl. Acad. Sci. U. S. A. *117*, 6599–6607.

Belanger, A.E., and Hatfull, G.F. (1999). Exponential-Phase Glycogen Recycling Is Essential for Growth of Mycobacterium smegmatis. J. Bacteriol. *181*, 6670–6678.

Belland, R.J., Zhong, G., Crane, D.D., Hogan, D., Sturdevant, D., Sharma, J., Beatty, W.L., and Caldwell, H.D. (2003). Genomic transcriptional profiling of the developmental cycle of Chlamydia trachomatis. Proc. Natl. Acad. Sci. U. S. A. *100*, 8478–8483.

Belocopitow, E., and Maréchal, L.R. (1970). Trehalose phosphorylase from Euglena gracilis. Biochim. Biophys. Acta *198*, 151–154.

Bernard, C. (1857). Sur le mécanisme physiologique de la formation du sucre dans le foie. Remarques sur la formation de la matière glycogène du foie. Comptes rendus de l'Académie des Sciences 44.

Berndsen, C.E., Albaugh, B.N., Tan, S., and Denu, J.M. (2007). Catalytic mechanism of a MYST family histone acetyltransferase. Biochemistry *46*, 623–629.

Binderup, K., Mikkelsen, R., and Preiss, J. (2000). Limited proteolysis of branching enzyme from Escherichia coli. Arch. Biochem. Biophys. *377*, 366–371.

Binderup, K., Mikkelsen, R., and Preiss, J. (2002). Truncation of the amino terminus of branching enzyme changes its chain transfer pattern. Arch. Biochem. Biophys. *397*, 279–285.

Birhanu, A.G., Yimer, S.A., Holm-Hansen, C., Norheim, G., Aseffa, A., Abebe, M., and Tønjum, T. (2017). Nε- and O-Acetylation in Mycobacterium tuberculosis Lineage 7 and Lineage 4 Strains: Proteins Involved in Bioenergetics, Virulence, and Antimicrobial Resistance Are Acetylated. J. Proteome Res. *16*, 4045–4059.

Blander, G., and Guarente, L. (2004). The Sir2 family of protein deacetylases. Annu. Rev. Biochem. *73*, 417–435.

Bonen, L., and Doolittle, W.F. (1975). On the prokaryotic nature of red algal chloroplasts. Proc. Natl. Acad. Sci. U. S. A. *72*, 2310–2314.

Bontemps-Gallo, S., Gaviard, C., Richards, C.L., Kentache, T., Raffel, S.J., Lawrence, K.A., Schindler, J.C., Lovelace, J., Dulebohn, D.P., Cluss, R.G., et al. (2018). Global Profiling of Lysine Acetylation in Borrelia burgdorferi B31 Reveals Its Role in Central Metabolism. Front. Microbiol. *9*.

Brown, J.L., and Roberts, W.K. (1976). Evidence that approximately eighty per cent of the soluble proteins from Ehrlich ascites cells are Nalpha-acetylated. J. Biol. Chem. *251*, 1009–1014.

Brownell, J.E., and Allis, C.D. (1995). An activity gel assay detects a single, catalytically active histone acetyltransferase subunit in Tetrahymena macronuclei. Proc. Natl. Acad. Sci. U. S. A. *92*, 6364–6368.

Brownell, J.E., Zhou, J., Ranalli, T., Kobayashi, R., Edmondson, D.G., Roth, S.Y., and Allis, C.D. (1996). Tetrahymena Histone Acetyltransferase A: A Homolog to Yeast Gcn5p Linking Histone Acetylation to Gene Activation. Cell *84*, 843–851.

Burckhardt, R.M., Buckner, B.A., and Escalante-Semerena, J.C. (2019). Staphylococcus aureus modulates the activity of acetyl-Coenzyme A synthetase (Acs) by sirtuin-dependent reversible lysine acetylation. Mol. Microbiol. *112*, 588–604.

Buschiazzo, A., Ugalde, J.E., Guerin, M.E., Shepard, W., Ugalde, R.A., and Alzari, P.M. (2004). Crystal structure of glycogen synthase: homologous enzymes catalyze glycogen synthesis and degradation. EMBO J. *23*, 3196–3205.

Cai, X., Seitl, I., Mu, W., Zhang, T., Stressler, T., Fischer, L., and Jiang, B. (2019). Characterization of a Recombinant Trehalose Synthase from Arthrobacter chlorophenolicus and its Unique Kinetics Indicating a Substrate Cooperativity. Appl. Biochem. Biotechnol. *187*, 1255–1271.

Cao, Y., Mahrenholz, A.M., DePaoli-Roach, A.A., and Roach, P.J. (1993). Characterization of rabbit skeletal muscle glycogenin. Tyrosine 194 is essential for function. J. Biol. Chem. *268*, 14687–14693.

Casson, N., Michel, R., Müller, K.-D., Aubert, J.D., and Greub, G. (2008). Protochlamydia naegleriophila as Etiologic Agent of Pneumonia. Emerg. Infect. Dis. *14*, 168–172.

Castaño-Cerezo, S., Bernal, V., Blanco-Catalá, J., Iborra, J.L., and Cánovas, M. (2011). cAMP-CRP co-ordinates the expression of the protein acetylation pathway with central metabolism in Escherichia coli. Mol. Microbiol. *82*, 1110–1128.

Castaño-Cerezo, S., Bernal, V., Post, H., Fuhrer, T., Cappadona, S., Sánchez-Díaz, N.C., Sauer, U., Heck, A.J.R., Altelaar, A.F.M., and Cánovas, M. (2014). Protein acetylation affects acetate metabolism, motility and acid stress response in Escherichia coli. Mol. Syst. Biol. *10*, 762.

Castaño-Cerezo, S., Bernal, V., Röhrig, T., Termeer, S., and Cánovas, M. (2015). Regulation of acetate metabolism in Escherichia coli BL21 by protein N(ε)-lysine acetylation. Appl. Microbiol. Biotechnol. *99*, 3533–3545.

Cenci, U., Nitschke, F., Steup, M., Minassian, B.A., Colleoni, C., and Ball, S.G. (2014). Transition from glycogen to starch metabolism in Archaeplastida. Trends Plant Sci. *19*, 18–28.

Cenci, U., Ducatez, M., Kadouche, D., Colleoni, C., and Ball, S.G. (2016). Was the Chlamydial Adaptative Strategy to Tryptophan Starvation an Early Determinant of Plastid Endosymbiosis? Front. Cell. Infect. Microbiol. *6*, 67.

Cenci, U., Bhattacharya, D., Weber, A.P.M., Colleoni, C., Subtil, A., and Ball, S.G. (2017). Biotic Host–Pathogen Interactions As Major Drivers of Plastid Endosymbiosis. Trends Plant Sci. *22*, 316–328.

Cenci, U., Qiu, H., Pillonel, T., Cardol, P., Remacle, C., Colleoni, C., Kadouche, D., Chabi, M., Greub, G., Bhattacharya, D., et al. (2018). Host-pathogen biotic interactions shaped vitamin K metabolism in Archaeplastida. Sci. Rep. *8*, 15243.

Chandra, G., Chater, K.F., and Bornemann, S. (2011). Unexpected and widespread connections between bacterial glycogen and trehalose metabolism. Microbiol. Read. Engl. *157*, 1565–1572.

Chen, G.S., and Segel, I.H. (1968). Purification and properties of glycogen phosphorylase from Escherichia coli. Arch. Biochem. Biophys. *127*, 175–186.

Chen, Y.-S., Lee, G.-C., and Shaw, J.-F. (2006). Gene Cloning, Expression, and Biochemical Characterization of a Recombinant Trehalose Synthase from Picrophilus torridus in Escherichia coli. J. Agric. Food Chem. *54*, 7098–7104.

Chiappino, M.L., Dawson, C., Schachter, J., and Nichols, B.A. (1995). Cytochemical localization of glycogen in Chlamydia trachomatis inclusions. J. Bacteriol. *177*, 5358–5363.

Choudhary, C., Kumar, C., Gnad, F., Nielsen, M.L., Rehman, M., Walther, T.C., Olsen, J.V., and Mann, M. (2009). Lysine acetylation targets protein complexes and co-regulates major cellular functions. Science *325*, 834–840.

Christensen, D.G., Meyer, J.G., Baumgartner, J.T., D'Souza, A.K., Nelson, W.C., Payne, S.H., Kuhn, M.L., Schilling, B., and Wolfe, A.J. (2018). Identification of Novel Protein Lysine Acetyltransferases in Escherichia coli. MBio *9*.

Christensen, D.G., Xie, X., Basisty, N., Byrnes, J., McSweeney, S., Schilling, B., and Wolfe, A.J. (2019a). Post-translational Protein Acetylation: An Elegant Mechanism for Bacteria to Dynamically Regulate Metabolic Functions. Front. Microbiol. *10*.

Christensen, D.G., Baumgartner, J.T., Xie, X., Jew, K.M., Basisty, N., Schilling, B., Kuhn, M.L., and Wolfe, A.J. (2019b). Mechanisms, Detection, and Relevance of Protein Acetylation in Prokaryotes. MBio *10*.

Cifuente, J.O., Comino, N., Trastoy, B., D'Angelo, C., and Guerin, M.E. (2019). Structural basis of glycogen metabolism in bacteria. Biochem. J. *476*, 2059–2092.

Clifton, D.R., Fields, K.A., Grieshaber, S.S., Dooley, C.A., Fischer, E.R., Mead, D.J., Carabeo, R.A., and Hackstadt, T. (2004). A chlamydial type III translocated protein is tyrosine-phosphorylated at the site of entry and associated with recruitment of actin. Proc. Natl. Acad. Sci. U. S. A. *101*, 10166–10171.

Colak, G., Xie, Z., Zhu, A.Y., Dai, L., Lu, Z., Zhang, Y., Wan, X., Chen, Y., Cha, Y.H., Lin, H., et al. (2013). Identification of lysine succinylation substrates and the succinylation regulatory enzyme CobB in Escherichia coli. Mol. Cell. Proteomics MCP *12*, 3509–3520.

Contreras, C.J., Segvich, D.M., Mahalingan, K., Chikwana, V.M., Kirley, T.L., Hurley, T.D., DePaoli-Roach, A.A., and Roach, P.J. (2016). INCORPORATION OF PHOSPHATE INTO GLYCOGEN BY GLYCOGEN SYNTHASE. Arch. Biochem. Biophys. *597*, 21–29.

Cossé, M.M., Hayward, R.D., and Subtil, A. (2018). One Face of Chlamydia trachomatis: The Infectious Elementary Body. Curr. Top. Microbiol. Immunol. *412*, 35–58.

Coulon, C., Eterpi, M., Greub, G., Collignon, A., McDonnell, G., and Thomas, V. (2012). Amoebal host range, host-free survival and disinfection susceptibility of environmental Chlamydiae as compared to Chlamydia trachomatis. FEMS Immunol. Med. Microbiol. *64*, 364–373.

Coutinho, P.M., Deleury, E., Davies, G.J., and Henrissat, B. (2003). An evolving hierarchical family classification for glycosyltransferases. J. Mol. Biol. *328*, 307–317.

Criscuolo, A., and Gribaldo, S. (2010). BMGE (Block Mapping and Gathering with Entropy): a new software for selection of phylogenetic informative regions from multiple sequence alignments. BMC Evol. Biol. *10*, 210.

Crosby, H.A., Heiniger, E.K., Harwood, C.S., and Escalante-Semerena, J.C. (2010). Reversible N epsilon-lysine acetylation regulates the activity of acyl-CoA synthetases involved in anaerobic benzoate catabolism in Rhodopseudomonas palustris. Mol. Microbiol. *76*, 874–888.

Dai, W., and Li, Z. (2014). Conserved type III secretion system exerts important roles in Chlamydia trachomatis. Int. J. Clin. Exp. Pathol. *7*, 5404–5414.

De Smet, K.A.L., Weston, A., Brown, I.N., Young, D.B., and Robertson, B.D. (2000). Three pathways for trehalose biosynthesis in mycobacteria. Microbiol. Read. Engl. *146 (Pt 1)*, 199–208.

Deschamps, P., Colleoni, C., Nakamura, Y., Suzuki, E., Putaux, J.-L., Buléon, A., Haebel, S., Ritte, G., Steup, M., Falcón, L.I., et al. (2008). Metabolic Symbiosis and the Birth of the Plant Kingdom. Mol. Biol. Evol. *25*, 536–548.

Deutscher, J., Francke, C., and Postma, P.W. (2006). How Phosphotransferase System-Related Protein Phosphorylation Regulates Carbohydrate Metabolism in Bacteria. Microbiol. Mol. Biol. Rev. *70*, 939–1031.

Devillers, C.H., Piper, M.E., Ballicora, M.A., and Preiss, J. (2003). Characterization of the branching patterns of glycogen branching enzyme truncated on the N-terminus. Arch. Biochem. Biophys. *418*, 34–38.

Dharamshi, J.E., Tamarit, D., Eme, L., Stairs, C., Martijn, J., Homa, F., Jørgensen, S.L., Spang, A., and Ettema, T.J.G. (2019). Marine sediments illuminate Chlamydiae diversity and evolution. BioRxiv.

Dittrich, C.R., Vadali, R.V., Bennett, G.N., and San, K.-Y. (2005). Redistribution of metabolic fluxes in the central aerobic metabolic pathway of E. coli mutant strains with deletion of the ackA-pta and poxB pathways for the synthesis of isoamyl acetate. Biotechnol. Prog. *21*, 627–631.

Drazic, A., Myklebust, L.M., Ree, R., and Arnesen, T. (2016). The world of protein acetylation. Biochim. Biophys. Acta BBA - Proteins Proteomics *1864*, 1372–1401.

Drepper, A., Peitzmann, R., and Pape, H. (1996). Maltokinase (ATP:maltose 1-phosphotransferase) from Actinoplanes sp.: demonstration of enzyme activity and characterization of the reaction product. FEBS Lett. *388*, 177–179.

Drochmans, P. (1962). Morphologie du glycogène: Etude au microscope électronique de colorations négatives du glycogène particulaire. J. Ultrastruct. Res. *6*, 141–163.

Ducatez, M. (2015). Nouvel aperçu dans l'évolution du métabolisme des polysaccharides de réserve chez les Archaeplastides. These de doctorat. Lille 1.

Edgar, R.C. (2004). MUSCLE: multiple sequence alignment with high accuracy and high throughput. Nucleic Acids Res. *32*, 1792–1797.

Elbein, A.D. (1974). The metabolism of alpha,alpha-trehalose. Adv. Carbohydr. Chem. Biochem. *30*, 227–256.

Elbein, A.D., Pastuszak, I., Tackett, A.J., Wilson, T., and Pan, Y.T. (2010). Last step in the conversion of trehalose to glycogen: a mycobacterial enzyme that transfers maltose from maltose 1-phosphate to glycogen. J. Biol. Chem. *285*, 9803–9812.

Elwell, C., Mirrashidi, K., and Engel, J. (2016). Chlamydia cell biology and pathogenesis. Nat. Rev. Microbiol. *14*, 385–400.

Everett, K.D., Bush, R.M., and Andersen, A.A. (1999). Emended description of the order Chlamydiales, proposal of Parachlamydiaceae fam. nov. and Simkaniaceae fam. nov., each containing one monotypic genus, revised taxonomy of the family Chlamydiaceae, including a new genus and five new species, and standards for the identification of organisms. Int. J. Syst. Bacteriol. *49 Pt 2*, 415–440.

Eydallin, G., Viale, A.M., Morán-Zorzano, M.T., Muñoz, F.J., Montero, M., Baroja-Fernández, E., and Pozueta-Romero, J. (2007a). Genome-wide screening of genes affecting glycogen metabolism in Escherichia coli K-12. FEBS Lett. *581*, 2947–2953.

Eydallin, G., Morán-Zorzano, M.T., Muñoz, F.J., Baroja-Fernández, E., Montero, M., Alonso-Casajús, N., Viale, A.M., and Pozueta-Romero, J. (2007b). An Escherichia coli mutant producing a truncated inactive form of GlgC synthesizes glycogen: Further evidences for the occurrence of various important sources of ADPglucose in enterobacteria. FEBS Lett. *581*, 4417–4422.

Eydallin, G., Montero, M., Almagro, G., Sesma, M.T., Viale, A.M., Muñoz, F.J., Rahimpour, M., Baroja-Fernández, E., and Pozueta-Romero, J. (2010). Genome-Wide Screening of Genes Whose Enhanced Expression Affects Glycogen Accumulation in Escherichia coli. DNA Res. *17*, 61–71.

Facchinelli, F., Colleoni, C., Ball, S.G., and Weber, A.P.M. (2013). Chlamydia, cyanobiont, or host: who was on top in the ménage à trois? Trends Plant Sci. *18*, 673–679.

Fang, T.-Y., Tseng, W.-C., Guo, M.-S., Shih, T.-Y., and Hung, X.-G. (2006). Expression, purification, and characterization of the maltooligosyltrehalose trehalohydrolase from the thermophilic archaeon Sulfolobus solfataricus ATCC 35092. J. Agric. Food Chem. *54*, 7105–7112.

Ferrell, J.C., and Fields, K.A. (2016). A working model for the type III secretion mechanism in Chlamydia. Microbes Infect. Inst. Pasteur *18*, 84–92.

Fields, K.A., Mead, D.J., Dooley, C.A., and Hackstadt, T. (2003). Chlamydia trachomatis type III secretion: evidence for a functional apparatus during early-cycle development. Mol. Microbiol. *48*, 671–683.

Filipkowski, P., Pietrow, O., Panek, A., and Synowiecki, J. (2012). Properties of recombinant trehalose synthase from Deinococcus radiodurans expressed in Escherichia coli. Acta Biochim. Pol. *59*.

Fischer, E.H., Graves, D.J., Crittenden, E.R.S., and Krebs, E.G. (1959). Structure of the site phosphorylated in the phosphorylase b to a reaction. J. Biol. Chem. *234*, 1698–1704.

Fontana, J.D. (1980). The presence of phosphate in glycogen. FEBS Lett. *109*, 85–92.

Fox, B.G., and Blommel, P.G. (2009). Autoinduction of Protein Expression. Curr. Protoc. Protein Sci. *CHAPTER 5*, Unit-5.23.

Fraga, J., Maranha, A., Mendes, V., Pereira, P.J.B., Empadinhas, N., and Macedo-Ribeiro, S. (2015). Structure of mycobacterial maltokinase, the missing link in the essential GlgE-pathway. Sci. Rep. *5*.

Fraiberg, M., Afanzar, O., Cassidy, C.K., Gabashvili, A., Schulten, K., Levin, Y., and Eisenbach, M. (2015). CheY's acetylation sites responsible for generating clockwise flagellar rotation in Escherichia coli. Mol. Microbiol. *95*, 231–244.

Friis, R.R. (1972). Interaction of L Cells and Chlamydia psittaci: Entry of the Parasite and Host Responses to Its Development. J. Bacteriol. *110*, 706–721.

Frydén, A., Kihlström, E., Maller, R., Persson, K., Romanus, V., and Anséhn, S. (1989). A clinical and epidemiological study of "ornithosis" caused by Chlamydia psittaci and Chlamydia pneumoniae (strain TWAR). Scand. J. Infect. Dis. *21*, 681–691.

Frye, R.A. (2000). Phylogenetic classification of prokaryotic and eukaryotic Sir2-like proteins. Biochem. Biophys. Res. Commun. *273*, 793–798.

Fuerst, J.A. (2013). The PVC superphylum: exceptions to the bacterial definition? Antonie Van Leeuwenhoek *104*, 451–466.

Fukushi, H., and Hirai, K. (1992). Proposal of Chlamydia pecorum sp. nov. for Chlamydia strains derived from ruminants. Int. J. Syst. Bacteriol. *42*, 306–308.

Gao, Y., Xi, Y., Lu, X.-L., Zheng, H., Hu, B., Liu, X.-Y., and Jiao, B.-H. (2013). Cloning, expression and functional characterization of a novel trehalose synthase from marine Pseudomonas sp. P8005. World J. Microbiol. Biotechnol. *29*, 2195–2206.

Gardner, J.G., Grundy, F.J., Henkin, T.M., and Escalante-Semerena, J.C. (2006). Control of acetyl-coenzyme A synthetase (AcsA) activity by acetylation/deacetylation without NAD(+) involvement in Bacillus subtilis. J. Bacteriol. *188*, 5460–5468.

Garg, S.K., Alam, M.S., Kishan, K.V.R., and Agrawal, P. (2007). Expression and characterization of alpha-(1,4)-glucan branching enzyme Rv1326c of Mycobacterium tuberculosis H37Rv. Protein Expr. Purif. *51*, 198–208.

Gehre, L., Gorgette, O., Perrinet, S., Prevost, M.-C., Ducatez, M., Giebel, A.M., Nelson, D.E., Ball, S.G., and Subtil, A. (2016). Sequestration of host metabolism by an intracellular pathogen. ELife *5*, e12552.

Gentry, M.S., Guinovart, J.J., Minassian, B.A., Roach, P.J., and Serratosa, J.M. (2018). Lafora disease offers a unique window into neuronal glycogen metabolism. J. Biol. Chem. *293*, 7117–7125.

Ghosh, S., Padmanabhan, B., Anand, C., and Nagaraja, V. (2016). Lysine acetylation of the Mycobacterium tuberculosis HU protein modulates its DNA binding and genome organization. Mol. Microbiol. *100*, 577–588.

Giaever, H.M., Styrvold, O.B., Kaasen, I., and Strøm, A.R. (1988). Biochemical and genetic characterization of osmoregulatory trehalose synthesis in Escherichia coli. J. Bacteriol. *170*, 2841–2849.

Gordiyenko, Y., Deroo, S., Zhou, M., Videler, H., and Robinson, C.V. (2008). Acetylation of L12 increases interactions in the Escherichia coli ribosomal stalk complex. J. Mol. Biol. *380*, 404–414.

Gottesman, S. (2017). Stress Reduction, Bacterial Style. J. Bacteriol. *199*.

Gueguen, Y., Rolland, J.-L., Schroeck, S., Flament, D., Defretin, S., Saniez, M.-H., and Dietrich, J. (2001). Characterization of the maltooligosyl trehalose synthase from the thermophilic archaeon Sulfolobus acidocaldarius. FEMS Microbiol. Lett. *194*, 201–206.

Gutierrez, A., Elez, M., Clermont, O., Denamur, E., and Matic, I. (2011). Escherichia coli YafP protein modulates DNA damaging property of the nitroaromatic compounds. Nucleic Acids Res. *39*, 4192–4201.

Hackstadt, T., Scidmore-Carlson, M.A., Shaw, E.I., and Fischer, E.R. (1999). The Chlamydia trachomatis IncA protein is required for homotypic vesicle fusion. Cell. Microbiol. *1*, 119–130.

Haferkamp, I., Schmitz-Esser, S., Wagner, M., Neigel, N., Horn, M., and Neuhaus, H.E. (2006). Tapping the nucleotide pool of the host: novel nucleotide carrier proteins of Protochlamydia amoebophila. Mol. Microbiol. *60*, 1534–1545.

Haider, S., Wagner, M., Schmid, M.C., Sixt, B.S., Christian, J.G., Häcker, G., Pichler, P., Mechtler, K., Müller, A., Baranyi, C., et al. (2010). Raman microspectroscopy reveals long-term extracellular activity of chlamydiae. *77*, 687–700.

Hayden, J.D., Brown, L.R., Gunawardena, H.P., Perkowski, E.F., Chen, X., and Braunstein, M. (2013). Reversible acetylation regulates acetate and propionate metabolism in Mycobacterium smegmatis. Microbiol. Read. Engl. *159*, 1986–1999.

Hayner, G.A., Khetan, S., and Paulick, M.G. (2017). Quantification of the Disaccharide Trehalose from Biological Samples: A Comparison of Analytical Methods. ACS Omega *2*, 5813–5823.

Helbig, A.O., Gauci, S., Raijmakers, R., van Breukelen, B., Slijper, M., Mohammed, S., and Heck, A.J.R. (2010). Profiling of N-Acetylated Protein Termini Provides In-depth Insights into the N-terminal Nature of the Proteome. Mol. Cell. Proteomics MCP *9*, 928–939.

Helsens, K., Van Damme, P., Degroeve, S., Martens, L., Arnesen, T., Vandekerckhove, J., and Gevaert, K. (2011). Bioinformatics analysis of a Saccharomyces cerevisiae N-terminal proteome provides evidence of alternative translation initiation and post-translational N-terminal acetylation. J. Proteome Res. *10*, 3578–3589.

Henrissat, B., Deleury, E., and Coutinho, P.M. (2002). Glycogen metabolism loss: a common marker of parasitic behaviour in bacteria? Trends Genet. TIG *18*, 437–440.

Hentchel, K.L., and Escalante-Semerena, J.C. (2015). Acylation of Biomolecules in Prokaryotes: a Widespread Strategy for the Control of Biological Function and Metabolic Stress. Microbiol. Mol. Biol. Rev. MMBR *79*, 321–346.

Hodawadekar, S.C., and Marmorstein, R. (2007). Chemistry of acetyl transfer by histone modifying enzymes: structure, mechanism and implications for effector design. Oncogene *26*, 5528–5540.

Hogan, R.J., Mathews, S.A., Mukhopadhyay, S., Summersgill, J.T., and Timms, P. (2004). Chlamydial Persistence: beyond the Biphasic Paradigm. Infect. Immun. *72*, 1843–1855.

Horn, M. (2008). Chlamydiae as symbionts in eukaryotes. Annu. Rev. Microbiol. *62*, 113–131.

Iglesias, A.A., Kakefuda, G., and Preiss, J. (1991). Regulatory and Structural Properties of the Cyanobacterial ADPglucose Pyrophosphorylases 1. Plant Physiol. *97*, 1187–1195.

Imai, S., Johnson, F.B., Marciniak, R.A., McVey, M., Park, P.U., and Guarente, L. (2000). Sir2: an NAD-dependent histone deacetylase that connects chromatin silencing, metabolism, and aging. Cold Spring Harb. Symp. Quant. Biol. *65*, 297–302.

INOUE, Y., ISHII, K., TOMITA, T., YATAKE, T., and FUKUI, F. (2002). Characterization of Trehalose Phosphorylase from Bacillus stearothermophilus SK-1 and Nucleotide Sequence of the Corresponding Gene. Biosci. Biotechnol. Biochem. *66*, 1835–1843.

Jarling, M., Cauvet, T., Grundmeier, M., Kuhnert, K., and Pape, H. (2004). Isolation of mak1 from Actinoplanes missouriensis and evidence that Pep2 from Streptomyces coelicolor is a maltokinase. J. Basic Microbiol. *44*, 360–373.

Jendrossek, D., and Pfeiffer, D. (2014). New insights in the formation of polyhydroxyalkanoate granules (carbonosomes) and novel functions of poly(3-hydroxybutyrate). Environ. Microbiol. *16*, 2357–2373.

Johnson, H.A. (2005). Fish bile and cautery: trachoma treatment in art. J. R. Soc. Med. *98*, 30–32.

Kaasen, I., Falkenberg, P., Styrvold, O.B., and Strøm, A.R. (1992). Molecular cloning and physical mapping of the otsBA genes, which encode the osmoregulatory trehalose pathway of Escherichia coli: evidence that transcription is activated by katF (AppR). J. Bacteriol. *174*, 889–898.

Kadouche, D. (2016). The comparative biochemistry of storage polysaccharide metabolism in Chlamydiales and Cyanobacteria : insights into the evolution of glycogen and starch metabolism in Eukaryotes. These de doctorat. Lille 1.

Kalscheuer, R., and Jacobs, W.R. (2010). The significance of GlgE as a new target for tuberculosis. Drug News Perspect. *23*, 619–624.

Kalscheuer, R., Syson, K., Veeraraghavan, U., Weinrick, B., Biermann, K.E., Liu, Z., Sacchettini, J.C., Besra, G., Bornemann, S., and Jacobs, W.R. (2010). Self-poisoning of Mycobacterium tuberculosis by targeting GlgE in an alpha-glucan pathway. Nat. Chem. Biol. *6*, 376–384.

Katoh, K., and Standley, D.M. (2013). MAFFT Multiple Sequence Alignment Software Version 7: Improvements in Performance and Usability. Mol. Biol. Evol. *30*, 772–780.

Kawaguchi, K., Fox, J., Holmes, E., Boyer, C., and Preiss, J. (1978). De Novo synthesis of Escherichia coli glycogen is due to primer associated with glycogen synthase and activation by branching enzyme. Arch. Biochem. Biophys. *190*, 385–397.

Keating, D.H., Shulla, A., Klein, A.H., and Wolfe, A.J. (2008). Optimized two-dimensional thin layer chromatography to monitor the intracellular concentration of acetyl phosphate and other small phosphorylated molecules. Biol. Proced. Online *10*, 36–46.

Kebbi-Beghdadi, C., Pilloux, L., Croxatto, A., Tosetti, N., Pillonel, T., and Greub, G. (2019). A predation assay using amoebae to screen for virulence factors unearthed the first W. chondrophila inclusion membrane protein. Sci. Rep. *9*, 19485.

Keeling, P.J., McCutcheon, J.P., and Doolittle, W.F. (2015). Symbiosis becoming permanent: Survival of the luckiest. Proc. Natl. Acad. Sci. U. S. A. *112*, 10101–10103.

Kehl-Fie, T.E., Zhang, Y., Moore, J.L., Farrand, A.J., Hood, M.I., Rathi, S., Chazin, W.J., Caprioli, R.M., and Skaar, E.P. (2013). MntABC and MntH contribute to systemic Staphylococcus aureus infection by competing with calprotectin for nutrient manganese. Infect. Immun. *81*, 3395–3405.

Kelley, L.A., Mezulis, S., Yates, C.M., Wass, M.N., and Sternberg, M.J.E. (2015). The Phyre2 web portal for protein modeling, prediction and analysis. Nat. Protoc. *10*, 845–858.

Kentache, T., Jouenne, T., Dé, E., and Hardouin, J. (2016). Proteomic characterization of Nα- and Nε-acetylation in Acinetobacter baumannii. J. Proteomics *144*, 148–158.

Kermani, A.A., Roy, R., Gopalasingam, C., Kocurek, K.I., Patel, T.R., Alderwick, L.J., Besra, G.S., and Fütterer, K. (2019). Crystal structure of the TreS-Pep2 complex, initiating α-glucan synthesis in the GlgE pathway of mycobacteria. J. Biol. Chem.

Kim, G.-W., and Yang, X.-J. (2011). Comprehensive lysine acetylomes emerging from bacteria to humans. Trends Biochem. Sci. *36*, 211–220.

Kim, K.H., An, D.R., Song, J., Yoon, J.Y., Kim, H.S., Yoon, H.J., Im, H.N., Kim, J., Kim, D.J., Lee, S.J., et al. (2012). Mycobacterium tuberculosis Eis protein initiates suppression of host immune responses by acetylation of DUSP16/MKP-7. Proc. Natl. Acad. Sci. U. S. A. *109*, 7729–7734.

Kim, S.C., Sprung, R., Chen, Y., Xu, Y., Ball, H., Pei, J., Cheng, T., Kho, Y., Xiao, H., Xiao, L., et al. (2006). Substrate and functional diversity of lysine acetylation revealed by a proteomics survey. Mol. Cell *23*, 607–618.

Kitamoto, Y., Akashi, H., Tanaka, H., and Mori, N. (1988). α-Glucose-1-phosphate formation by a novel trehalose phosphorylase from Flammulina velutipes. FEMS Microbiol. Lett. *55*, 147–149.

Kitaoka, M., and Hayashi, K. (2002). 糖質加リン酸分解酵素. Trends Glycosci. Glycotechnol. *14*, 35–50.

Kizawa, H., Miyagawa, K., and Sugiyama, Y. (1995). Purification and Characterization of Trehalose Phosphorylase from Micrococcus varians. Biosci. Biotechnol. Biochem. *59*, 1908–1912.

Klein, A.H., Shulla, A., Reimann, S.A., Keating, D.H., and Wolfe, A.J. (2007). The intracellular concentration of acetyl phosphate in Escherichia coli is sufficient for direct phosphorylation of two-component response regulators. J. Bacteriol. *189*, 5574–5581.

Koliwer-Brandl, H., Syson, K., van de Weerd, R., Chandra, G., Appelmelk, B., Alber, M., Ioerger, T.R., Jacobs, W.R., Geurtsen, J., Bornemann, S., et al. (2016). Metabolic Network for the Biosynthesis of Intra- and Extracellular α-Glucans Required for Virulence of Mycobacterium tuberculosis. PLoS Pathog. *12*, e1005768.

König, L., Siegl, A., Penz, T., Haider, S., Wentrup, C., Polzin, J., Mann, E., Schmitz-Esser, S., Domman, D., and Horn, M. (2017). Biphasic Metabolism and Host Interaction of a Chlamydial Symbiont. MSystems *2*.

Koshland, D.E. (1952). Effect of Catalysts on the Hydrolysis of Acetyl Phosphate. Nucleophilic Displacement Mechanisms in Enzymatic Reactions1. J. Am. Chem. Soc. *74*, 2286–2292.

Kosono, S., Tamura, M., Suzuki, S., Kawamura, Y., Yoshida, A., Nishiyama, M., and Yoshida, M. (2015). Changes in the Acetylome and Succinylome of Bacillus subtilis in Response to Carbon Source. PloS One *10*, e0131169.

Kouril, T., Zaparty, M., Marrero, J., Brinkmann, H., and Siebers, B. (2008). A novel trehalose synthesizing pathway in the hyperthermophilic Crenarchaeon Thermoproteus tenax: the unidirectional TreT pathway. Arch. Microbiol. *190*, 355–369.

Kretschmer, P.M., Bannister, A.M., O Brien, M.K., MacManus-Spencer, L.A., and Paulick, M.G. (2016). A liquid chromatography-tandem mass spectrometry assay for the detection and quantification of trehalose in biological samples. J. Chromatogr. B Analyt. Technol. Biomed. Life. Sci. *1033–1034*, 9–16.

Kuhn, M.L., Zemaitaitis, B., Hu, L.I., Sahu, A., Sorensen, D., Minasov, G., Lima, B.P., Scholle, M., Mrksich, M., Anderson, W.F., et al. (2014). Structural, kinetic and proteomic characterization of acetyl phosphate-dependent bacterial protein acetylation. PloS One *9*, e94816.

Labrie, S.D., Dimond, Z.E., Harrison, K.S., Baid, S., Wickstrum, J., Suchland, R.J., and Scott, P. (2019). CT339 as a ComEC Homolog Important for DNA Uptake and Lateral Gene Transfer. MBio *10*, 1–24.

Lamoth, F., Pillonel, T., and Greub, G. (2015). Waddlia: An emerging pathogen and a model organism to study the biology of chlamydiae. Microbes Infect. *17*, 732–737.

Lapteva, Y.S., Vologzhannikova, A.A., Sokolov, A.S., Ismailov, R.G., Uversky, V.N., and Permyakov, S.E. (2020). In Vitro N-Terminal Acetylation of Bacterially Expressed

Parvalbumins by N-Terminal Acetyltransferases from Escherichia coli. Appl. Biochem. Biotechnol.

Lartillot, N., Lepage, T., and Blanquart, S. (2009). PhyloBayes 3: a Bayesian software package for phylogenetic reconstruction and molecular dating. Bioinforma. Oxf. Engl. *25*, 2286–2288.

Leiba, J., Syson, K., Baronian, G., Zanella-Cléon, I., Kalscheuer, R., Kremer, L., Bornemann, S., and Molle, V. (2013). Mycobacterium tuberculosis maltosyltransferase GlgE, a genetically validated antituberculosis target, is negatively regulated by Ser/Thr phosphorylation. J. Biol. Chem. *288*, 16546–16556.

Lienard, J., Croxatto, A., Aeby, S., Jaton, K., Posfay-Barbe, K., Gervaix, A., and Greub, G. (2011). Development of a New Chlamydiales-Specific Real-Time PCR and Its Application to Respiratory Clinical Samples. J. Clin. Microbiol. *49*, 2637–2642.

Lin, Y., Fletcher, C.M., Zhou, J., Allis, C.D., and Wagner, G. (1999). Solution structure of the catalytic domain of GCN5 histone acetyltransferase bound to coenzyme A. Nature *400*, 86–89.

Linka, N., Hurka, H., Lang, B.F., Burger, G., Winkler, H.H., Stamme, C., Urbany, C., Seil, I., Kusch, J., and Neuhaus, H.E. (2003). Phylogenetic relationships of non-mitochondrial nucleotide transport proteins in bacteria and eukaryotes. Gene *306*, 27–35.

Lorberth, R., Ritte, G., Willmitzer, L., and Kossmann, J. (1998). Inhibition of a starch-granule-bound protein leads to modified starch and repression of cold sweetening. Nat. Biotechnol. *16*, 473–477.

Lou, J., Dawson, K.A., and Strobel, H.J. (1997). Glycogen biosynthesis via UDP-glucose in the ruminal bacterium Prevotella bryantii B1(4). Appl. Environ. Microbiol. *63*, 4355–4359.

Lu, C., Lei, L., Peng, B., Tang, L., Ding, H., Gong, S., Li, Z., Wu, Y., and Zhong, G. (2013). Chlamydia trachomatis GlgA is secreted into host cell cytoplasm. PloS One *8*, e68764.

Macek, B., Forchhammer, K., Hardouin, J., Weber-Ban, E., Grangeasse, C., and Mijakovic, I. (2019). Protein post-translational modifications in bacteria. Nat. Rev. Microbiol. *17*, 651–664.

Maruyama, S., Eveleigh, R.J., and Archibald, J.M. (2013). Treetrimmer: a method for phylogenetic dataset size reduction. BMC Res. Notes *6*, 145.

Mattoo, R.L., and Waygood, E.B. (1983). Determination of the levels of HPr and enzyme I of the phosphoenolpyruvate-sugar phosphotransferase system in Escherichia coli and Salmonella typhimurium. Can. J. Biochem. Cell Biol. Rev. Can. Biochim. Biol. Cell. *61*, 29–37.

McCoy, A.J., Sandlin, R.C., and Maurelli, A.T. (2003). In vitro and in vivo functional activity of Chlamydia MurA, a UDP-N-acetylglucosamine enolpyruvyl transferase involved in peptidoglycan synthesis and fosfomycin resistance. J. Bacteriol. *185*, 1218–1228.

McFadden, G.I. (2014). Origin and Evolution of Plastids and Photosynthesis in Eukaryotes. Cold Spring Harb. Perspect. Biol. *6*.

McKuen, M.J., Mueller, K.E., Bae, Y.S., and Fields, K.A. (2017). Fluorescence-Reported Allelic Exchange Mutagenesis Reveals a Role for Chlamydia trachomatis TmeA in Invasion That Is Independent of Host AHNAK. Infect. Immun. *85*.

Meile, L., Rohr, L.M., Geissmann, T.A., Herensperger, M., and Teuber, M. (2001). Characterization of the D-xylulose 5-phosphate/D-fructose 6-phosphate phosphoketolase gene (xfp) from Bifidobacterium lactis. J. Bacteriol. *183*, 2929–2936.

Meléndez, R., Meléndez-Hevia, E., and Cascante, M. (1997). How did glycogen structure evolve to satisfy the requirement for rapid mobilization of glucose? A problem of physical constraints in structure building. J. Mol. Evol. *45*, 446–455.

Meléndez, R., Meléndez-Hevia, E., Mas, F., Mach, J., and Cascante, M. (1998). Physical Constraints in the Synthesis of Glycogen That Influence Its Structural Homogeneity: A Two-Dimensional Approach. Biophys. J. *75*, 106–114.

Mendes, V., Maranha, A., Lamosa, P., da Costa, M.S., and Empadinhas, N. (2010). Biochemical characterization of the maltokinase from Mycobacterium bovis BCG. BMC Biochem. *11*, 21.

Mendes, V., Blaszczyk, M., Maranha, A., Empadinhas, N., and Blundell, T.L. (2015). Structure of Mycobacterium thermoresistibile GlgE defines novel conformational states that contribute to the catalytic mechanism. Sci. Rep. *5*, 17144.

Mendes, V., Acebrón-García-de-Eulate, M., Verma, N., Blaszczyk, M., Dias, M.V.B., and Blundell, T.L. (2019). Mycobacterial OtsA Structures Unveil Substrate Preference Mechanism and Allosteric Regulation by 2-Oxoglutarate and 2-Phosphoglycerate. MBio *10*.

Miah, F., Koliwer-Brandl, H., Rejzek, M., Field, R.A., Kalscheuer, R., and Bornemann, S. (2013). Flux through trehalose synthase flows from trehalose to the alpha anomer of maltose in mycobacteria. Chem. Biol. *20*, 487–493.

Miah, F., Bibb, M.J., Barclay, J.E., Findlay, K.C., and Bornemann, S. (2016). Developmental delay in a Streptomyces venezuelae glgE null mutant is associated with the accumulation of α-maltose 1-phosphate. Microbiology *162*, 1208–1219.

Michel, R., Müller, K.D., Hauröder, B., and Zöller, L. (2000). A coccoid bacterial parasite of Naegleria sp. (Schizopyrenida: Vahlkampfiidae) inhibits cyst formation of its host but not transformation to the flagellate stage. Acta Protozool. *39*, 199–207.

Minguez, P., Parca, L., Diella, F., Mende, D.R., Kumar, R., Helmer-Citterich, M., Gavin, A.-C., van Noort, V., and Bork, P. (2012). Deciphering a global network of functionally associated post-translational modifications. Mol. Syst. Biol. *8*, 599.

Minh, B.Q., Schmidt, H.A., Chernomor, O., Schrempf, D., Woodhams, M.D., von Haeseler, A., and Lanfear, R. (2020). IQ-TREE 2: New Models and Efficient Methods for Phylogenetic Inference in the Genomic Era. Mol. Biol. Evol. *37*, 1530–1534.

Mirrashidi, K.M., Elwell, C.A., Verschueren, E., Johnson, J.R., Frando, A., Von Dollen, J., Rosenberg, O., Gulbahce, N., Jang, G., Johnson, T., et al. (2015). Global Mapping of the Inc-Human Interactome Reveals that Retromer Restricts Chlamydia Infection. Cell Host Microbe *18*, 109–121.

Mitchell, A.L., Attwood, T.K., Babbitt, P.C., Blum, M., Bork, P., Bridge, A., Brown, S.D., Chang, H.-Y., El-Gebali, S., Fraser, M.I., et al. (2019). InterPro in 2019: improving coverage, classification and access to protein sequence annotations. Nucleic Acids Res. *47*, D351–D360.

Mittal, R., Peak-Chew, S.Y., Sade, R.S., Vallis, Y., and McMahon, H.T. (2010). The acetyltransferase activity of the bacterial toxin YopJ of Yersinia is activated by eukaryotic host cell inositol hexakisphosphate. J. Biol. Chem. *285*, 19927–19934.

Morán-Zorzano, M.T., Alonso-Casajús, N., Muñoz, F.J., Viale, A.M., Baroja-Fernández, E., Eydallin, G., and Pozueta-Romero, J. (2007). Occurrence of more than one important source of ADPglucose linked to glycogen biosynthesis in Escherichia coli and Salmonella. FEBS Lett. *581*, 4423–4429.

Mosser, M., Kapel, R., Chevalot, I., Olmos, E., Marc, I., Marc, A., and Oriol, E. (2015). Fractionation of yeast extract by nanofiltration process to assess key compounds involved in CHO cell culture improvement. Biotechnol. Prog. *31*, 875–882.

Moulder, J.W. (1964). The Psittacosis Group as Bacteria. Psittacosis Group Bact.

Moulder, J.W. (1991). Interaction of chlamydiae and host cells in vitro. Microbiol. Rev. *55*, 143–190.

Mueller, K.E., Wolf, K., and Fields, K.A. (2017). Chlamydia trachomatis transformation and allelic exchange mutagenesis. Curr. Protoc. Microbiol. *2017*, 11A.3.1-11A.3.15.

Mukherjee, S., Keitany, G., Li, Y., Wang, Y., Ball, H.L., Goldsmith, E.J., and Orth, K. (2006). Yersinia YopJ acetylates and inhibits kinase activation by blocking phosphorylation. Science *312*, 1211–1214.

Murakami, T., Kanai, T., Takata, H., Kuriki, T., and Imanaka, T. (2006). A novel branching enzyme of the GH-57 family in the hyperthermophilic archaeon Thermococcus kodakaraensis KOD1. J. Bacteriol. *188*, 5915–5924.

Mystkowska, A.A., Robb, C., Vidal-Melgosa, S., Vanni, C., Fernandez-Guerra, A., Höhne, M., and Hehemann, J.-H. (2018). Molecular recognition of the beta-glucans laminarin and pustulan by a SusD-like glycan-binding protein of a marine Bacteroidetes. FEBS J. *285*, 4465–4481.

Najjar, V.A., and Pullman, M.E. (1954). The Occurrence of a Group Transfer Involving Enzyme (phosphoglucomutase) and Substrate. Science *119*, 631–634.

Nakada, T., Maruta, K., Tsusaki, K., Kubota, M., Chaen, H., Sugimoto, T., Kurimoto, M., and Tsujisaka, Y. (1995). Purification and properties of a novel enzyme, maltooligosyl trehalose synthase, from Arthrobacter sp. Q36. Biosci. Biotechnol. Biochem. *59*, 2210–2214.

Nakayasu, E.S., Burnet, M.C., Walukiewicz, H.E., Wilkins, C.S., Shukla, A.K., Brooks, S., Plutz, M.J., Lee, B.D., Schilling, B., Wolfe, A.J., et al. (2017). Ancient Regulatory Role of Lysine Acetylation in Central Metabolism. MBio *8*.

Nambi, S., Basu, N., and Visweswariah, S.S. (2010). cAMP-regulated protein lysine acetylases in mycobacteria. J. Biol. Chem. *285*, 24313–24323.

Nicholson, T.L., Olinger, L., Chong, K., Schoolnik, G., and Stephens, R.S. (2003). Global Stage-Specific Gene Regulation during the Developmental Cycle of Chlamydia trachomatis. J. Bacteriol. *185*, 3179–3189.

Nobre, A., Alarico, S., Fernandes, C., Empadinhas, N., and da Costa, M.S. (2008). A unique combination of genetic systems for the synthesis of trehalose in Rubrobacter xylanophilus: properties of a rare actinobacterial TreT. J. Bacteriol. *190*, 7939–7946.

Noy, T., Xu, H., and Blanchard, J.S. (2014). Acetylation of acetyl-CoA synthetase from Mycobacterium tuberculosis leads to specific inactivation of the adenylation reaction. Arch. Biochem. Biophys. *550–551*, 42–49.

Okazaki, Y., Shimojima, M., Sawada, Y., Toyooka, K., Narisawa, T., Mochida, K., Tanaka, H., Matsuda, F., Hirai, A., Hirai, M.Y., et al. (2009). A chloroplastic UDP-glucose pyrophosphorylase from Arabidopsis is the committed enzyme for the first step of sulfolipid biosynthesis. Plant Cell *21*, 892–909.

Oldfors, A. (2017). Is Glycogenin Essential for Glycogen Synthesis? Cell Metab. *26*, 12–14.

Omsland, A., Sager, J., Nair, V., Sturdevant, D.E., and Hackstadt, T. (2012). Developmental stage-specific metabolic and transcriptional activity of Chlamydia trachomatis in an axenic medium. Proc. Natl. Acad. Sci. U. S. A. *109*, 19781–19785.

Omsland, A., Sixt, B.S., Horn, M., and Hackstadt, T. (2014). Chlamydial metabolism revisited: interspecies metabolic variability and developmental stage-specific physiologic activities. FEMS Microbiol. Rev. *38*, 779–801.

Opperdoes, F.R., and Michels, P.A.M. (1993). The glycosomes of the Kinetoplastida. Biochimie *75*, 231–234.

Opperdoes, F.R., De Jonckheere, J.F., and Tielens, A.G.M. (2011). Naegleria gruberi metabolism. Int. J. Parasitol. *41*, 915–924.

Otten, C., Brilli, M., Vollmer, W., Viollier, P.H., and Salje, J. (2018). Peptidoglycan in obligate intracellular bacteria. Mol. Microbiol. *107*, 142–163.

Pan, Y.T., Koroth Edavana, V., Jourdian, W.J., Edmondson, R., Carroll, J.D., Pastuszak, I., and Elbein, A.D. (2004). Trehalose synthase of Mycobacterium smegmatis: purification, cloning, expression, and properties of the enzyme. Eur. J. Biochem. *271*, 4259–4269.

Pan, Y.-T., Carroll, J.D., Asano, N., Pastuszak, I., Edavana, V.K., and Elbein, A.D. (2008). Trehalose synthase converts glycogen to trehalose. FEBS J. *275*, 3408–3420.

Paquette, N., Conlon, J., Sweet, C., Rus, F., Wilson, L., Pereira, A., Rosadini, C.V., Goutagny, N., Weber, A.N.R., Lane, W.S., et al. (2012). Serine/threonine acetylation of TGFβ-activated kinase (TAK1) by Yersinia pestis YopJ inhibits innate immune signaling. Proc. Natl. Acad. Sci. U. S. A. *109*, 12710–12715.

Park, J.-T., Shim, J.-H., Tran, P.L., Hong, I.-H., Yong, H.-U., Oktavina, E.F., Nguyen, H.D., Kim, J.-W., Lee, T.S., Park, S.-H., et al. (2011). Role of maltose enzymes in glycogen synthesis by Escherichia coli. J. Bacteriol. *193*, 2517–2526.

Paul, M.J., Primavesi, L.F., Jhurreea, D., and Zhang, Y. (2008). Trehalose metabolism and signaling. Annu. Rev. Plant Biol. *59*, 417–441.

Peebo, K., Valgepea, K., Nahku, R., Riis, G., Oun, M., Adamberg, K., and Vilu, R. (2014). Coordinated activation of PTA-ACS and TCA cycles strongly reduces overflow metabolism of acetate in Escherichia coli. Appl. Microbiol. Biotechnol. *98*, 5131–5143.

Phillips, D.M.P. (1963). The presence of acetyl groups in histones. Biochem. J. *87*, 258–263.

Pillonel, T., Bertelli, C., and Greub, G. (2018). Environmental Metagenomic Assemblies Reveal Seven New Highly Divergent Chlamydial Lineages and Hallmarks of a Conserved Intracellular Lifestyle. Front. Microbiol. *9*.

Pillonel, T., Tagini, F., Bertelli, C., and Greub, G. (2020). ChlamDB: a comparative genomics database of the phylum Chlamydiae and other members of the Planctomycetes-Verrucomicrobiae-Chlamydiae superphylum. Nucleic Acids Res. *48*, D526–D534.

Polevoda, B., and Sherman, F. (2003). N-terminal Acetyltransferases and Sequence Requirements for N-terminal Acetylation of Eukaryotic Proteins. J. Mol. Biol. *325*, 595–622.

Ponce-Toledo, R.I., Deschamps, P., López-García, P., Zivanovic, Y., Benzerara, K., and Moreira, D. (2017). An Early-Branching Freshwater Cyanobacterium at the Origin of Plastids. Curr. Biol. *27*, 386–391.

Posthuma, C.C., Bader, R., Engelmann, R., Postma, P.W., Hengstenberg, W., and Pouwels, P.H. (2002). Expression of the Xylulose 5-Phosphate Phosphoketolase Gene, xpkA, from Lactobacillus pentosus MD363 Is Induced by Sugars That Are Fermented via the Phosphoketolase Pathway and Is Repressed by Glucose Mediated by CcpA and the Mannose Phosphoenolpyruvate Phosphotransferase System. Appl. Environ. Microbiol. *68*, 831–837.

Prats, C., Graham, T.E., and Shearer, J. (2018). The dynamic life of the glycogen granule. J. Biol. Chem. *293*, 7089–7098.

Preiss, J. (1984). Bacterial glycogen synthesis and its regulation. Annu. Rev. Microbiol. *38*, 419–458.

Preiss, J. (2009). Glycogen: Biosynthesis and Regulation. EcoSal Plus *3*.

Preiss, J. (2014). Glycogen: Biosynthesis and Regulation. EcoSal Plus *6*.

Price, M.N., Dehal, P.S., and Arkin, A.P. (2010). FastTree 2 – Approximately Maximum-Likelihood Trees for Large Alignments. PLoS ONE *5*.

Qiu, H., Price, D.C., Weber, A.P.M., Facchinelli, F., Yoon, H.S., and Bhattacharya, D. (2013). Assessing the bacterial contribution to the plastid proteome. Trends Plant Sci. *18*, 680–687.

Qu, Q., Lee, S.-J., and Boos, W. (2004). TreT, a novel trehalose glycosyltransferring synthase of the hyperthermophilic archaeon Thermococcus litoralis. J. Biol. Chem. *279*, 47890–47897.

Rack, J.G.M., Morra, R., Barkauskaite, E., Kraehenbuehl, R., Ariza, A., Qu, Y., Ortmayer, M., Leidecker, O., Cameron, D.R., Matic, I., et al. (2015). Identification of a Class of Protein ADP-Ribosylating Sirtuins in Microbial Pathogens. Mol. Cell *59*, 309–320.

Radin, J.N., Zhu, J., Brazel, E.B., McDevitt, C.A., and Kehl-Fie, T.E. (2019). Synergy between Nutritional Immunity and Independent Host Defenses Contributes to the Importance of the MntABC Manganese Transporter during Staphylococcus aureus Infection. Infect. Immun. *87*.

Ramponi, G., Manao, G., and Camici, G. (1975). Nonenzymatic acetylation of histones with acetyl phosphate and acetyl adenylate. Biochemistry *14*, 2681–2685.

Rashid, A.M., Batey, S.F.D., Syson, K., Koliwer-Brandl, H., Miah, F., Barclay, J.E., Findlay, K.C., Nartowski, K.P., Khimyak, Y.Z., Kalscheuer, R., et al. (2016). Assembly of α-Glucan by GlgE and GlgB in Mycobacteria and Streptomycetes. Biochemistry *55*, 3270–3284.

Ren, J., Sang, Y., Lu, J., and Yao, Y.-F. (2017). Protein Acetylation and Its Role in Bacterial Virulence. Trends Microbiol. *25*, 768–779.

Reynolds, C.R., Islam, S.A., and Sternberg, M.J.E. (2018). EzMol: A Web Server Wizard for the Rapid Visualization and Image Production of Protein and Nucleic Acid Structures. J. Mol. Biol. *430*, 2244–2248.

Ripa, K.T. (1982). Microbiological diagnosis of Chlamydia trachomatis infection. Infection *10*, S19–S24.

Roach, P.J. (2015). Glycogen Phosphorylation and Lafora disease. Mol. Aspects Med. *46*, 78–84.

Roach, R.J., and Larner, J. (1977). Covalent phosphorylation in the regulation glycogen synthase activity. Mol. Cell. Biochem. *15*, 179–200.

Roach, P.J., Depaoli-Roach, A.A., Hurley, T.D., and Tagliabracci, V.S. (2012). Glycogen and its metabolism: some new developments and old themes. Biochem. J. *441*, 763–787.

Rodríguez-Ezpeleta, N., Brinkmann, H., Burey, S.C., Roure, B., Burger, G., Löffelhardt, W., Bohnert, H.J., Philippe, H., and Lang, B.F. (2005). Monophyly of primary photosynthetic eukaryotes: green plants, red algae, and glaucophytes. Curr. Biol. CB *15*, 1325–1330.

Rodríguez-Zaragoza, S. (1994). Ecology of free-living amoebae. Crit. Rev. Microbiol. *20*, 225–241.

Romeo, T., and Babitzke, P. (2018). Global Regulation by CsrA and Its RNA Antagonists. Microbiol. Spectr. *6*.

Romeo, T., Gong, M., Liu, M.Y., and Brun-Zinkernagel, A.M. (1993). Identification and molecular characterization of csrA, a pleiotropic gene from Escherichia coli that affects glycogen biosynthesis, gluconeogenesis, cell size, and surface properties. J. Bacteriol. *175*, 4744–4755.

Roy, R., Usha, V., Kermani, A., Scott, D.J., Hyde, E.I., Besra, G.S., Alderwick, L.J., and Fütterer, K. (2013). Synthesis of α-glucan in mycobacteria involves a hetero-octameric complex of trehalose synthase TreS and Maltokinase Pep2. ACS Chem. Biol. *8*, 2245–2255.

Rusconi, B., Lienard, J., Aeby, S., Croxatto, A., Bertelli, C., and Greub, G. (2013). Crescent and star shapes of members of the Chlamydiales order: impact of fixative methods. Antonie Van Leeuwenhoek *104*, 521–532.

Rusconi, B., Kebbi-Beghdadi, C., and Greub, G. (2015). Trafficking of Estrella lausannensis in human macrophages. Pathog. Dis. *73*.

Rybicka, K.K. (1996). Glycosomes — the organelles of glycogen metabolism. Tissue Cell *28*, 253–265.

Ryu, S.-I., Park, C.-S., Cha, J., Woo, E.-J., and Lee, S.-B. (2005). A novel trehalose-synthesizing glycosyltransferase from Pyrococcus horikoshii: molecular cloning and characterization. Biochem. Biophys. Res. Commun. *329*, 429–436.

Sambou, T., Dinadayala, P., Stadthagen, G., Barilone, N., Bordat, Y., Constant, P., Levillain, F., Neyrolles, O., Gicquel, B., Lemassu, A., et al. (2008). Capsular glucan and intracellular glycogen of Mycobacterium tuberculosis: Biosynthesis and Impact on the Persistence in mice. Mol. Microbiol. *70*, 762–774.

Sassetti, C.M., Boyd, D.H., and Rubin, E.J. (2003). Genes required for mycobacterial growth defined by high density mutagenesis. Mol. Microbiol. *48*, 77–84.

Schmidt, A., Kochanowski, K., Vedelaar, S., Ahrné, E., Volkmer, B., Callipo, L., Knoops, K., Bauer, M., Aebersold, R., and Heinemann, M. (2016). The quantitative and condition-dependent Escherichia coli proteome. Nat. Biotechnol. *34*, 104–110.

Schmidt, M.T., Smith, B.C., Jackson, M.D., and Denu, J.M. (2004). Coenzyme specificity of Sir2 protein deacetylases: implications for physiological regulation. J. Biol. Chem. *279*, 40122–40129.

Schneider, D., Bruton, C.J., and Chater, K.F. (2000). Duplicated gene clusters suggest an interplay of glycogen and trehalose metabolism during sequential stages of aerial mycelium development in Streptomyces coelicolor A3(2). Mol. Gen. Genet. MGG *263*, 543–553.

Schwarz, A., Goedl, C., Minani, A., and Nidetzky, B. (2007). Trehalose phosphorylase from Pleurotus ostreatus: characterization and stabilization by covalent modification, and application for the synthesis of alpha,alpha-trehalose. J. Biotechnol. *129*, 140–150.

Schwöppe, C., Winkler, H.H., and Neuhaus, H.E. (2002). Properties of the glucose-6-phosphate transporter from Chlamydia pneumoniae (HPTcp) and the glucose-6-phosphate sensor from Escherichia coli (UhpC). J. Bacteriol. *184*, 2108–2115.

Seibold, G.M., Breitinger, K.J., Kempkes, R., Both, L., Krämer, M., Dempf, S., and Eikmanns, B.J. (2011). The glgB-encoded glycogen branching enzyme is essential for glycogen accumulation in Corynebacterium glutamicum. Microbiol. Read. Engl. *157*, 3243–3251.

Seok, Y.J., Sondej, M., Badawi, P., Lewis, M.S., Briggs, M.C., Jaffe, H., and Peterkofsky, A. (1997). High affinity binding and allosteric regulation of Escherichia coli glycogen phosphorylase by the histidine phosphocarrier protein, HPr. J. Biol. Chem. *272*, 26511–26521.

Seok, Y.J., Koo, B.M., Sondej, M., and Peterkofsky, A. (2001). Regulation of E. coli glycogen phosphorylase activity by HPr. J. Mol. Microbiol. Biotechnol. *3*, 385–393.

Shearer, J., and Graham, T.E. (2002). New perspectives on the storage and organization of muscle glycogen. Can. J. Appl. Physiol. Rev. Can. Physiol. Appl. *27*, 179–203.

Shih, P.M., and Matzke, N.J. (2013). Primary endosymbiosis events date to the later Proterozoic with cross-calibrated phylogenetic dating of duplicated ATPase proteins. Proc. Natl. Acad. Sci. U. S. A. *110*, 12355–12360.

Sixt, B.S., Siegl, A., Müller, C., Watzka, M., Wultsch, A., Tziotis, D., Montanaro, J., Richter, A., Schmitt-Kopplin, P., and Horn, M. (2013). Metabolic Features of Protochlamydia amoebophila Elementary Bodies - A Link between Activity and Infectivity in Chlamydiae. PLoS Pathog. *9*.

Skipp, P.J.S., Hughes, C., McKenna, T., Edwards, R., Langridge, J., Thomson, N.R., and Clarke, I.N. (2016). Quantitative Proteomics of the Infectious and Replicative Forms of Chlamydia trachomatis. PloS One *11*, e0149011.

Smith, A.D. (1985). Biochemistry for the medical sciences: By E A Newsholme and A R Leech. pp 952. J. Wiley, Chichester, UK. 1983. £19.75 ISBN 0-471-90058-3. Biochem. Educ. *13*, 37–37.

Smythe, C., and Cohen, P. (1992). The discovery of glycogenin and the priming mechanism for glycogen biogenesis. In EJB Reviews 1991, P. Christen, and E. Hofmann, eds. (Berlin, Heidelberg: Springer), pp. 149–155.

Song, L., Carlson, J.H., Whitmire, W.M., Kari, L., Virtaneva, K., Sturdevant, D.E., Watkins, H., Zhou, B., Sturdevant, G.L., Porcella, S.F., et al. (2013). Chlamydia trachomatis Plasmid-Encoded Pgp4 Is a Transcriptional Regulator of Virulence-Associated Genes. Infect. Immun. *81*, 636–644.

Soppa, J. (2010). Protein Acetylation in Archaea, Bacteria, and Eukaryotes. Archaea *2010*.

Spellerberg, B., Cundell, D.R., Sandros, J., Pearce, B.J., Idanpaan-Heikkila, I., Rosenow, C., and Masure, H.R. (1996). Pyruvate oxidase, as a determinant of virulence in Streptococcus pneumoniae. Mol. Microbiol. *19*, 803–813.

Starai, V.J., and Escalante-Semerena, J.C. (2004). Identification of the protein acetyltransferase (Pat) enzyme that acetylates acetyl-CoA synthetase in Salmonella enterica. J. Mol. Biol. *340*, 1005–1012.

Starai, V.J., Celic, I., Cole, R.N., Boeke, J.D., and Escalante-Semerena, J.C. (2002). Sir2-dependent activation of acetyl-CoA synthetase by deacetylation of active lysine. Science *298*, 2390–2392.

Strøm, A.R., and Kaasen, I. (1993). Trehalose metabolism in Escherichia coli: stress protection and stress regulation of gene expression. Mol. Microbiol. *8*, 205–210.

Subtil, A., Parsot, C., and Dautry-Varsat, A. (2001). Secretion of predicted Inc proteins of Chlamydia pneumoniae by a heterologous type III machinery. Mol. Microbiol. *39*, 792–800.

Subtil, A., Delevoye, C., Balañá, M.-E., Tastevin, L., Perrinet, S., and Dautry-Varsat, A. (2005). A directed screen for chlamydial proteins secreted by a type III mechanism identifies a translocated protein and numerous other new candidates. Mol. Microbiol. *56*, 1636–1647.

Subtil, A., Collingro, A., and Horn, M. (2014). Tracing the primordial Chlamydiae: extinct parasites of plants? Trends Plant Sci. *19*, 36–43.

Sullivan, M.A., Vilaplana, F., Cave, R.A., Stapleton, D., Gray-Weale, A.A., and Gilbert, R.G. (2010). Nature of alpha and beta particles in glycogen using molecular size distributions. Biomacromolecules *11*, 1094–1100.

Sun, M., Xu, J., Wu, Z., Zhai, L., Liu, C., Cheng, Z., Xu, G., Tao, S., Ye, B.-C., Zhao, Y., et al. (2016). Characterization of Protein Lysine Propionylation in Escherichia coli: Global Profiling, Dynamic Change, and Enzymatic Regulation. J. Proteome Res. *15*, 4696–4708.

Suzuki, E., and Suzuki, R. (2016). Distribution of glucan-branching enzymes among prokaryotes. Cell. Mol. Life Sci. CMLS *73*, 2643–2660.

Suzuki, E., Onoda, M., Colleoni, C., Ball, S., Fujita, N., and Nakamura, Y. (2013). Physicochemical variation of cyanobacterial starch, the insoluble α-Glucans in cyanobacteria. Plant Cell Physiol. *54*, 465–473.

Syson, K., Stevenson, C.E.M., Rejzek, M., Fairhurst, S.A., Nair, A., Bruton, C.J., Field, R.A., Chater, K.F., Lawson, D.M., and Bornemann, S. (2011). Structure of Streptomyces Maltosyltransferase GlgE, a Homologue of a Genetically Validated Anti-tuberculosis Target. J. Biol. Chem. *286*, 38298–38310.

Syson, K., Stevenson, C.E.M., Lawson, D.M., and Bornemann, S. (2020). Structure of the Mycobacterium smegmatis α-maltose-1-phosphate synthase GlgM. Acta Crystallogr. Sect. F Struct. Biol. Commun. *76*, 175–181.

Szeredi, L., and Bacsadi, A. (2002). Detection of Chlamydophila (Chlamydia) abortus and Toxoplasma gondii in smears from cases of ovine and caprine abortion by the streptavidin-biotin method. J. Comp. Pathol. *127*, 257–263.

Taborisky, J. (1952). Historic and Ethnologic Factors in the Distribution of Trachoma. Am. J. Ophthalmol. *35*, 1305–1311.

Tagliabracci, V.S., Girard, J.M., Segvich, D., Meyer, C., Turnbull, J., Zhao, X., Minassian, B.A., DePaoli-Roach, A.A., and Roach, P.J. (2008). Abnormal Metabolism of Glycogen Phosphate as a Cause for Lafora Disease. J. Biol. Chem. *283*, 33816–33825.

Tagliabracci, V.S., Heiss, C., Karthik, C., Contreras, C.J., Glushka, J., Ishihara, M., Azadi, P., Hurley, T.D., DePaoli-Roach, A.A., and Roach, P.J. (2011). Phosphate incorporation during glycogen synthesis and Lafora disease. Cell Metab. *13*, 274–282.

Takamura, Y., and Nomura, G. (1988). Changes in the intracellular concentration of acetyl-CoA and malonyl-CoA in relation to the carbon and energy metabolism of Escherichia coli K12. J. Gen. Microbiol. *134*, 2249–2253.

Takata, H., Takaha, T., Okada, S., Takagi, M., and Imanaka, T. (1997). Characterization of a gene cluster for glycogen biosynthesis and a heterotetrameric ADP-glucose pyrophosphorylase from Bacillus stearothermophilus. J. Bacteriol. *179*, 4689–4698.

Takata, H., Takaha, T., Okada, S., Takagi, M., and Imanaka, T. (1998). Purification and characterization of α-glucan phosphorylase from bacillus stearothermophilus. J. Ferment. Bioeng. *85*, 156–161.

Tanaka, S., Matsushita, Y., Yoshikawa, A., and Isono, K. (1989). Cloning and molecular characterization of the gene rimL which encodes an enzyme acetylating ribosomal protein L12 of Escherichia coli K12. Mol. Gen. Genet. MGG *217*, 289–293.

Taunton, J., Hassig, C.A., and Schreiber, S.L. (1996). A mammalian histone deacetylase related to the yeast transcriptional regulator Rpd3p. Science *272*, 408–411.

Taylor-Brown, A., Vaughan, L., Greub, G., Timms, P., and Polkinghorne, A. (2015). Twenty years of research into Chlamydia-like organisms: a revolution in our understanding of the biology and pathogenicity of members of the phylum Chlamydiae. Pathog. Dis. *73*, 1–15.

Taylor-Robinson, D. (2017). The discovery of Chlamydia trachomatis. Sex. Transm. Infect. *93*, 10.

Testoni, G., Duran, J., García-Rocha, M., Vilaplana, F., Serrano, A.L., Sebastián, D., López-Soldado, I., Sullivan, M.A., Slebe, F., Vilaseca, M., et al. (2017). Lack of Glycogenin Causes Glycogen Accumulation and Muscle Function Impairment. Cell Metab. *26*, 256-266.e4.

Thao, S., and Escalante-Semerena, J.C. (2011). Control of protein function by reversible Nε-lysine acetylation in bacteria. Curr. Opin. Microbiol. *14*, 200–204.

Thao, S., and Escalante-Semerena, J.C. (2012). A positive selection approach identifies residues important for folding of Salmonella enterica Pat, an N(ε)-lysine acetyltransferase that regulates central metabolism enzymes. Res. Microbiol. *163*, 427–435.

Thevelein, J.M., and Hohmann, S. (1995). Trehalose synthase: guard to the gate of glycolysis in yeast? Trends Biochem. Sci. *20*, 3–10.

Thomas, V., Loret, J.-F., Jousset, M., and Greub, G. (2008). Biodiversity of amoebae and amoebae-resisting bacteria in a drinking water treatment plant. Environ. Microbiol. *10*, 2728–2745.

Thomason, M.J., Seabourne, C.R., Sattelle, B.M., Hembury, G.A., Stevens, J.S., Scott, A.J., Aziz, E.F., and Schroeder, S.L.M. (2015). Self-association of organic solutes in solution: a NEXAFS study of aqueous imidazole. Faraday Discuss. *179*, 269–289.

Thygeson, P. (1963). EPIDEMIOLOGIC OBSERVATIONS ON TRACHOMA IN THE UNITED STATES. Invest. Ophthalmol. *2*, 482–489.

Timmis, J.N., Ayliffe, M.A., Huang, C.Y., and Martin, W. (2004). Endosymbiotic gene transfer: organelle genomes forge eukaryotic chromosomes. Nat. Rev. Genet. *5*, 123–135.

Tjaden, J., Winkler, H.H., Schwöppe, C., Van Der Laan, M., Möhlmann, T., and Neuhaus, H.E. (1999). Two Nucleotide Transport Proteins in Chlamydia trachomatis, One for Net Nucleoside Triphosphate Uptake and the Other for Transport of Energy. J. Bacteriol. *181*, 1196–1202.

Torija, M.-J., Novo, M., Lemassu, A., Wilson, W., Roach, P.J., François, J., and Parrou, J.-L. (2005). Glycogen synthesis in the absence of glycogenin in the yeast Saccharomyces cerevisiae. FEBS Lett. *579*, 3999–4004.

Trentmann, O., Horn, M., van Scheltinga, A.C.T., Neuhaus, H.E., and Haferkamp, I. (2007). Enlightening energy parasitism by analysis of an ATP/ADP transporter from chlamydiae. PLoS Biol. *5*, e231.

Trievel, R.C., Rojas, J.R., Sterner, D.E., Venkataramani, R.N., Wang, L., Zhou, J., Allis, C.D., Berger, S.L., and Marmorstein, R. (1999). Crystal structure and mechanism of histone acetylation of the yeast GCN5 transcriptional coactivator. Proc. Natl. Acad. Sci. U. S. A. *96*, 8931–8936.

Tsusaki, K., Nishimoto, T., Nakada, T., Kubota, M., Chaen, H., Sugimoto, T., and Kurimoto, M. (1996). Cloning and sequencing of trehalose synthase gene from Pimelobacter sp. R48. Biochim. Biophys. Acta *1290*, 1–3.

Tu, S., Guo, S.-J., Chen, C.-S., Liu, C.-X., Jiang, H.-W., Ge, F., Deng, J.-Y., Zhou, Y.-M., Czajkowsky, D.M., Li, Y., et al. (2015). YcgC represents a new protein deacetylase family in prokaryotes. ELife *4*.

Turnquist, R.L., Gillett, T.A., and Hansen, R.G. (1974). Uridine Diphosphate Glucose Pyrophosphorylase CRYSTALLIZATION AND PROPERTIES OF THE ENZYME FROM RABBIT LIVER AND SPECIES COMPARISONS. J. Biol. Chem. *249*, 7695–7700.

Tyagi, J.S., and Sharma, D. (2002). Mycobacterium smegmatis and tuberculosis. Trends Microbiol. *10*, 68–69.

Ugalde, J.E., Parodi, A.J., and Ugalde, R.A. (2003). De novo synthesis of bacterial glycogen: Agrobacterium tumefaciens glycogen synthase is involved in glucan initiation and elongation. Proc. Natl. Acad. Sci. *100*, 10659–10663.

VanDrisse, C.M., and Escalante-Semerena, J.C. (2018). In Streptomyces lividans, acetyl-CoA synthetase activity is controlled by O-serine and Nε -lysine acetylation. Mol. Microbiol. *107*, 577–594.

VanDrisse, C.M., and Escalante-Semerena, J.C. (2019). Protein Acetylation in Bacteria. Annu. Rev. Microbiol. *73*, 111–132.

VanDrisse, C.M., Parks, A.R., and Escalante-Semerena, J.C. (2017). A Toxin Involved in Salmonella Persistence Regulates Its Activity by Acetylating Its Cognate Antitoxin, a Modification Reversed by CobB Sirtuin Deacetylase. MBio *8*.

Veleti, S.K., Lindenberger, J.J., Thanna, S., Ronning, D.R., and Sucheck, S.J. (2014). Synthesis of a poly-hydroxypyrolidine-based inhibitor of Mycobacterium tuberculosis GlgE. J. Org. Chem. *79*, 9444–9450.

Venkat, S., Gregory, C., Sturges, J., Gan, Q., and Fan, C. (2017). Studying the Lysine Acetylation of Malate Dehydrogenase. J. Mol. Biol. *429*, 1396–1405.

Verdin, E., and Ott, M. (2015). 50 years of protein acetylation: from gene regulation to epigenetics, metabolism and beyond. Nat. Rev. Mol. Cell Biol. *16*, 258–264.

Vetting, M.W., S de Carvalho, L.P., Yu, M., Hegde, S.S., Magnet, S., Roderick, S.L., and Blanchard, J.S. (2005). Structure and functions of the GNAT superfamily of acetyltransferases. Arch. Biochem. Biophys. *433*, 212–226.

Vidal, M., and Gaber, R.F. (1991). RPD3 encodes a second factor required to achieve maximum positive and negative transcriptional states in Saccharomyces cerevisiae. Mol. Cell. Biol. *11*, 6317–6327.

Viksø-Nielsen, A., Hao-Jie Chen, P., Larsson, H., Blennow, A., and Møller, B.L. (2002). Production of highly phosphorylated glycopolymers by expression of R1 in Escherichia coli. Carbohydr. Res. *337*, 327–333.

Visuttijai, K., Hedberg-Oldfors, C., Thomsen, C., Glamuzina, E., Kornblum, C., Tasca, G., Hernandez-Lain, A., Sandstedt, J., Dellgren, G., Roach, P., et al. (2019). Glycogenin is Dispensable for Glycogen Synthesis in Human Muscle, and Glycogenin Deficiency Causes Polyglucosan Storage. J. Clin. Endocrinol. Metab. *105*, 557–566.

de Vries, J., and Archibald, J.M. (2017). Endosymbiosis: Did Plastids Evolve from a Freshwater Cyanobacterium? Curr. Biol. *27*, R103–R105.

Wang, L., Regina, A., Butardo, V.M., Kosar-Hashemi, B., Larroque, O., Kahler, C.M., and Wise, M.J. (2015). Influence of in situ progressive N-terminal is still controversial truncation of glycogen branching enzyme in Escherichia coli DH5α on glycogen structure, accumulation, and bacterial viability. BMC Microbiol. *15*, 96.

Wang, M.-M., You, D., and Ye, B.-C. (2017). Site-specific and kinetic characterization of enzymatic and nonenzymatic protein acetylation in bacteria. Sci. Rep. *7*, 14790.

Wang, Y., Zhang, J., Wang, W., Liu, Y., Xing, L., and Li, M. (2012). Effects of the N-terminal and C-terminal domains of Meiothermus ruber CBS-01 trehalose synthase on thermostability and activity. Extremophiles *16*, 377–385.

Wannet, W.J., Hermans, J.H., van Der Drift, C., and Op Den Camp, H.J. (2000). HPLC detection of soluble carbohydrates involved in mannitol and trehalose metabolism in the edible mushroom Agaricus bisporus. J. Agric. Food Chem. *48*, 287–291.

Wannet, W.J.B., Op den Camp, H.J.M., Wisselink, H.W., van der Drift, C., Van Griensven, L.J.L.D., and Vogels, G.D. (1998). Purification and characterization of trehalose phosphorylase from the commercial mushroom Agaricus bisporus. Biochim. Biophys. Acta BBA - Gen. Subj. *1425*, 177–188.

Wayllace, N.Z., Valdez, H.A., Merás, A., Ugalde, R.A., Busi, M.V., and Gomez-Casati, D.F. (2012). An enzyme-coupled continuous spectrophotometric assay for glycogen synthases. Mol. Biol. Rep. *39*, 585–591.

Webb, S.G. (1990). Prehistoric eye disease (trachoma?) in Australian aborigines. Am. J. Phys. Anthropol. *81*, 91–100.

Weinert, B.T., Iesmantavicius, V., Wagner, S.A., Schölz, C., Gummesson, B., Beli, P., Nyström, T., and Choudhary, C. (2013). Acetyl-phosphate is a critical determinant of lysine acetylation in E. coli. Mol. Cell *51*, 265–272.

Weinert, B.T., Satpathy, S., Hansen, B.K., Lyon, D., Jensen, L.J., and Choudhary, C. (2017). Accurate Quantification of Site-specific Acetylation Stoichiometry Reveals the Impact of Sirtuin Deacetylase CobB on the E. coli Acetylome. Mol. Cell. Proteomics MCP *16*, 759–769.

Wilson, W.A., Roach, P.J., Montero, M., Baroja-Fernández, E., Muñoz, F.J., Eydallin, G., Viale, A.M., and Pozueta-Romero, J. (2010a). Regulation of glycogen metabolism in yeast and bacteria. FEMS Microbiol. Rev. *34*, 952–985.

Wilson, W.A., Roach, P.J., Montero, M., Baroja-Fernández, E., Muñoz, F.J., Eydallin, G., Viale, A.M., and Pozueta-Romero, J. (2010b). Regulation of glycogen metabolism in yeast and bacteria. FEMS Microbiol. Rev. *34*, 952–985.

Wolfe, A.J. (2005). The Acetate Switch. Microbiol. Mol. Biol. Rev. *69*, 12–50.

Xu, J.-Y., Xu, Z., Liu, X., Tan, M., and Ye, B.-C. (2018). Protein Acetylation and Butyrylation Regulate the Phenotype and Metabolic Shifts of the Endospore-forming Clostridium acetobutylicum. Mol. Cell. Proteomics MCP *17*, 1156–1169.

Yang, X.-J., and Grégoire, S. (2005). Class II Histone Deacetylases: from Sequence to Function, Regulation, and Clinical Implication. Mol. Cell. Biol. *25*, 2873–2884.

Yang, X.-J., and Seto, E. (2008). The Rpd3/Hda1 family of lysine deacetylases: from bacteria and yeast to mice and men. Nat. Rev. Mol. Cell Biol. *9*, 206–218.

Yoon, H.S., Hackett, J.D., Ciniglia, C., Pinto, G., and Bhattacharya, D. (2004). A molecular timeline for the origin of photosynthetic eukaryotes. Mol. Biol. Evol. *21*, 809–818.

Yoshikawa, A., Isono, S., Sheback, A., and Isono, K. (1987). Cloning and nucleotide sequencing of the genes rimI and rimJ which encode enzymes acetylating ribosomal proteins S18 and S5 of Escherichia coli K12. Mol. Gen. Genet. MGG *209*, 481–488.

You, D., Wang, M.-M., and Ye, B.-C. (2017). Acetyl-CoA synthetases of Saccharopolyspora erythraea are regulated by the nitrogen response regulator GlnR at both transcriptional and post-translational levels. Mol. Microbiol. *103*, 845–859.

Yu, B.J., Kim, J.A., Moon, J.H., Ryu, S.E., and Pan, J.-G. (2008). The diversity of lysine-acetylated proteins in Escherichia coli. J. Microbiol. Biotechnol. *18*, 1529–1536.

Yue, M., Wu, X.L., Gong, W.N., and Ding, H.B. (2009). Molecular cloning and expression of a novel trehalose synthase gene from Enterobacter hormaechei. Microb. Cell Factories *8*, 34.

Zaunbrecher, M.A., Sikes, R.D., Metchock, B., Shinnick, T.M., and Posey, J.E. (2009). Overexpression of the chromosomally encoded aminoglycoside acetyltransferase eis confers kanamycin resistance in Mycobacterium tuberculosis. Proc. Natl. Acad. Sci. U. S. A. *106*, 20004–20009.

Zea, C.J., and Pohl, N.L. (2004). General assay for sugar nucleotidyltransferases using electrospray ionization mass spectrometry. Anal. Biochem. *328*, 196–202.

Zeqiraj, E., and Sicheri, F. (2015). Getting a handle on glycogen synthase – Its interaction with glycogenin. Mol. Aspects Med. *46*, 63–69.

Zhang, R., Pan, Y.T., He, S., Lam, M., Brayer, G.D., Elbein, A.D., and Withers, S.G. (2011). Mechanistic Analysis of Trehalose Synthase from Mycobacterium smegmatis. J. Biol. Chem. *286*, 35601–35609.

Zhang, X., Leemhuis, H., and van der Maarel, M.J.E.C. (2019). Characterization of the GH13 and GH57 glycogen branching enzymes from Petrotoga mobilis SJ95 and potential role in glycogen biosynthesis. PloS One *14*, e0219844.

Zhao, K., Chai, X., and Marmorstein, R. (2004). Structure and Substrate Binding Properties of cobB, a Sir2 Homolog Protein Deacetylase from Escherichia coli. J. Mol. Biol. *337*, 731–741.

Zhao, M., Xu, X., Yang, S., Liu, T., and Liu, B. (2018). Cloning, expression and characterization of the maltooligosyl trehalose synthase from the archaeon Sulfolobus tokodaii. Pak. J. Pharm. Sci. *31*, 599–601.

Zhu, Y., Wei, D., Zhang, J., Wang, Y., Xu, H., Xing, L., and Li, M. (2010). Overexpression and characterization of a thermostable trehalose synthase from Meiothermus ruber. Extrem. Life Extreme Cond. *14*, 1–8.